Mathematical Models for the Dynamics of Tuberculosis and Hepatitis C Co-infection

Kizito Mohammed

2022/PhD/064/PS

A Thesis Submitted to Faculty of Science in Partial Fulfilment of the Requirements for the Award of the Degree of Doctor of Philosophy in Mathematics of Mbarara University of Science and Technology

August, 2025

DECLARATION

I hereby declare that all the information in this thesis has been obtained and presented in accordance with the academic rules and ethical conduct. Where I have used the work of others, due acknowledgen and sources have been provided.

Signed : _____

Date : 27/08/2025

APPROVAL

This thesis has been completed under our guidance and supervision, and we hereby approve it submission.

Hasifa Nampala, PhD
Department of Mathematics and Statistics
Kyambogo University, P. O. Box 1, Kyambogo, Uganda

Signed :_____

Date : 27/08/2025

Pius Ariho, PhD
Faculty of Computing and Informatics
Mbarara University of Science and Technology, P.O. Box 1410, Mbarara, Uganda

Signed :_____

Date : 28/08/2025

DEDICATION

To the loving memory of my mother, Dorothy Nakasi, whose unwavering support and guidanc inspired me to pursue my dreams. May this work be a testament to her enduring legacy.

ACKNOWLEDGEMENT

I acknowledge the contributions of several individuals and organisations to the completion of my PhI degree. I express heartfelt gratitude to my supervisors, Hasifa Nampala, PhD and Pius Ariho, PhI for their exceptional mentorship, guidance, encouragement and support. Your selfless dedication ha been instrumental in my success. I pray that God rewards you abundantly.

I would also like to extend my sincere appreciation to the management of Mbarara University o Science and Technology for waiving my tuition fees for the three academic years. Your generou support significantly facilitated my academic pursuit and I am deeply grateful for your investmen in my education.

I extend my sincere gratitude to the members of the Department of Mathematics at Mbarara University of Science and Technology for providing a conducive environment for my research anc academic growth. Michael Byamukama, PhD my colleague and friend, deserves a special mention fo his unrelenting encouragement, valuable insights, wise counsel and friendly ear whenever I needed it.

To my family, I offer my heartfelt thanks for your unwavering support, encouragement and patience. Your presence in my life has been a constant source of strength and motivation.

Contents

Declaration . . . .

Approval i

Dedication ii

Acknowledgement iv

List of Figures viii

List of Figures xi

List of Tables xi

List of Tables xii

Acronyms xiii

Acronyms xiv

Abstract xv

1 Introduction 1

1.1 Background 1

1.1.1 Tuberculosis 2

1.1.2 Hepatitis C 5

1.1.3 Co-infection of Tuberculosis and Hepatitis C 7

1.1.4 Mathematical Models in Infectious Disease Epidemiology 9

1.2 Statement of the Problem 10

1.3 Objectives of the Study 11

1.3.1 Main objective . . . .
1.3.2 Specific Objectives . . . .
1.4 Scope of the Study . . . .
1.5 Significance of the Study . . . .
1.6 Justification of the study . . . .
1.7 Structure of the Thesis . . . .

2 Literature Review . . . .
2.1 Introduction . . . .
2.2 Review of Tuberculosis Models . . . .
2.3 Review of Hepatitis C Models . . . .
2.4 Review of Optimal Control Analysis Models . . . .
2.5 Review of Co-infection models . . . .

3 Mathematical Modelling of TB-HCV Co-infection Dynamics with No Intervention
3.1 Introduction . . . .
3.2 Model Description . . . .
3.2.1 Compartmental TB-HCV Co-infection Model . . . .
3.2.2 Mathematical Model for TB-HCV Co-infection Dynamics . . . .
3.3 Analysis and Results of the Model . . . .
3.3.1 Positivity and Boundedness of Solutions . . . .
3.3.2 Existence of Equilibrium Points and their Stability based on the Basic Reproductic
Number . . . .
3.3.3 Sensitivity Analysis . . . .
3.4 Numerical Simulations . . . .
3.5 Discussion and Conclusion . . . .

4 Analysis of a Mathematical Model on the Dynamics of TB-HCV Co-infection with Medication . . . .
4.1 Introduction . . . .
4.2 Description and Formulation of the Model . . . .
4.2.1 Description of the TB-HCV Co-infection Dynamics . . . .
4.2.2 Compartmental Model Framework . . . .
4.2.3 Equations of the Model . . . .

4.3 Analysis and Results of the Model . . . .
4.3.1 Positivity and Boundedness Properties of Solutions in TB-HCV Co-infection Dynamics with Medication . . . .
4.3.2 TB-only sub model with Medication . . . .
4.3.3 TB Endemic Equilibrium, E^*_{TB} . . . .
4.3.4 The HCV-only Sub model with Medication . . . .
4.3.5 HCV Endemic Equilibrium E^*_{HCV} . . . .
4.3.6 Analysis of TB-HCV Co-infection Model with Medication . . . .
4.3.7 Sensitivity Analysis . . . .
4.4 Numerical Simulations . . . .
4.4.1 Effect of Treating TB on the Co-infection Dynamics of TB and HCV . . . .
4.4.2 Effect of Hospitalization on the Co-infection Dynamics of TB and HCV . . . .
4.4.3 Role of Treatment rates, r_1, r_2 and r_3 on the Co-infection Dynamics of TB and HCV . . . .
4.4.4 Effect of Treating HCV on the Co-infection Dynamics of TB and HCV . . . .
4.5 Discussion and Conclusion . . . .

5 Analysis of Optimal Control on the Dynamics of TB-HCV Co-infection . . . .
5.1 Introduction . . . .
5.2 Optimal Control Problem . . . .
5.2.1 Formulation of the Model . . . .
5.2.2 Existence and Characterization of Optimal Control Solution . . . .
5.3 Numerical Results and Discussions . . . .
5.3.1 Control with a Combination of all Intervention Strategies . . . .
5.3.2 Controls Fixed on TB only . . . .
5.3.3 Controls Fixed on HCV only . . . .
5.3.4 Controls with Screen and Treat against TB and HCV . . . .
5.3.5 Controls with Prevention against TB and HCV . . . .
5.4 Discussion and Conclusion . . . .

6 Discussion, Conclusion, Recommendations and Future Work 1
6.1 Discussion . . . .
6.1.1 TB-HCV Co-infection Dynamics with no Intervention . . . .

6.1.2 TB-HCV Co-infection Dynamics with Medication . . . . . .
6.1.3 Optimal Control Management Strategy for TB-HCV Co-infection . . . . . .
6.2 Conclusion . . . . . .
6.3 Recommendations . . . . . .
6.4 Future Work . . . . . .

Appendices . . . . . .

List of Figures

3.1 A compartmental diagram for TB-HCV co-infection dynamics . . . . . .
3.2 A graph of Susceptible humans against time with only values of Susceptible varied . .
3.3 A graph of Infected humans against time with varied values of Susceptibles only . . .
3.4 A graph of Co-infected humans against time with only values of Susceptible varied . .
3.5 Simulation results showing Susceptible, mono- infected and co-infected humans against time . . . . . .
3.6 Simulation results showing Susceptible humans against time . . . . . .
3.7 Simulation results showing mono-infected humans against time . . . . . .
3.8 Simulation results showing co-infected humans against time . . . . . .
3.9 Simulation results showing TB latent humans and HCV acute humans against time with ξ_1, ξ_2, q_1 and q_2 respectively varied . . . . . .
3.10 Graphs showing humans co-infected with chronic HCV and latent TB, I_{CL}, chronic HCV and active TB, I_{CT}, acute HCV and active TB I_{aT} and chronic HCV and active TB, I_{CT} against time when β_1, β_2, τ_1 and τ_2 are respectively varied. . . . . .

4.1 A compartmental diagram for TB-HCV co-infection dynamics with treatment . . . .
4.2 A graph of Susceptible humans against time with only values of Susceptible varied . . 1
4.3 Graphs of TB infected humans against time 1
4.4 Graphs of HCV infected humans against time 1
4.5 Graphs of co-infected humans against time 1
4.6 Simulation results showing TB infectious humans, HCV acute humans, HCV chronic humans and chronic HCV-infectious TB co-infected humans against time with ξ_1 and ξ_2 respectively varied 1
4.7 Figure displaying the number of chronic HCV-infectious TB co-infected humans against time with TB treatment rate ω_1 varied 1

4.8 Simulated data displaying the number of chronic HCV-latent TB co-infected humans against time, and number of acute HCV-infectious TB co-infected humans against time with TB treatment rate ω_1 varied . . . . . .
4.9 Simulated data displaying the number of chronic HCV-infectious TB co-infected humans against time with hospitalization rate ρ varied . . . . . .
4.10 Simulated data displaying the number of chronic HCV-latent TB co-infected humans against time, and number of acute HCV-infectious TB co-infected humans against time with hospitalization rate ρ varied . . . . . .
4.11 Simulated data displaying the number of chronic HCV-latent TB co-infected humans against time, and number of acute HCV-infectious TB co-infected humans against time with HCV treatment rate r_1 varied . . . . . .
4.12 Simulated data displaying the number of chronic HCV-latent TB co-infected humans against time, and number of acute HCV-infectious TB co-infected humans against time with TB treatment rate r_2 varied . . . . . .
4.13 Simulated data displaying the number of chronic HCV-infectious TB co-infected humans against time with treatment rate r_3 varied . . . . . .
4.14 Simulated data displaying the number of chronic HCV-latent TB co-infected humans against time, and number of acute HCV-infectious TB co-infected humans against time with treatment rate r_3 varied . . . . . .
4.15 Simulated data displaying the number of chronic HCV-infectious TB co-infected humans against time with HCV treatment rate c varied . . . . . .
4.16 Simulated data displaying the number of chronic HCV-latent TB co-infected humans against time, and number of acute HCV-infectious TB co-infected humans against time with HCV treatment rate c varied . . . . . .

5.1 Effect of all intervention strategies on susceptible and TB infected populations. . . . .
5.2 Effect of all intervention strategies on HCV infectious populations. . . . . .
5.3 Effect of all intervention strategies on co-infected populations. . . . . .
5.4 Effect of controls u_1 and u_2 on susceptible and TB infected populations. . . . . .
5.5 Effect of controls u_1 and u_2 on HCV infected populations. . . . . .
5.6 Effect of controls u_1 and u_2 on co-infected populations. . . . . .
5.7 Effect of controls u_3 and u_4 on susceptible and TB infected populations. . . . . .
5.8 Effect of controls u_3 and u_4 on HCV infected populations. . . . . .

5.9 Effect of controls u_3 and u_1 on co-infected populations. . . . . .
5.10 Effect of controls u_2 and u_1 on susceptible and TB infected populations. . . . . .
5.11 Effect of controls u_2 and u_1 on HCV infected populations. . . . . .
5.12 Effect of controls u_2 and u_1 on co-infected populations. . . . . .
5.13 Effect of controls u_1 and u_3 on susceptible and TB infected populations. . . . . .
5.14 Effect of controls u_1 and u_3 on HCV infected populations. . . . . .
5.15 Effect of controls u_1 and u_3 on co-infected populations. . . . . .

List of Tables

3.1 Variables used in the TB-HCV co-infection dynamics . . . . . .

3.2 Parameters used in the TB-HCV co-infection dynamics and their description . . . . .

3.3 Sensitivity indices of R_I and R_H with respect to parameters . . . . . .

3.4 The TB-HCV Co-infection Model Parameter values . . . . . .

4.1 Description of Parameters used in the TB-HCV Model Formulation . . . . . .

4.2 Sensitivity indices of R_{TB} and R_{HCV} with respect to parameters . . . . . .

4.3 The TB-HCV Co-infection Model Parameter values . . . . . .

ABBREVIATIONS AND ACRONYMS

AIDS	Acquired Immunodeficiency Syndrome
BCG	Bacillus Calmette-Guerin
CINAHL	Cummulative Index to Nursing and Allied Health Literature
COVID-19	Coronavirus disease of 2019
DAA	Direct-acting antiviral
Dots	Directly observed treatments
ELISA	Enzyme-Linked-Immunoassay
EMBASE	Excepta Medica database
HBV	Hepatitis B Virus
HCV	Hepatitis C Virus
HIV	Human Immunodeficiency Virus
HPV	Human Papillomavirus
HRP	Harm Reduction Programme
IFN	Interferon-$\alpha - 2b$
ISI	Institute for Scientific Information
MDR	Multidrug-resistant
MEDLINE	Medical Literature Analysis and Retrieval System Online
Mtb	Mycobacterium tuberculosis bacteria
PWID	People Who Inject Drugs
QALYs	Quality-adjusted life years
R_0	Basic reproduction number for TB-HCV co-infection
R_H	Basic reproduction number for HCV
R_T	Basic reproduction number for TB
R_{TH}	Effective reproduction number for TB-HCV co-infection
R_{HCV}	Effective reproduction number for HCV
R_{TB}	Effective reproduction number for TB

ABBREVIATIONS AND ACRONYMS

RNA	Ribonucleic acid
SVR	Sustained Viral Response
TB	Tuberculosis
VE	Varying-effectiveness
WHO	World Health Organisation

ABSTRACT

Tuberculosis (TB) and hepatitis C (HCV) impose substantial burdens on global health, significantly impacting morbidity and mortality worldwide. The high prevalence of TB and HCV makes co-infectio with both conditions a common occurrence. Existing mathematical models have not adequately accounted for the dynamics of TB-HCV co-infection. One-quarter of the world's population harbours latent TB infection. The chronic stage of HCV infection is characterized by its prolonged duration often involving asymptomatic yet infectious individuals. This necessitates an in-depth examination which has yet to be thoroughly explored. This study develops and analyses mathematical models to investigate the dynamics of TB-HCV co-infection with the aim of optimizing combination therapy strategies for effective management and control of both diseases. Stability analysis of equilibrium points was carried out and the effective reproduction number indicated that TB has a dominant role in TB-HCV co-infection dynamics, regardless of therapeutic interventions. Numerical simulations reveal that over time, increasing the rates at which individuals in co-infected classes are identified and put on TB and HCV treatment, decreases the incidence of TB and HCV infections among the population. Sensitivity analysis reveals that TB/HCV rate of human-to-human contact between the infected individuals and susceptible population and the likelihood of a contact resulting in TB/HCV transmission are equally likely to result into increased TB/HCV infections. Mathematical analysis shows that an integrated treatment strategy, combining pharmacological interventions with public health measures, optimises TB-HCV co-infection management. The study recommends that effective TB-HCV co-infection management requires an integrated care paradigm with concurrent treatmen and regular monitoring. Additionally, scaling up comprehensive screening and testing programme to facilitate early diagnosis, implementing multifaceted care models that address the complex need of co-infected individuals, and launching public awareness campaigns to reduce stigma and promote timely diagnosis and treatment adherence, ultimately optimizing patient outcomes and public healtl responses.

Key Words: Tuberculosis, Hepatitis C, Co-infection, Effective reproduction number, Mathematica model.

Chapter 1

Introduction

1.1 Background

Despite remarkable advancements in medical technology and healthcare, infectious diseases continue to pose a significant threat to global health, with tuberculosis (TB) and hepatitis C (HCV) co-infection emerging as a major public health concern [1]. According to World Health Organisation (WHO 2022), tuberculosis (TB) is one of the top 10 causes of death worldwide, with approximately 10 million people falling ill with TB and about 1.6 million dying from the disease annually [66]. WHO stated in its 2024 report [116] that in 2023, TB returned to being the world's leading cause of death from a single infectious agent, following 3 years in which it was replaced by coronavirus disease (COVID-19), and caused almost twice as many deaths as HIV/AIDS. In the same report, more than 10 million people continue to fall ill with TB every year with 6.0 million men, 3.6 million women and 1.3 million children, and the number has been rising since 2021. Following infection the risk of progressing to infectious TB disease is highest within the initial two-year period, with an estimated 5% likelihood, thereafter declining substantially [119]. Of the total number of people who develop TB disease each year, about 90% are adults, with more cases among men than women. The disease typically affects the lungs (pulmonary TB) but can affect other parts of the body as well [120].

Globally, an estimated 58 million people have chronic hepatitis C virus infection, with about 1.5 million new infections occurring per year [5]. There are an estimated 3.2 million adolescents and children with chronic hepatitis C infection. WHO (2023) [117], reports that approximately 1.3 million people die from hepatitis C each year, mostly from cirrhosis and hepatocellular carcinoma (primary liver cancer).

Infectious diseases are the result of a disharmonious ecological interaction between a microbia infectious agent (bacteria, fungi, parasites, or viruses, except for prions that are infectious proteins and a host. The dynamics in this interaction is subjected to the modulatory influence of severa factors, such as the environment, the biological properties of the pathogens and the host susceptibilitie to disease. In some cases, the influence of behavioural, cultural, and social patterns that can enhance or mitigate the host's exposure to the disease sources and consequently its transmission in the population do affect the dynamics of the infection [37]. In this sense, the connection between the above-mentioned factors is critical for a better understanding of the transmission patterns to support the development of effective strategies of control, health assistance, and policies [38].

Some infectious diseases such as Tuberculosis and Hepatitis C can be controlled and eradicated in most cases by antimicrobial drugs, as well as prevention by vaccination, proper hygienic sanitary and prophylactic measures. However, they also present great unpredictability regarding their epidemiolog magnitudes in the population. This is due to the biological evolution of infectious agents agains therapeutic drugs along with constant social and environmental changes intrinsic to the continuous and unstoppable process of globalization and urbanization [39, 40].

1.1.1 Tuberculosis

Tuberculosis (TB) is a bacterial infection that usually starts in the body of a susceptible person as a result of infection by *Mycobacterium tuberculosis* bacteria (Mtb). The disease is primarily transmitted when a person with infectious TB disease in the lungs coughs, sneezes, or talks, releasing droplet nuclei that contain *Mycobacterium tuberculosis.* These droplets can be inhaled by other persons potentially leading to infection. The common symptoms of TB include coughing blood, fever and weight loss [14]. Once infected, the individual will first undergo a period without visible clinica symptoms, called latent TB infection. The latent period is the timespan from the point of infection to the beginning of the state of infectiousness, which may last for weeks, months or the entire lifetime of the infected individual [82]. Latently infected people are asymptomatic and do not transmit the disease, but may progress to infectious (active TB) after a latency period [15]. The majority of these latently infected individuals live in developing countries where they are exposed to multiple TB risk factors. The risk of infection following TB exposure is primarily governed by exogenous factors This is determined by an intrinsic combination of the infectiousness of the source case, proximity to

contact and social and behavioural risk factors including smoking, alcohol, and indoor air pollution. In settings with increased chances of social mixing (together with overcrowding) transmission will be high. Similarly, delays in diagnosis within the healthcare system can prolong exposure to infectious individuals. Factors that increase the progression of infection to disease are primarily endogenous (host related). Persons with lowered immunity such as those with Human Immunodeficiency Virus, diabetes, immune disorders, end-stage renal disease, those on drugs that suppress immunity, young children, pregnant women among others are at a higher risk of contracting the disease [61]. Alcohol, malnutrition, tobacco smoke and indoor air pollution are also factors which impact a larger section of the population and accelerate progression to TB disease [46].

Several tests are used to diagnose tuberculosis, depending on the type of suspected TB. Diagnosing pulmonary TB requires a chest X-ray to look for changes in the appearance of your lungs that are suggestive of TB. Extrapulmonary TB, which is one outside the lungs requires a Computed Tomography (CT) scan, Magnetic Resonance Imaging (MRI) scan or ultrasound scan of the affected part of the body. Urine and blood tests could also be done as well as a biopsy, where a small sample of tissue or fluid is taken from the affected area and tested for TB bacteria.

Effective drug treatments were first developed in the 1940s. The latest WHO guidelines published in 2022 [66] include a strong recommendation for a 6-month regimen of isoniazid (H), rifampicin (R), ethambutol (E) and pyrazinamide (Z) for people with drug-susceptible TB (both pulmonary and extrapulmonary): all four drugs for the first two months, followed by H and R for the remaining 4 months. They also include new recommendations that people aged 12 years and older with drug-susceptible pulmonary TB may be treated with a 4-month regimen of rifapentine (P), H, Z and moxifloxacin (M), and that children and adolescents between 3 months and 16 years of age with non-severe TB (and without suspicion or evidence of resistance to R and H) may be treated with a 4-month regimen (2 months of H, R, Z and sometimes also E, followed by 2 months of H and R). Treatment success rates of at least 85% for people enrolled on the 6-month regimen are regularly reported to WHO by its 194 Member States. Nonetheless, inability to comply with the medication may lead to the emergence of drug-resistant TB [16, 116].

Various control interventions are available for TB prevention and treatment. Vaccination with *Bacillus Calmette-Guérin* (BCG) is the most preferred method of preventing TB which is used

to protect the susceptible individual from contracting the disease and subsequently prevent further dissemination of the infection [81]. However, the epidemiological framework for the prevention and care of TB is based on what is currently known about its transmission, the risk of developing infectious TB following infection and the effect of various interventions on these processes. Interventions for the prevention and management of TB ideally should encompass measures to: reduce exposure to Mycobacterium tuberculosis , identify all infected persons and provide preventive therapy to limit progression to active TB disease, especially for those persons at risk for this outcome, identify early, people with active TB and provide effective treatment to ensure relapse free cure, reduced risk of acquired drug resistance and prevention of long term morbidity from TB [85, 86, 87, 88]. These interventions need to be applied in the context of the health care system, preferably under the umbrella of universal health coverage and with the right level of political commitment which then leads to the mobilization of adequate financial resources to support care and prevention of the disease. Reactivation of TB in an exposed person (latently infected individuals) can be controlled through a control effort known as "case finding", which involves the monitoring action by public health workers to find and treat the exposed individuals to stop them from becoming infectious. Furthermore, the development of drug-resistant TB can be prevented by employing intervention program referred to as "case holding". The case holding control effort represent the interventions made by health workers to ensure adherence to the proper treatment of the infected people [16].

Despite the existence of treatment and vaccine, it is estimated that one-quarter of the world population serves as TB reservoirs. Individuals living in rural areas, mainly in developing countries, and in general below the poverty line, disproportionately contribute to the documented TB burden [18]. Data has shown that there is a strong association between poverty and TB, primarily in economically underprivileged countries [19]. According to WHO report, about 9.6 million people developed symptomatic TB infections resulting in about 1.5 million TB-associated deaths in 2019 [17]. In 2022, the WHO [116] estimated that the TB incidence in Africa was 2,780,000 with the incidence rate of about 233 per 100,000 population, while Uganda had 94,000 cases, translating to 198 per 100,000 population. TB mortality was estimated at 1,900 among HIV-negative persons, with an additional 2,800 death among people living with HIV. In the same report, Uganda is mentioned among the 30 high TB burden countries. Finally, the number of people acquiring infection and developing disease (and in turn the number of deaths caused by TB) can also be reduced through multisectoral action to address TB determinants such as poverty, undernutrition, HIV infection,

smoking and diabetes [116].

1.1.2 Hepatitis C

Hepatitis C virus (HCV) belongs to the Hepacivirus genus within the Flaviviridae family that also includes yellow fever virus, West Nile virus, and dengue virus. HCV is an enveloped and positive-strand ribonucleic acid (RNA) virus [62]. HCV is a blood-borne virus and is transmitted from infected person to non-infected person via exposure to infected blood, such as through intravenous drug use, blood transfusion, vertical transmissions or congenital (mother-to-child), organ transplant, or through sexual contact [68]. Originally, it was believed that most frequent routes of transmission of HCV was blood transfusion and intravenous drug abuse but recent epidemiological studies suggest the main route of HCV transmission is parental [11]. However, 90% intravenous drug users are at highest risk of getting HCV infection such as those who require multiple blood transfusions and blood products (hemophiliacs) or those who go through major surgery [12, 13].

Hepatitis C is a predominant cause of chronic liver complications. It is estimated that one third of the infected patients develop steatosis, hepatic cirrhosis (scarring of the liver) and liver cancer [1]. Hepatitis C is an asymptomatic infection and the patient remains unaware, but continuous fluctuation in liver enzymes may lead to hepatic injury [4]. The risk of progression to different disease stage may vary for HCV infection. For instance, a guideline developed for HCV infection epidemiology, treatment, and prevention among Persons Who Inject Drugs (PWID) shows that for every 100 people infected with HCV, 75–80%, 60–70%, and 5–20% will develop chronic infections, chronic liver diseases, and cirrhosis, respectively, and 1–5% will die of cirrhosis or liver cancer [83]. Symptoms of HCV can take decades to appear, and because of this about half of people with HCV do not know they are infected [60]. However, the incubation period for HCV ranges from 2 weeks up to six months [49]. The majority, about 80%, of HCV-infected individuals do not show any symptoms. The HCV is cleared spontaneously without any treatment from 30% of infected individuals within 6 months of infection, and the remaining develops chronic HCV infection [54, 68]. The Global Health Sector strategy on viral hepatitis set goals to be achieved by 2030 to eliminate HCV as a public threat by a 90% and 65% reduction in global incidence and mortality, respectively [65]. Hepatitis C virus infection is a major public health concern particularly in African countries, which have the highest prevalence rates of HCV in the world (1–26%) [3]. HCV is more prevalent in developing countries than in developed ones due to lack of healthcare facilities, poor prognosis

and high cost of the available treatments [3]. According to the 2024 WHO Global Hepatitis Report [125], the burden of HCV remains a significant public health challenge globally with approximately 50 million people worldwide living with chronic HCV infection, representing about 0.7% of the global population. Particularly in sub-Saharan Africa, an estimated 11 million people are living with HCV, with a prevalence rate of approximately 1%. The region also recorded about 1.2 million new hepatitis infections and 125,000 hepatitis-related deaths in 2022, a substantial proportion of which were attributable to HCV [125]. At the regional level, a recent systematic review and meta-analysis indicated that the seroprevalence of HCV in East Africa is approximately 2.71%, with around 54.8% of those seropositive being viraemic, indicating active infection [126]. Among high-risk populations such as people who inject drugs (PWID), the prevalence is significantly higher, reaching 20.6% [127]. Despite of all therapeutic interventions, hepatitis C and its associated causes are responsible for about 1.3 global deaths annually [3, 116]. Several HCV studies have been conducted in Uganda, most of them clinical, including children with sickle cell anaemia, patients in medical emergency units, and HIV infected patients [118, 119]. These studies have shown an HCV antibody prevalence varying from 0 to 7%, and viremia ranging from 2 to 3%. An initial study performed among blood donors using radio immunoblot assay (RIBA) showed an antibody prevalence of 4.1% but this study was conducted in one region and could not establish if samples that tested positive had chronic HCV infection as nucleic acid testing (NAT) was not done [120]. According to the study conducted by [128], the estimated national prevalence of chronic HCV infection (HCV RNA positive) in Uganda is 0.75%. These figures highlight the urgent need for targeted HCV screening, diagnosis, and treatment strategies to meet the WHO's target of eliminating viral hepatitis as a public health threat by 2030.

Detection of antibody against hepatitis C (anti-HCV) by Enzyme-Linked Immunoassay (ELISA) test is the initial step in diagnosis of HCV infection and it is more than 99% sensitive and specific [8]. Polymerase Chain Reaction (PCR) is the second main step in the analysis of chronic HCV infection and exposure of virus is usually detectable within 7 to 21 days [9, 10]. Liver biopsy is also an important parameter in diagnosis of chronic HCV infection [2, 10].

Several treatment options of HCV exist such as using antivirals like zepatier, mavyret, ribavirin and many more, intended to clear the virus from your body. The goal of treatment is to have no hepatitis C virus detected in your body at least 12 weeks after one completes treatment. However, infection with HCV takes long to manifest unlike infection with TB. Therefore, most of the individuals infected

with HCV may not be aware that they are infected until many years later [66], and thus would not seek for treatment. Screening, diagnosis and treatment of HCV infected individuals remains a global challenge. Globally, in most countries there is: lack of prioritization, political will and hence lack of dedicated budgets or programmes for hepatitis C [71]. According to the Global hepatitis report of 2021 [64], it was revealed that globally, between 2015-2019, of the 57.8 million people living with HCV, only 26% had been tested for HCV and knew their status (Africa had the lowest proportion diagnosed of 6%); 7% started treatment; and cumulatively, 7.7% had ever received HCV treatment with direct-acting antiviral drugs. The WHO estimates that during 2022, the percentage of persons estimated to have hepatitis C who were diagnosed and treated were 36% and 20% respectively. Unlike in developed countries, where it is recommended that all TB infected patients should be screened for HCV on entry into the healthcare system; in most resource limited countries in Sub-Saharan Africa, there is no mandatory HCV screening even among TB infected individuals who are under health care. This is due to the high HCV screening and treatment costs [7]. However, HCV screening is only recommended when investigating whether HCV is the possible cause of liver disease among TB infected patients [7].

There are several interventions that can help to reduce the risk of virus infection, such as controlling injectors, proper sterilization and disinfection, screening of blood and blood products, media campaign etc. As hepatitis C virus infection is not preventable by vaccination, WHO urges member states to act to improve surveillance, prevention, and access to screening and treatment at the national and regional levels [5]. In addition, media campaigns may be carried out for the public to gain knowledge about hepatitis C, and its potential to become a pandemic. Due to the great diversity in prevalence and modes of transmission, accurate epidemiological information on HCV infections is urgently needed to guide national and regional plans for prevention, treatment, and reduction of complications of the infection [5].

1.1.3 Co-infection of Tuberculosis and Hepatitis C

A co-infection is the simultaneous infection or colonisation of the same host with two or more different organisms or different strains or serotypes of the same organism, leading to co-existence of organisms or strains within the host or at population level. Both TB and HCV are threatening infectious diseases and they constitute major health problems, particularly in the endemic countries. Co-infection with tuberculosis (TB) and hepatitis C virus (HCV) is a significant clinical and public-health challenge,

particularly in high-prevalence regions as it may cause serious health hazards and place a significant bio-burden on the community.

Both TB and HCV infections are prevalent worldwide, with high co-infection rates in certain regions especially among vulnerable populations like prisoners, HIV patients, and injection drug users Studies have shown that TB-HCV co-infection is a significant public health concern, with a prevalence ranging from 2% to 30% in different populations. In some countries, up to 30% of TB patients are also infected with HCV [84]. Both TB and HCV infections weaken the immune system, making individuals more susceptible to co-infection. TB infection can suppress the immune system, making it harder for the body to fight off HCV. Conversely, HCV infection can weaken the immune system increasing the risk of TB reactivation. Co-infection can complicate diagnosis, as symptoms may overlap or mask each other. Screening for both TB and HCV is crucial in high-risk populations Humans infected with TB tend to register more new cases of HCV chronic infection than the general population which increases the risk of the occurrence of drug-induced hepatotoxicity [41, 84] and it is a well-known independent risk factor for the development of drug induced hepatotoxicity [42]. HCV chronic infection makes the already complex management of multidrug-resistant TB (MDR-TB) patients even more difficult.

Tuberculosis co-infection with hepatitis C activates latent tuberculosis, increases the risk of mortality and drug-induced liver injury [20]. Moreover, liver damage induced by HCV increases the risk of anti-TB drug-induced hepatotoxicity. This is because liver toxicity is a common side effect of anti-TB drugs and this leads to increased complexity in the treatment of TB-HCV patients [20, 21] Co-infection requires careful management, as TB treatment can affect HCV treatment outcomes and vice versa. Healthcare providers must balance treatment regimens to address both infections effectively. Co-infection is associated with poorer treatment outcomes and higher mortality rates compared to single infections. Delayed diagnosis and inadequate treatment can worsen outcomes Integrated prevention and control strategies, including screening, testing, and treatment, are essential for managing TB and HCV co-infection. Harm reduction programs, like needle exchange and substance abuse treatment, can reduce HCV transmission among injection drug users.
Generally, the prevalence of TB infection in HCV patients or otherwise has not been extensively analyzed. Although co-infection with TB and HCV is probably very common, understanding how the two infections interact could be of great importance for the control of both diseases, yet few

mathematical studies have been conducted on this potential association. Therefore, this study intends to formulate and analyse mathematical models that explain transmission and control dynamics of TB and HCV co-infection.

1.1.4 Mathematical Models in Infectious Disease Epidemiology

Epidemiology is a discipline which deals with the study of infectious diseases in a population. It is concerned with all aspects of epidemic, for example spread, control, vaccination strategy etc. Mathematical modelling is the process of creating a simplified mathematical representation of a real-life phenomenon by use of functions and equations. The aim of epidemic modelling is to understand and if possible control the spread of the disease. With mathematical models, we are able to generate a concrete background upon which we can build experiments and formulate hypotheses. In healthcare settings, mathematical modelling serves as a tool for investigating complex phenomena, obviating the need for unethical experimentation involving human subjects. Mathematical models are used to predict disease transmission, total population infected or will be infected, the duration of an epidemic, control measures and persistence of the disease. In addition, mathematical models are used for various epidemiological parameter estimation such as the reproduction number, R_0. Mathematical models are very crucial in the formation and assessment of the effectiveness of the disease prevention and control strategies.

In this study, deterministic models are used to investigate the dynamics of TB-HCV co-infection because of their simplicity. Compartmental mathematical models shall be used to describe the dynamics of the disease. In these models, the population shall be divided into compartments and the variables shall be used to denote populations in the different compartments. The interactions between these compartments shall be used to explain the way an individual gets infected and how the infection is transmitted. Ordinary differential equations shall be used to relate the interactions between the variables.

1.2 Statement of the Problem

The study of co-infections is critical for understanding how the two diseases are related, and how prevention and treatment efforts can be most effective. Mathematical models can provide insight into the complicated infection dynamics, and into effective control measures. TB disease can be controlled and cured, however, it continues to be a major health problem in the world and is now one of the top ten causes of death and the leading cause of death from a single infectious disease agent. In 2019, approximately 10 million people contracted TB resulting in about 1.4 million fatalities [34]. In 2023, an estimated 10.8 million people fell ill with TB worldwide, including 6.0 million men, 3.6 million women and 1.3 million children [116]. Chronic infection with hepatitis C virus (HCV) is prevalent (2 to 15%) throughout the world; 20 to 30% of infected people may develop cirrhosis and 1 to 3% may develop liver cancer [7]. HCV infection can cause liver damage, which may affect the metabolism of TB medications, leading to reduced efficacy or increased toxicity [20]. The WHO estimates that during 2022, about 1.0 million people were newly infected with hepatitis C virus (HCV). Nearly 50 million people have chronic HCV which causes approximately 1.3 million deaths each year due to liver disease and cancer [117]. TB and HCV continue to pose a great threat in the Sub-Saharan Africa, with their death rate and prevalence on the rise, together they accounted for more than 2.0 million deaths worldwide in 2019 [6, 17]. Such alarming statistics may retard the milestones so far achieved in meeting the Sustainable Development Goal 3 whose target is to end the epidemics of AIDS, tuberculosis, malaria and neglected tropical diseases and combat hepatitis, water-borne diseases and other communicable diseases by 2030.

Understanding the complex dynamics between TB and HCV co-infection is crucial for developing effective management and treatment strategies to address this significant public health concern. Therefore, this study intended to formulate and analyse mathematical models and use numerical solutions to explain TB and HCV co-infection dynamics, by determining the role of dual treatment of TB and HCV on the dynamics of the co-infection. By incorporating optimal control strategies, the model enabled the investigation of optimal management scenarios for TB-HCV co-infection, ultimately informing public health strategies.

1.3 Objectives of the Study

1.3.1 Main objective

The main objective of this study was to formulate and analyse mathematical models for the dynamics of TB and HCV co-infection.

1.3.2 Specific Objectives

The specific objectives of the study were to;

(i) analyse the transmission dynamics of TB and HCV co-infection using a mathematical model so as to find the conditions for the disease control.

(ii) determine the synergistic effects of dual therapy on TB-HCV co-infection progression.

(iii) investigate the optimal strategy in management of TB-HCV co-infection.

1.4 Scope of the Study

The study examined the dynamics of pulmonary tuberculosis and hepatitis C virus co-infection. Deterministic mathematical models for tuberculosis and hepatitis C virus co-infection were developed to provide an in-depth look at the diseases. The models examined the dynamics of the co-infection without treatment and the role of treatment on the dynamics of TB-HCV co-infection. The study was further extended to incorporate optimal control analysis so as to find the best strategies to the management of the co-infection.

1.5 Significance of the Study

The outcomes of this study shall help the government and policy makers to establish policies, programmes and optimal plan on how to control the diseases. The study shall help health workers on the front line in the control of the diseases quantify the effect of the diseases and set strategies for treatment and other control measures. To the researcher, this study shall act as a base for further research on the co-infection dynamics of TB and HCV. This study shall also add to existing body of knowledge on mathematical application in the field of epidemiology.

1.6 Justification of the study

TB and HCV infections present a significant burden to global health. The dual epidemics of TE and HCV have a devastating impact on global health outcomes, driving high rates of morbidity and mortality. TB is a complex disease that requires a long treatment period, making it difficult to manage and control. In many resource-poor settings, access to healthcare services, including TB diagnosis and treatment, is limited. The presence of HCV co-infection in TB-infected individuals substantially increases their risk of death, complicating TB management. TB medication, such as isoniazid and rifampicin can be hepatotoxic and HCV co-infection can increase this risk, leading to liver damage or failure, hence increasing liver-related morbidity and mortality. A notable characteristic of HCV infection is that it is not preventable by vaccination, unlike other types of hepatitis. Advances in HCV treatment have led to the development of direct-acting antiretroviral (DAA) medications, which offer improved efficacy compared to traditional interferon-based therapies. Despite its high prevalence and significant disease burden, HCV surveillance remains woefully under addressed, with screening, diagnosis and treatment of infected individuals posing a major global health challenge. Worldwide, hepatitis C remains a low priority in most countries, resulting in inadequate funding and programming to address the disease [115]. The high likelihood of HCV infection progressing to chronic disease, rather than being naturally cleared, underscores the importance of addressing this infection as a significant public health concern. Given the asymptomatic progression and lack of a vaccine for HCV, a neglected disease worldwide, and its common co-infection with TB, this thesis investigated the dynamics of TB-HCV co-infection to inform evidence-based control strategies.

1.7 Structure of the Thesis

This thesis develops and analyses mathematical models to simulate the dynamics of TB-HCV co-infection under different control interventions. The thesis is organized as follows: Chapter 2 provides a comprehensive review of existing literature on TB, HCV and TB-HCV co-infection. Chapter 3 introduces a deterministic model designed to investigate the dynamics of TB-HCV co-infectio in absence of treatment. Chapter 4 develops a deterministic model to investigate the dynamics of TB-HCV co-infection under the presence of treatment for both diseases. The model in Chapter 4 is an extension of the model presented in Chapter 3, with additional components to account for treatment of both TB and HCV. The model is employed to evaluate the impact of treatment on TB-HCV co-infection. Chapter 5 focuses on the development of an optimal control model to

determine the most effective strategies for managing TB-HCV co-infection. In Chapter 6, we discuss the implications of the findings, summarize the key conclusions, recommendations for addressing TB-HCV co-infection and outline potential avenues for future research.

Chapter 2

Literature Review

2.1 Introduction

This Chapter provides a comprehensive review of existing mathematical models that investigate the dynamics of TB, HCV and TB-HCV co-infection, highlighting their strengths, limitations and contributions to our understanding of this complex disease interaction. By synthesizing the current state of knowledge in this field, this review aims to identify gaps in existing research, inform the development of our models, and ultimately support the design of effective control strategies for mitigating the burden of TB-HCV co-infection.

2.2 Review of Tuberculosis Models

The first TB model for the transmission dynamics of TB was developed by Waaler and Anderson [26], who used a mathematical model to study the epidemiology of TB. The model had three compartments: non-infected (susceptible), infected non-cases (latent TB), and infected cases (infectio His model illustrated how it could help in predicting the trend of TB in a given situation, either spontaneously or under influence of specific control programs. The model emphasized in particular that it would be profitable in evaluating specific control programs by reflecting their interference in the natural trend of tuberculosis in the controlled area.

Trauer, *et al.* [27], used a mathematical model to simulate TB transmission in the highly endemic regions of the Asian-pacific. Their findings indicate that their model can not be calibrated to the estimated incidence rate without allowing for re-infection during latency and that even in the presence

of a moderate fitness cost and a lower value of the basic reproduction number R_0, Multidrug-resistan (MDR) TB becomes the dominant strain at equilibrium. Improved treatment of drug susceptible TI does not result in decreased rates of MDR TB through prevention of the new resistance but rathe results in a modest increase in MDR TB.

Castillo-Chavez, *et al.* [28], focused their study on an age-structure model for the disease transmissio dynamics of TB in populations that were subjected to a vaccination program. They first showed that the infection-free steady state is globally stable if the basic reproductive number R_0 is below one, and that an endemic steady state exists when the reproductive number in the presence of vaccine is above one. They then applied the theoretical results to vaccination policies to determine the optimal age or ages at which an individual will be vaccinated.

Kasereka *et al.* [29], analysed and simulated a mathematical model of the dynamics of pulmonary TB with eight compartments that included groups of individuals lost to follow-up and transferred. Results obtained showed that lost to follow-up and transferred individuals constitute a risk, but less than the cases carrying germs. That is, if some people are lost to follow-up and/or transferred (not followed), the number of these individuals who are untreated have an impact on the incidence of the disease but negligible compared to people with latent TB.

Mengistu *et al.* [33], investigated the dynamical behaviour of a TB disease model with vaccination and a saturated incidence rate. In their model, they divided the total population into four compartments, namely, susceptible, high risk latent, infective, and low-risk latent population. For the proposed model, two equilibria, the disease-free equilibrium and endemic equilibrium, are derived and their stability determined. They also found the basic reproduction number, which helps to determine the dynamical behaviour of the model. They recommend early detection and isolation of infectious people, conducting health campaigns and educating the community, screening of high-risk exposed individuals, and the treatment of latent TB as strategies to control and eradicate TB from the community. At the same time, they realised that *Bacillus Calmette-Guérin* (BCG) vaccine plays an important role in the prevention of the disease, and immunization of the children should be continued.

Porco *et al.* [90], presented time-dependent uncertainty and sensitivity analyses in order to quantitatively understand the transmission dynamics of TB epidemics in the absence of treatment. The time-dependent

uncertainty analysis enabled them to evaluate the variability in the epidemiological outcome variable of the model during the progression of a TB epidemic. Calculated values (from the uncertainty analysis) for the disease incidence, disease prevalence, and mortality rates were found to be approximately consistent with historical data. The time-dependent sensitivity analysis revealed that only a few of the model's input parameters significantly affected the severity of a TB epidemic; these parameters were the disease reactivation rate, the fraction of infected individuals who develop TB soon after infection, the number of individuals that an infectious individual infects per year, the disease death rate, and the population recruitment rate. Their analysis demonstrates that it is possible to improve the understanding of the behaviour of TB epidemics by applying time-dependent uncertainty and sensitivity analysis to a transmission model.

Zhao *et al.* [91], proposed a susceptible-exposed-infectious-recovered (SEIR) epidemic model with age groupings, involving three categories: children, the middle-aged, and senior to investigate the role of age on the transmission of TB in Mainland China from 2005 to 2016. They then evaluated the parameters by the Least Square method and simulated the model and it had good alignment with the reported infected TB data in Mainland China. Furthermore, they estimated the basic reproduction number R_0 of 1.7858, with an obtained 95% confidence interval for R_0 of (1.7752, 1.7963) by Latin hypercube sampling, and later completed a sensitivity analysis of R_0 in terms of some parameters. The study demonstrated that diverse age groups have different effects on TB infection.

Dodd *et al.* [92], aimed at producing a global mortality burden estimate in children using a complementary approach not dependent on vital registration data. In their mathematical modelling study, they estimated deaths in children younger than 5 years and those aged 5–14 years for 217 countries and territories using a case-fatality-based approach. They used paediatric TB notification data and HIV and antiretroviral treatment estimates to disaggregate the WHO paediatric TB incidence estimates by age, HIV, and treatment status. They then applied systematic review evidence on corresponding case-fatality ratios. They later interpreted that TB is a top ten cause of death in children worldwide and a key omission from previous analyses of under-5 mortality. Almost all these deaths occur in children not on TB treatment, implying substantial scope to reduce this burden.

2.3 Review of Hepatitis C Models

Mathematical epidemiological models have been developed to assess the dynamics of HCV infection. Neumann *et al.* [22], developed a deterministic mathematical model to better understand the dynamics of hepatitis C and the antiviral effect of interferon-α-2b (IFN). Viral decline in 23 patients during therapy was analysed. The analysis indicated that the major initial effect of IFN is to block virion production or release, with blocking efficacies of 81, 95, and 96% for daily doses of 5, 10, and 15 million international units, respectively. The findings show that infection with hepatitis C is highly dynamic and that early monitoring of viral load can help guide therapy.

According to Dahari *et al.* [23], a typical therapy response shows a rapid viral decline at the start followed by a second slower decline until the virus becomes undetectable. A triphasic decline is also observed in some patients that indicate a promising initial rapid decline in viral load, followed by "shoulder phase" (slow or remains constant), and final phase of resumed viral decay. However, upon therapy cessation, approximately 50% of treated HCV infection patients exhibit a rebound of viral plateau, to pre-treatment levels that define whether, the antiviral therapy is only partially effective during treatment phase or successful in eradicating HCV infection.

Khan *et al.* [24], studied the transmission dynamics of hepatitis C and eventually formulated an optimal control strategy to prevent disease spread. A deterministic epidemic model for the spread of HCV infection, which incorporates the possibility of an isolation state, was formulated. Global analysis of the equilibrium solution was performed. The existence of a disease-free equilibrium and an endemic equilibrium was shown. The study further demonstrated that the disease-free equilibrium is globally asymptotically stable for values of the basic reproduction number $R_0 < 1$. The disease uniformly persists when $R_0 > 1$. Since endemic equilibrium point is stable, they formulated time-dependent optimal control strategies to fight HCV infection. They considered the two most effective strategies known to prevent disease spread, vaccination and isolation separately. In their conclusion, therapy along with an effective isolation strategy can greatly reduce the prevalence of HCV infection.

Ayobami *et al.* [30], formulated and analysed a mathematical model for the spread and transmission dynamics of hepatitis C using a system of first order ordinary differential equations. Treatment and other control measures were incorporated and analysis carried out on the developed model by

considering the different modes of transmitting the disease. The effective reproduction number of the model was computed and the equilibrium states were obtained and analysed for their stability relatively to the effective reproduction number. The result shows that, the disease-free equilibrium was stable and the criteria for stability of the endemic equilibrium were established. It is also shown that the model's infectious and disease-free equilibria are locally and globally asymptotically stable if $R_0 < 1$, and it is endemic equilibrium or unstable if $R_0 > 1$. Numerical simulations of the model show that the hepatitis C will be eradicated or reduced to the minimum from the proposed population in consideration if there is proper education, adequate awareness, and proper intensive treatment given at the initial phase of the disease outbreak with the proposed interventions of the model in due time.

Behzadifar *et al.* [31], conducted an investigation in Iran to assess the prevalence of HCV infection among people who inject drugs (PWID). The aim of the study was to synthesize the literature performing a comprehensive search and meta-analysis. Forty-two studies were included. 15,072 PWID were assessed for determining the prevalence of HCV infection. The overall prevalence of HCV infection among PWID in Iran was computed to be 47% (CI 95%: 39–56). The prevalence ranged between 7% and 96%. Men and subjects using a common/shared syringe were 1.46 and 3.95 times more likely to be at risk, respectively. The findings of the present study showed that the prevalence of HCV infection among PWIDs in Iran is high.

Fang *et al.* [97], developed a mathematical model to predict the impact of different HCV intervention strategies on the HCV infection burden in Chinese people who inject drugs (PWID) by 2030. A dynamic deterministic mathematical model was used to simulate the transmission of HCV among PWID in China between 2016 and 2030, using domestic data based on the real cascade of HCV infection care. They considered various intervention scenarios, including treatment regimens, harm reduction programme (HRP) coverage, enhanced testing and referral for treatment. Their study indicates that achieving WHO elimination targets is an extremely challenging goal that requires substantial improvements in HCV infection testing and treatment among PWID. The findings suggest that coordinated improvements in testing, treatment, and harm reduction programs could greatly reduce the HCV infection burden among PWID in China, and urgent policy changes are needed to integrate HCV testing and treatment into existing harm reduction programmes.

Simple models of therapy for viral diseases such as hepatitis C or human immunodeficiency virus

assume that, once therapy is started, the drug has a constant effectiveness. More realistic models have assumed either that the drug effectiveness depends on the drug concentration or that the effectiveness varies over time. Conway *et al.* [98], studied mathematically a varying-effectiveness (VE) model in the context of HCV infection. They show that while the model is linear, it has no closed-form solution due to the time-varying nature of the effectiveness. They then showed that the model can be transformed into a Bessel equation and derive an analytic solution in terms of modified Bessel functions, which are defined as infinite series, with time-varying arguments. Fitting the solution to data from HCV infected patients under therapy yielded values for the parameters in the model. They also showed that for biologically realistic parameters, the predicted viral decay on therapy is generally biphasic and resembles that predicted by constant-effectiveness (CE) models. Later, they introduced a general method for determining the time at which the transition between decay phases occurs based on calculating the point of maximum curvature of the viral decay curve. For the parameter regimes of interest, they also found approximate solutions for the VE model and establish the asymptotic behaviour of the system. It is concluded that the rate of second phase decay is determined by the death rate of infected cells multiplied by the maximum effectiveness of therapy, whereas the rate of first phase decline depends on multiple parameters including the rate of increase of drug effectiveness with time.

In Australian prisons, approximately 20% of inmates are chronically infected with hepatitis C [100], providing an important population for targeted treatment and prevention. Kwon *et al.* [99], used a dynamic mathematical model of HCV infection transmission to assess the impact of increasing direct-acting antiviral (DAA) treatment uptake on HCV incidence and prevalence in the prisons in New South Wales, Australia, and to assess the cost-effectiveness of alternate treatment strategies. They developed four separate models reflecting different average prison lengths of stay (LOS) of 2, 6, 24, and 36 months. Each model considered four DAA treatment coverage scenarios of 10% (status-quo), 25%, 50%, and 90% over 2016–2045. For each model and scenario, they estimated the lifetime burden of disease, costs and changes in quality-adjusted life years (QALYs) in prison and in the community during 2016–2045. Costs and QALYs were discounted 3.5% annually and adjusted to 2015 Australian dollars. Compared to treating 10% of infected prisoners, increasing DAA coverage to 25%, 50%, and 90% reduced HCV incidence in prisons by 9–33% (2-months LOS), 26–65% (6-months LOS), 37–70% (24-months LOS), and 35–65% (36-months LOS). DAA treatment was highly cost-effective among all LOS models at conservative willingness-to-pay thresholds. DAA

therapy became increasingly cost-effective with increasing coverage. Compared to 10% treatment coverage, the incremental cost per QALY ranged from $497-$569 (2-months LOS), -$280–$323 (6-months LOS), -$432– $426 (24-months LOS), and -$245–$477 (36-months LOS). Treating more than 25% of HCV-infected prisoners with DAA therapy is highly cost-effective. Their study shows that treating HCV-infected prisoners is highly cost-effective and should be a government priority for the global HCV elimination effort.

Elbasha, *et al.* [101], presented a deterministic model for HCV infection transmission and used the model to assess the potential impact of antiviral therapy. The model is based on the susceptible-infect (SIRS) compartmental structure with chronic primary infection and possibility of reinfection. Importa epidemiologic thresholds such as the basic and control reproduction numbers and a measure o treatment impact were derived. They found that if the control reproduction number is greater than unity, there is a locally unstable infection-free equilibrium and a unique, globally asymptotically stable endemic equilibrium. If the control reproduction number is less than unity, the infection-free equilibrium is globally asymptotically stable, and hepatitis C will be eliminated. Numerical simulation suggest that, besides the parameters that determine the basic reproduction number, reinfection plays an important role in HCV transmissions and magnitude of the public health impact of antiviral therapy. Further, they realized that treatment regimens with better efficacy holds great promise for lowering the public health burden of HCV disease.

The revolution in hepatitis C treatment through the development of direct-acting antivirals (DAAs) has generated international interest in the global elimination of the disease as a public health threat. In 2017, this led WHO to establish elimination targets for 2030. Now, evaluation of the impact of public health interventions on the global HCV epidemic and investigation whether WHO's elimination targets could be met is key. Heffernan *et al.* [102], developed a dynamic transmission model of the global HCV epidemic, calibrated to 190 countries, which incorporates data on demography, people who inject drugs (PWID), current coverage of treatment and prevention programmes, natural history of the disease, HCV prevalence, and HCV-attributable mortality. They estimated the worldwide impact of scaling up interventions that reduce risk of transmission, improve access to treatment and increase screening for HCV infection by considering six scenarios: no change made to existing levels of diagnosis or treatment; sequentially adding the following interventions: blood safety and infection control, PWID harm reduction, offering of DAAs at diagnosis, and outreach screening to

increase the number diagnosed; and a scenario in which DAAs are not introduced (ie, treatment i only with pegylated interferon and oral ribavirin) to investigate the effect of DAA use. They alsc explored the effect of varying the coverage or impact of these interventions in sensitivity analyse: and also assessed the impact on the global epidemic of removing certain key countries from thc package of interventions. In their findings, reducing global burden depends upon success of preventior interventions, implementation of outreach screening, and progress made in key high-burden countrie: including China, India, and Pakistan. In conclusion, further improvements in blood safety anc infection control, expansion or creation of PWID harm reduction services, and extensive screening for HCV with concomitant treatment for all are necessary to reduce the burden of HCV infection. These findings should inform the ongoing global action to eliminate the HCV epidemic.

The main aim of antiviral treatment is to eradicate the hepatitis C which is defined as a viral RNA that is undetectable by highly sensitive methods. Until a few years ago, the combination of pegylated interferon and ribavirin (PEG/RBV) was the only treatment strategy available and the rates of viral clearance response did not surpass 50% in certain genotypes (1 and 4) with these treatments. In 2011, the first direct acting antiviral agents (DAA), boceprevir and telaprevir were approved for treatment of genotype 1, in combination with traditional dual therapy which accomplished to increase the rates of sustained viral response (SVR) in both naive patients and in retreated patients. Singh *et al.* [107], studied about newer Advances in the Management of Hepatitis C. In their study, it is revealed that with direct acting antiviral (DAAs) drugs, the management of patients with chronic hepatitis C has radically changed owing to their high rates of sustained viral response (SVR) and improved safety profile. This has led to the reduction of the risk of progression to cirrhosis and a lower incidence of complications even in established cirrhosis. It is also observed that in order to achieve elimination of hepatitis C, improvement in screening by using rapid and simple tests to diagnose HCV infection, access to antiviral treatment and reduction of new infections are essential. Other strategies include local and national screening programmes, lowering the costs of drug and developing simple management algorithms that enable unspecialized physicians and even nurses to initiate and guide treatment of HCV infection.

Nankya-Mutyoba *et al.* [121], performed a survey among blood donors across 4 regions of Uganda. Their survey found a prevalence of active HCV infection of 7.8% among donors who screened anti-HCV positive at the blood bank. The finding of 7.8% of active infections in HCV antibody

positive blood donors is high when compared to the blood bank protocol. They also identified 3 genotypes with genotype 4 as the predominant one across regions, followed by genotype 1. This finding is consistent with current data on genotype distribution within Sub-Sahara Africa, where genotype 4 is common in Eastern Africa and genotype 1 and 2 in West Africa. They identified age, region of birth and residence as well as marital status, as important factors associated to active HCV infection which could be effectively targeted for micro-elimination. These findings support the efforts to scale-up testing and linkage to care and antiviral treatment, as key steps towards elimination of the public health risk due to HCV.

2.4 Review of Optimal Control Analysis Models

Gao, *et al.* [73], extended the model of Liu and Zhang [78] by incorporating three control terms case finding, case holding (considered twice) and later applied optimal control theory to the resulting model. Optimal control strategies were proposed to minimize both the disease burden and the intervention cost. They proved the existence and uniqueness of optimal control paths and obtained these optimal paths analytically using Pontryagin's Maximum Principle. They further analysed their results numerically to compare various strategies of proposed controls. It is observed that implementation of the three controls is most effective and less expensive among all the strategies. Thus, they concluded that in order to reduce tuberculosis threat, all the three controls must be taken into consideration concurrently.

Kereyu, *et al.* [44], used a compartmental non-linear deterministic mathematical model to investigate the effect of different optimal control strategies in controlling tuberculosis (TB) disease transmission in the community. They employed stability theory of differential equations to investigate the qualitativ behaviour of the model by obtaining the basic reproduction number and determining the local stability conditions for the disease-free and endemic equilibria. They considered three control strategies representing distancing, case finding, and treatment efforts and numerically compare the levels of exposed and infectious populations with and without control strategies. The results suggest that combination of all controls is the best strategy to eradicate TB disease from the community at an optimal level with minimum cost of interventions.

Okosun *et al.* [74], considered a deterministic hepatitis C virus (HCV) model and studied the

impact of optimal control on the screening of immigrants and treatment of HCV on the transmission dynamics of the disease in a homogeneous population with constant immigration of susceptible individuals. Their investigations were about the impact of each control mechanism individually and the combinations of these strategies in the control of HCV. The costs associated with each of these strategies were also investigated by formulating the costs function problem as an optimal control problem, and then used the Pontryagin's Maximum Principle to solve the optimal control problems. They suggest the treatment of acute-infected and chronic-infected individuals control strategy be optimized where resources are scarce, because the implementation of the three strategies (combination of screening of immigrants, treatment of acute-infected and chronic-infected individuals) will imply additional cost.

Jung *et al.* [75], applied optimal control theory to a system of ordinary differential equations modelling a two-strain tuberculosis model. They sought to reduce the latent and infectious groups with the resistant-strain tuberculosis by using controls representing two types of treatments. The optimal controls were characterized in terms of the optimality system, which was solved numerically for several scenarios. Their results show how a cost-effective combination of treatment efforts (case holding and case finding) depends on the population size, cost of implementing treatments controls and the parameters of the model.

Kim *et al.* [93], developed a mathematical TB model which fitted to the Philippine data that was used to understand the transmission dynamics of TB. Different control strategies such as distancing, latent case finding, case holding, active case finding controls, and combinations thereof were investigated within the framework of optimal control theory. Their study proposed optimal control strategies for reducing the number of high-risk latent and infectious TB patients with minimum intervention implementation costs. Their results suggest that distancing control is the most efficient control strategy when a single intervention is utilized. However, full scale employment of the distancing control measure is a daunting task. Thus, this burden can be circumvented by the combination of other control interventions. The noble finding in their study is that enhancing active case finding control instead of case holding control together with distancing and latent case finding control is shown to have significant potential for curtailing the spread of TB in the Philippines.

Ullah *et al.* [94], formulated a deterministic model to study the dynamics and possible control

of TB disease. Initially, they developed the model without control variables and presented the basic mathematical analysis of the model. The stability results of the model at the disease-free case were presented when $R_0 < 1$, and further it was proven that the infection would persist uniformly when $R_0 > 1$. The model biological parameters were estimated using the confirmed TB infected cases reported in Khyber Pakhtunkhwa, Pakistan, from 2002 to 2017. Based on the estimated and fitted parameters, they obtained that $R_0 = 1.2928$. The model stability was investigated graphically when R_0 is greater or less than one. Further, the sensitivity analysis of the threshold parameter was performed in order to formulate an appropriate optimal strategy for curtailing the TB infection. Later, they developed the control model using three control variables. The existence of the optimal control problem and the necessary mathematical results for the control characterization was obtained. Finally, the simulations were presented to highlight the importance and impact of suggested control interventions on the disease dynamics. The proposed set of controls could be used for the elimination of TB infection in a community.

Choi *et al.* [95], developed a mathematical control model for the transmission dynamics of tuberculosis (TB) in South Korea on the basis of the reported active-TB and relapse-TB incidence data. In their study, optimal control theory was used to propose optimal TB prevention and control strategy and rearrange the South Korea government TB budget for the best TB elimination plan. The impact of distancing, case finding, and/or case holding controls were investigated when the number of infected and infectious individuals are minimized, while the intervention costs are kept low. The implementation of optimal control measures shows that the distancing control, such as isolation of infectious people, early TB patient detection, and educational program/campaign for healthy control is the most effective control factor for the prevention of TB transmission in South Korea.

Directly observed treatment and short course chemotherapy (Dots) strategy combines medicine care and modern health system firmly, and it has been carried out by World Health Organization (WHO) since 1997. In the struggle with TB, China promoted the process of controlling the disease actively, and the full coverage of Dots strategy had been reached. Understanding the impact of Dots strategy on the control of TB is important for designing further prevention strategy. Liu *et al.* [96], investigated the impact of control strategy on the transmission of TB in China by dynamic model. They then further discussed control for TB aiming at developing new vaccine and improving treatment. The optimal control problem, minimizing the total number of infectious individual

with the lowest cost, was proposed and analysed by Pontryagin's maximum principle. Numerical simulations were provided to illustrate the theoretical results. In their conclusion, they observed that the diagnosis and treatment of TB in China have been promoted a lot and the R_0 is reduced by the full coverage of Dots strategy. However, the R_0 in China is still greater than 1 now. The relationship between R_0 and vaccination strategy was shown. Optimal strategy aiming at exposed and infected population was suggested for further control.

Yang *et al.* [112], formulated a mathematical model to explore the impact of vaccination and treatment on the transmission dynamics of tuberculosis (TB). They developed a technique to prove that the basic reproduction number is the threshold of global stability of the disease-free and endemic equilibria. To control the spread of TB, the optimal regulations of an extended model with vaccination and treatment was proposed, and optimal control strategies for several scenarios identified. Numerical simulations of the optimal system of extended TB model indicated that the vaccination and treatment strategies are effective in reducing TB disease transmission. Especially, if the BCG vaccine works, maximum strategy during the procedure should be adopted. The simulation results of optimal control also show that a cost-effective control strategy depends on the cost of the implementation of the control.

2.5 Review of Co-infection models

Nampala *et al.* [48], studied the HIV/HBV co-infection. Mathematical models coupled with numerica simulations were used in their study with the aim of investigating the optimal combination of antiretroviral therapy (ART) in HIV/HBV co-infection. Emtricitabine, tenofovir and efavirenz is the optimal combination that maximises the therapeutic effect of therapy and minimises the toxic response to medication in HIV/HBV co-infection.

Mayanja *et al.* [54], formulated and analysed a deterministic model to study the HIV and HCV co-infection dynamics in absence of therapy. Their findings reveal that, in the long run, there is a substantial number of individuals co-infected with HIV and latent HCV. Therefore, HIV and latently HCV-infected individuals need to seek early treatment so as to slow down the progression of HIV to AIDS and latent HCV to advanced HCV.

Bhunu *et al.* [56], formulated and analysed a deterministic model of the co-dynamics of hepatitis C virus and HIV/AIDS in order to assess their impact on the dynamics of each disease in the presence of treatment. They realized that, there are more HIV-only infected individuals not yet showing AIDS symptoms and the number of dually infected individuals first increases and then declines to asymptotically low level due to full recovery from hepatitis C. In their conclusion, HCV has an ongoing prolonged negative effect on the health of the population, irrespective of their HIV status, and as such, its control should be reinforced in resource limited settings.

Bowong *et al.* [49], formulated and analyzed a deterministic mathematical model of the co-dynamics of HBV/TB co-infection. Through simulations, they mainly found that, the two diseases will co-exist whenever their partial reproductive numbers exceed unity; the increased progression rate due to exogenous reinfection from latent to active TB in co-infected individuals may play a significant role in the rising prevalence of TB and the increased progression rates from acute stage to chronic stage of HBV infection have increased the prevalence levels of HBV and TB.

Bhunu *et al.* [51], studied a TB/HIV co-infection model that considered antiretroviral therapy for the AIDS cases and treatment of all forms of TB. The thresholds and equilibria quantities for the models were determined and stabilities analysed. From their study, they conclude that treatment of AIDS cases results in a significant reduction of numbers of individuals progressing to active TB. Further, treatment of latent and active forms of TB results in delayed onset of the AIDS stages of HIV infection.

Nino *et al.* [79], conducted a study to determine whether HCV co-infection increases the risk of incident drug-induced hepatitis among patients on first-line anti-TB drug therapy. Among 326 study patients with culture-confirmed TB, 68 (21%) were HCV co-infected. A high prevalence of HCV co-infection was found among patients with TB infection. Drug-induced hepatotoxicity is significantly associated with HCV co-infection but severe drug-induced hepatotoxicity is rare.

El-Mokhtar *et al.* [32], conducted a study to evaluate the impact of HCV on the T-cell-mediated immune response to TB in co-infected patients. Sixty-four patients with active TB infections were screened for co-infection with HCV. They concluded that different subsets of TB-specific $CD4^+$ T cells in TB-HCV-infected individuals are partially impaired in early-stage HCV infection. This is

combined with increased serum IL-10 level. Such immune modulations may represent a powerful risk factor for disease progression in patients with TB-HCV co-infection.

Infection with Hepatitis C Virus (HCV) increases the hepatotoxicity of anti-tuberculosis drugs. Meysam *et al.* [80], carried out a systematic review and meta-analysis with a purpose of determining the prevalence of HCV infection in patients with TB infection. PubMed/MEDLINE, ISI/Web of Sciences, CINAHL, EMBASE, the Cochrane Library and Scopus were searched from January 2000 to March 2018. The overall prevalence of HCV in patients with TB was calculated using the random-effect model with 95% confidence interval (CI). To evaluate heterogeneity, I^2 test was used. Egger's regression test was utilized to check publication bias. Twenty-one articles were selected for the final analysis based on the inclusion/exclusion criteria. A total of 15,542 patients with TB participated in the studies. The overall prevalence of HCV infection in patients with TB was 7% [95%CI: 6-9]. Subgroup analysis revealed that diagnostic test (P=0.0039), geographical background (P=0.0076) and gender distribution (P=0.0672) were statistically significant moderators. Men had a higher risk for HCV than women (Odds Ratio, OR=2.02; 95%CI: 1.28-3.18). The results of their study highlight the importance of screening HCV in TB patients. Knowing whether HCV is present or not in these patients can be helpful in effectively treating them.

Feleke *et al.* [103], conducted a study to estimate the prevalence, determinants of hepatitis B, hepatitis C and the survival of tuberculosis patients until drug-induced hepatitis. Prospective cohort study design was implemented. The data were collected from September 2016 to May 2019. Systematic random sampling was used to select the study participants. Baseline data were collected before the patient starts directly observed treatment strategy (DOTS), the sign of liver toxicity was assessed every week. Tuberculosis treatment outcomes and WHO clinical stage was recorded at the end of 6th months. Descriptive statistics were used to estimate the prevalence of hepatitis B, hepatitis C viral infections and their effect on tuberculosis treatment outcomes. Binary logistic regression was used to identify the determinants of hepatitis B and C infections. The Kaplan Meier survival curve was used to estimate the survival of tuberculosis patient and Cox regression was used to identify the predictors of drug-induced hepatitis. A total of 3537 tuberculosis patients were followed. The prevalence of hepatitis B and C viral infection among tuberculosis patients were 15.1 and 17.3% respectively. Their results revealed that hepatitis B and C viral infection among tuberculosis patients was associated with alcohol, sex, HIV, chronic illness. The incidence density for liver toxicity among

tuberculosis patients was 843 cases per 15707 person-months and liver toxicity was determined b HIV, Hepatitis B, Hepatitis C, the severity of tuberculosis and underlying chronic illnesses. I their conclusion, decision-makers should consider incorporating screening for hepatitis B and C vira infection during tuberculosis treatment.

Musso *et al.* [104], carried out a study to evaluate if treating at the same time HCV infection and pulmonary MDR-TB is feasible and effective. In their study, they described two cases of patients with pulmonary MDR-TB and concurrent HCV chronic infection cured with DAAs at a Tertiary Infectious Diseases Hospital in Italy. During antitubercular treatment, both patients experienced a Drug-Induced Liver Injury (DILI) before treating HCV infection. After DAAs liver enzymes normalized and hepatitis C virus Ribonucleic acid (HCV RNA) was undetectable. Then antitubercular regimen was started according to the institutional protocol, drawn up following WHO MDR-TB guidelines. It was completed without further liver side effects and patients were declared cured from both HCV infection and MDR-TB. They concluded by suggesting to always considering treatment of chronic hepatitis C with DAAs as a useful intervention for reintroduction of second-line antitubercular agents in those patients who developed DILI, reducing the risk of treatment interruption when re-exposed to these drugs.

Aggarwal *et al.* [131], developed a non-linear mathematical model for HIV-TB co-infection. They introduced a time delay parameter to capture the delay in diagnosis and treatment initiation for co-infected individuals. The local stability analysis of equilibrium points was analysed in presence of delay, revealing specific conditions for hopf bifurcation to occur. Numerical simulations were carried out using different parameter sets to examine the effects of detection and treatment delays on co-infected individuals at each equilibrium point.

To assess the prevalence of HCV infection among tuberculosis patients and to investigate its impact on tuberculosis and its treatment outcome, Nageeb *et al.* [105], carried out a cross-sectional study on 500 tuberculosis patients. Socio-demographic data, clinical history and examination, clinical severity, response to drugs, laboratory and radiological investigation, Tuberculin skin test, and HCV screening were done. According to their results, HCV infection was detected among 54 tuberculosis patients (10.8%). HCV- positive patients suffered more from almost all clinical presentation than HCV- negative patients but without statistical significant difference. Tuberculin skin test induration

and reactions were more in HCV- negative patients with 17.9 ± 4.9 mm compared to 12.9 ± 2 mm in HCV positive patients. Lung cavitation and lung infiltration were the most predominant radiological finding among HCV- positive patients. Classification and Treatment (CAT) IV and modified CAT I were the most treatment regimen used in HCV- positive patients. Failure of treatment was significantly higher among HCV- positive patients (59.3%) compared to 9.9% of their counterparts. Moreover, multidrug resistance (MDR) and rifampicin resistance were significantly higher in HCV- positive group than their comparable group (31.5% and 29.6%, and 9% and 4.3% respectively). They revealed that co-infection of HCV in Patients with TB is frequent. It increases the frequency of almost all clinical presentation and had its predominant findings on laboratory and radiological investigations. Co-infection also alters the response to TB treatment and should be screened among tuberculous patients before treatment and closely monitored during treatment to detect early any drug resistance or treatment failure.

Wahid *et al.* [106], carried out a study aimed at suggesting proper management of patients co-infected with both HCV and TB. They monitored a 77-year-old female patient who visited a primary care physician for a routine follow-up because she had past history of HCV in 2011, but she was successfully treated with interferon-therapy. The patient experienced HCV relapse in 2016 but did not respond to sofosbuvir and ribavirin and it was later on confirmed that she had TB which made the treatment of HCV more challenging. According to their results, this is the first evidence that highlights sofosbuvir, daclatasvir and ribavirin as an optimal treatment regimen for patients co-infected with TB. Furthermore, it is necessary to treat TB before initiating HCV treatment because of risk of hepatotoxicity. In conclusion, co-infection of TB in HCV patients alters treatment response towards sofosbuvir, an approved anti-HCV drug with high rate of sustained virological response.

Kempker *et al.* [129], reviewed the drug metabolism of anti-TB and HCV drugs and the known potential drug-drug interactions between recommended HCV regimens and individual anti-TB drugs. They realized that rifampin is the only anti-TB drug to have been formally studied for potential drug interactions with anti-HCV direct-acting antivirals (DAAs), and existing data preclude these combinations. They however, discovered that based on known pathways of drug metabolism and enzyme effects, the combination of HCV DAA regimens with all other anti-TB drugs may be feasible. In their conclusion, pharmacokinetic studies are needed next to help move cotreatment regimens forward for clinical use among patients co-infected with TB and HCV.

Tanvi *et al.* [130], formulated a non-linear population model for HIV-TB co-infection. Their model examined how the timing of HIV treatment initiation (early or late) in TB-treated co-infected individuals influenced the incidence of Immune Reconstitution Inflammatory syndrome (IRIS). With fixed control parameters, the model analysis demonstrated the existence and local stability of disease-f and endemic equilibria. They formulated and solved an optimal control problem incorporating time-dependent parameters, using Pontryagin's maximum principle to minimize the number of infecte individuals, disease-induced deaths, and treatment costs. Numerical results suggested that implement optimal control strategies is more effective than constant treatment rates in minimizing the burden of the co-infection.

This literature review has provided an overview of the current state of modelling research on TB. HCV and TB-HCV co-infection. While significant progress has been made in understanding the individual diseases, further research is needed to develop integrated models that accurately capture the interactions between TB and HCV infections.

Tuberculosis and hepatitis C virus infections are both common infectious diseases. Although HCV infection is frequent in patients with TB, few studies have been conducted worldwide and there is still little evidence concerning this topic [105]. The TB-HCV deterministic models were rare in literature and the few existing statistical models did not explicitly address treatment effects and optimal control strategies for managing the co-infection dynamics. This was the basis for our study. In this study therefore, mathematical models of TB and HCV co-infection were developed to determine the role of dual treatment of TB and HCV on the dynamics of the co-infection. By incorporating optimal control strategies, the model enabled the investigation of optimal management scenarios for TB-HCV co-infection.

Chapter 3

Mathematical Modelling of TB-HCV Co-infection Dynamics with No Intervention

3.1 Introduction

In this Chapter, a deterministic mathematical model is developed and analysed with an aim of investigating the dynamics of TB infection as a result of HCV co-infection and vice versa in absence of treatment. Despite the availability of antibiotics, TB infected humans may not be under medication in the view of the fact that they may not have been detected or if detected, they could just choose to delay to start the antibiotics. In some developing countries like Uganda, and in general those below the poverty line, some TB infected humans may have no access to antibiotics. Others may decide to drop out since the treatment takes a long period of time and rather expensive [66]. Comparably, HCV infected humans especially in the chronic stage may be undetected and therefore cannot quest medication. Further, screening, detection and medication of HCV infected humans continues to remain a challenge globally [56]. Therefore, there is a need to investigate the TB-HCV co-infection dynamics in absence of intervention. The model intends to inform policy makers of factors that fuel the transmission of both TB and HCV infections and hence the measures that can be put to curtail the transmission rate.

3.2 Model Description

The model divides the human population into the following sub-populations; susceptible humans at a risk of contracting TB or HCV (S(t)), TB latently-infected but not infectious of TB ($I_L(t)$), TB infectious humans assumed not under medication ($I_T(t)$), Acute HCV humans without symptoms but infectious of HCV ($I_A(t)$), Chronic HCV humans with symptoms and infectious of HCV ($I_C(t)$), co-infected humans with acute HCV and latent TB, ($I_{AL}(t)$), co-infected humans with chronic HCV and latent TB ($I_{CL}(t)$), co-infected humans with acute HCV and infectious TB ($I_{AT}(t)$), and co-infected humans with chronic HCV and infectious TB ($I_{CT}(t)$), all as summarised in Table 3.1.

It is supposed that humans in the susceptible sub-group increase at a rate, Λ due to birth and immigration. All humans in different subgroups go through natural death at a constant rate. μ. Susceptible humans contract TB infection after a contact with TB infectious human at a rate, λ_T and acquire HCV infection after contact with an HCV infectious human at a rate, λ_H.

The total population size at time, t is $N(t)$ and is given by

$$N(t) = S(t) + I_L(t) + I_T(t) + I_A(t) + I_C(t) + I_{AL}(t) + I_{CL}(t) + I_{AT}(t) + I_{CT}(t). \tag{3.1}$$

The rate at which humans acquire TB infection is given by

$$\lambda_T(t) = \frac{\xi_1 q_1 \big(I_T(t) + a(I_{AT}(t) + I_{CT}(t))\big)}{N(t)}, \tag{3.2}$$

with ξ_1 the rate of human-to-human contact between the TB infected individuals and susceptible population; q_1 is the likelihood of a contact resulting in TB transmission; a is the enhancement factor for the increased risk of easily contracting TB from a dually infected individual in classes I_{AT} and I_{CT}, respectively. The parameter accounts for increased infectiousness in dually infected humans compared to those with TB only [49].

Similarly, the rate of HCV infection in humans is

$$\lambda_H(t) = \frac{\xi_2 q_2 \big(\phi I_A(t) + I_C(t) + b_1 I_{AL}(t) + b_2 I_{CL}(t) + b_3 I_{AT}(t) + b_4 I_{CT}(t)\big)}{N(t)}, \tag{3.3}$$

where, ξ_2 is the rate of human-to-human contact between the HCV infected individuals and susceptible population; q_2 is the likelihood of a contact resulting in HCV transmission; b_1, b_2, b_3 and b_4 are enhancement factors for the increased risk of easily contracting HCV from a dually infected individual in classes I_{AL}, I_{CL}, I_{AT} and I_{CT}, respectively. Dual infected individuals are more infectious of HCV as compared to their counterparts who are mono-infected. We note that $b_1, b_3 > b_2, b_4 > 1$, considering the fact that an HCV acutely infected human is more infectious than the HCV chronically infected human due to higher viral loads during the early stages of the infection. ϕ is the amplification parameter catering for the increased risk of being infected with HCV from a singly-acute HCV infected individual.

Susceptible humans, once infected with TB, enter TB latently infected class $I_L(t)$. Some humans in $I_L(t)$ sub-group progress to the infectious class, $I_T(t)$ at a rate θ while the rest gain natural recovery at a rate η. Humans in the TB infectious class die from both natural death, at a rate μ and TB induced death at a rate σ_1. Conversely, on contracting HCV, susceptible humans join the acute HCV human class, $I_A(t)$. Here, we have some humans in $I_A(t)$ class who recover from the acute HCV instinctively at a rate π where as the rest join the chronic HCV class $I_C(t)$ at a rate α. Humans in acute HCV class only die from natural death with an assumption that acute HCV is not fatal whereas humans in chronic HCV class die from both natural death and chronic HCV at a per capita rate of δ.

When humans in classes $I_L(t)$ and $I_A(t)$ interact, they become dually infected with latent TB and acute HCV and enter a class of the humans co-infected with latent TB and acute HCV, $I_{AL}(t)$. The humans in $I_{AL}(t)$ class only die from natural death, at a rate μ. Similarly, when humans in class $I_L(t)$ and $I_C(t)$ interact, they are projected to become dually infected with both latent TB and chronic HCV, thus entering a class of humans co-infected with latent TB and chronic HCV, $I_{CL}(t)$. These humans not only die from natural death at a rate μ, but also die due to the co-infection at a rate δ. Humans in class $I_{AL}(t)$ progress to $I_{AT}(t)$ class at a rate τ_1 and they also progress to $I_{CL}(t)$ at a rate β_1. Humans in $I_{CL}(t)$ and $I_{AT}(t)$ classes progress to $I_{CT}(t)$ class at rates τ_2 and β_2 respectively. Humans in classes $I_{AT}(t)$ and $I_{CT}(t)$ die from both natural death and co-infection induced death at rates d_1 and d_2 respectively. We note that, $d_1, d_2 > \delta$, because the disease induced death rate from the co-infection is expected to be greater than that of mono-infection. In the formulation of TB-HCV co-infection model, it is assumed that all susceptible humans are equally susceptible to TB and HCV.

Table 3.1: Variables used in the TB-HCV co-infection dynamics

Variable	Description
$S(t)$	Susceptible humans
$I_L(t)$	Tuberculosis latently-infected but not infectious humans
$I_T(t)$	Infectious TB humans assumed not under medication
$I_A(t)$	Infectious acute HCV humans
$I_C(t)$	Infectious chronic HCV humans
$I_{AL}(t)$	Co- infected humans with acute HCV and latent TB
$I_{CL}(t)$	Co-infected humans with chronic HCV and latent TB
$I_{AT}(t)$	Co-infected humans with acute HCV and infectious TB
$I_{CT}(t)$	Co-infected humans with chronic HCV and infectious TB

Table 3.2: Parameters used in the TB-HCV co-infection dynamics and their description

Parameter	Definition
Λ	Per capita recruitment rate into susceptible population
μ	Per capita natural mortality rate
σ_1	Per capita mortality rate for individuals with infectious TB
δ	Per capita death rate for humans with chronic form of HCV
d_1	Per capita mortality rate due to infectious TB in individuals with acute HCV and infectious TB
d_2	Per capita mortality rate due to either chronic HCV or infectious TB
θ	Rate of progress from latent stage to active stage of TB
α	Rate of progress from acute class to chronic HCV
τ_1	Rate of progress from I_{AL} class to I_{AT} class
τ_2	Rate of progress from I_{CL} class to I_{CT} class
β_1	Rate of progress from I_{AL} class to I_{CL} class
β_2	Rate of progress from I_{AT} class to I_{CT} class
η	Natural recovery rate of TB latent humans
π	Natural recovery rate of HCV acute humans
ϕ	Transmission coefficient for the HCV acute humans

Both TB and HCV are transmitted by contact (direct or indirect) between an infected human and a susceptible human. It is also assumed that HCV infection starts as acute and may progress to chronic; both stages are infectious [73]. By [66], TB begins as latent; some recover without treatment, but active TB requires medication. The variables and parameters presented in the description of TB-HCV co-infection dynamics are summarised in Table 3.1 and 3.2 respectively.

3.2.1 Compartmental TB-HCV Co-infection Model with no Intervention

Based on the described dynamics of TB-HCV co-infection and the associated assumptions, the resultant compartmental model is depicted in the compartmental diagram shown in Figure 3.1.

The arrows indicate movement of humans between states or compartments.

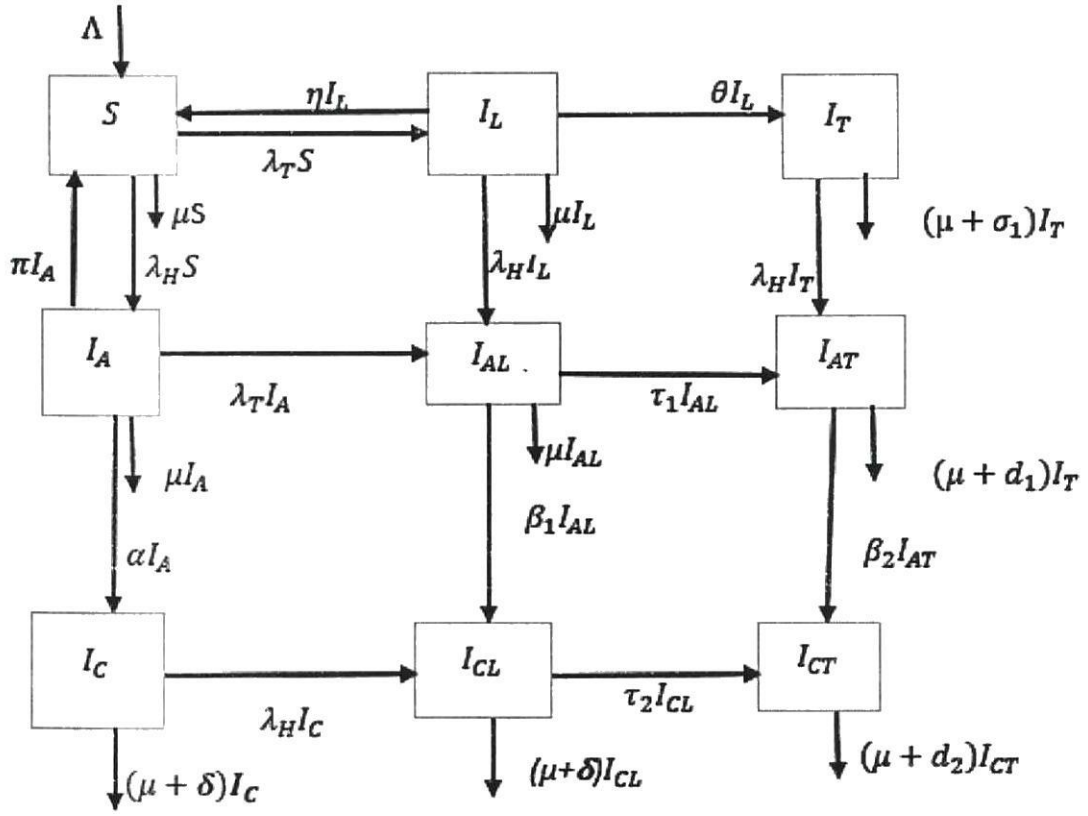

Figure 3.1: A compartmental diagram for TB-HCV co-infection dynamics in absence of treatment

3.2.2 Mathematical Model for TB-HCV Co-infection Dynamics with n Intervention

From the compartmental diagram, in Figure 3.1, the associated model equations are as in Equatio system (3.4).

$$\begin{aligned}
\frac{dS(t)}{dt} &= \Lambda + \pi I_A(t) + \eta I_L(t) - (\lambda_T + \lambda_H + \mu)S(t),\\
\frac{dI_L(t)}{dt} &= \lambda_T S(t) - (\theta + \eta + \mu + \lambda_H)I_L(t),\\
\frac{dI_T(t)}{dt} &= \theta I_L(t) - (\mu + \sigma_1 + \lambda_H)I_T(t),\\
\frac{dI_A(t)}{dt} &= \lambda_H S(t) - (\pi + \alpha + \mu + \lambda_T)I_A(t),\\
\frac{dI_C(t)}{dt} &= \alpha I_A(t) - (\mu + \delta + \lambda_T)I_C(t),\\
\frac{dI_{AL}(t)}{dt} &= \lambda_T I_A(t) + \lambda_H I_L(t) - (\tau_1 + \mu + \beta_1)I_{AL}(t),\\
\frac{dI_{CL}(t)}{dt} &= \beta_1 I_{AL}(t) + \lambda_T I_C(t) - (\tau_2 + \mu + \delta)I_{CL}(t),\\
\frac{dI_{AT}(t)}{dt} &= \tau_1 I_{AL}(t) + \lambda_H I_T(t) - (\beta_2 + \mu + d_1)I_{AT}(t),\\
\frac{dI_{CT}(t)}{dt} &= \tau_2 I_{CL}(t) + \beta_2 I_{AT}(t) - (\mu + d_2)I_{CT}(t),
\end{aligned} \tag{3.4}$$

where λ_T and λ_H are defined in (3.2) and (3.3) respectively. The initial conditions for the variables of the system are as follows:

$S(0) > 0$, $I_L(0) \geq 0$, $I_T(0) \geq 0$, $I_A(0) \geq 0$, $I_C(0) \geq 0$, $I_{AL}(0) \geq 0$, $I_{CL}(0) \geq 0$, $I_{AT}(0) \geq 0$ and $I_{CT}(0) \geq 0$.

3.3 Analysis and Results of the Model

3.3.1 Positivity and Boundedness of Solutions

This subsection investigates the basic properties of solutions generated by model system (3.4). The model system (3.4) defines the population of humans. Thus, it is imperative to show that all the population sizes $S(t), I_L(t), I_T(t), I_A(t), I_C(t), I_{AL}(t), I_{CL}(t), I_{AT}(t)$ and $I_{CT}(t)$ remain non-negative for all time and bounded, meaning that the population sizes do not grow indefinitely, thereby maintaining the model's feasibility.

Theorem 1. *Solutions of the model system* (3.4) *with non-negative starting values remain non-negati for all* $t \geq 0$ *as stated by [54, 114].*

Proof. Let the starting values of the model system (3.4) be non-negative. We prove that each solution component of the system remains non-negative. Otherwise, we assume a contradiction:
that there exists a first time $t_1 : S(t_1) = 0, S'(t_1) < 0$ and $S(t) > 0, I_L(t) > 0, I_T(t) > 0,$
$I_A(t) > 0, I_C(t) > 0, I_{AL}(t) > 0, I_{CL}(t) > 0, I_{AT}(t) > 0, I_{CT}(t) > 0$ for $0 < t < t_1$
or there exists a
$t_2 : I_L(t_2) = 0, I'_L(t_2) < 0$ and $S(t) > 0, I_L(t) > 0, I_T(t) > 0, I_A(t) > 0, I_C(t) > 0, I_{AL}(t) > 0,$
$I_{CL}(t) > 0, I_{AT}(t) > 0, I_{CT}(t) > 0$ for $0 < t < t_2$
or there exists a
$t_3 : I_T(t_3) = 0, I'_T(t_3) < 0$ and $S(t) > 0, I_L(t) > 0, I_T(t) > 0, I_A(t) > 0, I_C(t) > 0, I_{AL}(t) > 0,$
$I_{CL}(t) > 0, I_{AT}(t) > 0, I_{CT}(t) > 0$ for $0 < t < t_3$
or there exists a
$t_4 : I_A(t_2) = 0, I'_A(t_4) < 0$ and $S(t) > 0, I_L(t) > 0, I_T(t) > 0, I_A(t) > 0, I_C(t) > 0, I_{AL}(t) > 0,$
$I_{CL}(t) > 0, I_{AT}(t) > 0, I_{CT}(t) > 0$ for $0 < t < t_4$
or there exists a
$t_5 : I_C(t_5) = 0, I'_C(t_5) < 0$ and $S(t) > 0, I_L(t) > 0, I_T(t) > 0, I_A(t) > 0, I_C(t) > 0, I_{AL}(t) > 0,$
$I_{CL}(t) > 0, I_{AT}(t) > 0, I_{CT}(t) > 0$ for $0 < t < t_5$
or there exists a
$t_6 : I_{AL}(t_6) = 0, I'_{AL}(t_6) < 0$ and $S(t) > 0, I_L(t) > 0, I_T(t) > 0, I_A(t) > 0, I_C(t) > 0,$
$I_{AL}(t) > 0, I_{CL}(t) > 0, I_{AT}(t) > 0, I_{CT}(t) > 0$ for $0 < t < t_6$
or there exists a
$t_7 : I_{CL}(t_7) = 0, I'_{CL}(t_7) < 0$ and $S(t) > 0, I_L(t) > 0, I_T(t) > 0, I_A(t) > 0, I_C(t) > 0,$
$I_{AL}(t) > 0, I_{CL}(t) > 0, I_{AT}(t) > 0, I_{CT}(t) > 0$ for $0 < t < t_7$

or there exists a

$t_8 : I_{AT}(t_8) = 0, I'_{AT}(t_8) < 0$ and $S(t) > 0, I_L(t) > 0, I_T(t) > 0, I_A(t) > 0, I_C(t) > 0,$

$I_{AL}(t) > 0, I_{CL}(t) > 0, I_{AT}(t) > 0, I_{CT}(t) > 0$ for $0 < t < t_8$

or there exists a

$t_9 : I_{CT}(t_9) = 0, I'_{CT}(t_9) < 0$ and $S(t) > 0, I_L(t) > 0, I_T(t) > 0, I_A(t) > 0, I_C(t) > 0,$

$I_{AL}(t) > 0, I_{CL}(t) > 0, I_{AT}(t) > 0, I_{CT}(t) > 0$ for $0 < t < t_9$.

From the first Equation of model system (3.4), we have

$$\begin{aligned}\frac{dS(t_1)}{dt} &= \Lambda + \pi I_A(t_1) + \eta I_L(t_1) - (\lambda_T(t_1) + \lambda_H(t_1) + \mu)S(t_1),\\ &= \Lambda + \pi I_A(t_1) + \eta I_L(t_1) > 0,\end{aligned}$$

thus, a contradiction, implying that $S(t)$ shall be non-negative.

From the second Equation of model system (3.4), we have

$$\begin{aligned}\frac{dI_L(t_2)}{dt} &= \lambda_T(t_2)S(t_2) - (\theta + \eta + \mu + \lambda_H(t_2))I_L(t_2),\\ &= \lambda_T(t_2)S(t_2) > 0,\end{aligned}$$

thus, a contradiction, implying that $I_L(t)$ shall be non-negative.

From the third Equation of model system (3.4), we have

$$\begin{aligned}\frac{dI_T(t_3)}{dt} &= \theta I_L(t_3) - (\mu + \sigma_1 + \lambda_H(t_3))I_T(t_3),\\ &= \theta I_L(t_3) > 0,\end{aligned}$$

thus, a contradiction, implying that $I_T(t)$ shall remain non-negative.

From the fourth Equation of model system (3.4), we have

$$\begin{aligned}\frac{dI_A(t_4)}{dt} &= \lambda_H(t_4)S(t_4) - (\pi + \alpha + \mu + \lambda_T(t_4))I_A(t_4),\\ &= \lambda_H(t_4)S(t_4) > 0,\end{aligned}$$

thus, a contradiction, implying that $I_A(t)$ shall be non-negative.

From the fifth Equation of model system (3.4), we have

$$\begin{aligned}\frac{dI_C(t_5)}{dt} &= \alpha I_A(t_5) - (\mu + \delta + \lambda_T(t_5))I_C(t_5),\\ &= \alpha I_A(t_5) > 0,\end{aligned}$$

thus, a contradiction, implying that $I_C(t)$ remains non-negative.

From the sixth Equation of model system (3.4), we have

$$\begin{aligned}\frac{dI_{AL}(t_6)}{dt} &= \lambda_T(t_6)I_A(t_6) + \lambda_H(t_6)I_L(t_6) - (\tau_1 + \mu + \beta_1)I_{AL}(t_6),\\ &= \lambda_T(t_6)I_A(t_6) + \lambda_H(t_6)I_L(t_6) > 0,\end{aligned}$$

giving is a contradiction, implying that $I_{AL}(t)$ remains non-negative.

From the seventh Equation of model system (3.4), we have

$$\begin{aligned}\frac{dI_{CL}(t_7)}{dt} &= \beta_1 I_{AL}(t_7) + \lambda_T(t_7)I_C(t_7) - (\tau_2 + \mu + \delta)I_{CL}(t_7),\\ &= \beta_1 I_{AL}(t_7) + \lambda_T(t_7)I_C(t_7) > 0,\end{aligned}$$

giving a contradiction, implying that $I_{CL}(t)$ remains non-negative.

From the eighth Equation of model system (3.4), we have

$$\begin{aligned}\frac{dI_{AT}(t_8)}{dt} &= \tau_1 I_{AL}(t_8) + \lambda_H(t_8)I_I(t_8) - (\beta_2 + \mu + d_1)I_{AT}(t_8),\\ &= \tau_1 I_{AL}(t_8) + \lambda_H(t_8)I_I(t_8) > 0,\end{aligned}$$

giving a contradiction, implying that $I_{AT}(t)$ remains non-negative.

From the ninth Equation of model system (3.4), we have

$$\begin{aligned}\frac{dI_{CT}(t_9)}{dt} &= \tau_2 I_{CL}(t_9) + \beta_2 I_{AT}(t_9) - (\mu + d_2)I_{CT}(t_9),\\ &= \tau_2 I_{CL}(t_9) + \beta_2 I_{AT}(t_9) > 0,\end{aligned}$$

which is a contradiction, meaning that $I_{CT}(t)$ remains non-negative.

Thus, in all cases, $S(t), I_L(t), I_T(t), I_A(t), I_C(t), I_{AL}(t), I_{CL}(t), I_{AT}(t), I_{CT}(t)$ remain non-negative for

$t \geq 0$. □

Theorem 2. *The region*

$$\Omega = \{S(t), I_L(t), I_T(t), I_A(t), I_C(t), I_{AL}(t), I_{CL}(t), I_{AT}(t), I_{CT}(t) \in \mathbb{R}^9_+ : 0 \leq N(t) \leq \frac{\Lambda}{\mu}\}$$

is positively invariant and all solutions starting in Ω approach, enter or stay in Ω.

Proof. Let

$$(S(t), I_L(t), I_T(t), I_A(t), I_C(t), I_{AL}(t), I_{CL}(t), I_{AT}(t), I_{CT}(t) \in \mathbb{R}^9_+)$$

be any solution of the model system (3.4), with non-negative initial condition given by

$$S(0), I_L(0), I_T(0), I_A(0), I_C(0), I_{AL}(0), I_{CL}(0), I_{AT}(0), I_{CT}(0).$$

The total population is given by $N(t)$ in Équation (3.1).
Adding all the differential equations in the model system (3.4), we have

$$\frac{dN(t)}{dt} = \Lambda - \mu N - \sigma_1 I_T - \delta(I_C + I_{CL}) - d_1 I_{AT} - d_2 I_{CT}. \tag{3.5}$$

Since all parameter values are greater than zero and

$$I_T(t) > 0, I_A(t) > 0, I_{AL}(t) > 0, I_{CL}(t) > 0, I_{CT}(t) > 0 I_C(t) > 0 \text{ and } I_{AT}(t) > 0 \text{ for all } t > 0,$$

then Equation (3.5) yields the inequality

$$\frac{dN(t)}{dt} + \mu N(t) \leq \Lambda. \tag{3.6}$$

On solving the inequality (3.6) by integrating factor method with initial conditions $N(0) = N_0$, we have

$$0 \leq N(t) \leq \frac{\Lambda}{\mu} + (N_0 - \frac{\Lambda}{\mu})e^{-\mu t},$$

so that, as $t \to \infty$,

$$0 \leq N(t) \leq \frac{\Lambda}{\mu}.$$

Consequently, all possible feasible solution of the model system (3.4) that begin in the region

$$\Omega = \{S(t), I_L(t), I_T(t), I_A(t), I_C(t), I_{AL}(t), I_{CL}(t), I_{AT}(t), I_{CT}(t) \in \mathbb{R}^9_+ : 0 \leq N(t) \leq \frac{\Lambda}{\mu}\},$$

remains in the region for all values of t. Thus, the region Ω is positively invariant, that is, for all values of t, the solution is well-posed and biologically meaningful. □

3.3.2 Existence of Equilibrium Points and their Stability based on the Basic Reproduction Number

In this subsection, we derive and analyse the stability of equilibrium solutions using basic reproduction numbers. The basic reproduction number R_0 is defined as the average number of secondary cases arising from an average primary case in an entirely susceptible population over the period of infection (Diekman et al., [63]). The basic reproduction number is an important non-dimensional quantity in epidemiology as it sets the threshold in the study of a disease. We compute the basic reproduction number, R_0 using the next generation operator approach by Van den Driessche and Watmough [35].

Remark 3.1: The condition $R_0 < 1$ means that every infectious individual will cause less than one secondary infection and hence the disease will die out and when $R_0 > 1$ every infectious individual will cause more than one secondary infection and hence the disease will invade the population. A large value of R_0 may indicate the possibility of a major epidemic. The properties and complexities of R_0 depend on the number of infectives and intervention strategies. Therefore, all health control measures or strategies of a disease, if effective, should lower R_0 to less than unity.

Remark 3.2: Our computation of the basic reproduction numbers involves deriving separate TB and HCV sub models, culminating in a comprehensive TB-HCV co-infection model.

3.3.2.1 The Equilibrium and Basic Reproduction Number for TB-only sub model with no Intervention

The TB-only sub model is obtained by equating all the variables concerning HCV in the model system (3.4) to zero, that is,

$$I_A(t) = I_C(t) = I_{AL}(t) = I_{CL}(t) = I_{AT}(t) = I_{CT}(t) = \lambda_H = 0.$$

Hence, the TB-only sub model is as in system (3.7).

$$\begin{aligned}\frac{dS}{dt} &= \Lambda + \eta I_L - (\lambda_T + \mu)S,\\ \frac{dI_L}{dt} &= \lambda_T S - (\theta + \eta + \mu)I_L,\\ \frac{dI_T}{dt} &= \theta I_L - (\mu + \sigma_1)I_T,\end{aligned} \tag{3.7}$$

with

$$S(0) = S_0 \geq 0, I_L(0) = I_{L0} \geq 0, I_T(0) = I_{T0} \geq 0,$$

as the starting values,

$$\lambda_T = \frac{\xi_1 q_1 I_T(t)}{N_T(t)},$$

is the force of infection and the total population is given by

$$N_T(t) = S(t) + I_L(t) + I_T(t).$$

To determine the TB-free equilibrium point for the TB-only sub model, we suppose that there is no TB infection in the community, such that $I_L = I_T = 0$. Thus, the sub model system (3.7) reduces to:

$$\frac{dS}{dt} = \Lambda + \mu S, \tag{3.8}$$

Now, the right-hand side of the equation (3.8) is set to zero and solving the resulting equation gives

$$S^0 = \frac{\Lambda}{\mu}.$$

Thus, the TB-free equilibrium point for the TB-only sub model is given by

$$F_T^0 = (S^0, I_L^0, I_T^0) = (\frac{\Lambda}{\mu}, 0, 0).$$

In this instance, we shall define the basic reproduction number R_T as the number of new TB cases given rise to by an infectious TB human during their entire infectious period. Now, the next generation matrix method suggested by Van den Driesche and Watmough, [35] is applied to to establish the basic reproduction number R_T of system (3.7). Let $\mathcal{F}$ represent the matrix of components of new infection and $\mathcal{V}$ the matrix of the rest of transfer components in system (3.7)

The infected compartments are I_L and I_T. Thus, we have

$$\mathcal{F} = \begin{bmatrix} \lambda_T S \\ 0 \end{bmatrix}, \tag{3.9}$$

and

$$\mathcal{V} = \begin{bmatrix} (\theta + \eta + \mu) I_L \\ -\theta I_L + (\mu + \sigma_1) I_T \end{bmatrix}. \tag{3.10}$$

The Jacobian matrices of Equations (3.9) and (3.10) are computed at the disease-free equilibrium, E_T^0, thus yielding matrices F_T and V_T respectively as,

$$F_T = \begin{bmatrix} 0 & \xi_1 q_1 \frac{S}{N_T} \\ 0 & 0 \end{bmatrix},$$

and

$$V_T = \begin{bmatrix} (\theta + \eta + \mu) & 0 \\ -\theta & (\mu + \sigma_1) \end{bmatrix}.$$

At E_T^0, $\frac{S}{N_T} = 1$, thus,

$$F_T(E_T^0) = \begin{bmatrix} 0 & \xi_1 q_1 \\ 0 & 0 \end{bmatrix}, \tag{3.11}$$

and

$$V_T(E_T^0) = \begin{bmatrix} (\theta + \eta + \mu) & 0 \\ -\theta & (\mu + \sigma_1) \end{bmatrix}. \tag{3.12}$$

Then,

$$V_T^{-1} = \begin{bmatrix} (\theta + \eta + \mu) & 0 \\ -\theta & (\mu + \sigma_1) \end{bmatrix}.$$

$$F_T V_T^{-1} = \frac{1}{(\mu + \sigma_1)(\theta + \eta + \mu)} \begin{bmatrix} 0 & \xi_1 q_1 \\ 0 & 0) \end{bmatrix} \begin{bmatrix} (\mu + \sigma_1) & 0 \\ \theta & (\theta + \eta + \mu \end{bmatrix},$$

$$F_T V_T^{-1} = \begin{bmatrix} \frac{\xi_1 q_1 \theta}{(\mu + \sigma_1)(\theta + \eta + \mu)} & \frac{\xi_1 q_1}{(\mu + \sigma_1)} \\ 0 & 0) \end{bmatrix}. \tag{3.13}$$

For the eigenvalues, λ, we solve the equation

$$P(\lambda) = \det(FV^{-1} - \lambda I) = 0.$$

From which we have,

$$\det \begin{bmatrix} \frac{\xi_1 q_1 \theta}{(\mu+\sigma_1)(\theta+\eta+\mu)} - \lambda & 0 \\ 0 & -\lambda \end{bmatrix} = 0. \tag{3.14}$$

Therefore,

$$\lambda_1 = 0 \text{ and } \lambda_2 = \frac{\xi_1 q_1 \theta}{(\mu+\sigma_1)(\theta+\eta+\mu)}.$$

Thus, the TB basic reproduction number, R_T, which is the spectral radius of the dominant eigenvalue is

$$R_T = \frac{\xi_1 q_1 \theta}{(\theta+\eta+\mu)(\mu+\sigma_1)}.$$

The decrease of the infection in a human population is influenced by the parameters that will reduce the value of the reproduction number to less than unity. Clearly, it can be observed that when the rate of human-to-human contact between the TB infected individuals and susceptible population ξ_1, the likelihood of a contact resulting in TB transmission, q_1 and the rate of progression, θ, of latent TB humans to the active TB class become large, this leads to an increase in the TB secondary infections. Thus, intervention measures to mitigate TB infection should mainly target decreasing ξ_1, q_1 and θ while increasing the natural recovery rate, η, of TB latent humans.

Using Theorem 2 from [35], the following result is established.

Lemma 3.1: The local and asymptotic stability of the disease-free equilibrium point, E_T^0, of TB-only sub model with no intervention exists if $R_T < 1$.

Proof. To establish the local and asymptotic stability of the TB infection-free equilibrium point E_T^0, we use the eigenvalue technique. The approach requires that all the eigenvalues of the Jacobian matrix, $J(E_T)$ at E_T^0 have negative real parts as used in [54, 114].

The Jacobian matrix, $J(E_T)$ of the TB-only sub model (3.7) is obtained as follows:

$$J(E_T) = \begin{bmatrix} -(\frac{\xi_1 q_1 I_T}{N_T} + \mu) & \eta & \frac{-\xi_1 q_1 S}{N_T} \\ \frac{\xi_1 q_1 I_T}{N_T} & -k_1 & \frac{\xi_1 q_1 S}{N_T} \\ 0 & \theta & -k_2 \end{bmatrix}, \tag{3.15}$$

where

$$k_1 = \theta + \eta + \mu \text{ and } k_2 = \mu + \sigma_2.$$

Evaluating the Jacobian matrix (3.15) at $E_T^0 = (\frac{\Lambda}{\mu}, 0, 0)$, leads to

$$J(E_T^0) = \begin{bmatrix} -\mu & \eta & -\xi_1 q_1 \\ 0 & -k_1 & \xi_1 q_1 \\ 0 & \theta & -k_2 \end{bmatrix}. \tag{3.16}$$

Now, applying Trace/determinant method,

$$\text{Trace}(J(E_T^0)) = -(\mu + k_1 + k_2) < 0. \tag{3.17}$$

Then determinant for a reduced 2×2 matrix is given by,

$$\det = (k_1 k_2 - \xi_1 q_1 \theta). \tag{3.18}$$

For stability, $\det > 0$. That is

$$k_1 k_2 > \xi_1 q_1 \theta. \tag{3.19}$$

Since $\xi_1 q_1 \theta = k_1 k_2 R_T$, this implies

$$k_1 k_2 > k_1 k_2 R_T. \tag{3.20}$$

Thus, $R_T < 1$.

Therefore, E_T^0 is locally asymptotically stable only if $R_T < 1$. A local and asymptotic stability o E_T^0 implies that in case some few TB infected humans are introduced into the population, then ove time, the system returns to TB-free equilibrium. □

3.3.2.2 Global stability of TB-free equilibrium point for TB-only sub model with nc intervention

To investigate the global and asymptotic stability of the system of differential Equations (3.7), th approach described by Castillo-Chavez *et al.* [76] and also applied in [54, 114] is used.

The TB-only system (3.7) is re-written in the form:

$$\begin{aligned} \frac{dX_T}{dt} &= F(X_T, Z_T), \\ \frac{dZ_T}{dt} &= G(X_T, Z_T), G(X_T, 0) = 0. \end{aligned} \tag{3.21}$$

Where $X_T = (S)$ and $Z_T = (I_L, I_T)$, with $X_T \in \mathbb{R}_+$ indicating the number of uninfected humans and $Z_T \in \mathbb{R}_+^2$ showing the number of humans infected with TB. Let the TB-free equilibrium of this system be denoted by $E_T^0 = (X_T^0, 0) = (\frac{\Lambda}{\mu}, 0)$. It is necessary to ensure that the following conditions are met to guarantee global asymptotic stability.

$$\begin{aligned} &(H1) : \text{For } \frac{dX_T}{dt} = F(X_T, 0), X_T^0 \text{ is globally asymptotically stable,} \\ &(H2) : G(X_T, Z_T) = MZ_T - \hat{G}(X_T, Z_T), \hat{G}(X_T, Z_T) \geq 0, \end{aligned}$$

for $(X_T, Z_T) \in \Omega_T$. where $M = D_Z G(X_T^0, 0)$ is a Metzler matrix (the off diagonal elements of M are no-negative) and Ω_T is the region where the model makes biological meaning. Thus, when system (3.21) satisfies conditions $(H1)$ and $(H2)$, we have the following Theorem satisfied.

Theorem 3. *The equilibrium point $E_T^0 = (X_T^0, 0)$ is globally asymptotically stable point of system (3.21) provided $R_T < 1$ and that conditions $(H1)$ and $(H2)$ are satisfied.*

Proof. By Lemma 3.1, if $R_T < 1$, then E_T^0 is locally asymptotically stable.
For the first condition $(H1)$, that is, the global asymptotic stability of X_T, we have,

$$\frac{dX_T}{dt} = F(X_T, 0) = \Lambda - \mu S_T,$$

which is a linear differential equation. Solving it gives,

$$S_T(t) = \frac{\Lambda}{\mu}(1 - e^{-\mu t}) + S_T(0)e^{-\mu t}.$$

Now, as $t \to \infty$, $S_T \to \frac{\Lambda}{\mu}$ regardless of the value of $S_T(0)$. Thus, X_T is globally asymptotically stable.

For the second condition $(H2)$, consider

$$G(X_T, Z_T) = \begin{bmatrix} \lambda_T S - k_1 I_L \\ \theta I_L - k_2 I_T \end{bmatrix},$$
$$= \begin{bmatrix} \xi_1 q_1 I_T \frac{S}{N_T} - k_1 I_L \\ \theta I_L - k_2 I_T \end{bmatrix}.$$

Then

$$M = D_Z G(X_T^0, 0) = \begin{bmatrix} -k_1 & \xi_1 q_1 \frac{S}{N_T} \\ \theta & -k_2 \end{bmatrix}.$$

At E_T^0,

$$M = \begin{bmatrix} -k_1 & \xi_1 q_1 \\ \theta & -k_2 \end{bmatrix}.$$

Therefore,

$$\hat{G}(X_T, Z_T) = MZ_T - G(X_T, Z_T),$$
$$= \begin{bmatrix} \xi_1 q_1 I_T (1 - \frac{S}{N_T}) \\ 0 \end{bmatrix}.$$

Since $0 < S \leq N_T$, then $\hat{G}(X_T, Z_T) \geq 0$. We also notice that matrix M is actually a Metzler matrix since both of its off diagonal elements are positive. Thus, it clearly implies that condition $(H2)$ is satisfied. Hence, the TB-free equilibrium point E_T^0 is globally asymptotically stable for $R_T < 1$. This implies that no matter the number of TB cases that are brought into the population, TB infection shall not persist in the population. □

3.3.2.3 The Existence of TB Endemic State

Here, we consider the persistence of TB in the population and determine the TB endemic equilibrium point, $E_T^* = (S^*, I_L^*, I_T^*)$. By setting the derivatives of system 3.7 to zero, we have

$$\Lambda + \dot{\eta} I_L - (\lambda_T + \mu) S = 0, \tag{3.22}$$

$$\lambda_T S - (\theta + \eta + \mu) I_L = 0, \tag{3.23}$$

$$\theta I_L - (\mu + \sigma_1) I_T = 0, \tag{3.24}$$

with

$$\lambda_T = \frac{\xi_1 q_1 I_T}{N_T}, \tag{3.25}$$

and

$$N_T = S + I_L + I_T. \tag{3.26}$$

Now, substituting for λ_T in Equations (3.22) and (3.23), gives

$$\Lambda N_T + \eta I_L N_T - (\xi_1 q_1 I_T + \mu) S = 0, \tag{3.27}$$

$$\xi_1 q_1 I_T S - k_1 I_L N_T = 0, \tag{3.28}$$

$$\theta I_L - k_2 I_T = 0. \tag{3.29}$$

Now, solving for S from Equation (3.28), yields

$$S = \frac{k_1 I_L N_T}{\xi_1 q_1 I_T}. \tag{3.30}$$

Substituting for S in Equation (3.27), gives

$$\Lambda N_T + \eta N_T I_L - k_1 I_L N_T + \frac{\mu k_1 I_L N_T}{\xi_1 q_1 I_T} = 0. \tag{3.31}$$

From Equation (3.29),

$$I_T = \frac{\theta I_L}{k_2}. \tag{3.32}$$

Now, substituting I_T in Equation (3.31) and solving for I_L, yields

$$I_L = \frac{\Lambda \xi_1 q_1 + \mu k_1 k_2}{\xi_1 q_1 (k_1 - \eta)}. \tag{3.33}$$

Substituting for I_L in Equation (3.32), we get

$$I_T = \frac{\theta(\Lambda \xi_1 q_1 + \mu k_1 k_2)}{\xi_1 q_1 k_2 (k_1 - \eta)}. \tag{3.34}$$

Substituting for I_L and I_T in Equation (3.30), gives

$$S = \frac{k_1 k_2 N_T}{\theta \xi_1 q_1}. \tag{3.35}$$

Hence, the TB endemic equilibrium point E_T^*, is given by

$$E_T^* = (S^*, I_L^*, I_T^*) = \Big(\frac{k_1 k_2 N_T}{\theta \xi_1 q_1}, \frac{\Lambda \xi_1 q_1 + \mu k_1 k_2}{\xi_1 q_1 (k_1 - \eta)}, \frac{\theta(\Lambda \xi_1 q_1 + \mu k_1 k_2)}{\xi_1 q_1 k_2 (k_1 - \eta)}\Big)$$

Lemma 3.2: The TB-only sub model (3.7) has a unique endemic equilibrium point if $R_T > 1$.

Proof. If the infection is consistently present in the population, then $\frac{dI_L}{dt} > 0$ and $\frac{dI_T}{dt} > 0$ as used in [114], that is

$$\frac{\xi_1 q_1 I_T S}{N_T} - k_1 I_L > 0, \tag{3.36}$$

$$\theta I_L - k_2 I_T > 0. \tag{3.37}$$

From Inequality (3.36),

$$k_1 I_L < \xi_1 q_1 I_T \frac{S}{N_T}. \tag{3.38}$$

Using the fact that $\frac{S}{N_T} \leq 1$, inequality (3.38) becomes

$$I_L < \frac{\xi_1 q_1 I_T}{k_1}. \tag{3.39}$$

From Inequality (3.37),

$$I_T < \frac{\theta I_L}{k_2}. \tag{3.40}$$

Substituting for I_T into inequality (3.39), gives

$$I_L < \frac{\theta \xi_1 q_1 I_L}{k_1 k_2}, \tag{3.41}$$

$$1 < \frac{\theta \xi_1 q_1}{k_1 k_2} = R_T. \tag{3.42}$$

Therefore, an endemic equilibrium point E_T^* which is distinctive does exist when $R_T > 1$. □

Lemma 3.3: The local and asymptotic stability of the TB-endemic equilibrium, E_T^* exists if $R_T > 1$.

Proof. The local and asymptotic stability of E_T^* is established using the trace and determinant method. The approach requires that trace of the Jacobian matrix $J(E_T^*)$ is less than zero and the determinant of the Jacobian matrix $J(E_T^*)$ is greater than zero.

The Jacobian matrix $J(E_T)$ of the TB-only sub model is given by

$$J(E_T) = \begin{bmatrix} -(\lambda_T + \mu) & \eta & -\xi_1 q_1 \frac{S}{N_T} \\ \lambda_T & -k_1 & \xi_1 q_1 \frac{S}{N_T} \\ 0 & \theta & -k_2 \end{bmatrix}. \tag{3.43}$$

Evaluating the Jacobian matrix (3.43) at E_T^* gives Thus,

$$J(E_T^*) = \begin{bmatrix} -(\lambda_T^* + \mu) & \eta & \frac{-\xi_1 q_1}{R_T} \\ \lambda_T^* & -k_1 & \frac{\xi_1 q_1}{R_T} \\ 0 & \theta & -k_2 \end{bmatrix}.$$

Now

$$\text{tr}(J(E_T^*)) = -(\lambda^* + \mu + k_1 + k_2) < 0.$$

Then

$$\begin{aligned} \det(J(E_T^*)) &= 2\frac{\lambda_T^* q_1 \theta \xi_1}{R_T} + \frac{\mu q_1 \theta \xi_1}{R_T} + \eta k_2 \lambda_T^* - k_1 k_2 \lambda_T^* - k_1 k_2, \mu \\ &= \frac{q_1 \theta \xi_1}{R_T}(2\lambda_T^* + \mu) + \eta k_2 \lambda_T^* - k_1 k_2 (\lambda_T^* + \mu), \\ &= k_1 k_2 (R_T - 1)(\lambda_T^* + \mu) + \lambda_T^* (\frac{q_1 \theta \xi_1}{R_T} + \eta k_2). \end{aligned}$$

Since the

$$\text{tr}(J(E_T^*)) = -(\lambda_T^* + \mu + k_1 + k_2) < 0,$$

and the determinant is positive when $R_T > 1$, then, the TB-endemic equilibrium, E_T^*, is locally asymptotically stable. □

3.3.2.4 Global stability of the endemic equilibrium point for TB-only sub model with no intervention

Lemma 3.4: If $R_T > 1$, then the TB-endemic equilibrium E_T^* of TB-only sub model is globally asymptotically stable.

Proof. The global stability of TB-endemic equilibrium E_T^* for the TB-only sub model is analysed

using the following constructed Lyapunov function by Cai and Li [70]. Let the Lyapunov function be

$$L(S^*, I_L^*, I_T^*) = L_1\Big(S - S^* - S^* In\Big(\frac{S^*}{S}\Big)\Big) + L_2\Big(I_L - I_L^* - I_L^* In\Big(\frac{I_L^*}{I_L}\Big)\Big) + L_3\Big(I_T - I_T^* - I_T^* In\Big(\frac{I_T^*}{I_T}\Big)\Big).$$

Taking derivative of the Lyapunov function L with respect to time along the positive solution of the above equation, we obtain,

$$\begin{aligned}\frac{dL}{dt} &= L_1\Big(1 - \frac{S^*}{S}\Big)\frac{dS}{dt} + L_2\Big(1 - \frac{I_L^*}{I_L}\Big)\frac{dI_L}{dt} + L_3\Big(1 - \frac{I_T^*}{I_T}\Big)\frac{dI_T}{dt},\\ &= L_1\Big(1 - \frac{S^*}{S}\Big)\Big(\Lambda + \eta I_L - \frac{\xi_1 q_1 I_T S}{N_T} - \mu S\Big) + L_2\Big(1 - \frac{I_L^*}{I_L}\Big)\Big(\frac{\xi_1 q_1 I_T S}{N_T} - k_1 I_L\Big)\\ &\quad + L_3\Big(1 - \frac{I_T^*}{I_T}\Big)\Big(\theta I_L - k_2 I_T\Big). \qquad (3.44)\end{aligned}$$

At the TB-endemic equilibrium, we have

$$\Lambda = \frac{\xi_1 q_1 I_L^* S^*}{N_T^*} + \mu S^* - \eta I_L^*, \qquad (3.45)$$

$$k_1 = \frac{\xi_1 q_1 I_T^* S^*}{N_T^* I_L^*}, \qquad (3.46)$$

$$k_2 = \frac{\theta I_L^*}{I_T^*}. \qquad (3.47)$$

Substituting Λ, k_1 and k_2 into Equation (3.44), we get

$$\begin{aligned}\frac{dL}{dt} &= L_1\Big(1 - \frac{S^*}{S}\Big)\Big(\frac{\xi_1 q_1 I_L^* S^*}{N_T^*} + \mu S^* - \eta I_L^* + \eta I_L - \frac{\xi_1 q_1 I_T S}{N_T} - \mu S\Big)\\ &\quad + L_2\Big(1 - \frac{I_L^*}{I_L}\Big)\Big(\frac{\xi_1 q_1 I_T S}{N_T} - \frac{\xi_1 q_1 I_T^* S^*}{N_T^* I_L^*} I_L\Big) + L_3\Big(1 - \frac{I_T^*}{I_T}\Big)\Big(\theta I_L - \frac{\theta I_L^*}{I_T^*} I_T\Big). \qquad (3.48)\end{aligned}$$

Expanding and putting together terms of similar signs in Equation (3.48), we have

$$\begin{aligned}\frac{dL}{dt} &= \frac{\xi_1 q_1 I_T^* S^* L_1}{N_T^*} + \mu S^* L_1 + \eta I_L L_1 - \frac{\xi_1 q_1 I_T^* S^{*2} L_1}{N_T S} - \frac{\mu S^{*2} L_1}{S} - \frac{\eta I_L S^* L_1}{S} \\ &+ \frac{\xi_1 q_1 I_T S L_2}{N_T} - \frac{\xi_1 q_1 I_T S I_L^* L_2}{I_L N_T} + \theta I_L L_3 - \frac{\theta I_L I_T^* L_3}{I_T} - L_1 \eta I_L^* - \frac{\xi_1 q_1 I_T S L_1}{N_T} - \mu S L_1 \\ &+ \frac{\eta S^* I_L^* L_1}{S} + \frac{\xi_1 q_1 I_T S^* L_1}{N_T} + \mu S^* L_1 - \frac{\xi_1 q_1 I_T^* S^*}{N_T^* I_L^*} I_L L_2 + \frac{\xi_1 q_1 I_T^* S^*}{N_T^*} L_2 - \frac{\theta I_L^*}{I_T^*} I_T L_3 + \theta I_L^* L_3.\end{aligned} \tag{3.49}$$

$\frac{dL}{dt} = A - B.$

where

$$\begin{aligned}A &= \frac{\xi_1 q_1 I_T^* S^* L_1}{N_T^*} + \mu S^* L_1 + \eta I_L L_1 + \frac{\xi_1 q_1 I_T S L_2}{N_T} + \theta I_L L_3 + \frac{\eta S^* I_L^* L_1}{S} \\ &+ \frac{\xi_1 q_1 I_T S^* L_1}{N_T} + \mu S^* L_1 + \frac{\xi_1 q_1 I_T^* S^*}{N_T^*} L_2 + \theta I_L^* L_3,\end{aligned}$$

and

$$\begin{aligned}B &= \frac{\xi_1 q_1 I_T^* S^{*2} L_1}{N_T S} + \frac{\mu S^{*2} L_1}{S} + \frac{\eta I_L S^* L_1}{S} + \frac{\xi_1 q_1 I_T S I_L^* L_2}{I_L N_T} + \frac{\theta I_L I_T^* L_3}{I_T} + L_1 \eta I_L^* \\ &+ \frac{\xi_1 q_1 I_T S L_1}{N_T} + \mu S L_1 + \frac{\xi_1 q_1 I_T^* S^*}{N_T^* I_L^*} I_L L_2 + \frac{\theta I_L^*}{I_T^*} I_T L_3.\end{aligned}$$

Thus, if $A < B$, then we obtain that $\frac{dL}{dt} \leq 0$, noting that $\frac{dL}{dt} = 0$ if and only if $S = S^*, I_L = I_L^*, I_T = I_T^*$. Therefore, the largest compact invariant set in $\{(S^*, I_L^*, I_T^*) \in \Omega_T : \frac{dL}{dt} = 0\}$ is singleton $\{E_T^*\}$ where E_T^* is the endemic equilibrium point of the system (3.7). Thus, by Lasalle's Invariant principle, (Lasalle J, [71]), it implies that E_T^* is globally asymptotically stable in Ω_T if $A < B$. □

3.3.2.5 The HCV-free Equilibrium and Basic Reproduction Number for HCV-only sub model with no intervention

By setting all the variables concerning TB infection in model system (3.4) to zero, we obtain the HCV-only sub model. Let $I_L = I_T = I_{AL} = I_{AT} = I_{CL} = I_{CT} = \lambda_T = 0$. Then, the HCV-only sub

model is given in Equation (3.50).

$$\begin{aligned}
\frac{dS}{dt} &= \Lambda + \pi I_A - (\lambda_H + \mu)S, \\
\frac{dI_A}{dt} &= \lambda_H S - (\pi + \alpha + \mu)I_A, \\
\frac{dI_C}{dt} &= \alpha I_A - (\mu + \delta)I_C,
\end{aligned} \tag{3.50}$$

with

$$S(0) = S_0 \geq 0, I_A(0) = I_{A0} \geq 0, I_C(0) = I_{C0} \geq 0 \text{ as the initial conditions,}$$

$$N_H = S + I_A + I_C \text{ as the total population}$$

and

$$\lambda_H = \frac{\xi_2 q_2(\phi I_A + I_C)}{N_H} \text{ as the force of infection.}$$

To determine the HCV-free equilibrium point, we assume that there is no HCV infection in the population such that $I_A = I_C = 0$. Thus, the model system 3.50 reduces to:

$$\frac{dS}{dt} = \Lambda - \mu S. \tag{3.51}$$

Now, setting the right-hand side of Equation (3.51) to zero and solving for the values of the HCV-free equilibrium point, we get

$$\Lambda - \mu S^0 = 0, \text{ giving } S^0 = \frac{\Lambda}{\mu}$$

Therefore, the HCV-free equilibrium for the HCV-only sub model is given by:

$$E_H^0 = (S^0, I_A^0, I_C^0) = (\frac{\Lambda}{\mu}, 0, 0).$$

The basic reproduction number, R_H, for the sub model system (3.50) is defined as the number of secondary HCV cases produced by one HCV positive human during their entire life. Applying the method of the next generation matrix for calculating the basic reproduction number as proposed in [35], the matrices for rate of emergence of new infections in compartment i, F_i, and for the rate of movement into and out of compartment i by all other ways, V_i, for the HCV-only sub model in (3.50) are obtained as follows:

The infected compartments are I_A and I_C. Thus, we have

$$F_i = \begin{bmatrix} \lambda_H S \\ 0 \end{bmatrix}$$

and

$$V_i = \begin{bmatrix} (\pi + \alpha + \mu) I_A \\ -\alpha I_A + (\mu + \delta) I_C \end{bmatrix}$$

The Jacobian matrix of the new HCV infections, F_H and that for the rate of transfer into and out of the compartment i by all other processes, V_H, computed at HCV-free equilibrium point are got as follows:

$$F_H = \begin{bmatrix} \frac{\xi_2 q_2 \phi S}{N_H} & \frac{\xi_2 q_2 S}{N_H} \\ 0 & 0 \end{bmatrix}.$$

At $E_H^0 = (\frac{\Lambda}{\mu}, 0, 0)$,

$$F_H = \begin{bmatrix} \xi_2 q_2 \phi & \xi_2 q_2 \\ 0 & 0 \end{bmatrix},$$

and

$$V_H = \begin{bmatrix} k_3 & 0 \\ -\alpha & k_4 \end{bmatrix},$$

where $k_3 = \pi + \alpha + \mu$ and $k_4 = \mu + \delta$.

$$V_H^{-1} = \frac{1}{k_1 k_2} \begin{bmatrix} k_3 & 0 \\ \alpha & k_4 \end{bmatrix}.$$

Now, the next generation matrix is given by:

$$\begin{aligned} FV_H^{-1} &= \frac{1}{k_1 k_2} \begin{bmatrix} \xi_2 q_2 \phi & \xi_2 q_2 \\ 0 & 0 \end{bmatrix} \begin{bmatrix} k_3 & 0 \\ \alpha & k_4 \end{bmatrix}, \\ &= \begin{bmatrix} \frac{\xi_2 q_2 (\phi k_4 + \alpha)}{k_3 k_4} & \frac{\xi_2 q_2}{k_4} \\ 0 & 0 \end{bmatrix}. \end{aligned} \tag{3.52}$$

To determine the eigenvalues, λ, we solve the characteristic equation below:

$$\det(F_H V_H^{-1} - \lambda I) = 0. \tag{3.53}$$

Thus,

$$\det \begin{bmatrix} \frac{\xi_2 q_2(\phi k_4+\alpha)}{k_3 k_4} - \lambda & \frac{\xi_2 q_2}{k_4} \\ 0 & -\lambda \end{bmatrix} = 0.$$

From which

$$-\lambda(\frac{\xi_2 q_2(\phi k_4 + \alpha)}{k_3 k_4} - \lambda) = 0. \tag{3.54}$$

Now, on solving Equation (3.54), we have

$$\lambda_1 = 0 \text{ and } \lambda_2 = \frac{\xi_2 q_2(\phi k_4 + \alpha)}{k_3 k_4}.$$

But the basic reproduction number for the HCV-only sub model, R_H, is given by the spectral radius of the dominant eigenvalue.

Thus,

$$\rho(F_H V_H^{-1}) = R_H = \frac{\xi_2 q_2(\phi k_4 + \alpha)}{k_3 k_4}.$$

Therefore, it can be deduced that an increase in HCV transmission probability q_2 and the average number of HCV contact persons, ξ_2, per year, leads to an increase in the HCV secondary infections. An increase in the average period a human remains latently infected with HCV increases the number of secondary HCV infections. Increase in spontaneous clearance of acute HCV, π leads to reduced number of secondary HCV infections. Thus, intervention measures should target reducing both the average number of HCV contact persons, ξ_2, and HCV transmission probability, q_2, while increasing the natural recovery rate of HCV acute humans, π. This conclusion agrees with [54].

Using Theorem 2 from [35], the following result is established.

Lemma 3.5: The local and asymptotic stability of HCV infection-free equilibrium point, E_H^0 exists if $R_H < 1$.

Proof. The local and asymptotic stability of HCV infection-free equilibrium exists if and only if all the eigenvalues of the Jacobian matrix at E_H^0 have negative real parts. The Jacobian matrix $J(E_H)$ of the HCV-only sub model (3.50) at, E_H^0, is given by

$$J(E_H) = \begin{bmatrix} -\left(\frac{\xi_2 q_2(\phi I_A + I_C)}{N_H} + \mu\right) & \pi - \frac{\xi_2 q_2 \phi S}{N_H} & -\frac{\xi_2 q_2 S}{N_H} \\ \frac{\xi_2 q_2(\phi I_A + I_C)}{N_H} & \frac{\xi_2 q_2 \phi S}{N_H} - k_3 & \frac{\xi_2 q_2 S}{N_H} \\ 0 & \alpha & -k_4 \end{bmatrix}.$$

At $E_H^0 = (\frac{\Lambda}{\mu}, 0, 0)$,

$$J(E_H^0) = \begin{bmatrix} -\mu & \pi - \xi_2 q_2 \phi & -\xi_2 q_2 \\ 0 & \xi_2 q_2 \phi - k_3 & \xi_2 q_2 \\ 0 & \alpha & -k_4 \end{bmatrix}.$$

The eigenvalues are determined from the characteristic equation given by

$$\det(\lambda I - J(F_H^0)) = 0.$$

Thus,

$$\det \begin{bmatrix} (\lambda + \mu) & \pi - \xi_2 q_2 \phi & -\xi_2 q_2 \\ 0 & \lambda - \xi_2 q_2 \phi - k_3 & \xi_2 q_2 \\ 0 & \alpha & \lambda + k_4 \end{bmatrix} = 0.$$

$$(\lambda + \mu)(\lambda - (\xi_2 q_2 \phi - k_3))(\lambda + k_4) - \alpha \xi_2 q_2) = 0. \tag{3.55}$$

Now, solving Equation (3.55), we have

$$\lambda_1 = -\mu, \lambda_2 = \frac{-(k_4 - (\xi_2 q_2 \phi - k_3)) - \sqrt{(k_4 - (\xi_2 q_2 \phi - k_3))^2 + 4((\xi_2 q_2 \phi - k_3)k_4 + \alpha \xi_2 q_2)}}{2}$$

$$\text{and } \lambda_3 = \frac{-(k_4 - (\xi_2 q_2 \phi - k_3)) + \sqrt{(k_4 - (\xi_2 q_2 \phi - k_3))^2 + 4((\xi_2 q_2 \phi - k_3)k_4 + \alpha \xi_2 q_2)}}{2}.$$

Clearly, λ_1 and λ_2 have negative real parts. However, the real part of λ_3 is negative when

$$\frac{\sqrt{(k_4 - (\xi_2 q_2 \phi - k_3))^2 + 4((\xi_2 q_2 \phi - k_3)k_4 + \alpha \xi_2 q_2)}}{2} < 0. \tag{3.56}$$

On simplifying inequality (3.56), yields

$$\xi_2 q_2 (\phi k_4 + \alpha) - k_3 k_< - \frac{(k_3 + k_4 - \xi_2 q_2 \phi)^2}{4}.$$

But

$$\xi_2 q_2 (\phi k_4 + \alpha) = R_H k_3 k_4.$$

Therefore,

$$R_H < \left(1 - \frac{(k_3 k_4 - \xi_2 q_2 \phi)^2}{4 k_3 k_4}\right), \text{ implying } R_H < 1.$$

Hence, E_H^0 is locally asymptotically stable if and only if $R_H < 1$. □

3.3.2.6 Global stability of HCV infection free equilibrium for HCV-only sub model with no intervention

Lemma 3.6: The HCV-free equilibrium point E_H^0 of model (3.50) is globally asymptotically stable if $R_H \leq 1$.

Proof. Let $V = Q_1 I_A + Q_2 I_C$ be the Lyapunov function that contains humans who participate in proliferation of the HCV infection in the community, with Q_1 and Q_2 being random positive constants. The derivative of the Lyapunov function with respect to time is computed as

$$\begin{aligned}\frac{dV}{dt} &= Q_1(\lambda_H S - k_3 I_A) + Q_2(\alpha I_A - k_4 I_c),\\ &= Q_1\big(\xi_2 q_2(\phi I_A + I_C)\frac{S}{N} - k_3 I_A\big) + Q_2(\alpha I_A - k_4 I_C).\end{aligned}$$

Since $\frac{S}{N_H} \leq 1$,

$$\frac{dV}{dt} \leq ((\xi_2 q_2 \phi - k_3) + \alpha Q_2) I_A + (\xi_2 q_2 Q_1 - k_4 Q_2) I_C. \tag{3.57}$$

Since constants Q_1 and Q_2 are arbitrarily chosen and are positive, we can let $Q_2 = \frac{\xi_2 q_2 Q_1}{k_4}$. Thus inequality (3.57) becomes

$$\frac{dV}{dt} \leq \frac{Q_1 I_A}{k_4}(\xi_2 q_2(\phi k_4 + \alpha) - k_3 k_4). \tag{3.58}$$

But

$$\xi_2 q_2(\phi k_4 + \alpha) = k_3 k_4 R_H.$$

Thus, inequality (3.58) simplifies to

$$\frac{dV}{dt} \leq Q_1 k_3 I_A(R_H - 1).$$

Therefore, $\frac{dV}{dt} \leq 0$ whenever $R_H \leq 1$. Additionally, $\frac{dV}{dt} = 0$ if either $I_A = I_C = 0$ or $R_H = 1$. In both cases, the greatest compact invariant set of $\Omega_H = \{(S(t), I_A(t), I_C(t) \in \mathbb{R}_+^3) : \frac{dV}{dt} = 0\}$ is the singleton E_H^0. Thus, Lasalle's invariance principle [71] suggests that provided $R_H \leq 1$, E_H^0 is globally asymptotically stable. □

3.3.2.7 The Existence of HCV Endemic State

By considering the persistence of HCV infection in the population, we determine the HCV-endemic equilibrium point, $E_H^* = (S^*, I_A^*, I_C^*)$. Evaluating the derivatives of sub model system (3.50) to zero, we get

$$\Lambda + \pi I_A - (\lambda_H + \mu)S = 0, \tag{3.59}$$

$$\lambda_H S - (\pi + \alpha + \mu + \delta_1)I_A = 0, \tag{3.60}$$

$$\alpha I_A - (\mu + \delta_2)I_C = 0, \tag{3.61}$$

with

$$\lambda_H = \frac{\xi_2 q_2(\phi I_A + I_C)}{N_H}. \tag{3.62}$$

and

$$N_H = S + I_A + I_C. \tag{3.63}$$

Now, substituting for λ_H in Equations (3.59) and (3.60), we get

$$\Lambda + \pi I_A - (\frac{\xi_2 q_2(\phi I_A + I_C)}{N_H} + \mu)S = 0, \tag{3.64}$$

$$\frac{\xi_2 q_2(\phi I_A + I_C)}{N_H} S - k_3 I_A, \tag{3.65}$$

$$\alpha I_A - k_4 I_C = 0, \tag{3.66}$$

Solving for S in Equation (3.65), we have

$$S = \frac{k_3 I_A N_H}{\xi_1 q_1(\phi I_A + I_C)} \tag{3.67}$$

Substituting for S in Equation (3.64) and simplifying, we have

$$\Lambda + \pi I_A - k_3 I_A - \frac{k_3 I_A N_H \mu}{\xi_2 q_2(\phi I_A + I_C)} = 0. \tag{3.68}$$

Now, from Equation (3.66), we have

$$I_C = \frac{\alpha I_A}{k_4}. \tag{3.69}$$

Substituting for I_C in Equation (3.68), we get

$$\Lambda + \pi I_A - k_3 I_A - \frac{k_3 I_A N_H \mu}{\xi_2 q_2 (\phi I_A + \frac{\alpha I_A}{k_4})} = 0. \tag{3.70}$$

Solving for I_A in Equation (3.70), gives

$$I_A = \frac{\Lambda \xi_2 q_2 (\phi k_4 + \alpha) - k_3 k_4 \mu N_H}{\xi_2 q_2 (\phi k_4 + \alpha)(k_3 - \pi)}. \tag{3.71}$$

Solving for I_C in Equation (3.69), we have

$$I_C = \frac{\Lambda \alpha \xi_2 q_2 (\phi k_4 + \alpha) - k_3 k_4 \alpha \mu N_H}{\xi_2 q_2 k_4 (\phi k_4 + \alpha)(k_3 - \pi)}. \tag{3.72}$$

Substituting for I_A and I_C in Equation (3.67) and simplifying, we get the expression for S as

$$S = \frac{N_H k_3 k_4}{\xi_2 q_2 (\phi k_4 + \alpha)} \tag{3.73}$$

Then, the endemic equilibrium point for the HCV-only sub model is given by

$$E_H^* = \Big(\frac{N_H k_3 k_4}{\xi_2 q_2 (\phi k_4 + \alpha)}, \frac{\mu N_H k_3 k_4 - \Lambda \xi_2 q_2 (\phi k_4 + \alpha)}{\xi_2 q_2 (\phi k_4 + \alpha)(\pi - k_3)}, \frac{\alpha \mu N_H k_3 k_4 - \alpha \Lambda \xi_2 q_2 (\phi k_4 + \alpha)}{\xi_2 q_2 k_4 (\phi k_4 + \alpha)(\pi - k_3)} \Big).$$

Lemma 3.7: Whenever $R_H > 1$, then HCV-only sub model (3.50) has a distinctive endemic equilibrium point.

Proof. If the infection stays in the population for some time, then $\frac{dI_A}{dt} > 0$ and $\frac{dI_C}{dt} > 0$, that is

$$\frac{\xi_2 q_2 (\phi I_A + I_C) S}{N_H} - k_3 I_A > 0, \tag{3.74}$$

and

$$\alpha I_A - k_4 I_C > 0. \tag{3.75}$$

Re-writing inequality (3.74), we have

$$k_3 I_A < \xi_2 q_2 (\phi I_A + I_C) \frac{S}{N_H}. \tag{3.76}$$

Using the fact that $\frac{S}{N_H} \leq 1$, inequality (3.76) simplifies to

$$I_A < \frac{\xi_2 q_2(\phi I_A + I_C)}{k_3}. \tag{3.77}$$

Solving for I_C in inequality (3.75), we have

$$I_C < \frac{\alpha I_A}{k_4}. \tag{3.78}$$

Substituting for I_A and I_C in inequality (3.77) and simplifying, we get

$$1 < \frac{\alpha \xi_2 q_2}{k_3 k_4 - k_4 \xi_2 q_2 \phi}. \tag{3.79}$$

Thus, $R_H > 1$.

Hence, a unique endemic equilibrium point E_H^* exists when $R_H > 1$. □

Lemma 3.8: If $R_H > 1$, then the endemic equilibrium E_H^* of the system (3.50) is locally asymptotically stable in Ω_H.

Proof. In order to determine the local and asymptotic stability of E_H^*, the Jacobian matrix of HCV-only sub model at E_H^* should have a negative trace and a positive determinant. Evaluating the Jacobian matrix $J(E_H)$ of the HCV sub-model (3.50) at the endemic equilibrium gives

$$J(E_H^*) = \begin{bmatrix} -(\lambda_H^* + \mu) & (\pi - \frac{\xi_2 q_2 \phi}{R_H}) & -\frac{\xi_2 q_2}{R_H} \\ \lambda_H^* & (\frac{\xi_2 q_2 \phi}{R_H} - k_3) & \frac{\xi_2 q_2}{R_H} \\ 0 & \alpha & -k_4 \end{bmatrix}, \tag{3.80}$$

where λ_H^* is defined as the rate at which susceptible humans acquire HCV infection, evaluated at the endemic equilibrium point.

Now

$$\mathrm{tr}(J(E_H^*)) = \frac{\xi_2 q_2 \phi}{R_H} - (\lambda_H^* + \mu + k_3 + k_4).$$

For negative trace,

$$\frac{\xi_2 q_2 \phi}{R_H} - (\lambda_H^* + \mu + k_3 + k_4) < 0. \tag{3.81}$$

Re-arranging inequality (3.81), gives

$$\frac{R_H(\lambda_H^* + \mu + k_3 + k_4)}{\xi_2 q_2 \phi} > 1. \tag{3.82}$$

Next, consider

$$\det(J(E_H^*)) = \frac{\alpha\mu\xi_2 q_2}{R_H} + \frac{k_4\mu\xi_2 q_2\phi}{R_H} + k_4\pi\lambda_H^* - k_3k_4(\lambda_H^* + \mu).$$

Thus, the $\det(J(E_H^*)) > 0$ when

$$\frac{\alpha\mu\xi_2 q_2 + k_4\mu\xi_2 q_2\phi + k_4\pi\lambda_H^* R_H}{\xi_2 q_2(\phi k_4 + \alpha)(\lambda_H^* + \mu)} > 1. \tag{3.83}$$

However, inequalities (3.82) and (3.83) hold when $R_H > 1$. Hence, the HCV endemic equilibrium, E_H^* is locally asymptotically stable whenever $R_H > 1$ and unstable otherwise. □

3.3.2.8 Global stability of the endemic equilibrium for HCV-only sub model with no intervention

To establish the global stability of the HCV-endemic equilibrium point E_H^* for the HCV-only sub model (3.50), we use the same approach as in Lemma (3.4).

Lemma 3.9: If $R_H > 1$, then the global and asymptotic stability of the HCV endemic equilibrium E_H^* of sub model system (3.50) exists.

Proof. Let the Lyapunov function $U = U(S, I_A, I_C)$ be defined as:

$$U = U_1\Big(S - S^* - S^* In\Big(\frac{S^*}{S}\Big)\Big) + U_2\Big(I_A - I_A^* - I_A^* In\Big(\frac{I_A^*}{I_A}\Big)\Big) + U_3\Big(I_C - I_C^* - I_C^* In\Big(\frac{I_C^*}{I_C}\Big)\Big).$$

Taking derivative of the Lyapunov function U with respect to time along the positive solution of the above system, we obtain,

$$\begin{aligned}
\frac{dU}{dt} &= U_1\Big(1 - \frac{S^*}{S}\Big)\frac{dS}{dt} + U_2\Big(1 - \frac{I_A^*}{I_A}\Big)\frac{dI_A}{dt} + U_3\Big(1 - \frac{I_C^*}{I_C}\Big)\frac{dI_C}{dt}, \\
\frac{dU}{dt} &= U_1\Big(1 - \frac{S^*}{S}\Big)\Big(\Lambda + \pi I_A + \frac{\xi_2 q_2(\phi I_A + I_C)S}{N_H} - \mu S\Big) + U_2\Big(1 - \frac{I_A^*}{I_A}\Big)\Big(\frac{\xi_2 q_2(\phi I_A + I_C)S}{N_H} - k_3 I_A\Big) \\
&\quad + U_3\Big(1 - \frac{I_C^*}{I_C}\Big)\Big(\alpha I_A - k + 4I_C\Big).
\end{aligned}$$

At the HCV endemic equilibrium, we have

$$\Lambda = -\pi I_A^* + \frac{\xi_2 q_2(\phi I_A^* + I_C^*)S^*}{N_H^*} + \mu S^*,$$

$$k_3 = \frac{\xi_2 q_2(\phi I_A^* + I_C^*)S^*}{N_H^* I_A^*},$$

and

$$k_4 = \alpha \frac{I_A^*}{I_C^*}.$$

Now, substituting for Λ, k_3 and k_4 in $\frac{dU}{dt}$, we have

$$\begin{aligned}\frac{dU}{dt} &= U_1\Big(1 - \frac{S^*}{S}\Big)\Big(- \pi I_A^* + \frac{\xi_2 q_2(\phi I_A^* + I_C^*)S^*}{N_H^*} + \mu S^* + \pi I_A + \frac{\xi_2 q_2(\phi I_A + I_C)S}{N_H} - \mu S\Big)\\ &+ U_2\Big(1 - \frac{I_A^*}{I_A}\Big)\Big(\frac{\xi_2 q_2(\phi I_A + I_C)S}{N_H} - \frac{\xi_2 q_2(\phi I_A^* + I_C^*)S^*}{N_H^* I_A^*} I_A\Big) + U_3\Big(1 - \frac{I_C^*}{I_C}\Big)\Big(\alpha I_A - \alpha \frac{I_A^*}{I_C^*} I_C\Big).\end{aligned}$$

Expanding and collecting the positive terms together and the negative terms together, we have

$$\frac{dU}{dt} = C - D,$$

where

$$\begin{aligned}C = &\frac{\xi_2 q_2(\phi I_A^* + I_C^*)S^* U_1}{N_H^*} + \mu S^* U_1 + \pi I_A U_1 + \frac{\pi I_A^* S^* U_1}{S} + \frac{\xi_2 q_2(\phi I_A + I_C)S^* U_1}{S N_H}\\ &+ \mu S^* U_1 + \frac{\xi_2 q_2(\phi I_A + I_C)S U_2}{N_H} + \frac{\xi_2 q_2(\phi I_A^* + I_C^*)S^* U_2}{N_H^*} + \alpha I_A U_3 + \alpha I_A^* U_3,\end{aligned}$$

and

$$\begin{aligned}D = &\pi I_A^* U_1 + \frac{\xi_2 q_2(\phi I_A + I_C)U_1}{N_H} + \mu S U_1 + \frac{\xi_2 q_2(\phi I_A^* + I_C^*)S^* U_1}{S N_H^*} + \frac{\mu S^{*2} U_1}{S} + \frac{\pi I_A S^* U_1}{S}\\ &+ \frac{\xi_2 q_2(\phi I_A^* + I_C^*)S^* I_A U_2}{N_H^* I_A^*} + \frac{\xi_2 q_2(\phi I_A + I_C)S^* I_A^* U_2}{N_H I_A} + \frac{\alpha I_A^* I_C U_3}{I_C^*} + \frac{\alpha I_A I_C^* U_3}{I_C}.\end{aligned}$$

Hence, if $C < D$, then we obtain that $\frac{dU}{dt} \leq 0$, with $\frac{dU}{dt} = 0$ if and only if $S = S^*, I_A = I_A^*, I_C = I_C^*$. Therefore, the largest compact invariant set in $\{(S^*, I_A^*, I_C^*) \in \Omega_H : \frac{dU}{dt} = 0\}$ is singleton $\{E_H^*\}$ where E_H^* is the endemic equilibrium point of the system (3.50). Thus, by Lasalle's Invariant principle [71], it implies that E_H^* is globally asymptotically stable in Ω_H if $C < D$. □

3.3.2.9 The Basic Reproduction number and Equilibrium points for the TB-HCV Co-infection Model with no Intervention

We first consider determining the disease-free equilibrium point E^0, for the TB-HCV co-infection model system (3.4).

The disease-free equilibrium point, $E^0 = (S^0, I_L^0, I_T^0, I_A^0, I_C^0, I_{AL}^0, I_{CL}^0, I_{AT}^0, I_{CT}^0)$ is determined by setting all the infective compartments to zero, that is, $I_L = I_T = I_A = I_C = I_{AL} = I_{CL} = I_{AT} = I_{CT} = 0$.

Thus, model system ((3.4)) reduces to

$$\frac{dS(t)}{dt} = \Lambda - \mu S. \tag{3.84}$$

Now, equating the right-hand side of Equation (3.84) to zero and solving the state variable, we have $S^0 = \frac{\Lambda}{\mu}$.

Therefore, the disease-free equilibrium point, E^0, for the TB-HCV co-infection model is given by $E^0 = (S^0, I_L^0, I_T^0, I_A^0, I_C^0, I_{AL}^0, I_{CL}^0, I_{AT}^0, I_{CT}^0) = (\frac{\Lambda}{\mu}, 0, 0, 0, 0, 0, 0, 0, 0)$.

Next, we consider determining the basic reproduction number R_0 for the TB-HCV co-infection model.

Lemma 3.10: The basic reproduction number R_0 for TB-HCV co-infection model is given by:

$$R_0 = \max\{R_T, R_H\}$$

Proof. The basic reproduction number is calculated using the method of the next generation matrix proposed by [35] for model system (3.4). By determining the matrix, F_i, for the rate of emergence of new cases in component i, and the matrix, V_i, for the rate of movement into and out of component i by all other means, given as below:

$$F_i = \begin{bmatrix} \lambda_T S \\ 0 \\ \lambda_H S \\ 0 \\ \lambda_T I_A + \lambda_H I_L \\ \lambda_T I_C \\ \lambda_H I_T \\ 0 \end{bmatrix},$$

and

$$V_i = \begin{bmatrix} (\theta+\eta+\mu+\lambda_H)I_L \\ -\theta I_L + (\mu+\sigma_1+\lambda_H)I_T \\ (\pi+\alpha+\mu+\lambda_T)I_A \\ -\alpha I_A + (\mu+\delta+\lambda_T)I_C \\ (\tau_1+\mu+\beta_1)I_{AL} \\ -\beta_1 I_{AL} + (\tau_2+\mu+\delta)I_{CL} \\ -\tau_1 I_{AL} + (\beta_2+\mu+d_1)I_{AT} \\ -\tau_2 I_{CL} - \beta_2 I_{AT} + (\mu+d_2)I_{CT} \end{bmatrix}.$$

Now, the Jacobian matrix, F, of the new cases at the disease-free equilibrium, E^0, is determined as

$$F(E^0) = \begin{bmatrix} 0 & \xi_1 q_1 & 0 & 0 & 0 & 0 & \xi_1 q_1 a_1 & \xi_1 q_1 a_2 \\ 0 & 0 & 0 & 0 & 0 & 0 & 0 & 0 \\ 0 & 0 & \xi_2 q_2 \phi & \xi_2 q_2 & \xi_2 q_2 b_1 & \xi_2 q_2 b_2 & \xi_2 q_2 b_3 & \xi_2 q_2 b_4 \\ 0 & 0 & 0 & 0 & 0 & 0 & 0 & 0 \\ 0 & 0 & 0 & 0 & 0 & 0 & 0 & 0 \\ 0 & 0 & 0 & 0 & 0 & 0 & 0 & 0 \\ 0 & 0 & 0 & 0 & 0 & 0 & 0 & 0 \\ 0 & 0 & 0 & 0 & 0 & 0 & 0 & 0 \end{bmatrix}.$$

Then, the Jacobian matrix, V, for the rate of movement from one compartment to another at disease free equilibrium point, E^0, is determined as

$$V(E^0) = \begin{bmatrix} (\theta+\eta+\mu) & 0 & 0 & 0 & 0 & 0 & 0 & 0 \\ -\theta & (\mu+\sigma_1) & 0 & 0 & 0 & 0 & 0 & 0 \\ 0 & 0 & (\pi+\alpha+\mu) & 0 & 0 & 0 & 0 & 0 \\ 0 & 0 & -\alpha & (\mu+\delta) & 0 & 0 & 0 & 0 \\ 0 & 0 & 0 & 0 & (\tau_1+\mu+\beta_1) & 0 & 0 & 0 \\ 0 & 0 & 0 & 0 & -\beta & (\tau_2+\mu+\delta) & 0 & 0 \\ 0 & 0 & 0 & 0 & -\tau_1 & 0 & (\beta_2+\mu+d_1) & 0 \\ 0 & 0 & 0 & 0 & 0 & -\tau_2 & -\beta_2 & (\mu+d_2) \end{bmatrix}.$$

The inverse matrix V^{-1} of $V(E^0)$ is given by

$$V^{-1} = \begin{bmatrix} \frac{1}{(\theta+\eta+\mu)} & 0 & 0 & 0 & 0 & 0 & 0 & 0 \\ \frac{\theta}{(\theta+\eta+\mu)(\mu+\sigma_1)} & \frac{1}{(\mu+\sigma_1)} & 0 & 0 & 0 & 0 & 0 & 0 \\ 0 & 0 & \frac{1}{(\pi+\alpha+\mu)} & 0 & 0 & 0 & 0 & 0 \\ 0 & 0 & \frac{\alpha}{(\pi+\alpha+\mu)(\mu+\delta)} & \frac{1}{(\mu+\delta)} & 0 & 0 & 0 & 0 \\ 0 & 0 & 0 & 0 & \frac{1}{(\tau_1+\mu+\beta_1)} & 0 & 0 & 0 \\ 0 & 0 & 0 & 0 & \frac{\beta}{(\tau_1+\mu+\beta_1)(\tau_2+\mu+\delta)} & \frac{1}{(\tau_2+\mu+\delta)} & 0 & 0 \\ 0 & 0 & 0 & 0 & \frac{\tau_1}{(\tau_1+\mu+\beta_1)(\beta_2+\mu+d_1)} & 0 & \frac{1}{(\beta_2+\mu+d_1)} & 0 \\ 0 & 0 & 0 & 0 & \frac{\beta_2\tau_1(\tau_2+\mu+\delta)+\beta_1\tau_2(\beta_2+\mu+d_1)}{\mathrm{W}} & \frac{\tau_2}{(\tau_2+\mu+\delta)(\mu+d_2)} & \frac{\beta_2}{(\beta_2+\mu+d_1)(\mu+d_2)} & \frac{1}{(\mu+d_2)} \end{bmatrix}.$$

where $\mathrm{W} = (\tau_1 + \mu + \beta_1)(\tau_2 + \mu + \delta)(\beta_2 + \mu + d_1)(\mu + d_2)$.
Then,

$$FV^{-1} = \begin{bmatrix} \frac{\xi_1 q_1 \theta}{(\theta+\eta+\mu)(\mu+\sigma_1)} & \frac{\xi_1 q_1}{(\mu+\sigma_1)} & 0 & 0 & \mathrm{K} & \frac{\xi_1 q_1 a_2 \tau_2}{(\tau_2+\mu+\delta)(\mu+d_2)} & \frac{\xi_1 q_1 (a_1(\mu+d_2)+a_2\beta_2)}{(\eta_2+\mu+d_1)(\mu+d_2)} & \frac{\xi_1 q_1 a_2}{(\mu+d_2)} \\ 0 & 0 & 0 & 0 & 0 & 0 & 0 & 0 \\ 0 & 0 & \frac{\xi_2 q_2(\phi(\mu+\delta)+\alpha)}{(\pi+\alpha+\mu)(\mu+\delta)} & \frac{\xi_2 q_2}{(\mu+\delta)} & \mathrm{T} & \frac{\xi_2 q_2 (b_2(\mu+d_2)+b_1\tau_2)}{(\tau_2+\mu+\delta)(\mu+d_2)} & \frac{\xi_2 q_2 (b_3(\mu+d_2)+b_4\beta_2)}{(\beta_2+\mu+d_1)(\mu+d_2)} & \frac{\xi_2 q_2 b_4}{(\mu+d_2)} \\ 0 & 0 & 0 & 0 & 0 & 0 & 0 & 0 \\ 0 & 0 & 0 & 0 & 0 & 0 & 0 & 0 \\ 0 & 0 & 0 & 0 & 0 & 0 & 0 & 0 \\ 0 & 0 & 0 & 0 & 0 & 0 & 0 & 0 \\ 0 & 0 & 0 & 0 & 0 & 0 & 0 & 0 \end{bmatrix}.$$

where $\mathrm{K} = \frac{\tau_1\xi_1 q_1 a_1(\tau_2+\mu+\delta)(\mu+d_2)+\xi_1 q_1 a_2\left(\beta_2\tau_1(\tau_2+\mu+\delta)+\beta_1\tau_2(\beta_2+\mu+d_1)\right)}{(\tau_1+\mu+\beta_1)(\tau_2+\mu+\delta)(\beta_2+\mu+d_1)(\mu+d_2)}$,

and

$$\mathrm{T} = \frac{\xi_2 q_2(\beta_2+\mu+d_1)(\mu+d_1)\left(b_1(\tau_2+\mu+\delta)+b_2\beta_1\right)+\xi_2 q_2\left(b_3\tau_1(\tau_2+\mu+\delta)(\mu+d_2)+b_4(\beta_2\tau_1\left(\beta_2\tau_1(\tau_2+\mu+\delta)+\beta_1\tau_2(\beta_2+\mu+d_1)\right)\right)}{(\tau_1+\mu+\beta_1)(\tau_2+\mu+\delta)(\beta_2+\mu+d_2)(\mu+d_2)}.$$

Now, on solving the eigenvalues, the dominant eigenvalues for the matrix FV^{-1} are

$$\lambda_1 = \frac{\xi_1 q_1 \theta}{(\mu+\sigma_1)(\theta+\eta+\mu)}, \lambda_2 = \frac{\xi_2 q_2(\phi(\mu+\delta)+\alpha)}{(\pi+\alpha+\mu)(\mu+\delta)}, \lambda_3 =, ..., = \lambda_8 = 0.$$

However, λ_1 and λ_2 correspond to the reproduction numbers for the TB infection sub model and HCV infection sub model respectively. Thus, the basic reproduction number, R_0, for TB-HCV co-infection model is given by

$$\dot{R_0} = \max\{R_T, R_H\}.$$

□

This implies that if $R_T > R_H$, then the dynamics of the co-infection is dependant on TB and vice versa. It is noted that in absence of TB, $R_0 = R_H$ and in absence of HCV, $R_0 = R_T$.

Using Theorem 2 from [35], the subsequent result is proved.

Lemma 3.11: The local and asymptotic stability of the disease-free equilibrium point, E^0, of model system (3.4) exists if $R_0 < 1$.

Proof. The local stability of the disease-free equilibrium, E^0, is determined by computing the Jacobian matrix of the TB-HCV co-infection model system (3.4) and establishing the signs of the eigenvalues of its submatrices, in the upper left corner, J_{11}, the inner submatrix, J_{22} and the lower right-hand corner submatrix, J_{33}.
The disease-free equilibrium is locally asymptotically stable if and only if all the eigenvalues of J_{11}, J_{22} and J_{33} have negative real parts [54, 64]. The Jacobian matrix of the TB-HCV co-infection model at, E^0, is given by

$$J(E^0) = \begin{bmatrix} -\mu & \eta & \xi_1 q_1 & (\pi - \xi_2 q_2 \phi) & -\xi_2 q_2 & -\xi_2 q_2 b_1 & -\xi_2 q_2 b_2 & -(\xi_1 q_1 a_1 + \xi_2 q_2 b_3) & -(\xi_1 q_1 a_2 + \xi_2 q_2 b_4) \\ 0 & -(\theta+\eta+\mu) & \xi_1 q_1 & 0 & 0 & 0 & 0 & \xi_1 q_1 a_1 & \xi_1 q_1 a_2 \\ 0 & \theta & -(\mu+\sigma_1) & 0 & 0 & 0 & 0 & 0 & 0 \\ 0 & 0 & 0 & x_1 & \xi_2 q_2 & \xi_2 q_2 b_1 & \xi_2 q_2 b_2 & \xi_2 q_2 b_3 & \xi_2 q_2 b_4 \\ 0 & 0 & 0 & \alpha & (\mu+\delta) & 0 & 0 & 0 & 0 \\ 0 & 0 & 0 & 0 & 0 & -x_2 & 0 & 0 & 0 \\ 0 & 0 & 0 & 0 & 0 & \beta_1 & -(\tau_2+\mu+\delta) & 0 & 0 \\ 0 & 0 & 0 & 0 & 0 & \tau_1 & 0 & (\beta_2+\mu+d_1) & 0 \\ 0 & 0 & 0 & 0 & 0 & 0 & \tau_2 & \beta_2 & -(\mu+d_2) \end{bmatrix},$$

where $x_1 = (\xi_2 q_2 \phi - (\pi + \alpha + \mu))$ and $x_2 = (\tau_1 + \mu + \beta_1)$.

We now re-write the Jacobian matrix, J, at E^0 as

$$J(E^0) = \begin{bmatrix} J_{11} & J_{12} & J_{13} \\ J_{21} & J_{22} & J_{23} \\ J_{31} & J_{32} & J_{33} \end{bmatrix},$$

where

$$J_{11} = \begin{bmatrix} -\mu & \eta & \xi_1 q_1 \\ 0 & -(\theta+\eta+\mu) & \xi_1 q_1 \\ 0 & \theta & -(\mu+\sigma_1) \end{bmatrix}, J_{12} = \begin{bmatrix} (\pi - \xi_2 q_2 \phi) & -\xi_2 q_2 & -\xi_2 q_2 b_1 \\ 0 & 0 & 0 \\ 0 & 0 & 0 \end{bmatrix},$$

$$J_{13} = \begin{bmatrix} -\xi_2 q_2 b_2 & -(\xi_1 q_1 a_1 + \xi_2 q_2 b_3) & -(\xi_1 q_1 a_2 + \xi_2 q_2 b_4) \\ 0 & \xi_1 q_1 a_1 & \xi_1 q_1 a_2 \\ 0 & 0 & 0 \end{bmatrix},$$

$$J_{21} = \begin{bmatrix} 0 & 0 & 0 \\ 0 & 0 & 0 \\ 0 & 0 & 0 \end{bmatrix}, J_{22} = \begin{bmatrix} (\xi_2 q_2 \phi - (\pi + \alpha + \mu)) & \xi_2 q_2 & \xi_2 q_2 b_1 \\ \alpha & -(\mu + \delta) & 0 \\ 0 & 0 & -(\tau_1 + \mu + \beta_1) \end{bmatrix},$$

$$J_{23} = \begin{bmatrix} \xi_2 q_2 b_2 & \xi_2 q_2 b_3 & \xi_2 q_2 b_4 \\ 0 & 0 & 0 \\ 0 & 0 & 0 \end{bmatrix}$$

and

$$J_{31} = \begin{bmatrix} 0 & 0 & 0 \\ 0 & 0 & 0 \\ 0 & 0 & 0 \end{bmatrix}, J_{32} = \begin{bmatrix} (0 & 0 & \beta_1 \\ 0 & 0 & \tau_1 \\ 0 & 0 & 0 \end{bmatrix}, J_{33} = \begin{bmatrix} -(\tau_2 + \mu + \delta) & 0 & 0 \\ 0 & -(\beta_2 + \mu + d_1) & 0 \\ \tau_2 & \beta_2 & -(\mu + d_2) \end{bmatrix}.$$

Then, we continue to determine the eigenvalues of the sub-matrices J_{11}, J_{22} and J_{33} to establish their signs.

For J_{33}, the corresponding eigenvalues are

$$-(\tau_2 + \mu + \delta), -(\beta_2 + \mu + d_1) \text{ and } -(\mu + d_2).$$

We observe that all the eigenvalues of J_{33} are negative.

For J_{22}, the eigenvalues are

$$\xi_2 q_2 \phi - (\pi + \alpha + \mu), -(\mu + \delta) \text{ and } -(\tau_1 + \mu + \beta_1).$$

We observe that the eigenvalues of J_{22} are all negative when

$$\xi_2 q_2 \phi < (\pi + \alpha + \mu + \delta),$$

from which

$$\frac{\xi_2 q_2 \phi}{(\pi + \alpha + \mu + \delta)} < 1. \tag{3.85}$$

But

$$(\pi + \alpha + \mu + \delta) = \frac{\xi_2 q_2 (\phi(\mu + \delta) + \alpha)}{R_{II}(\mu + \delta)}.$$

Thus, inequality (3.85) becomes

$$\frac{(\mu+\delta)R_H}{\phi(\mu+\delta)+\alpha} < 1. \tag{3.86}$$

However, inequality (3.86) is satisfied only if $R_H < 1$.

Finally, the corresponding eigenvalues of submatrix J_{11} are

$$-\mu, \frac{-(y_1+y_2)-\sqrt{(y_1+y_2)^2-4(y_1y_2-\xi_1q_1\theta)}}{2} \text{ and } \frac{-(y_1+y_2)+\sqrt{(y_1+y_2)^2-4(y_1y_2-\xi_1q_1\theta)}}{2},$$

where

$$y_1 = (\theta+\eta+\mu) \text{ and } y_2 = (\mu+\sigma_1).$$

However, the third eigenvalue is a negative when

$$\sqrt{(y_1+y_2)^2-4(y_1y_2-\xi_1q_1\theta)} < 0,$$
$$4\xi_1q_1\theta < 2y_1y_2-(y_1^2+y_2^2).$$

But

$$\xi_1q_1\theta = y_1y_2R_T.$$

Thus,

$$R_T < \frac{-(y_1-y_2)^2}{4y_1y_2}. \tag{3.87}$$

Thus,

$$R_T < 1. \tag{3.88}$$

Therefore, if inequalities (3.86) and (3.87) are satisfied, then $R_0 < 1$ and hence the disease-free equilibrium point E^0 for model system (3.4), is locally asymptotically stable. □

3.3.2.10 Global stability of the disease-free equilibrium point for TB-HCV co-infection with no intervention

To understand the global behaviour of the system ((3.4)), the method described by Castillo-Chavez *et al.* [76] is deployed. Our model system (3.4) is now expressed in the form:

$$\begin{aligned} \frac{dX}{dt} &= F(X,Y), \\ \frac{dY}{dt} &= G(X,Y), G(X,0) = 0, \end{aligned} \tag{3.89}$$

where $X = (S)$ with $X \in \mathbb{R}_+$ denoting the number of uninfected humans and $Y = (I_L, I_T, I_A, I_C, I_{AL}, I_{CL}, I_{AT}, I_{CT})$ with $Y \in \mathbb{R}_+^8$ whose components denote the number of humans infected with TB-only or HCV-only or both TB and HCV. Let the disease-free equilibrium of our system (3.4) be denoted by $E^0 = (X^0, 0) = (\frac{\Lambda}{\mu}, 0)$. We have to establish that the subsequent conditions are met to guarantee global asymptotic stability.

$$\begin{aligned} &(C1) : \text{For } \frac{dX}{dt} = F(X,0), X^0 \text{ is globally asymptotically stable,} \\ &(C2) : G(X,Y) = AY - \hat{G}(X,Y), \hat{G}(X,Y) \geq 0, \text{for } (X,Y) \in \Omega, \end{aligned}$$

where $A = D_Y G(X^0, 0)$ is a Metzler matrix (the off diagonal elements of Metzler are no-negative) and Ω is the region where the model makes biological meaning.

Thus, when system (3.89) satisfies conditions$(C1)$ and $(C2)$, we have the following Theorem satisfied.

Theorem 4. *The equilibrium point $E^0 = (X^0, 0)$ is globally asymptotically stable point of system (3.89) provided $R_0 < 1$ and that conditions $(C1)$ and $(C2)$ are satisfied.*

Proof. From Lemma 3.11, E^0 is locally asymptotically stable if $R_0 < 1$. For the first condition $(C1)$, that is, the global asymptotic stability of X^0, we have,

$$F(X,Y) = \Big[\Lambda + \pi I_A + \eta I_L - (\lambda_T + \lambda_H + \mu)S\Big]$$

and

$$\frac{dX}{dt} = F(X,0) = \Lambda - \mu S,$$

which is a linear differential equation. Solving it we get

$$S(t) = \frac{\Lambda}{\mu} - \frac{\Lambda}{\mu}e^{-\mu t} + S(0)e^{-\mu t}.$$

Now, as $t \to \infty$, $S \to \frac{\Lambda}{\mu}$ regardless of the value of $S(0)$. Thus, there is convergence in Ω implying that $(C1)$ holds.

For the second condition $(C2)$, consider

$$G(X,Y) = \begin{bmatrix} G_1(X,Y) \\ G_2(X,Y) \\ G_3(X,Y) \\ G_4(X,Y) \\ G_5(X,Y) \\ G_6(X,Y) \\ G_7(X,Y) \\ G_8(X,Y) \end{bmatrix} = \begin{bmatrix} \lambda_T S - (\theta + \eta + \mu + \lambda_H) I_L \\ \theta I_L - (\mu + \sigma_1 + \lambda_H) I_T \\ \lambda_H S - (\pi + \alpha + \mu + \lambda_T) I_A \\ \alpha I_A - (\mu + \delta + \lambda_T) I_C \\ \lambda_T I_A + \lambda_H I_L - (\tau_1 + \mu + \beta_1) I_{AL} \\ \beta_1 I_{AL} + \lambda_T I_C - (\tau_2 + \mu + \delta) I_{CL} \\ \tau_1 I_{AL} + \lambda_H I_T - (\beta_2 + \mu + d_1) I_{AT} \\ \tau_2 I_{CL} + \beta_2 I_{AT} - (\mu + d_2) I_{CT} \end{bmatrix},$$

and

$$A = \begin{bmatrix} -(\theta + \eta + \mu) & \xi_1 q_1 & 0 & 0 & 0 & 0 & 0 & 0 \\ \theta & -(\mu + \sigma_1) & 0 & 0 & 0 & 0 & 0 & 0 \\ 0 & 0 & (\xi_2 q_2 \phi - (\pi + \alpha + \mu)) & \xi_2 q_2 & \xi_2 q_2 b_1 & \xi_2 q_2 b_2 & \xi_2 q_2 b_3 & \xi_2 q_2 b_4 \\ 0 & 0 & \alpha & -(\mu + \delta) & 0 & 0 & 0 & 0 \\ 0 & 0 & 0 & 0 & -(\tau_1 + \mu + \beta_1) & 0 & 0 & 0 \\ 0 & 0 & 0 & 0 & \beta_1 & -(\tau_2 + \mu + \delta) & 0 & 0 \\ 0 & 0 & 0 & 0 & \tau_1 & 0 & -(\beta_2 + \mu + d_1) & 0 \\ 0 & 0 & 0 & 0 & 0 & \tau_2 & \beta_2 & -(\mu + d_2) \end{bmatrix}.$$

Now, from

$$\hat{G}(X,Y) = AY - G(X,Y)$$

$$\hat{G}(X,Y) = \begin{bmatrix} \hat{G}_1(X,Y) \\ \hat{G}_2(X,Y) \\ \hat{G}_3(X,Y) \\ \hat{G}_4(X,Y) \\ \hat{G}_5(X,Y) \\ \hat{G}_6(X,Y) \\ \hat{G}_7(X,Y) \\ \hat{G}_8(X,Y) \end{bmatrix} = \begin{bmatrix} \xi_1 q_1 I_T - \lambda_T S + \lambda_H I_L \\ \lambda_H I_T \\ \xi_2 q_2 \big(\phi I_A + I_C + I_{AL} + I_{CL} + b_3 I_{AT} + b_4 I_{CT}\big) - \lambda_H S + \lambda_T I_A \\ \lambda_T I_C \\ -\lambda_T I_A - \lambda_H I_L \\ -\lambda_T I_C \\ -\lambda_H I_T \\ 0 \end{bmatrix}$$

Since $\hat{G}_5(X,Y) < 0, \hat{G}_6(X,Y) < 0$ and $\hat{G}_7(X,Y) < 0$, then $\hat{G}(X,Y) \not> 0$. This implies that condition $C2$ is not satisfied. Therefore, the disease-free equilibrium, $E^0 = (X^0, 0)$, may not be globally asymptotically stable for $R_0 < 1$. □

3.3.2.11 Existence of TB-HCV co-infection with no Intervention Endemic Equilibr

The endemic equilibrium point for TB-HCV co-infection model (3.4) does exist if $R_T > 1$ $R_H > 1$, that is $R_0 = \max\{R_T, R_H\} > 1$. However, the explicit computation of the enc equilibrium for the TB-HCV co-infection in terms of the model parameters is analytically cl Thus, the existence and stability are investigated through numerical simulations. The starting v of the variables, $S, I_L, I_T, I_A, I_C, I_{AL}, I_{CL}, I_{AT}, I_{CT}$ are changed to establish whether they settle t same values greater than zero with time, regardless of the dissimilar starting values of the varia In the numerical analysis, the values of the parameters used are shown in Table 3.4.

In Figures 3.2, 3.3 and 3.4, the starting values of humans who are at a risk of contracting

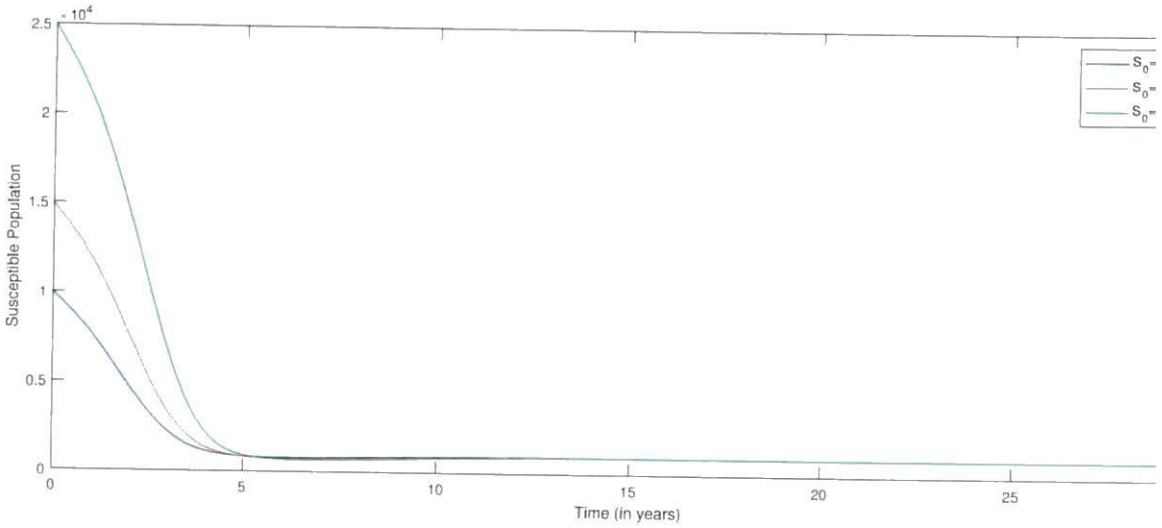

Figure 3.2: A graph of Susceptible humans against time with varied values of Susceptibles only

and HCV infections, $S(0)$; TB latently infected humans, $I_L(0)$; Infectious TB humans, $I_T(0)$; a HCV infectious humans, $I_A(0)$; chronic HCV infectious humans, $I_C(0)$; TB latent and acute H co-infected humans, $I_{AL}(0)$; TB latent and chronic HCV co-infected humans, $I_{CL}(0)$; TB infect and acute HCV dually infected humans, $I_{AT}(0)$ and TB infectious and chronic HCV dually infe humans, $I_{CT}(0)$ are changed for each variable at a time while maintaining starting values of the ot variables.

Figure 3.2 shows that over time, regardless of the starting value of humans at a risk of contracting and HCV infections, the number of humans that remain likely to contract TB and HCV infecti is identical. Similarly, in Figures 3.3 and 3.4, initial values of each of the respective infected co-infected variables are changed while maintaining values of other state variables. Over time i

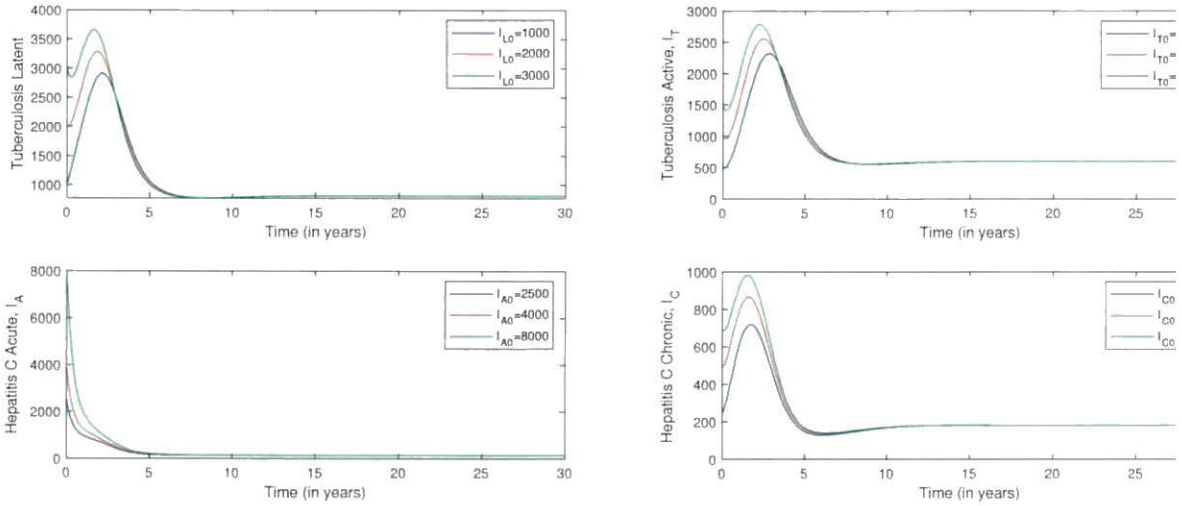

Figure 3.3: A graph of Infected humans against time with varied values of respective infectives only

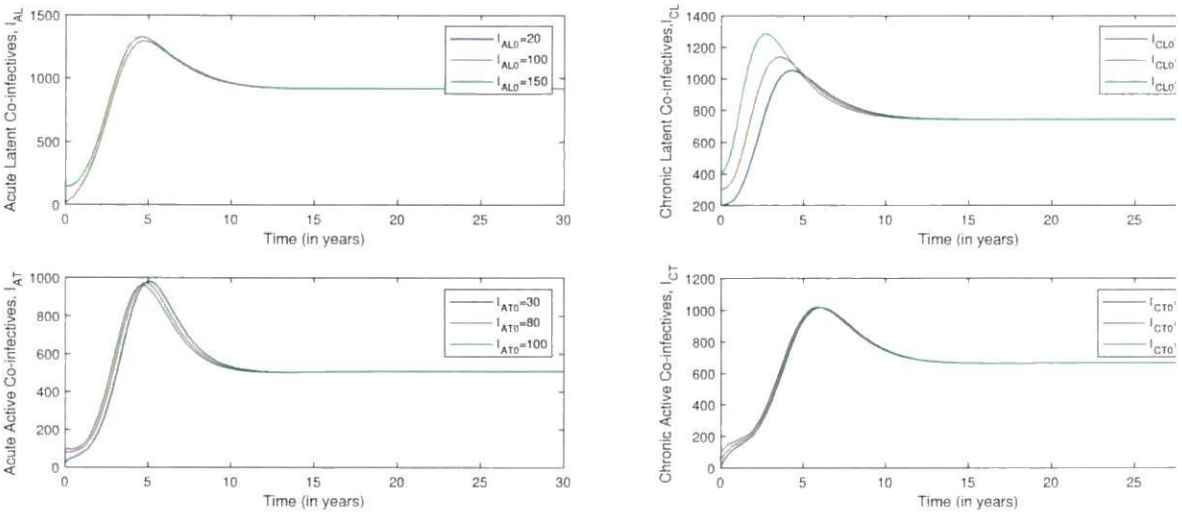

Figure 3.4: A graph of Co-infected humans against time with varied values of respective co-infectives o

revealed that the number of humans left infected and co-infected is the same. This can be conclu that there is a globally stable endemic equilibrium for TB-HCV co-infection model.

3.3.3 Sensitivity Analysis

With the aim of establishing how to decrease human death and morbidity rates due to TB infect HCV infection and their co-infection, it is imperative to be aware of the significance of the gi parameters in the dynamics of the infection. This helps us to know the suitable intervention pla action that can be taken to curb the infection. Here, we compute the sensitivity indices of the b reproduction number, $R_0 = \max\{R_T, R_H\}$, with respect to the parameters in TB-HCV co-infect model (3.4). This is done using the normalized forward sensitivity index method by Chitnis *et al.* [

Definition: The normalized forward sensitivity index of a variable, Z, that depends differentiable on a parameter, p, is defined as a ratio of relative change in Z to the relative change in parameter, p, that is

$$i_p^Z = \frac{\partial Z}{\partial p} \times \frac{p}{Z}.$$

Now, since $R_0 = \max\{R_T, R_H\}$, the sensitivity analysis of R_0 with respect to each of the parameters is analysed by way of the sensitivity indices of R_T and R_H. Thus, implicitly, the decisive parameters shall entirely be dependent on the predominant infection.

3.3.3.1 Sensitivity Indices of R_T

These are computed using the formula

$$i_p^{R_T} = \frac{\partial R_T}{\partial p} \times \frac{p}{R_T}.$$

Thus, the sensitivity indices of R_T with respect to $\xi_1, q_1, \theta, \mu, \sigma_1$ and η are:

$$\begin{aligned}
i_{\xi_1}^{R_T} &= \frac{\partial R_T}{\partial \xi_1} \times \frac{\xi_1}{R_T} = \frac{q_1\theta}{(\mu+\sigma_1)(\theta+\eta+\mu)} \times \frac{\xi_1}{R_T} = 1, \\
i_{q_1}^{R_T} &= \frac{\partial R_T}{\partial q_1} \times \frac{q_1}{R_T} = \frac{\xi_1\theta}{(\mu+\sigma_1)(\theta+\eta+\mu)} \times \frac{q_1}{R_T} = 1, \\
i_{\sigma_1}^{R_T} &= \frac{\partial R_T}{\partial \sigma_1} \times \frac{\sigma_1}{R_T} = \frac{-\sigma_1}{(\mu+\sigma_1)} = -0.7877, \\
i_{\eta}^{R_T} &= \frac{\partial R_T}{\partial \eta} \times \frac{\eta}{R_T} = \frac{-\eta}{(\theta+\eta+\mu)} = -0.6239, \\
i_{\theta}^{R_T} &= \frac{\partial R_T}{\partial \theta} \times \frac{\theta}{R_T} = \frac{(\eta+\mu)}{(\theta+\eta+\mu)} = 0.3219, \\
i_{\mu}^{R_T} &= \frac{\partial R_T}{\partial \mu} \times \frac{\mu}{R_T} = -\mu\Big(\frac{1}{(\theta+\eta+\mu)} + \frac{1}{(\mu+\sigma_1)}\Big) = -0.0949.
\end{aligned}$$

3.3.3.2 Sensitivity Indices of R_H

These are computed using the formula

$$i_p^{R_H} = \frac{\partial R_H}{\partial p} \times \frac{p}{R_H}.$$

Table 3.3: Sensitivity indices of R_T and R_H with respect to parameters

Basic Reproduction Number	Parameter	Sensitivity Index
R_T	ξ_1	+1.0000
	q_1	+1.0000
	σ_1	-0.7877
	η	-0.6239
	θ	+0.3219
	μ	-0.0949
R_H	ξ_2	+1.0000
	q_2	+1.0000
	δ	-0.7568
	α	+0.1640
	π	-0.0973
	ϕ	+0.0771
	μ	-0.0227

Therefore, the sensitivity indices of R_H with respect to $\xi_2, q_2, \phi, \delta, \alpha, \pi$ and μ are:

$$
\begin{aligned}
i_{\xi_2}^{R_H} &= \frac{\partial R_H}{\partial \xi_2} \times \frac{\xi_2}{R_H} = \frac{q_2(\phi(\mu+\delta)+\alpha)}{(\pi+\alpha+\mu)(\mu+\delta)} \times \frac{\xi_2}{R_H} = 1,\\
i_{q_2}^{R_H} &= \frac{\partial R_H}{\partial q_2} \times \frac{q_2}{R_H} = \frac{\xi_2(\phi(\mu+\delta)+\alpha)}{(\pi+\alpha+\mu)(\mu+\delta)} \times \frac{\xi_2}{R_H} = 1,\\
i_{\phi}^{R_H} &= \frac{\partial R_H}{\partial \phi} \times \frac{\phi}{R_H} = \frac{\phi(\mu+\delta)}{\phi(\mu+\delta)+\alpha} = 0.0771,\\
i_{\pi}^{R_H} &= \frac{\partial R_H}{\partial \pi} \times \frac{\pi}{R_H} = \frac{-\pi}{(\pi+\alpha+\mu)} = -0.0973,\\
i_{\delta}^{R_H} &= \frac{\partial R_H}{\partial \delta} \times \frac{\delta}{R_H} = \frac{-\alpha\delta}{\phi(\mu+\delta)+\alpha} = -0.7567,\\
i_{\alpha}^{R_H} &= \frac{\partial R_H}{\partial \alpha} \times \frac{\alpha}{R_H} = \frac{\alpha\big(-\phi(\mu+\delta)+(\pi+\mu)\big)}{(\pi+\alpha+\mu)(\phi(\mu+\delta)+\alpha)} = 0.1640,\\
i_{\mu}^{R_H} &= \frac{\partial R_H}{\partial \mu} \times \frac{\mu}{R_H} = \mu\Big(\frac{\phi}{(\phi\mu+\phi\delta+\alpha)} - \frac{1}{(\mu+\pi+\alpha)} - \frac{1}{(\mu+\delta}\Big) = -0.0227.
\end{aligned}
$$

Sensitivity indices for both R_T and R_H are presented in Table 3.3 in which the parameters are arranged from the most sensitive to the least ones.

3.3.3.3 Interpretation of the Sensitivity Indices

From Table 3.3, for a parameter with a positive index, it signifies that the corresponding basic reproduction number decreases (or increases) with decrease (or increase) in that parameter, while keeping other parameters unchanged. For example, $i_{\xi_1}^{R_T} = 1$, means that decreasing (or increasing)

the value of the rate of human-to-human contact between the TB infected individuals and susceptible population, ξ_1 by say, 10%, while keeping the other parameter values constant, decreases (or increases) the value of R_T by 10%. Similarly, $i_\theta^{R_T} = 0.3219$ means that increasing (or decreasing) of θ by 10% increases (or decreases) R_T by 3.219%.

On the other hand, the negative sign of the sensitivity index of say R_T with respect to σ_1, η and μ means an inverse relationship between the parameters and R_T. For instance, a 20% decrease (or increase) in the value of the natural recovery rate of TB latent humans, η, while maintaining the value of the other parameters, increases (or decreases) the value of R_T by about 12.4%.

It is noted that the spread of TB infection rises when the values of ξ_1, q_1 and θ are increased and the ones of σ_1, η and μ are decreased. The most sensitive parameters in TB infection are the rate of human-to-human contact between the TB infected individuals and susceptible population ξ_1 and the likelihood of a contact resulting in TB transmission, q_1 followed by the disease induced death rate, σ, for humans infected with active TB. Therefore, the interventions need to target and aim at reducing the values of ξ_1, q_1 and the rate of progression, θ, from latent to infectious TB stage.

It is also noted that the endemicity of HCV infection increases when the values of the rate of human-to-human contact between the HCV infected individuals and susceptible population, ξ_2, the likelihood of a contact resulting in HCV transmission, q_2 and the progression rate, α, from acute HCV to chronic stage are increased and those of δ, π and μ are decreased. The most sensitive parameters in HCV infection are ξ_2 and q_2 followed by α. Thus, interventions to reduce HCV infection should aim and concentrate on decreasing values of ξ_2, q_2 and α. Therefore, strategies for TB and HCV control should target behaviours that reduce the contact rates for both diseases. Such strategies include screening and isolation, wearing of face masks for TB infected humans and screening, sterilization of surgical instruments and use of condoms for HCV cases.

It is noted from sensitivity analysis that, the rate of human-to-human contact between the TB (or HCV) infected individuals and susceptible population together with the likelihood of a contact resulting in TB or HCV transmission are equally likely to increase TB (or HCV) infection. Besides, their increase leads to increase in almost all other parameters.

Therefore, efforts such as screening and isolation, wearing face masks by TB infected persons and avoiding sharing surgical instruments during blood transfusion should be undertaken. Also, early treatment needs to be sought by the latent TB humans and acute HCV humans to avoid progression to infectious TB and chronic HCV stages respectively.

Now, substituting for the parameter values in Table 3.4 into R_T and R_H, we have $R_T = 3.816$ and $R_H = 1.378$. We observe that, the basic reproduction number R_0 of the TB-HCV co-infection model is concluded as

$$R_0 = \max\{R_T, R_H\} = \max\{3.816, 1.378\} = 3.816.$$

Thus, the dynamics of TB-HCV co-infection is majorly influenced by TB.

3.4 Numerical Simulations

In the above sections, we have discussed the analytical behaviours of the TB-HCV co-infection model as well as the sub models. Here, we carry out numerical simulations to support the analytical solutions by studying the TB-HCV co-infection dynamics without intervention. We assume initial values of the state variables to be $S(0) = 10000, I_L(0) = 200, I_T(0) = 500, I_A(0) = 150, I_C(0) = 400, I_{AL}(0) = 100, I_{CL}(0) = 100, I_{AT}(0) = 100$ and $I_{CT}(0) = 100$ and parameter values as described in Table 3.4, the model was simulated using ODE 45 solver coded in MATLAB computer software. Both situations for $R_0 > 1$ and $R_0 < 1$ are considered with parameter modifications.

In Figure 3.5, we note that the local stability of the endemic equilibrium of TB-HCV co-infection model does exist since the system goes to equilibria after about 10 years. This happens for $R_T = 3.816 > 1$ and $R_H = 1.378 > 1$.

Figure 3.6, we realize that without treatment for both TB and HCV, the number of humans susceptible to TB and HCV, decrease asymptotically to less than 10% in about 5 years. This is because more humans continue contracting TB and HCV with no intervention.

Figure 3.7, the number of humans infected with latent TB, I_L, starts increasing and over time tends to a steady state at a low level. This is due to progression to infectious TB and natural

Table 3.4: The TB-HCV Co-infection Model Parameter values

Parameter	Value/yr^{-1}	Source
μ	0.02	[49]
σ_1	0.0575	[49]
δ	0.82	[58]
d_1	0.6	Assumed
d_2	0.8	Assumed
θ	0.25	[57]
α	2	[54]
τ_1	0.00013	Assumed
τ_2	0.00015	Assumed
β_1	0.00014	Assumed
β_2	0.00016	Assumed
η	0.4405	[54]
π	0.27	[54]
ϕ	0.20	Assumed
ξ_1, ξ_2	4, 2 people respectively	[57, 58]
q_1, q_2	0.08, 0.07 respectively	[57, 58]
a	1.002	Assumed
b_1, b_2, b_3 and b_4	1.003, 1.002, 1.005, 1.001 respectively	Assumed

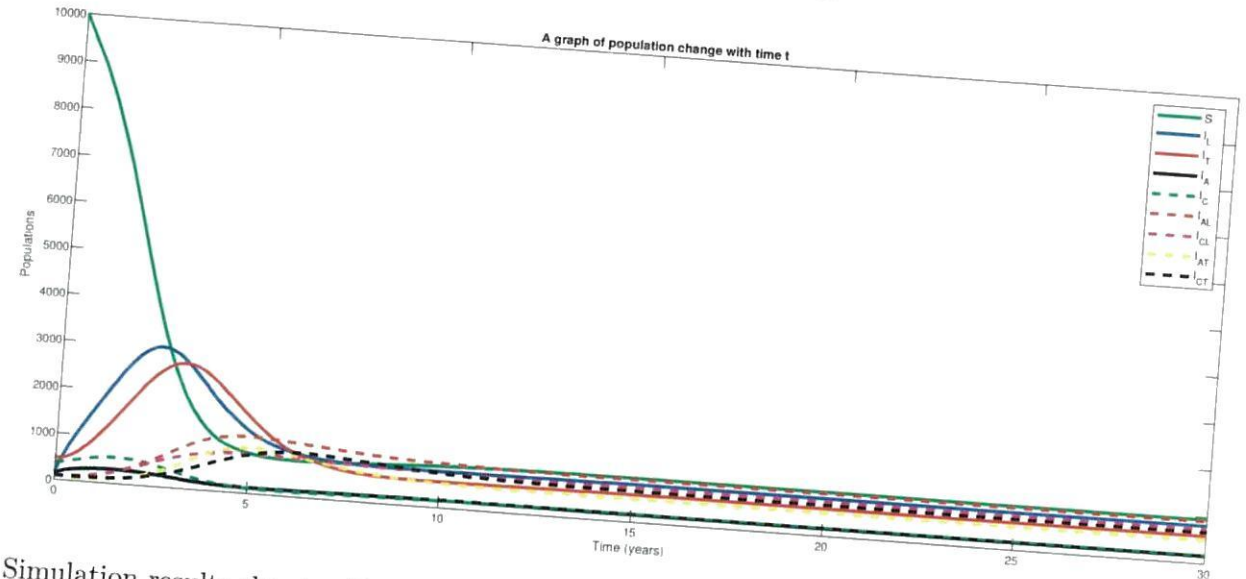

ure 3.5: Simulation results showing Susceptible, mono-infected and co-infected humans against time

overy to susceptible class. The number of infectious TB humans, I_T, starts by increasing and in process decline to a steady state at a low level. This is due to progression to dually infected ses.

number of acute HCV humans, I_A, is seen to increase at the start and over time reduce to steady . Due to progression of acute HCV humans to chronic HCV class, the number of chronic HCV ans, I_C, increase at first and later on reduce to steady state.

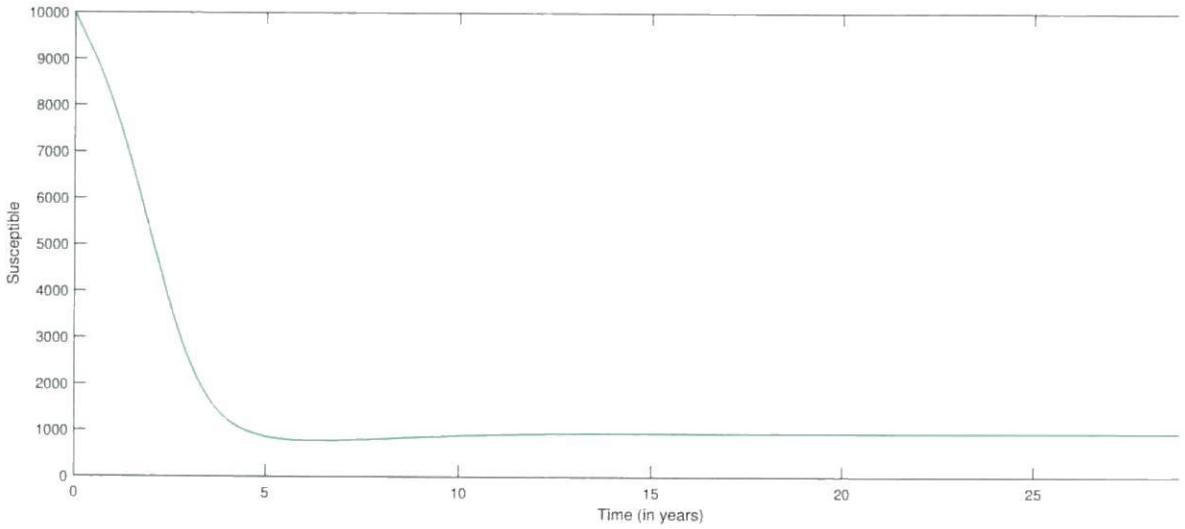

Figure 3.6: Simulation results showing Susceptible humans against time

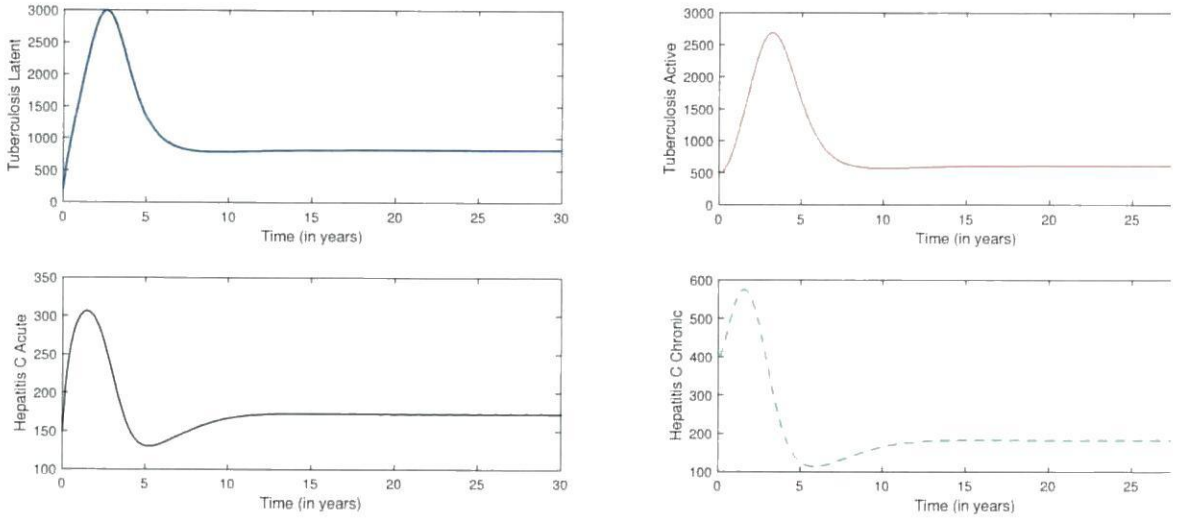

Figure 3.7: Simulation results showing mono-infected humans against time

From Figure 3.8, the number of humans co-infected with latent TB and acute HCV begins to and later on reduce asymptotically to slightly low steady level. Similarly, the number of infec humans from the dually infected classes I_{CL}, I_{AT} and I_{CT} increases in the beginning and over t reduce asymptotically to slightly lower steady levels.

From Figures 3.7 and 3.8 it is observed that:

1. Co-infected classes, I_{AL}, I_{CL}, I_{AT} and I_{CT}, over time decline asymptotically to attain stabi to levels higher than those at which mono-infected classes I_L, I_T, I_A and I_C attain stability

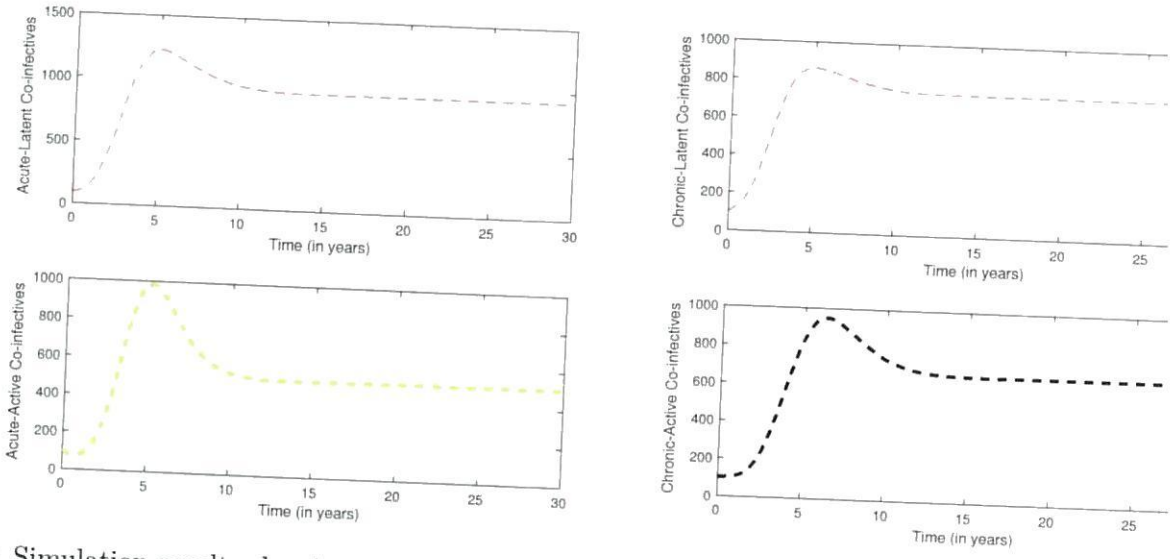

Figure 3.8: Simulation results showing co-infected humans against time

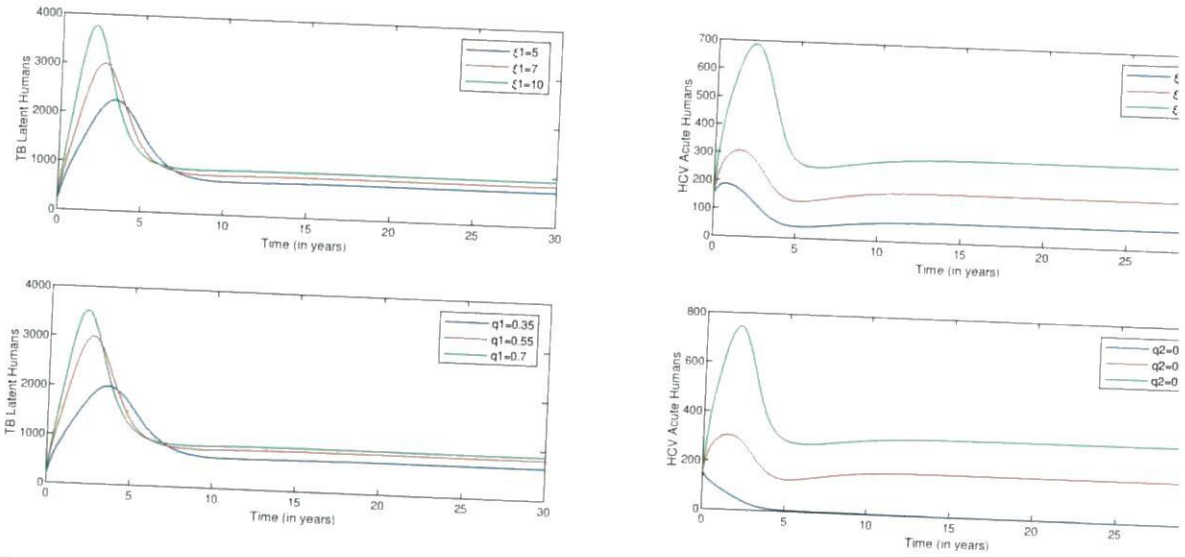

Figure 3.9: Simulation results showing TB latent humans and HCV aute humans against time with varie values of ξ_1, ξ_2, q_1 and q_2

2. Co-infected classes over time take longer to attain steady state compared to mono-infecte classes. Whereas mono-infected classes take about 5 years, the dually infected classes tak about 10 years to attain stability.

Figure 3.9 explains the effect of the rate of human-to-human contact between the TB (or HCV infected individuals and susceptible population on the number of TB latent or HCV acute humans It shows that an increase in the rate of human-to-human contact between the TB (or HCV) infected individuals and susceptible population leads to the increase in the number of TB latent or HCV acute humans and vice versa. Relatedly, an increase in the likelihood of a contact resulting in TB (or HCV) transmission leads to increase in the rate of transmission of TB-HCV infection and vice

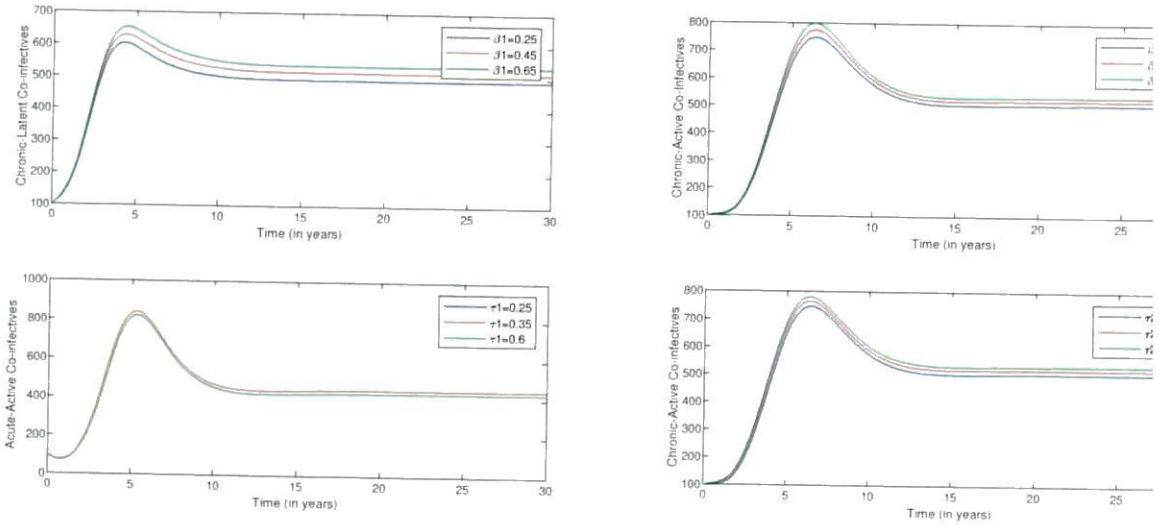

Figure 3.10: Graphs of humans co-infected with chronic HCV and latent TB, I_{CL}, chronic HCV and ac TB, I_{CT}, acute HCV and active TB I_{aT} and chronic HCV and active TB, I_{CT} against time when β_1, β_2 and τ_2 are respectively varied.

versa.

Figure 3.10 shows the dynamics of humans co-infected with chronic HCV and latent TB, I_{CL}, chr HCV and active TB, I_{CT}, acute HCV and active TB I_{AT} and chronic HCV and active TB, I_{CT} v changing values of β_1, β_2, τ_1 and τ_2 respectively.

Generally, the graphs indicate that an increase in the rates of progression, say β_1, β_2, τ_1 or τ_2 fr one co-infected class leads to increase in the number of co-infected humans in another class. T leads to escalation of the disease among the humans. However, as time passes by, all the gra begin to fly horizontally regardless of the dissimilar values of the individual parameters. Thus, th is dire need to introduce the dually infected humans to some interventions, say treatment.

3.5 Discussion and Conclusion

In this Chapter, a TB-HCV co-infection model with no intervention was developed and analys The positivity and boundedness properties of the model solutions in a biologically feasible regi were verified. The steady-states of the sub models and their stability with respect to the ba reproduction numbers were analysed. In both sub models, the disease-free equilibrium points a found to be locally asymptotically stable provided their respective reproduction numbers are l than unity. The unique endemic equilibrium points, E_T, for TB sub model and E_H, for HCV s model exist whenever their corresponding reproduction numbers R_T and R_H are greater than uni

The disease-free equilibrium, E^0, may not be globally asymptotically stable for $R_0 < 1$, indicating a backward bifurcation will occur at $R_0 = 1$ as proved in Feng et al. (2000). However, the equilibrium points, E^0 and E^*, for TB-HCV co-infection model are both locally asymptotically stable.

From numerical simulations, the number of TB latent humans, HCV acute humans and the number of dually infected humans increase with the rate of human-to-human contact between the TB (or HCV) infected individuals and susceptible population. The number is also proportional to the likelihood of a contact resulting in TB (or HCV) transmission and the progression rate from TB latent or HCV acute to TB active or HCV chronic stage. Therefore, it is necessary to mitigate and eradicate the infections.

From sensitivity analysis, decreasing the rate of human-to-human contact between the TB (or HCV) infected individuals and susceptible population is the major effective way to manage the spread of TB or HCV infection. Hence, strategies such as health education campaigns to communities targeting reducing the transmission rates of TB and HCV could help to reduce the progression of latent TB and acute HCV humans to infectious TB and chronic HCV humans respectively. These could include screening and isolation, wearing of face masks for TB cases and screening, sterilization of surgical instruments and use of condoms for HCV infected humans. The current model comes with limitations in accessing real data since there are no mathematical studies that deeply explore the co-infection burden of TB and HCV. Including intervention strategies against both TB and HCV infections in the current model could further improve our understanding of the control dynamics of both diseases.

Chapter 4

Analysis of a Mathematical Model on the Dynamics of TB-HCV Co-infection with Medication

4.1 Introduction

The model in this Chapter provides new insights through a dynamic modelling framework that highlights the crucial role of treatment in reducing the transmission of TB and HCV infections, ultimately informing policymakers on evidence-based interventions to decrease the spread of both infections.

4.2 Description and Formulation of the Model

4.2.1 Description of the TB-HCV Co-infection Dynamics

The model categorises the human population into thirteen distinct and separate groups ascending to their epidemiological status, namely susceptible individuals capable of acquiring TB or HCV ($S(t)$), TB infected, latent and not contagious ($I_L(t)$), tuberculosis infectious individuals ($I_T(t)$), tuberculosis infectious hospitalized individuals on medication ($H(t)$), tuberculosis treated individuals ($R_T(t)$), HCV acutely infectious individuals but with no symptoms ($I_A(t)$), HCV chronically infectious individuals with symptoms ($I_C(t)$), HCV under treatment individuals ($R_H(t)$), individuals with acute HCV infection and latent TB, not infectious with TB but infectious with HCV ($I_{AL}(t)$), dually infected

humans with HCV chronic infection in the latent TB stage, non-infectious for TB but infectious for HCV ($I_{CL}(t)$), individuals with acute HCV infection in the infectious stage of TB ($I_{AT}(t)$), individuals with chronic HCV infection in infectious stage of TB ($I_{CT}(t)$) and individuals under treatment of the dual infection ($R(t)$).

The medication for HCV patients shall be considered only at the HCV chronic stage. This is because HCV acute stage is often short and asymptomatic in relation to the lengthy and symptomatic HCV chronic stage. Thus, diagnosis of HCV patients is at the chronic phase of the infection [45, 112]. The total population at time t, represented by $N(t)$, is defined as

$$N(t) = S(t)+I_L(t)+I_T(t)+H(t)+R_T(t)+I_A(t)+I_C(t)+R_H(t)+I_{AL}(t)+I_{CL}(t)+I_{AT}(t)+I_{CT}(t)+R(t).$$

No matter when, there is a steady inflow into the susceptible class, $S(t)$, through birth and immigration at a rate Λ. A constant natural mortality rate, μ exists in all sub-populations.
Susceptible humans acquire TB to move to latent TB class, $I_L(t)$ at a rate λ_T defined by:

$$\lambda_T(t) = \frac{\xi_1 q_1 \big(I_T(t) + \epsilon H(t) + a(I_{AT}(t) + I_{CT}(t))\big)}{N(t)}, \tag{4.1}$$

where ξ_1 is the rate of human-to-human contact between the TB infected individuals and susceptible population; q_1 is the likelihood of a contact resulting in TB transmission; a is the enhancement factor for the increased risk of easily contracting TB from a dually infected human in classes I_{AT} and I_{CT}. The parameter a accounts for increased infectiousness in dually infected humans compared to those with TB only [49]. ϵ is the reduction parameter considering for the reduced risk of being infected with TB by a hospitalized TB infected human.

Similarly, susceptible humans get infected with HCV to move to the acute class, $I_A(t)$, at a rate λ_H, defined by (4.2),

$$\lambda_H(t) = \frac{\xi_2 q_2 \big(\phi I_A(t) + I_C(t) + b_1 I_{AL}(t) + b_2 I_{CL}(t) + b_3 I_{AT}(t) + b_4 I_{CT}(t)\big)}{N(t)}, \tag{4.2}$$

where, ξ_2 is the rate of human-to-human contact between the HCV infected individuals and susceptible population; q_2 is the likelihood of a contact resulting in HCV transmission; b_1, b_2, b_3 and b_4 are enhancement factors for the increased risk of easily contracting HCV from a dually infected individual

in classes I_{AL}, I_{CL}, I_{AT} and I_{CT}, respectively. Dual infected individuals are more infectious of HCV as compared to their counterparts who are mono-infected. We note that $b_1, b_3 > b_2, b_4 > 1$, considering the fact that an HCV acutely infected human is more infectious than the HCV chronically infected human due to higher viral loads during the early stages of the infection. ϕ is the amplification parameter catering for the increased risk of being infected with HCV from a singly-acute HCV infected individual.

TB latently infected humans, I_L, either recover naturally due to strong immune system at a rate η and return to susceptible class or progress to active TB class, $I_T(t)$, at a rate θ. Once humans infected with active TB are tested positive, some are put on medication while attended to from home at a rate ω_1 to join the $R_T(t)$ class, whereas others are hospitalized at a rate ρ to join the $H(t)$ class. While in hospital, the active TB patients receive treatment at a rate ω_2 to also join the $R_T(t)$ class. Individuals in classes $I_T(t)$ and $H(t)$ not only die naturally, but also die from active TB at a rate σ_1 and σ_2 respectively. Acute HCV humans that happen to recover naturally return to the susceptible class at a rate π, while others progress to the chronic HCV class, $I_C(t)$, at a rate α. Having been detected with chronic HCV, the infected humans are put on treatment at a rate ψ to join the $R_H(t)$ class. Latent TB and active TB individuals in classes $I_L(t)$ and $I_T(t)$ respectively, at a rate of λ_H, become infected with HCV and transit to state $I_{AL}(t)$ and $I_{AT}(t)$ respectively. Similarly, acute and chronic HCV humans in classes $I_A(t)$ and $I_C(t)$ are respectively infected with TB at a rate λ_T to join classes $I_{AL}(t)$ and $I_{CL}(t)$ respectively. Humans in I_{AL} progress to $I_{AT}(t)$ and $I_{CL}(t)$ at rates τ_1 and β_1 respectively. Similarly, humans in classes $I_{CL}(t)$ and $I_{AT}(t)$ both progress to $I_{CT}(t)$ class at rates τ_2 and β_2 respectively. Having tested positive to the co-infection, humans in classes $I_{CL}(t)$, $I_{AT}(t)$ and $I_{CT}(t)$ are put on treatment at rates r_1, r_2 and r_3 to join $R(t)$ class. In addition to natural death, humans in classes $I_C(t)$ and $I_{CL}(t)$ classes also die from chronic HCV-induced death at a rate δ and those in classes $I_{AT}(t)$ and $I_{CT}(t)$ also die from co-infection induced death at rates d_1 and d_2 respectively. Because previous infection does not provide permanent immunity, humans in classes $R_H(t)$, $R_T(t)$ and $R(t)$ return to susceptible class having been treated to clearance of the infection at rates ν_1, ν_2 and ν_3 respectively.

In order to formulate the dynamical system, all susceptible individuals have the same risk of acquiring either infection, the diseases are spread by contact with an infected individual. TB infected individuals first get latently infected and go on to become infectious. However, latent tuberculosis individuals are not infectious. Similarly, before developing chronic HCV, all hepatitis C infected persons first contract

Table 4.1: Description of Parameters used in the TB-HCV Model Formulation

Parameter	Definition
Λ	Per capita recruitment rate into susceptible population
μ	Per capita natural mortality rate
σ_1	Per capita mortality rate for individuals with infectious TB
σ_2	Per capita mortality rate for individuals hospitalized with infectious TB
δ	Per capita mortality rate for individuals with chronic form of HCV
d_1	Per capita mortality rate due to infectious TB in individuals with acute HCV and infectious TB
d_2	Per capita mortality rate due to either chronic HCV or infectious TB
θ	Rate of progression from latent to infectious TB
ρ	Rate at which the TB infectious individuals are hospitalized
ω_1	Rate at which TB infectious individuals are put on treatment
ω_2	Rate at which hospitalized infectious TB individuals are put on treatment
α	Progression rate from acute class to chronic HCV class
τ_1	Progression rate from I_{AL} class to I_{AT} class
τ_2	Progression rate from I_{CL} class to I_{CT} class
β_1	Progression rate from I_{AL} class to I_{CL} class
β_2	Progression rate from I_{AT} class to I_{CT} class
ψ	Rate at which chronic HCV individuals are put on treatment
r_1	Rate at which individuals in I_{CL} class are put on HCV treatment
r_2	Rate at which individuals in I_{AT} class are put on TB treatment
r_3	Rate at which individuals in I_{CT} class are put on treatment
ν_1	Rate of loss of temporary immunity to HCV
ν_2	Rate of loss of temporary immunity to TB
ν_3	Rate of loss of temporary immunity to both TB and HCV
η	Rate of natural recovery of latent TB individuals
π	Rate of natural recovery of acute HCV individuals
ϵ	Transmission coefficient for the hospitalized individuals
ϕ	Transmission coefficient for the HCV acute individuals

acute HCV and both forms of HCV are infectious. Acute HCV individuals either advance to the chronic stage or recover naturally. However, since the acute form of HCV is primarily asymptomatic, there is hardly any possibility of medication at this stage. Individuals co-infected with acute HCV and latent TB are less likely to recover naturally due to the combined burden of both infections. Tuberculosis and hepatitis C recovered humans acquire temporary immunity before re-infection. Table 4.1 provides a comprehensive summary of the parameters governing TB-HCV co-infection dynamics.

4.2.2 Compartmental Model Framework

Figure 4.1 illustrates the TB-HCV co-infection dynamics, as informed by our model description a assumptions. The arrows indicate movement of individuals between states or compartments.

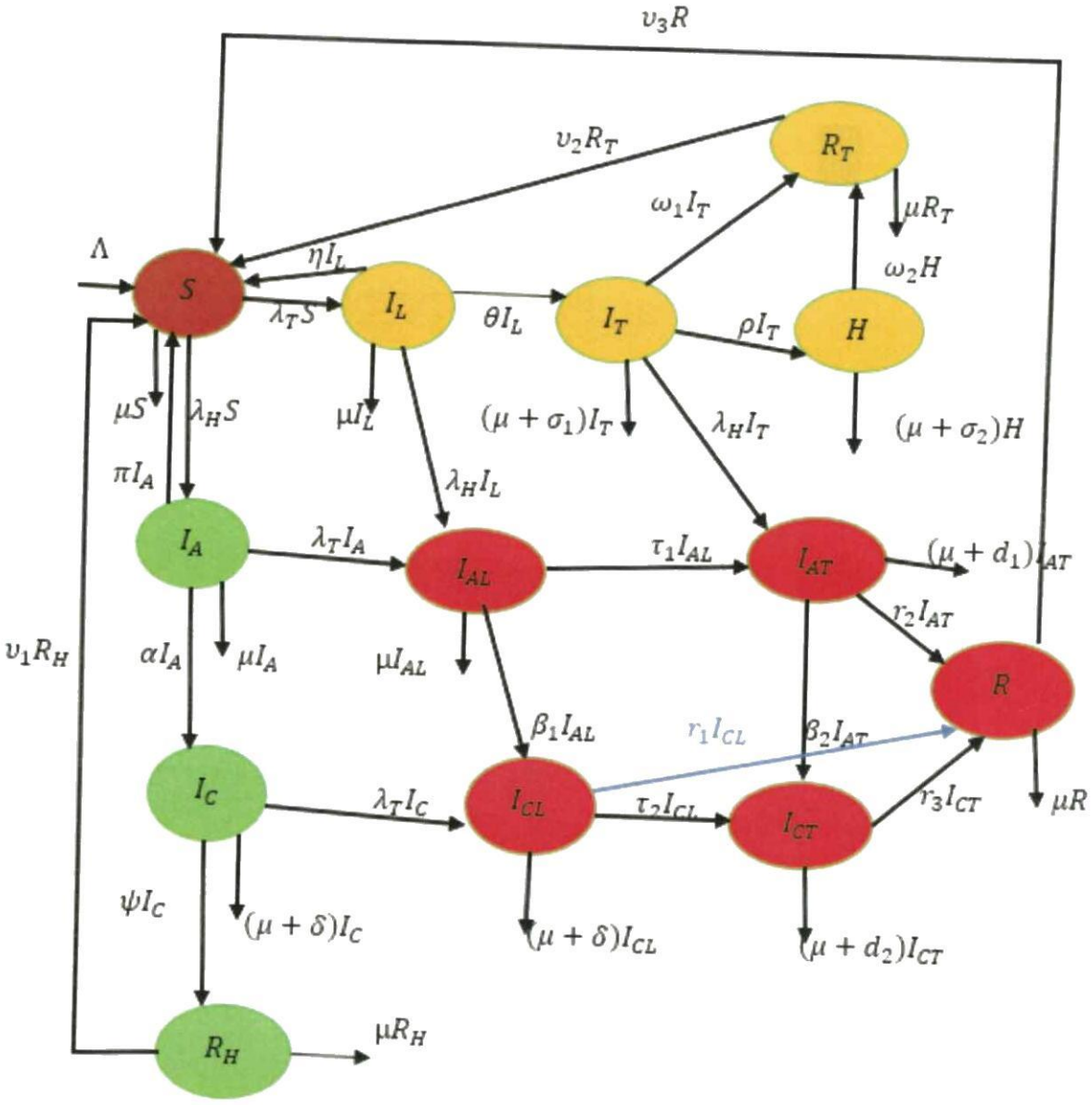

Figure 4.1: A compartmental diagram for TB-HCV co-infection dynamics with treatment

4.2.3 Equations of the Model

Using the parameters in Table 4.1 and the model flow diagram in Figure 4.1, the model is derived on the basis of the descriptions above using first order nonlinear ordinary differential equations as

follows:

$$\begin{aligned}
\frac{dS(t)}{dt} &= \Lambda + \nu_1 R_H(t) + \nu_2 R_T(t) + \nu_3 R(t) + \pi I_A(t) + \eta I_L(t) - (\lambda_T + \lambda_H + \mu)S(t),\\
\frac{dI_L(t)}{dt} &= \lambda_T S(t) - (\theta + \eta + \mu + \lambda_H)I_L(t),\\
\frac{dI_T(t)}{dt} &= \theta I_L(t) - (\omega_1 + \rho + \mu + \sigma_1 + \lambda_H)I_T(t),\\
\frac{dH(t)}{dt} &= \rho I_T(t) - (\omega_2 + \mu + \sigma_2)H(t),\\
\frac{dR_T(t)}{dt} &= \omega_2 H(t) + \omega_1 I_T(t) - (\nu_2 + \mu)R_T(t),\\
\frac{dI_A(t)}{dt} &= \lambda_H S(t) - (\pi + \alpha + \mu + \lambda_T)I_A(t),\\
\frac{dI_C(t)}{dt} &= \alpha I_A(t) - (\psi + \mu + \delta + \lambda_T)I_C(t),\\
\frac{dR_H(t)}{dt} &= \psi I_C(t) - (\nu_1 + \mu)R_H(t),\\
\frac{dI_{AL}(t)}{dt} &= \lambda_T I_A(t) + \lambda_H I_L(t) - (\tau_1 + \mu + \beta_1)I_{AL}(t),\\
\frac{dI_{CL}(t)}{dt} &= \beta_1 I_{AL}(t) + \lambda_T I_C(t) - (r_1 + \tau_2 + \mu + \delta)I_{CL}(t),\\
\frac{dI_{AT}(t)}{dt} &= \tau_1 I_{AL}(t) + \lambda_H I_T(t) - (r_2 + \beta_2 + \mu + d_1)I_{AT}(t),\\
\frac{dI_{CT}(t)}{dt} &= \tau_2 I_{CL}(t) + \beta_2 I_{AT}(t) - (r_3 + \mu + d_2)I_{CT}(t),\\
\frac{dR(t)}{dt} &= r_1 I_{CL}(t) + r_2 I_{AT}(t) + r_3 I_{CT}(t) - (\nu_3 + \mu)R(t).
\end{aligned} \tag{4.3}$$

where λ_T and λ_H are as defined in Equations (4.1) and (4.2) respectively. The initial values of the solution to the system are:

$$\begin{aligned}
&S(0) > 0, I_L(0) \geq 0, I_T(0) \geq 0, H(0) \geq 0, R_T(0) \geq 0, I_A(0) \geq 0, I_C(0) \geq 0, R_H(0) \geq 0,\\
&I_{AL}(0) \geq 0, I_{CL}(0) \geq 0, I_{AT}(0) \geq 0, I_{CT}(0) \geq 0 \text{ and } R(0) \geq 0.
\end{aligned} \tag{4.4}$$

4.3 Analysis and Results of the Model

4.3.1 Positivity and Boundedness Properties of Solutions in TB-HCV Co-infection Dynamics with Medication

Since the model system (4.3) studies human population, we need to verify that the model system is both mathematically well-defined and biologically relevant. In this subsection, we analyse the solution

properties of the TB-HCV co-infection model (4.3) focusing on non-negativity and boundedness.

Theorem 5. *The solutions* $S(t), I_L(t), I_T(t), H(t), R_T(t), I_A(t), I_C(t),$
$R_H(t), I_{AL}(t), I_{CL}(t), I_{AT}(t), I_{CT}(t)$ *and* $R(t)$ *of the model system* (4.3) *are non-negative for* $t > 0$.

Proof. Let the starting values of the variables of the system (4.3) be as defined in expression (4.4). Each component of the system's solution is demonstrated to be non-negative. Assuming the contrary, suppose there exists a first instant

$t_1 : S(t_1) = 0, S'(t_1) < 0$ and $S(t) > 0, I_L(t) > 0, ..., R(t) > 0$ for $0 < t < t_1$,

or there exists a

$t_2 : I_L(t_2) = 0, I'_L(t_2) < 0$ and $S(t) > 0, I_L(t) > 0, ..., R(t) > 0$ for $0 < t < t_2$,

or there exists a

$t_3 : I_T(t_3) = 0, I'_T(t_3) < 0$ and $S(t) > 0, I_L(t) > 0, ..., R(t) > 0$ for $0 < t < t_3$,

or there exists a

$t_4 : H(t_4) = 0, H'(t_4) < 0$ and $S(t) > 0, I_L(t) > 0, ..., R(t) > 0$ for $0 < t < t_4$,

or there exists a

$t_5 : R_T(t_5) = 0, R'_T(t_5) < 0$ and $S(t) > 0, I_L(t) > 0, ..., R(t) > 0$ for $0 < t < t_5$,

or there exists a

$t_6 : I_A(t_6) = 0, I'_A(t_6) < 0$ and $S(t) > 0, I_L(t) > 0, ..., R(t) > 0$ for $0 < t < t_6$,

or there exists a

$t_7 : I_C(t_7) = 0, I'_C(t_7) < 0$ and $S(t) > 0, I_L(t) > 0, ..., R(t) > 0$ for $0 < t < t_7$,

or there exists a

$t_8 : R_H(t_8) = 0, R'_H(t_8) < 0$ and $S(t) > 0, I_L(t) > 0, ..., R(t) > 0$ for $0 < t < t_8$,

or there exists a

$t_9 : I_{AL}(t_9) = 0, I'_{AL}(t_9) < 0$ and $S(t) > 0, I_L(t) > 0, ..., R(t) > 0$ for $0 < t < t_9$,

or there exists a

$t_{10} : I_{CL}(t_{10}) = 0, I'_{CL}(t_{10}) < 0$ and $S(t) > 0, I_L(t) > 0, ..., R(t) > 0$ for $0 < t < t_{10}$,

or there exists a

$t_{11} : I_{AT}(t_{11}) = 0, I'_{AT}(t_{11}) < 0$ and $S(t) > 0, I_L(t) > 0, ..., R(t) > 0$ for $0 < t < t_{11}$,

or there exists a

$t_{12} : I_{CT}(t_{12}) = 0, I'_{CT}(t_{12}) < 0$ and $S(t) > 0, I_L(t) > 0, ..., R(t) > 0$ for $0 < t < t_{12}$,

or there exists a

$t_{13} : R(t_{13}) = 0, R'(t_{13}) < 0$ and $S(t) > 0, I_L(t) > 0, ..., R(t) > 0$ for $0 < t < t_{13}$.

Considering differential equation one of model system (4.3), we get

$$\begin{aligned}\frac{dS(t_1)}{dt} &= \Lambda + \nu_1 R_H(t_1) + \nu_2 R_T(t_1) + \nu_3 R(t_1) + \pi I_A(t_1) + \eta I_L(t_1) - (\lambda_T + \lambda_H + \mu)S(t_1).\\ &= \Lambda + \nu_1 R_H(t_1) + \nu_2 R_T(t_1) + \nu_3 R(t_1) + \pi I_A(t_1) + \eta I_L(t_1) > 0,\end{aligned}$$

leading to a discrepancy, thus, $S(t)$ stays positive.

Considering differential equation two of model system (4.3), we get

$$\begin{aligned}\frac{dI_L(t_2)}{dt} &= \lambda_T S(t_2) - (\theta + \eta + \mu + \lambda_H)I_L(t_2),\\ &= \lambda_T S(t_2) > 0,\end{aligned}$$

leading to a discrepancy, thus, $I_L(t)$ stays positive.

Considering differential equation three of model system (4.3), we get

$$\begin{aligned}\frac{dI_T(t_3)}{dt} &= \theta I_L(t_3) - (\omega_1 + \rho + \mu + \sigma_1 + \lambda_H)I_T(t_3),\\ &= \theta I_L(t_3) > 0,\end{aligned}$$

leading to a discrepancy, thus, $I_T(t)$ stays positive.

Considering differential equation four of model system (4.3), we get

$$\begin{aligned}\frac{dH(t_4)}{dt} &= \rho I_T(t_4) - (\omega_2 + \mu + \sigma_2)H(t_4),\\ &= \rho I_T(t_4) > 0,\end{aligned}$$

leading to a discrepancy, thus, $H(t)$ stays positive.

Considering differential equation five of model system (4.3), we get

$$\begin{aligned}\frac{dR_T(t_5)}{dt} &= \omega_2 H(t_5) + \omega_1 I_T(t_5) - (\nu_2 + \mu)R_T(t_5),\\ &= \omega_2 H(t_5) + \omega_1 I_T(t_5) > 0,\end{aligned}$$

leading to a discrepancy, thus, $R_T(t)$ stays positive.

Considering differential equation six of model system (4.3), we get

$$\begin{aligned}\frac{dI_A(t_6)}{dt} &= \lambda_H S(t_6) - (\pi + \alpha + \mu + \lambda_T) I_A(t_6), \\ &= \lambda_H S(t_6) > 0,\end{aligned}$$

leading to a discrepancy, thus, $I_A(t)$ stays positive.

Considering differential equation seven of model system (4.3), we get

$$\begin{aligned}\frac{dI_C(t_7)}{dt} &= \alpha I_A(t_7) - (\psi + \mu + \delta + \lambda_T) I_C(t_7), \\ &= \alpha I_A(t_7) > 0,\end{aligned}$$

leading to a discrepancy, thus, $I_C(t)$ stays positive.

Considering differential equation eight of model system (4.3), we get

$$\begin{aligned}\frac{dR_H(t_8)}{dt} &= \psi I_C(t_8) - (\nu_1 + \mu) R_H(t_8), \\ &= \psi I_C(t_8) > 0,\end{aligned}$$

leading to a discrepancy, thus, $R_H(t)$ stays positive.

Considering differential equation nine of model system (4.3), we get

$$\begin{aligned}\frac{dI_{AL}(t_9)}{dt} &= \lambda_T I_A(t_9) + \lambda_H I_L(t_9) - (\tau_1 + \mu + \beta_1) I_{AL}(t_9), \\ &= \lambda_T I_A(t_9) + \lambda_H I_L(t_9) > 0,\end{aligned}$$

leading to a discrepancy, thus, $I_{AL}(t)$ stays positive.

Considering differential equation ten of model system (4.3), we get

$$\begin{aligned}\frac{dI_{CL}(t_{10})}{dt} &= \beta_1 I_{AL}(t_{10}) + \lambda_T I_C(t_{10}) - (r_1 + \tau_2 + \mu + \delta) I_{CL}(t_{10}), \\ &= \beta_1 I_{AL}(t_{10}) + \lambda_T I_C(t_{10}) > 0,\end{aligned}$$

leading to a discrepancy, thus, $I_{CL}(t)$ stays positive.

Considering differential equation eleven of model system (4.3), we get

$$\begin{aligned}\frac{dI_{AT}(t_{11})}{dt} &= \tau_1 I_{AL}(t_{11}) + \lambda_H I_T(t_{11}) - (r_2 + \beta_2 + \mu + d_1) I_{AT}(t_{11}),\\ &= \tau_1 I_{AL}(t_{11}) + \lambda_H I_T(t_{11}) > 0,\end{aligned}$$

leading to a discrepancy, thus, $I_{AT}(t)$ stays positive.

Considering differential equation twelve of model system (4.3), we get

$$\begin{aligned}\frac{dI_{CT}(t_{12})}{dt} &= \tau_2 I_{CL}(t_{12}) + \beta_2 I_{AT}(t_{12}) - (r_3 + \mu + d_2) I_{CT}(t_{12}),\\ &= \tau_2 I_{CL}(t_{12}) + \beta_2 I_{AT}(t_{12}) > 0,\end{aligned}$$

leading to a discrepancy, thus, $I_{CT}(t)$ stays positive.

Considering differential equation thirteen of model system (4.3), we get

$$\begin{aligned}\frac{dR(t_{13})}{dt} &= r_1 I_{CL}(t_{13}) + r_2 I_{AT}(t_{13}) + r_3 I_{CT}(t_{13}) - (\nu_3 + \mu) R(t_{13}).\\ &= r_1 I_{CL}(t_{13}) + r_2 I_{AT}(t_{13}) + r_3 I_{CT}(t_{13}) > 0,\end{aligned}$$

leading to a discrepancy, thus, $R(t)$ stays positive.

Therefore, in all cases, the solutions of the variables $S(t), I_L(t), I_T(t), H(t), R_T(t), I_A(t), I_C(t)$, $R_H(t), I_{AL}(t), I_{CL}(t), I_{AT}(t), I_{CT}(t)$ and $R(t)$ remain positive. □

Theorem 6. *The region*

$$\begin{aligned}\Omega = \{&\big(S(t), I_L(t), I_T(t), H(t), R_T(t), I_A(t), I_C(t), R_H(t), I_{AL}(t), I_{CL}(t), I_{AT}(t), I_{CT}(t),\\ &R(t)\big) \in \mathbb{R}^{13}_+ : 0 \leq N(t) \leq \frac{\Lambda}{\mu}\},\end{aligned}$$

is positively invariant and attractive set with respect to the model.

Proof. Let

$$\big(S(t), I_L(t), I_T(t), H(t), R_T(t), I_A(t), I_C(t), R_H(t), I_{AL}(t), I_{CL}(t), I_{AT}(t), I_{CT}(t), R(t)\big) \in \mathbb{R}^{13}_+$$

be a solution to the system (4.3) chosen arbitrarily, subject to non-negative values as in expression (4.4).

By adding the equations in system (4.3) together, we obtain

$$\frac{dN}{dt} = \Lambda - \mu N - \eta I_L - \sigma_1 I_T - \sigma_2 H - \delta(I_C + I_{CL}) - d_1 I_{AT} - d_2 I_{CT}. \tag{4.5}$$

Since $I_L, I_T, H, I_A, I_C, I_{AL}, I_{CL}, IAT, I_{CT} \geq 0$ for $t > 0$, then Equation (4.5) simplifies to

$$\frac{dN}{dt} \leq \Lambda - \mu N, \tag{4.6}$$

which we can re-write as

$$\frac{dN}{dt} + \mu N \leq \Lambda. \tag{4.7}$$

Now, solving inequality (4.7) using integrating factor method, together with initial conditions $N(t = 0) = N_0$, we have

$$Ne^{\mu t} \leq \frac{\Lambda}{\mu} e^{\mu t} + N_0 - \frac{\Lambda}{\mu}. \tag{4.8}$$

Re-arranging inequality (4.8) leads to

$$N \leq \frac{\Lambda}{\mu} + \left(N_0 - \frac{\Lambda}{\mu}\right) e^{-\mu t}. \tag{4.9}$$

Thus, we have

$$0 \leq N(t) \leq \frac{\Lambda}{\mu} + N_0 e^{-\mu t}.$$

Clearly, as $t \to \infty$, we have

$$0 \leq N(t) \leq \frac{\Lambda}{\mu}.$$

This result implies that any feasible solution of the model system (4.3) once in the region Ω, it remains confined to that region for all time t. Consequently, region Ω is a biologically meaningful and trapping region, meaning it remains stable under the system's dynamics. Therefore, the model is both mathematically well-defined and biologically relevant.

Calculation of the effective reproduction numbers is carried out, by first gaining insights into the distinct behaviour of the TB-only and HCV-only sub models with treatment and thereafter the TB-HCV co-infection model with treatment.

By effective reproduction number, we mean the average number of secondary infections caused by a single infective, at a given susceptible fraction [132] □

$$
\begin{aligned}
\frac{dI_L(t)}{dt} &= \lambda_T S(t) - (\theta + \eta + \mu) I_L(t), \\
\frac{dI_T(t)}{dt} &= \theta I_L(t) - (\omega_1 + \rho + \mu + \sigma_1) I_T(t), \\
\frac{dH(t)}{dt} &= \rho I_T(t) - (\omega_2 + \mu + \sigma_2) H(t), \\
\frac{dR_T(t)}{dt} &= \omega_1 I_T(t) + \omega_2 H(t) - (\nu_2 + \mu) R_T(t),
\end{aligned} \tag{4.10}
$$

where,

$$
\lambda_T(t) = \frac{\xi_1 q_1 \big(I_T(t) + \epsilon H(t)\big)}{N_{TB}(t)}, \tag{4.11}
$$

and

$$
N_{TB}(t) = S(t) + I_L(t) + I_T(t) + H(t) + R_T(t). \tag{4.12}
$$

The TB-free equilibrium point for the TB-only sub model is determined by assuming that there is no TB infection in the population, that is to say, $I_L = I_T = H = R_T = 0$. Thus, the TB-only sub model (4.10) reduces to

$$
\frac{dS(t)}{dt} = \Lambda - \mu S(t). \tag{4.13}
$$

Now, solving Equation (4.13), we have

$$
S(t) = \frac{\Lambda}{\mu}. \tag{4.14}
$$

Thus, the TB-free equilibrium point for the TB-only sub model is given by

$$
E^o_{TB} = (S(t), I_L(t), I_T(t), H(t), R_T(t)) = \big(\frac{\Lambda}{\mu}, 0, 0, 0, 0\big). \tag{4.15}
$$

The next generation matrix method developed by Driessche and Watmough [35] is used to compute the effective reproduction number R_{TB} for the TB-only sub model with treatment. The matrix representing the rate of new TB cases emerging in compartment i, F_i, specific to the TB-only sub

model (4.10) is

$$\cdot F_i = \begin{bmatrix} \lambda_T S \\ 0 \\ 0 \end{bmatrix}.$$

The matrix, V_i, which represents the transfer rates between compartments i and all other compartment is given by

$$V_i = \begin{bmatrix} (\eta+\mu+\theta)I_L \\ -\theta I_L + (\omega_1+\rho+\mu+\sigma_1)I_T \\ -\rho I_T + (\omega_2+\mu+\sigma_2)H \end{bmatrix}.$$

The Jacobian matrix of the new TB infections in compartment i at TB-free equilibrium point, E^0_{TB}, is given by

$$F_{TB} = \begin{bmatrix} 0 & \xi_1 q_1 & \xi_1 q_1 \epsilon \\ 0 & 0 & 0 \\ 0 & 0 & 0 \end{bmatrix}.$$

The Jacobian matrix V_{TB} for the rate of transfer into and out of compartment i by all other processes at TB-free equilibrium is given by

$$V_{TB} = \begin{bmatrix} (\eta+\mu+\theta) & 0 & 0 \\ -\theta & (\omega_1+\rho+\mu+\sigma_1) & 0 \\ 0 & -\rho & (\omega_2+\mu+\sigma_2) \end{bmatrix}.$$

The inverse of matrix V_{TB} is calculated and obtained as

$$V_{TB}^{-1} = \begin{bmatrix} \frac{1}{(\eta+\mu+\theta)} & 0 & 0 \\ \frac{\theta}{(\eta+\mu+\theta)(\omega_1+\rho+\mu+\sigma_1)} & \frac{1}{(\omega_1+\rho+\mu+\sigma_1)} & 0 \\ \frac{\rho\theta}{(\eta+\mu+\theta)(\omega_1+\rho+\mu+\sigma_1)(\omega_2+\mu+\sigma_2)} & \frac{\rho}{(\omega_1+\rho+\mu+\sigma_1)(\omega_2+\mu+\sigma_2)} & \frac{1}{(\omega_2+\mu+\sigma_2)} \end{bmatrix}.$$

The next generation matrix $F_{TB}V_{TB}^{-1}$ is given by

$$F_{TB}V_{TB}^{-1} = \begin{bmatrix} \frac{\xi_1 q_1 \theta}{(\eta+\mu+\theta)(\omega_1+\rho+\mu+\sigma_1)} + \frac{\xi_1 q_1 \epsilon \rho \theta}{(\eta+\mu+\theta)(\omega_1+\rho+\mu+\sigma_1)(\omega_2+\mu+\sigma_2)} & \frac{\xi_1 q_1}{(\eta+\mu+\theta)} + \frac{\xi_1 q_1 \epsilon \rho}{(\omega_1+\rho+\mu+\sigma_1)(\omega_2+\mu+\sigma_2)} & \frac{\xi_1 q_1 \epsilon}{(\omega_2+\mu+\sigma_2)} \\ 0 & 0 & 0 \\ 0 & 0 & 0 \end{bmatrix}.$$

Now, the eigenvalues, λ are calculated from the characteristic equation given as

$$\det\Big(F_{TB}V_{TB}^{-1} - \lambda I\Big) = 0,$$

from which we have

$$\det\begin{bmatrix} \Big(\frac{\xi_1 q_1\theta}{(\eta+\mu+\theta)(\omega_1+\rho+\mu+\sigma_1)} + \frac{\xi_1 q_1\epsilon\rho\theta}{(\eta+\mu+\theta)(\omega_1+\rho+\mu+\sigma_1)(\omega_2+\mu+\sigma_2)}\Big) - \lambda & \frac{\xi_1 q_1}{(\eta+\mu+\theta)} + \frac{\xi_1 q_1\epsilon\rho}{(\omega_1+\rho+\mu+\sigma_1)(\omega_2+\mu+\sigma_2)} & \frac{\xi_1 q_1\epsilon}{(\omega_2+\mu+\sigma_2)} \\ 0 & -\lambda & 0 \\ 0 & 0 & -\lambda \end{bmatrix} = 0.$$

and

$$\Big[\Big(\frac{\xi_1 q_1\theta}{(\eta+\mu+\theta)(\omega_1+\rho+\mu+\sigma_1)} + \frac{\xi_1 q_1\epsilon\rho\theta}{(\eta+\mu+\theta)(\omega_1+\rho+\mu+\sigma_1)(\omega_2+\mu+\sigma_2)}\Big) - \lambda\Big][-\lambda][-\lambda] = 0 \tag{4.16}$$

Now, on solving Equation (4.16), we have

$$\lambda_1 = \frac{\xi_1 q_1\theta}{(\eta+\mu+\theta)(\omega_1+\rho+\mu+\sigma_1)}\Big(1 + \frac{\epsilon\rho}{(\omega_2+\mu+\sigma_2)}\Big), \lambda_2 = 0 \text{ and } \lambda_3 = 0.$$

But

$$\begin{aligned} R_{TB} &= \max\{\lambda_1, \lambda_2, \lambda_3\} \\ &= \max\Big\{\frac{\xi_1 q_1\theta}{(\eta+\mu+\theta)(\omega_1+\rho+\mu+\sigma_1)}\Big(1 + \frac{\epsilon\rho}{(\omega_2+\mu+\sigma_2)}\Big), 0, 0\Big\}. \end{aligned}$$

Thus, the TB induced effective reproduction number, R_{TB}, is given as

$$R_{TB} = \frac{\xi_1 q_1\theta}{(\eta+\mu+\theta)(\omega_1+\rho+\mu+\sigma_1)}\Big(1 + \frac{\epsilon\rho}{(\omega_2+\mu+\sigma_2)}\Big). \tag{4.17}$$

Lemma 4.1: The TB infection-free equilibrium, E_{TB}^0, is locally asymptotically stable if $R_{TB} < 1$ and unstable otherwise.

Proof. The Jacobian matrix of the TB-only sub model (4.10), is given by:

$$J(E_{TB}) = \begin{bmatrix} -\left(\xi_1 q_1 \frac{(I_T+\epsilon H)}{N_{TB}} + \mu\right) & \eta & -\xi_1 q_1 & \xi_1 q_1 \epsilon & \nu_2 \\ \xi_1 q_1 \frac{(I_T+\epsilon H)}{N_{TB}} & -\kappa_1 & \xi_1 q_1 & \xi_1 q_1 \epsilon & 0 \\ 0 & \theta & -\kappa_2 & 0 & 0 \\ 0 & \rho & 0 & -k_3 & 0 \\ 0 & 0 & \omega_1 & \omega_2 & -(\nu_2+\mu) \end{bmatrix}. \tag{4.18}$$

where

$$\kappa_1 = \theta + \eta + \mu, \kappa_2 = \omega_1 + \rho + \mu + \sigma_1 \text{ and } \kappa_3 = \omega_2 + \mu + \sigma_2.$$

At TB infection free equilibrium point, $E^0_{TB} = (\frac{\Lambda}{\mu}, 0, 0, 0, 0)$, the Jacobian matrix becomes:

$$J(E_{TB}) = \begin{bmatrix} -\mu & \eta & -\xi_1 q_1 & \xi_1 q_1 \epsilon & \nu_2 \\ 0 & -k_1 & \xi_1 q_1 & \xi_1 q_1 \epsilon & 0 \\ 0 & \theta & -\kappa_2 & 0 & 0 \\ 0 & \rho & 0 & -\kappa_3 & 0 \\ 0 & 0 & \omega_1 & \omega_2 & -(\nu_2+\mu) \end{bmatrix}. \tag{4.19}$$

However, $J(E^0_{TB})$ can be expressed in the form

$$J(E^0_{TB}) = \begin{bmatrix} J_{11} & J_{12} \\ J_{21} & J_{22} \end{bmatrix},$$

where

$$J_{11} = \begin{bmatrix} -\mu & \eta & -\xi_1 q_1 \\ 0 & -\kappa_1 & \xi_1 q_1 \\ 0 & \theta & -\kappa_2 \end{bmatrix}, J_{12} = \begin{bmatrix} -\xi_1 q_1 \epsilon & \nu_2 \\ \xi_1 q_1 \epsilon, & 0 \\ 0 & 0 \end{bmatrix}, J_{21} = \begin{bmatrix} 0 & \rho & 0 \\ 0 & 0 & \omega_1 \end{bmatrix} \text{ and } J_{22} = \begin{bmatrix} -\kappa_3 & 0 \\ \omega_2 & -(\nu_2+\mu) \end{bmatrix}.$$

An essential and requisite condition for local asymptotic stability of the disease-free equilibrium is that all the eigenvalues of submatrices J_{11} and J_{22} have negative real parts [29, 34, 54]. For the eigenvalues of submatrix J_{22}, we have

$$\det(J_{22} - \lambda I) = 0,$$

where I is a 2×2 matrix. Therefore

$$\det \begin{bmatrix} -k_3 - \lambda & 0 \\ \omega_2 & -(\nu_2 + \mu) - \lambda \end{bmatrix} = 0 \tag{4.20}$$

On solving Equation (4.20) for the eigenvalues, we get

$$\lambda_1 = -\kappa_3 \text{ and } \lambda_2 = -(\nu_2 + \mu).$$

Thus, the eigenvalues of J_{22} are $-\kappa_3$ and $-(\nu_2 + \mu)$ which are both negative.
Now, the eigenvalues of J_{11} are calculated as follows:

$$\det(J_{11} - \lambda I) = 0, \tag{4.21}$$

$$\det \begin{bmatrix} -\mu - \lambda & \eta & -\xi_1 q_1 \\ 0 & -\kappa_1 - \lambda & \xi_1 q_1 \\ 0 & \theta & -\kappa_2 - \lambda \end{bmatrix} = 0, \tag{4.22}$$

On solving Equation (4.22) for the eigenvalues, we get

$$\lambda_3 = -\mu, \lambda_4 = \frac{-(\kappa_1 + \kappa_2) - \sqrt{(\kappa_1 + \kappa_2)^2 - 4(\kappa_1\kappa_2 - \theta\xi_1 q_1)}}{2} \text{ and}$$
$$\lambda_5 = \frac{-(\kappa_1 + \kappa_2) + \sqrt{(\kappa_1 + \kappa_2)^2 - 4(\kappa_1\kappa_2 - \theta\xi_1 q_1)}}{2}.$$

For λ_4 and λ_5 to be negative, then

$$-(\kappa_1 + \kappa_2) \pm \sqrt{(\kappa_1 + \kappa_2)^2 - 4(\kappa_1\kappa_2 - \theta\xi_1 q_1)} < 0. \tag{4.23}$$

Re-arranging inequality (4.23), we get

$$(\kappa_1 + \kappa_2)^2 < (\kappa_1 + \kappa_2)^2 - 4(\kappa_1\kappa_2 - \theta\xi_1 q_1). \tag{4.24}$$

On simplifying inequality (4.24), we have

$$\frac{\theta\xi_1 q_1}{\kappa_1\kappa_2} < 1. \tag{4.25}$$

Now, from

$$R_{TB} = \frac{\xi_1 q_1 \theta}{\kappa_1 \kappa_2}\left(\frac{\kappa_3 + \epsilon\rho}{\kappa_3}\right). \tag{4.26}$$

Re-arranging Equation (4.26), yields

$$\frac{\theta \xi_1 q_1}{\kappa_1 \kappa_2} = \frac{\kappa_3 R_{TB}}{\kappa_3 + \epsilon\rho}.$$

Thus, inequality (4.25) can be re-written as

$$\frac{\kappa_3 R_{TB}}{\kappa_3 + \epsilon\rho} < 1. \tag{4.27}$$

Therefore, λ_4 and λ_5 are negative eigenvalues if inequality (4.27) is satisfied. Hence, the TB infection-free equilibrium E^0_{TB}, is locally asymptotically stable if $R_{TB} < 1$ and unstable otherwise. This suggests that in the event that a small group of TB-infected persons enter the population, the system will eventually return to the TB-free equilibrium over time. □

4.3.2.1 Global stability of TB infection-free equilibrium for TB-only sub model with medication

The global behaviour of model system (4.10) is analysed by applying the approach by Castillo-Chavez et al. [76] as also applied by [114]. Re-writing the TB-only sub model (4.10) in the form

$$\begin{aligned} \frac{dX_{TB}}{dt} &= F(X_{TB}, Z_{TB}) \\ \frac{dZ_{TB}}{dt} &= G(X_{TB}, Z_{TB}), G(X_{TB}, 0) = 0, \end{aligned} \tag{4.28}$$

where $X_{TB} = (S_{TB})$ and $Z_{TB} = (I_L, I_T, H, R_T)$, with $X_{TB} \in \mathbb{R}_+$ denoting (its components) the number of uninfected humans and $Z_{TB} \in \mathbb{R}^4_+$ whose components denote the number of humans infected with TB including those ones on treatment. Let the TB infection free equilibrium of system (4.28) be denoted by $E^0_{TB} = (X^0_{TB}, 0) = (\frac{\Lambda}{\mu}, 0, 0, 0, 0)$.

Theorem 7. *The fixed point $E^0_{TB} = (X_{TB}, 0)$ is a globally asymptotic stable equilibrium of system (4.28) provided $R_{TB} < 1$ and that the following conditions are satisfied.*

$$D1: \text{ For } \frac{dX_{TB}}{dt} = F(X_{TB}, 0), X^0_{TB} \text{ is globally asymptotically stable.}$$

$$D2: G(X_{TB}, Z_{TB}) = MZ_{TB} - \hat{G}(X_{TB}, Z_{TB}), \hat{G}(X_{TB}, Z_{TB}) \geq 0 \text{ for } (X_{TB}, Z_{TB}) \in \Omega_{TB},$$

where $M = \frac{\partial}{\partial Z_{TB}} G(X^0_{TB}, 0)$ is a Metzler matrix and Ω_{TB} is the invariant region in which the model

makes biological sense.

Proof. From Lemma (4.1), E^0_{TB} is locally asymptotically stable if $R_{TB} < 1$.
For the first condition $(D1)$, that is , the global asymptotic stability of X^0_{TB}, we have

$$F(X_{TB}, Z_{TB}) = \begin{bmatrix} \Lambda + \eta I_L + \nu_2 R_T - (\lambda_T + \mu)S \\ 0 \end{bmatrix} \tag{4.29}$$

and

$$\frac{dX_{TB}}{dt} = F(X_{TB}, 0) = \Lambda - \mu S, \tag{4.30}$$

which is a linear differential equation. On solving Equation (4.30), we get

$$S(t) = \frac{\Lambda}{\mu} - \frac{\Lambda}{\mu} e^{-\mu t} + S(0)e^{-\mu t}. \tag{4.31}$$

Now, as $t \to \infty$, $S_{TB}(t) \to \frac{\Lambda}{\mu}$ regardless of the value of $S(0)$. Thus, there is convergence in Ω_{TB}, implying that condition $(D1)$ holds.
For the second condition $(D2)$, consider

$$\begin{aligned} G(X_{TB}, Z_{TB}) &= \begin{bmatrix} \lambda_T S - \kappa_1 I_L \\ \theta I_L - \kappa_2 I_T \\ \rho I_T - \kappa_3 H \\ \omega_1 I_T + \omega_2 H - (\nu_2 + \mu) R_T \end{bmatrix} \\ &= \begin{bmatrix} \xi_1 q_1 \left(I_T + \epsilon H\right) \frac{S}{N_{TB}} - \kappa_1 I_L \\ \theta I_L - \kappa_2 I_T \\ \rho I_T - \kappa_3 H \\ \omega_1 I_T + \omega_2 H - (\nu_2 + \mu) R_T \end{bmatrix} \end{aligned} \tag{4.32}$$

and

$$M = \frac{\partial}{\partial Z_{TB}} G(X^0_{TB}, 0) = \begin{bmatrix} -\kappa_1 & \xi_1 q_1 \frac{S}{N_{TB}} & \xi_1 q_1 \epsilon \frac{S}{N_{TB}} & 0 \\ \theta & -\kappa_2 & 0 & 0 \\ 0 & \rho & -\kappa_3 & 0 \\ 0 & \omega_1 & \omega_2 & -(\nu_2 + \mu) \end{bmatrix}. \tag{4.33}$$

Now, at $E^0_{TB} = (\frac{\Lambda}{\mu}, 0, 0, 0.0)$, $\frac{S}{N_{TB}} \leq 1$, thus Equation (4.33) reduces to

$$M = \frac{\partial}{\partial Z_{TB}} G(X^0_{TB}, 0) = \begin{bmatrix} -\kappa_1 & \xi_1 q_1 & \xi_1 q_1 \epsilon & 0 \\ \theta & -\kappa_2 & 0 & 0 \\ 0 & \rho & -\kappa_3 & 0 \\ 0 & \omega_1 & \omega_2 & -(\nu_2 + \mu) \end{bmatrix}. \tag{4.34}$$

But

$$\hat{G}(X_{TB}, Z_{TB}) = MZ_{TB} - G(X_{TB}, Z_{TB}). \tag{4.35}$$

Substituting Equations (4.32) and (4.34) into (4.35), and on simplifying, we have

$$\hat{G}(X_{TB}, Z_{TB}) = \begin{bmatrix} -\kappa_1 & \xi_1 q_1 & \xi_1 q_1 \epsilon & 0 \\ \theta & -\kappa_2 & 0 & 0 \\ 0 & \rho & -\kappa_3 & 0 \\ 0 & \omega_1 & \omega_2 & -(\nu_2 + \mu) \end{bmatrix} \begin{bmatrix} I_L \\ I_T \\ H \\ R_T \end{bmatrix} - \begin{bmatrix} \xi_1 q_1 (I_T + \epsilon H) \frac{S}{N_{TB}} - \kappa_1 I_L \\ \theta I_L - \kappa_2 I_T \\ \rho I_T - \kappa_3 H \\ \omega_1 I_T + \omega_2 H - (\nu_2 + \mu) R_T \end{bmatrix}, \tag{4.36}$$

$$= \begin{bmatrix} \xi_1 q_1 I_T (1 - \frac{S}{N_{TB}}) + \xi_1 q_1 \epsilon H (1 - \frac{S}{N_{TB}}) \\ 0 \\ 0 \\ 0 \end{bmatrix}. \tag{4.37}$$

Given that $0 < S \leq N_{TB}$, it follows easily that $\hat{G}(X_{TB}, Z_{TB}) \geq 0$. Additionally, matrix M is a Metzler matrix with all off-diagonal entries being positive or zero. It follows that, E^0_{TB} is globally asymptotically stable when $R_{TB} < 1$. This means that irrespective of the number of TB infectives introduced into the population, TB will gradually phase out. □

4.3.3 TB Endemic Equilibrium, E^*_{TB}

The TB endemic equilibrium, E^*_{TB}, occurs when TB infection persists in the population. Now, setting the derivatives of Equations (4.10) of the TB-only sub model to zero, we get:

$$\Lambda + \eta I_L(t) + \nu_2 R_T(t) - \lambda_T S(t) - \mu S(t) = 0, \tag{4.38}$$

$$\lambda_T S(t) - \kappa_1 I_L(t) = 0, \tag{4.39}$$

$$\theta I_L(t) - \kappa_2 I_T(t) = 0, \tag{4.40}$$

$$\rho I_T(t) - \kappa_3 H(t) = 0, \tag{4.41}$$

$$\omega_1 I_T(t) + \omega_2 H(t) - (\nu_2 + \mu) R_T(t) = 0, \tag{4.42}$$

where,

$$\lambda_T(t) = \frac{\xi_1 q_1 \big(I_T(t) + \epsilon H(t)\big)}{N_{TB}(t)}, \tag{4.43}$$

$$\kappa_1 = (\theta + \eta + \mu), \kappa_2 = (\omega_1 + \rho + \mu + \sigma_1), \kappa_3 = (\omega_2 + \mu + \sigma_2)$$

and

$$\frac{dN}{dt} = \Lambda - \mu N_{TB} - \sigma_1 I_T - \sigma_2 H. \tag{4.44}$$

But at equilibrium, $\frac{dN}{dt} = 0$, thus, Equation (4.44) becomes

$$\Lambda - \mu N_{TB} - \sigma_1 I_T - \sigma_2 H = 0. \tag{4.45}$$

Re-writing Equation (4.41), we have

$$I_T = \frac{\kappa_3}{\rho} H. \tag{4.46}$$

Substituting I_T in Equation (4.45) and simplifying, we get

$$H = \frac{\rho(\Lambda - \mu N_{TB})}{(\sigma_1 \kappa_3 + \sigma_2 \rho)}. \tag{4.47}$$

Substituting H in Equation (4.46) and re-arranging, we get

$$I_T = \frac{\kappa_3(\Lambda - \mu N_{TB})}{(\sigma_1 \kappa_3 + \sigma_2 \rho)}. \tag{4.48}$$

Putting I_T in Equation (4.40) and simplifying, we have

$$I_L = \frac{\kappa_2\kappa_3(\Lambda - \mu N_{TB})}{\theta(\sigma_1\kappa_3 + \sigma_2\rho)}. \tag{4.49}$$

Substituting H and I_T in Equation (4.42), we have

$$R_T = \frac{(\dot{\Lambda} - \mu N_{TB})(\omega_2\rho + \omega_1\kappa_3)}{\kappa_4(\sigma_1\kappa_3 + \sigma_2\rho)}. \tag{4.50}$$

Now, substituting H, I_T and I_L in Equation (4.39) and simplifying we get

$$S = \frac{\kappa_1\kappa_2\kappa_3 N_{TB}}{\xi_1 q_1\theta(\kappa_3 + \epsilon\rho)}. \tag{4.51}$$

Thus, the endemic equilibrium point E^*_{TB} is given by

$$E^*_{TB} = \Big(\frac{\kappa_1\kappa_2\kappa_3 N_{TB}}{\xi_1 q_1\theta(\kappa_3 + \epsilon\rho)}, \frac{\kappa_2\kappa_3(\Lambda - \mu N_{TB})}{\theta(\sigma_1\kappa_3 + \sigma_2\rho)}, \frac{\kappa_3(\Lambda - \mu N_{TB})}{(\sigma_1\kappa_3 + \sigma_2\rho)}, \frac{\rho(\Lambda - \mu N_{TB})}{(\sigma_1\kappa_3 + \sigma_2\rho)}, \frac{(\Lambda - \mu N_{TB})(\omega_2\rho + \omega_1\kappa_3)}{(\nu_2 + \mu)(\sigma_1\kappa_3 + \sigma_2\rho)}\Big). \tag{4.52}$$

Lemma 4.2: The TB-only sub model (4.10) has a unique endemic equilibrium point if $R_{TB} > 1$.

Proof: If the disease is endemic in the population, then $\frac{dI_L}{dt} > 0$, $\frac{dI_T}{dt} > 0$ and $\frac{dH}{dt} > 0$, that is

$$\xi_1 q_1(I_T + \epsilon H)\frac{S}{N_{TB}} - \kappa_1 I_L > 0, \tag{4.53}$$

$$\theta I_L - \kappa_2 I_T > 0. \tag{4.54}$$

$$\rho I_T - \kappa_3 H > 0. \tag{4.55}$$

From inequality (4.53), we have

$$\kappa_1 I_L < \xi_1 q_1(I_T + \epsilon H)\frac{S}{N_{TB}}. \tag{4.56}$$

Using the fact that $\frac{S}{N_{TB}} \leq 1$, inequality (4.56) becomes

$$I_L < \frac{\xi_1 q_1}{\kappa_1}(I_T + \epsilon H). \tag{4.57}$$

From Inequality (4.55), we have

$$H < \frac{\rho I_T}{\kappa_3}. \tag{4.58}$$

Substituting H into inequality (4.57) and simplifying, we get

$$I_L < \frac{\xi_1 q_1}{\kappa_1}(1 + \frac{\epsilon\rho}{\kappa_3})I_T. \tag{4.59}$$

Now, re-arranging inequality (4.54), we have

$$I_T < \frac{\theta I_L}{\kappa_2}. \tag{4.60}$$

Substituting I_T into inequality (4.59) and simplifying, we get

$$1 < \frac{\xi_1 q_1 \theta}{\kappa_1 \kappa_2}(1 + \frac{\epsilon\rho}{\kappa_3}). \tag{4.61}$$

Thus, $R_{TB} > 1$.

Hence, a unique endemic equilibrium point E^*_{TB} exists when $R_{TB} > 1$.

Lemma 4.3: If $R_{TB} > 1$, the TB endemic equilibrium E^*_{TB} is locally stable, otherwise, it is unstable.

Proof. We study the local stability of the TB endemic equilibrium by applying the Routh-Hurwitz criterion. The Jacobian matrix of TB-only sub model is given by

$$J(E_{TB}) = \begin{bmatrix} -\left(\xi_1 q_1 \frac{(I_T + \epsilon H)}{N_{TB}} + \mu\right) & \eta & -\xi_1 q_1 & -\xi_1 q_1 \epsilon & \nu_2 \\ \xi_1 q_1 \frac{(I_T + \epsilon H)}{N_{TB}} & -\kappa_1 & \xi_1 q_1 & \xi_1 q_1 \epsilon & 0 \\ 0 & \theta & -\kappa_2 & 0 & 0 \\ 0 & \rho & 0 & -\kappa_3 & 0 \\ 0 & 0 & \omega_1 & \omega_2 & -(\nu_2 + \mu) \end{bmatrix}. \tag{4.62}$$

At the TB endemic equilibrium, the Jacobian matrix $J(E_{TB})$ becomes

$$J(E^*_{TB}) = \begin{bmatrix} -(z^* + \mu) & \eta & -\xi_1 q_1 & -\xi_1 q_1 \epsilon & \nu_2 \\ z^* & -\kappa_1 & \xi_1 q_1 & \xi_1 q_1 \epsilon & 0 \\ 0 & \theta & -\kappa_2 & 0 & 0 \\ 0 & \rho & 0 & -\kappa_3 & 0 \\ 0 & 0 & \omega_1 & \omega_2 & -(\nu_2 + \mu) \end{bmatrix}, \tag{4.63}$$

where

$z^* = \xi_1 q_1 \dfrac{(I_T^* + \epsilon H^*)}{N_{TB}^*}$, is the force of TB infection at the equilibrium where the disease persists.

The characteristic polynomial of the Jacobian matrix $J(E_{TB}^*)$ is obtained as

$$P(\lambda) = \det(\lambda I - J(E_{TB}^*)) = \lambda^5 + e_1\lambda^4 + e_2\lambda^3 + e_3\lambda^2 + e_4\lambda + e_5, \tag{4.64}$$

where I is a 5×5 identity matrix and

$$\begin{aligned}
e_1 &= \kappa_1 + \kappa_2 + \kappa_3 + z^* + \mu + \nu_2.\\
e_2 &= \kappa_2\kappa_3 + (\kappa_1 + z^* + \mu)(\kappa_2 + \kappa_3) + \kappa_1(z^* + \mu) + \nu_2(\kappa_2 + \kappa_3) + \nu_2(\kappa_1 + z^* + \mu)\\
&\quad - \xi_1 q_1 \epsilon\rho - \xi_1 q_1\theta - \eta z^*.\\
e_3 &= \kappa_2\kappa_3(\kappa_1 + z^* + \mu) + (\kappa_1(\kappa_2 + \kappa_3)(z^* + \mu) + \kappa_2\kappa_3\nu_2 + \nu_2(\kappa_1 + z^* + \mu)(\kappa_2 + \kappa_3)\\
&\quad + \kappa_1\nu_2(z^* + \mu) - \xi_1 q_1 z^*\theta - \xi_1 q_1\epsilon\rho(z^* + \mu + \kappa_2) - \xi_1 q_1\epsilon\rho\nu_2 - \xi_1 q_1\theta(z^* + \mu + \kappa_3)\\
&\quad - \xi_1 q_1\theta\nu_2 - \eta z^*(\kappa_2 + \kappa_3) - \eta z^*\nu_2 - \xi_1 q_1\epsilon z^*\rho,\\
e_4 &= \kappa_1\kappa_2\kappa_3(z^* + \mu) + \kappa_2\kappa_3\nu_2(\kappa_1 + z^* + \mu) + \kappa_1\nu_2(\kappa_2 + \kappa_3)(z^* + \mu) + \xi_1 q_1 z^*\theta(\kappa_3 + \nu_2)\\
&\quad - \xi_1^2 q_1^2\epsilon\rho\kappa_2 - \xi_1 q_1\epsilon\rho\nu_2(z^* + \mu + \kappa_2) - \xi_1^2 q_1^2\epsilon\theta\kappa_3 - \xi_1 q_1\theta\nu_2(z^* + \mu + \kappa_3) - \nu_2\omega_2\rho z^*\\
&\quad - \nu_2\omega_2 z^*\theta - \eta z^*\kappa_2\kappa_3 - \eta z^*\nu_2(\kappa_2 + \kappa_3) - \xi_1 q_1\epsilon z^*\rho(\kappa_1 + \nu_2),\\
e_5 &= \kappa_1\kappa_2\kappa_3\nu_2(z^* + \mu) - \xi_1 q_1 z^*\theta\nu_2\kappa_3 - \xi_1^2 q_1^2\epsilon\rho\nu_2\kappa_2 - \xi_1^2 q_1^2\epsilon\theta\nu_2\kappa_3 - \nu_2\omega_2\rho z^*\kappa_2 - \omega_2\nu_2 z^*\theta\kappa_2\\
&\quad - \eta z^*\nu_2\kappa_2\kappa_3 - \xi_1 q_1\epsilon z^*\rho\kappa_2\nu_2.
\end{aligned}$$

The TB endemic equilibrium is locally asymptotically stable if and only if the Routh-Hurwitz criterion is satisfied. The criterion states that the polynomial, $P(\lambda)$, has all roots with negative real parts if and only if the determinants, H, of all Hurwitz matrices are positive, that is $H_i > 0$, $i = 1, 2, 3, 4, 5$

[77]. According to [77], for a characteristic polynomial of degree five, the determinants are given by

$$\begin{aligned} H_1 &= e_1 > 0, \\ H_2 &= e_1e_2 - e_3 > 0. \\ H_3 &= e_1e_2e_3 + e_1e_3 + e_1e_5 - e_1e_4 - e_3 > 0, \\ H_4 &= (e_3e_4 - e_2e_5)(e_1e_2 - e_3) - (e_1e_4 - e_5) > 0, \\ H_5 &= e_5H_4 > 0. \end{aligned} \tag{4.65}$$

Now, when the determinants in system (4.65) are satisfied, then a conclusion can be made that the TB endemic equilibrium is locally asymptotically stable. □

4.3.3.1 Global stability of TB endemic equilibrium for TB-only sub model with medicati

Here, we investigate the global stability of the TB endemic equilibrium, E^*_{TB}.

Lemma 4.4: If $R_{TB} > 1$, then the TB endemic equilibrium, E^*_{TB}, of TB-only sub model system is globally asymptotically stable and unstable otherwise.

Proof. To investigate the global stability of, E^*_{TB}, the Lyapunov function $L = L(S, I_L, I_T, H, R_T)$, is constructed as:

$$\begin{aligned} L = U_1\Big((S - S^* - S^*In(\frac{S}{S^*})\Big) + U_2\Big(I_L - I^*_L - I^*_L In(\frac{I_L}{I^*_L})\Big) + U_3\Big(I_T - I^*_T - I^*_T In(\frac{I_T}{I^*_T})\Big) \\ + U_4\Big(H - H^* - H^*In(\frac{H}{H^*})\Big) + U_5\Big(R_T - R^*_T - R^*_T In(\frac{R_T}{R^*_T})\Big), \end{aligned}$$

where $U_1, U_2, ..., U_5$ are positive constants.

The time derivative of the Lyapunov function is given by:

$$\begin{aligned} \frac{dL}{dt} &= U_1\Big(1 - \frac{S^*}{S}\Big)\frac{dS}{dt} + U_2\Big(1 - \frac{I^*_L}{I_L}\Big)\frac{dI_L}{dt} + U_3\Big(1 - \frac{I^*_T}{I_T}\Big)\frac{dI_T}{dt} + U_4\Big(1 - \frac{H^*}{H}\Big)\frac{dH}{dt} \\ &\quad + U_5\Big(1 - \frac{R^*_T}{R_T}\Big)\frac{dR_T}{dt}, \\ &= U_1\Big(1 - \frac{S^*}{S}\Big)\Big(\Lambda + \eta I_L + \nu_2 R_T - \xi_1 q_1 \frac{(I_T + \epsilon H)}{N_{TB}} S - \mu S\Big) \\ &\quad + U_2\Big(1 - \frac{I^*_L}{I_L}\Big)\Big(\xi_1 q_1 \frac{(I_T + \epsilon H)}{N_{TB}} S - \kappa_1 I_L\Big) + U_3\Big(1 - \frac{I^*_T}{I_T}\Big)(\theta I_L - \kappa_2 I_T) \\ &\quad + U_4\Big(1 - \frac{H^*}{H}\Big)(\rho I_T - \kappa_3 H) + U_5\Big(1 - \frac{R^*_T}{R_T}\Big)(\omega_1 I_T + \omega_2 H - \kappa_4 R_T), \end{aligned} \tag{4.66}$$

where $\kappa_4 = \nu + \mu$.

At the TB endemic equilibrium, we have

$$\begin{aligned}
\Lambda &= \xi_1 q_1 \frac{(I_T^* + \epsilon H^*)}{N_{TB}^*} S^* + \mu S^* - \eta I_L^* - \nu_2 R_T^*, \\
\kappa_1 &= \xi_1 q_1 \frac{(I_T^* + \epsilon H^*)}{N_{TB}^* I_L^*} S^*, \\
\kappa_2 &= \frac{\theta I_L^*}{I_T^*}, \\
\kappa_3 &= \frac{\rho I_L^*}{H^*}, \\
\kappa_4 &= \frac{(\omega_1 I_T^* + \omega_2 H^*)}{R_T^*}.
\end{aligned} \tag{4.67}$$

Now, substituting for $\Lambda, \kappa_1, \kappa_2, \kappa_3$ and κ_4 in Equation (4.66), we get

$$\begin{aligned}
\frac{dL}{dt} &= U_1\Big(1 - \frac{S^*}{S}\Big)\Big(\xi_1 q_1 \frac{(I_T^* + \epsilon H^*)}{N_{TB}^*} S^* + \mu S^* - \eta I_L^* - \nu_2 R_T^* + \eta I_L + \nu_2 R_T - \xi_1 q_1 \frac{(I_T + \epsilon H)}{N_{TB}} S - \mu S\Big) \\
&+ U_2\Big(1 - \frac{I_L^*}{I_L}\Big)\Big(\xi_1 q_1 \frac{(I_T + \epsilon H)}{N_{TB}} S - \xi_1 q_1 \frac{(I_T^* + \epsilon H^*)}{N_{TB}^* I_L^*} S^* I_L\Big) + U_3\Big(1 - \frac{I_T^*}{I_T}\Big)(\theta I_L - \frac{\theta I_L^*}{I_T^*} I_T) \\
&+ U_4\Big(1 - \frac{H^*}{H}\Big)(\rho I_T - \frac{\rho I_L^*}{H^*} H) + U_5\Big(1 - \frac{R_T^*}{R_T}\Big)(\omega_1 I_T + \omega_2 H - \frac{(\omega_1 I_T^* + \omega_2 H^*)}{R_T^*} R_T).
\end{aligned}$$

Expanding and collecting the positive terms together and negative terms together, we have:

$$\frac{dL}{dt} = -X + Y,$$

where

$$\begin{aligned}
X = &\frac{U_1 \xi_1 q_1 I_T S}{N_{TB}} + \frac{U_1 \xi_1 q_1 \epsilon H S}{N_{TB}} + U_1 \eta I_L^* + U_1 \mu S + \frac{U_1 \xi_1 q_1 I_T^* S^*}{N_{TB}^*} \frac{S^*}{S} + \frac{U_1 \xi_1 q_1 \epsilon H S^*}{N_{TB}^*} \frac{S^*}{S} + U_1 \mu S^* \frac{S^*}{S} \\
&+ U_1 \eta I_L \frac{S^*}{S} + U_1 \nu_2 R_T \frac{S^*}{S} + \frac{U_1 \xi_1 q_1 \epsilon H S^*}{N_{TB}} + \frac{U_2 \xi_1 q_1 I_T^* S^*}{N_{TB}^*} \frac{I_L}{I_L^*} + \frac{U_2 \xi_1 q_1 \epsilon H^* S^*}{N_{TB}^*} \frac{I_L}{I_L^*} + \frac{U_2 \xi_1 q_1 I_T S}{N_{TB}} \frac{I_L^*}{I_L} \\
&+ \frac{U_2 \xi_1 q_1 \epsilon H S}{N_{TB}} \frac{I_L^*}{I_L} + U_3 \theta I_L^* \frac{I_T}{I_T^*} + U_3 \theta I_L^* \frac{I_T^*}{I_T} + U_4 \rho I_L^* \frac{H}{H^*} + U_4 \rho I_T \frac{H^*}{H} + U_5 \omega_1 I_T^* \frac{R_T}{R_T^*} + U_5 \omega_2 H \frac{R_T}{R_T^*} \\
&+ U_5 \omega_1 I_T \frac{R_T^*}{R_T} + U_5 \omega_2 H \frac{R_T^*}{R_T}
\end{aligned}$$

and

$$Y = \frac{U_1\xi_1 q_1 I_T^* S^*}{N_{TB}^*} + \frac{U_1\xi_1 q_1 \epsilon H S^*}{N_{TB}^*} + U_1\mu S^* + U_1\eta I_L + U_1\nu_2 R_T + U_1\eta I_L^*\frac{S^*}{S} + U_1\nu_2 R_T^*\frac{S^*}{S}$$
$$+ \frac{U_1\xi_1 q_1 I_T S^*}{N_{TB}} + U_1\mu S^* + \frac{U_2\xi_1 q_1 I_T S}{N_{TB}} + \frac{U_2\xi_1 q_1 \epsilon H S}{N_{TB}} + \frac{U_2\xi_1 q_1 I_T^* S^*}{N_{TB}^*} + \frac{U_2\xi_1 q_1 \epsilon H^* S^*}{N_{TB}^*}$$
$$+ U_3\theta I_L + U_3\theta I_L^* + U_4\rho I_L + U_4\rho I_L^* + U_5\omega_1 I_T + U_5\omega_2 H + U_5\omega_1 I_T^* + U_5\omega_2 H^*.$$

Hence, $\frac{dI_L}{dt} \leq 0$ when $Y < X$; and $\frac{dI_L}{dt} = 0$ when $S = S^*, I_L = I^*L, I_T = I_T^*, H = H^*$ and $R_T = R_T^*$. Therefore, the largest invariant set $(S, I_L, I_T, H, R_T) \in \Omega$ such that $\frac{dL}{dt} = 0$ is the singleton (E_{TB}^*), E_{TB}^* is the TB endemic equilibrium for TB-only sub model system. According to Lasalle's invariant principle (Lasalle, [71]), the global asymptotic stability of E_{TB}^* is guaranteed when $Y < X$. □

4.3.4 The HCV-only Sub model with Medication

The HCV-only sub model is derived by setting all the variables concerning TB infection to zero; that is $I_L(t) = I_T(t) = H(t) = R_T(t) = I_{AL}(t) = I_{CL}(t) = I_{AT}(t) = I_{CT}(t) = R(t) = 0$. Then the HCV-only sub model is as in Equation (4.68).

$$\begin{aligned}
\frac{dS}{dt} &= \Lambda + \pi I_A + \nu_1 R_H - \lambda_H S - \mu S,\\
\frac{dI_A}{dt} &= \lambda_H S - (\pi + \alpha + \mu) I_A,\\
\frac{dI_C}{dt} &= \alpha I_A - (\psi + \mu + \delta) I_C,\\
\frac{dR_H}{dt} &= \psi I_C - (\mu + \nu_1) R_H,
\end{aligned} \tag{4.68}$$

where

$$\lambda_H = \xi_2 q_2 \frac{(\phi I_A + I_C)}{N_{HCV}} \tag{4.69}$$

and

$$N_{HCV} = S + I_A + I_C + R_H. \tag{4.70}$$

The HCV infection-free equilibrium is calculated by modelling a scenario where HCV has been entirely eliminated from the population, such that $I_A = I_C = R_H = 0$. Therefore, the HCV-only sub model reduces to:

$$\frac{dS}{dt} = \Lambda - \mu S. \tag{4.71}$$

Setting the right-hand side of the Equation (4.71) to zero and solving the resulting equation, we have

$$S^0 = \frac{\Lambda}{\mu}.$$

Consequently, the HCV infection-free equilibrium point for the HCV-only sub model is given as:

$$E^0_{HCV} = (S^0, I^0_A, I^0_C, R^0_H) = (\frac{\Lambda}{\mu}, 0, 0, 0).$$

Lemma 4.5: The effective reproduction number for HCV-only sub model (4.68) is

$$R_{HCV} = \frac{\xi_2 q_2 \big(\phi(\psi + \mu + \delta) + \alpha\big)}{(\pi + \alpha + \mu)(\psi + \mu + \delta)}.$$

Proof. To compute R_{HCV}, the next generation matrix technique (Driessche and Watmough, [35]) is employed.

The matrix for the rate of appearance of new HCV infections in compartment i, F_i, for the HCV-only sub model (4.68) is given by

$$F_i = \begin{bmatrix} \lambda_H S \\ 0 \\ 0 \end{bmatrix}.$$

The rate of transfer into and out of compartment, i by all other processes, V_i, is given by

$$V_i = \begin{bmatrix} (\pi + \alpha + \mu) I_A \\ -\alpha I_A + (\psi + \mu + \delta) I_C \\ -\psi I_C + (\mu + \nu_1) R_H \end{bmatrix}.$$

Now, the Jacobian matrix, F_{HCV}, of the new HCV infections in compartment i at HCV infection free equilibrium point, is given by

$$F_{HCV} = \begin{bmatrix} \xi_2 q_2 \phi & \xi_2 q_2 & 0 \\ 0 & 0 & 0 \\ 0 & 0 & 0 \end{bmatrix}.$$

At the disease-free equilibrium, the Jacobian matrix, V_{HCV}, corresponding to the rate of exchange

between compartment i through all processes is given by

$$V_{HCV} = \begin{bmatrix} (\pi+\alpha+\mu) & 0 & 0 \\ -\alpha & (\psi+\mu+\delta) & 0 \\ 0 & -\psi & (\mu+\nu_1) \end{bmatrix}$$

and

$$V_{HCV}^{-1} = \begin{bmatrix} \frac{1}{(\pi+\alpha+\mu)} & 0 & 0 \\ \frac{\alpha}{(\pi+\alpha+\mu)(\psi+\mu+\delta)} & \frac{1}{(\psi+\mu+\delta)} & 0 \\ \frac{\alpha\psi}{(\pi+\alpha+\mu)(\psi+\mu+\delta)(\mu+\nu_1)} & \frac{\psi}{(\psi+\mu+\delta)(\mu+\nu_1)} & \frac{1}{(\mu+\nu_1)} \end{bmatrix}.$$

Now,

$$F_{HCV}V_{HCV}^{-1} = \begin{bmatrix} \frac{\xi_2 q_2 \phi}{(\pi+\alpha+\mu)} + \frac{\xi_2 q_2 \alpha}{(\pi+\alpha+\mu)(\psi+\mu+\delta)} & \frac{\xi_2 q_2}{(\psi+\mu+\delta)} & 0 \\ 0 & 0 & 0 \\ 0 & 0 & 0 \end{bmatrix}.$$

For the eigenvalues, λ, we solve the equation

$$\det(\lambda I - F_{HCV}V_{HCV}^{-1}) = 0,$$

$$\det \begin{bmatrix} \lambda - \frac{\xi_2 q_2(\phi(\psi+\mu+\delta)+\alpha)}{(\pi+\alpha+\mu)(\psi+\mu+\delta)} & \frac{\xi_2 q_2}{(\psi+\mu+\delta)} & 0 \\ 0 & \lambda & 0 \\ 0 & 0 & \lambda \end{bmatrix} = 0. \tag{4.72}$$

On solving Equation (4.72), we have the eigenvalues

$$\lambda_1 = \frac{\xi_2 q_2(\phi(\psi+\mu+\delta)+\alpha)}{(\pi+\alpha+\mu)(\psi+\mu+\delta)}, \lambda_2 = 0 \text{ and } \lambda_3 = 0.$$

However, the effective reproduction number for the HCV-only sub model, R_{HCV}, is given by the spectral radius of the dominant eigenvalue as

$$\rho(F_{HCV}V_{HCV}^{-1}) = R_{HCV} = \frac{\xi_2 q_2(\phi(\psi+\mu+\delta)+\alpha)}{(\pi+\alpha+\mu)(\psi+\mu+\delta)}. \tag{4.73}$$

□

The parameters that are crucial in increasing or decreasing the value of R_{HCV} are discussed under sensitivity analysis in subsection (4.3.7).

Lemma 4.6: The HCV infection-free equilibrium, E^0_{HCV}, is locally asymptotically stable if $R_{HCV} < 1$ and unstable otherwise.

Proof. The Jacobian matrix, $J(E_{HCV})$, of the HCV-only sub model (4.68) is given by

$$J(E_{HCV}) = \begin{bmatrix} -\left(\xi_2 q_2 (\frac{\phi I_A + I_C}{N_{HCV}}) + \mu\right) & \pi - \xi_2 q_2 \phi \frac{S}{N_{HCV}} & -\xi_2 q_2 \frac{S}{N_{HCV}} & \nu_1 \\ \xi_2 q_2 (\frac{\phi I_A + I_C}{N_{HCV}}) & \xi_2 q_2 \phi \frac{S}{N_{HCV}} - (\pi + \alpha + \mu) & \xi_2 q_2 \frac{S}{N_{HCV}} & 0 \\ 0 & \alpha & -(\psi + \mu + \delta) & 0 \\ 0 & 0 & \psi & -(\mu + \nu_1) \end{bmatrix}. \quad (4.74)$$

At HCV infection-free equilibrium, E^0_{HCV}, the Jacobian matrix reduces to

$$J(E^0_{HCV}) = \begin{bmatrix} -\mu & \pi - \xi_2 q_2 \phi & -\xi_2 q_2 & \nu_1 \\ 0 & \xi_2 q_2 \phi - (\pi + \alpha + \mu) & \xi_2 q_2 & 0 \\ 0 & \alpha & -(\psi + \mu + \delta) & 0 \\ 0 & 0 & \psi & -(\mu + \nu_1) \end{bmatrix}. \quad (4.75)$$

Now, the characteristic polynomial $P(\lambda)$ is given by

$$P(\lambda) = \det \begin{bmatrix} (\lambda + \mu) & \pi - \xi_2 q_2 \phi & -\xi_2 q_2 & \nu_1 \\ 0 & \lambda + (\pi + \alpha + \mu) - \xi_2 q_2 \phi & \xi_2 q_2 & 0 \\ 0 & \alpha & \lambda + (\psi + \mu + \delta) & 0 \\ 0 & 0 & \psi & \lambda + (\mu + \nu_1) \end{bmatrix}. \quad (4.76)$$

On solving Equation (4.76), we have

$$P(\lambda) = (\lambda + \mu)(\lambda + (\mu + \nu_1))\left(\lambda^2 + a_1 \lambda + a_0\right), \quad (4.77)$$

where

$$a_1 = (\psi + \mu + \delta) + (\pi + \alpha + \mu) - \xi_2 q_2 \phi > 0 \text{ if } (\psi + \mu + \delta) + (\pi + \alpha + \mu) > \xi_2 q_2 \phi$$

and

$$\begin{aligned} a_0 &= (\psi+\mu+\delta)((\pi+\alpha+\mu)-\xi_2 q_2\phi)-\alpha\xi_2 q_2, \\ &= (\psi+\mu+\delta)(\pi+\alpha+\mu)(1-R_{HCV})>0 \text{ if } R_{HCV}<1. \end{aligned}$$

By Routh-Hurwitz criterion, the characteristic polynomial $\lambda^2+a_1\lambda+a_0$ has negative eigenvalues if $a_1>0$ and $a_0>0$ which is satisfied when $R_{HCV}<1$. Therefore, since all the eigenvalues of the characteristic polynomial (4.77) are negative for $R_{HCV}<1$, then the HCV infection-free equilibrium point of system (4.68) is locally asymptotically stable. □

4.3.4.1 Global stability of HCV infection-free equilibrium for HCV-only sub model with medication

The global behaviour of HCV-only sub model (4.68) is studied by applying the Theorem by Castillo-Chav et al. [76]. Re-writing the HCV-only sub model (4.68) in the form:

$$\begin{aligned} \frac{dX_{HCV}}{dt} &= F(X_{HCV}, Z_{HCV}) \\ \frac{dZ_{HCV}}{dt} &= G(X_{HCV}, Z_{HCV}), G(X_{HCV}, 0)=0, \end{aligned} \tag{4.78}$$

where $X_{HCV}=(S_{HCV})$ and, $Z_{HCV}=(I_A, I_C, R_H)$, with $X_{HCV}\in\mathbb{R}_+$ denoting (its components) the number of uninfected humans and $Z_{HCV}\in\mathbb{R}_+^3$ whose components denote the number of humans infected with HCV including those ones under treatment class. Let the HCV infection-free equilibrium of system (4.78) be denoted by $E^0_{HCV}=(X^0_{HCV},0)=(\frac{\Lambda}{\mu},0,0,0)$.
It is necessary to ensure that the following conditions are satisfied to guarantee global asymptotic stability.

$\mathcal{H}1$: For $\frac{dX_{HCV}}{dt}=F(X_{HCV},0), X^0_{HCV}$ is globally asymptotically stable.

$\mathcal{H}2: G(X_{HCV},Z_{HCV})=AZ_{HCV}-\hat{G}(X_{HCV},Z_{HCV}), \hat{G}(X_{HCV},Z_{HCV})\geq 0$ for $(X_{HCV},Z_{HCV})\in\Omega_{HCV}$,

where $A=\frac{\partial}{\partial Z_{HCV}}G(X^0_{HCV},0)$ is an M-matrix and Ω_{HCV} is the invariant region in which the model takes biological sense.

Theorem 8. *The fixed point $E^0_{HCV}=(X_{HCV},0)$ is a globally asymptotic stable equilibrium of system (4.78) provided $R_{HCV}<1$ and that the conditions $(\mathcal{H}1)$ and $(\mathcal{H}2)$ are satisfied.*

Proof. From Lemma (4.6), E^0_{HCV} is locally asymptotically stable if $R_{HCV} < 1$.

For the first condition $(E1)$, that is , the global asymptotic stability of X^0_{HCV}, we have

$$F(X_{HCV}, Z_{HCV}) = \begin{bmatrix} \Lambda + \pi I_A + \nu_1 R_H - (\lambda_H + \mu)S \\ 0 \end{bmatrix} \tag{4.79}$$

and

$$\frac{dX_{HCV}}{dt} = F(X_{HCV}, 0) = \Lambda - \mu S, \tag{4.80}$$

which is a linear differential equation. On solving equation (4.80), we get

$$S(t) = \frac{\Lambda}{\mu} - \frac{\Lambda}{\mu}e^{-\mu t} + S(0)e^{-\mu t}. \tag{4.81}$$

Now, as $t \to \infty$, $S_{HCV}(t) \to \frac{\Lambda}{\mu}$ regardless of the value of $S(0)$. Thus, there is convergence in Ω_{HCV}, implying that condition $(E1)$ holds.

For the second condition, $(E2)$, consider

$$G(X_{HCV}, Z_{HCV}) = \begin{bmatrix} \xi_2 q_2 \frac{(\phi I_A + I_C)S}{N_{HCV}} - (\pi + \alpha + \mu)I_A \\ \alpha I_A - (\psi + \mu + \delta) \\ \psi I_C - (\mu + \nu_1)R_H \end{bmatrix}$$

and

$$A = \frac{\partial}{\partial Z_{HCV}} G(X^0_{HCV}, 0) = \begin{bmatrix} \xi_2 q_2 \phi \frac{S}{N_{HCV}} - (\pi + \alpha + \mu) & \xi_2 q_2 \frac{S}{N_{HCV}} & 0 \\ \alpha & -(\psi + \mu + \delta) & 0 \\ 0 & \psi & -(\mu + \nu_1) \end{bmatrix}.$$

Now, at

$$E^0_{HCV} = (\frac{\Lambda}{\mu}, 0, 0, 0), \qquad \frac{S}{N_{HCV}} \leq 1.$$

Thus,

$$A = \begin{bmatrix} \xi_2 q_2 \phi - (\pi + \alpha + \mu) & \xi_2 q_2 & 0 \\ \alpha & -(\psi + \mu + \delta) & 0 \\ 0 & \psi & -(\mu + \nu_1) \end{bmatrix},$$

and

$$\hat{G}(X_{HCV}, Z_{HCV}) = AZ_{HCV} - G(X_{HCV}, Z_{HCV})$$

$$\hat{G}(X_{HCV}, Z_{HCV}) = \begin{bmatrix} \xi_2 q_2 \phi - (\pi + \alpha + \mu) & \xi_2 q_2 & 0 \\ \alpha & -(\psi + \mu + \delta) & 0 \\ 0 & \psi & -(\mu + \nu_1) \end{bmatrix} \begin{bmatrix} I_A \\ I_C \\ R_H \end{bmatrix} - \begin{bmatrix} \xi_2 q_2 \frac{(\phi I_A + I_C)S}{N_{HCV}} - (\pi + \alpha + \mu) I_A \\ \alpha I_A - (\psi + \mu + \delta) \\ \psi I_C - (\mu + \nu_1) R_H \end{bmatrix}$$

$$= \begin{bmatrix} \xi_2 q_2 \phi I_A (1 - \frac{S}{N_{HCV}}) + \xi_2 q_2 I_C (1 - \frac{S}{N_{HCV}}) \\ 0 \\ 0 \end{bmatrix}. \tag{4.82}$$

Since $0 < S \leq N_{HCV}$, it is clearly noticeable from Equation (4.82) that $\hat{G}(X_{HCV}, Z_{HCV}) \geq 0$. However, matrix A is not a Metzler matrix since not all it off-diagonal elements are non-negative. Hence, E^0_{HCV} may lack global asymptotic stability for $R_{HCV} < 1$. Consequently, a backward bifurcation takes place as established by Feng at el. [69] at $R_{HCV} = 1$. The system can exhibit two stable states: disease-free and disease-present with the initial conditions determining which state the system converges to. □

4.3.5 HCV Endemic Equilibrium E^*_{HCV}

The HCV infection equilibrium point, $E^*_{HCV} = (S^*, I^*_A, I^*_C, R^*_H)$ occurs when HCV infection persists in the population. Equating the derivatives of HCV-only sub model (4.68) to zero, gives

$$\Lambda + \pi I_A + \nu_1 R_H - \lambda_H S - \mu S = 0, \tag{4.83}$$

$$\lambda_H S - (\pi + \alpha + \mu) I_A = 0, \tag{4.84}$$

$$\alpha I_A - (\psi + \mu + \delta) I_C = 0, \tag{4.85}$$

$$\psi I_C - (\mu + \nu_1) R_H = 0, \tag{4.86}$$

where

$$\lambda_H = \xi_2 q_2 \frac{(\phi I_A + I_C)}{N_{HCV}} \tag{4.87}$$

and

$$\frac{dN}{dt} = \Lambda - \mu N_{HCV} - \delta I_C.$$

But at equilibrium point, $\frac{dN}{dt} = 0$. This implies

$$\Lambda - \mu N_{HCV} - \delta I_C = 0. \tag{4.88}$$

Re-arranging Equation (4.88), we have

$$I_C = \frac{(\Lambda - \mu N_{HCV})}{\delta}. \tag{4.89}$$

Substituting I_C in Equation (4.84) and simplifying, we get

$$I_A = \frac{(\psi + \mu + \delta)(\Lambda - \mu N_{HCV})}{\alpha\delta}. \tag{4.90}$$

Substituting I_C in Equation (4.86) and simplifying yields

$$R_H = \frac{\psi(\Lambda - \mu N_{HCV})}{\delta(\mu + \nu_1)}. \tag{4.91}$$

Now, substituting I_A, I_C and R_H in Equation (4.83) and simplifying, we have

$$S = \frac{(\pi + \alpha + \mu)(\psi + \mu + \delta)N_{HCV}}{\xi_2 q_2(\phi(\psi + \mu + \delta) + \alpha)}. \tag{4.92}$$

Thus, the HCV infection endemic equilibrium point, $E^*_{HCV} = \left(S^*, I^*_A, I^*_C, R^*_H\right)$ is given by

$$\Big(\frac{(\pi + \alpha + \mu)(\psi + \mu + \delta)N_{HCV}}{\xi_2 q_2(\phi(\psi + \mu + \delta) + \alpha)}, \frac{(\psi + \mu + \delta)(\Lambda - \mu N_{HCV})}{\alpha\delta}, \frac{(\Lambda - \mu N_{HCV})}{\delta}, \frac{\psi(\Lambda - \mu N_{HCV})}{\delta(\mu + \nu_1)}\Big).$$

Lemma 4.7: The HCV-only sub model (4.68) has a unique endemic equilibrium point if $R_{HCV} > 1$.

Proof: If the disease stays in the population, then $\frac{dI_A}{dt} > 0$ and $\frac{dI_C}{dt} > 0$, that is

$$\xi_2 q_2(\phi I_A + I_C)\frac{S}{N_{HCV}} - (\pi + \alpha + \mu)I_A > 0, \tag{4.93}$$

$$\alpha I_A - (\psi + \mu + \delta)I_C > 0. \tag{4.94}$$

Re-arranging inequality (4.93), we have

$$I_A < \frac{\xi_2 q_2(\phi I_A + I_C)}{(\pi + \alpha + \mu)}\frac{S}{N_{HCV}}. \tag{4.95}$$

Using the fact that $\frac{S}{N_{HCV}} \leq 1$, (4.95) reduces to

$$I_A < \frac{\xi_2 q_2(\phi I_A + I_C)}{(\pi + \alpha + \mu)}. \tag{4.96}$$

From inequality (4.94), we have

$$I_C < \frac{\alpha I_A}{(\psi + \mu + \delta)}. \tag{4.97}$$

Substituting I_C into inequality (4.96) and simplifying, we get

$$1 < \frac{\xi_2 q_2(\phi(\pi + \alpha + \mu) + \alpha)}{(\pi + \alpha + \mu)(\psi + \mu + \delta)}. \tag{4.98}$$

Thus, $R_{HCV} > 1$.

Hence, a unique endemic equilibrium point E^*_{HCV} exists when $R_{HCV} > 1$.

Lemma 4.8: The HCV infection endemic equilibrium point $E^*_{HCV} = (S^*, I^*_A, I^*_C, R^*_H)$ is locally asymptotically stable for the effective reproduction number, $R_{HCV} > 1$, and unstable otherwise.

Proof. To study the local stability of the HCV endemic equilibrium point, we use the method of Routh-Hurwitz criterion. At the HCV endemic equilibrium point, E^*_{HCV}, the Jacobian matrix is

$$J(E^*_{HCV}) = \begin{bmatrix} -(f^* + \mu) & \pi - \frac{\xi_2 q_2 \phi}{R_{HCV}} & \frac{-\xi_2 q_2}{R_{HCV}} & \nu_1 \\ f^* & \frac{\xi_2 q_2 \phi}{R_{HCV}} - (\pi + \alpha + \mu) & \frac{\xi_2 q_2}{R_{HCV}} & 0 \\ 0 & \alpha & -(\psi + \mu + \delta) & 0 \\ 0 & 0 & \psi & -(\mu + \nu_1) \end{bmatrix}, \tag{4.99}$$

where

$f^* = \frac{\xi_2 q_2(\Lambda - \mu N_{HCV})(\phi(\psi + \mu + \delta) + \alpha)}{\alpha \delta N_{HCV}}$, is the force of HCV infection evaluated at E^*_{HCV}.

The characteristic polynomial $P(\lambda)$ of $J(E^*_{HCV})$ is given as

$$
\begin{aligned}
P(\lambda) &= \det(\lambda I - J(E^*_{HCV})), \\
&= \det \begin{bmatrix} \lambda + (f^* + \mu) & \pi - \frac{\xi_2 q_2 \phi}{R_{HCV}} & \frac{-\xi_2 q_2}{R_{HCV}} & \nu_1 \\ f^* & \lambda + (\pi + \alpha + \mu) - \frac{\xi_2 q_2 \phi}{R_{HCV}} & \frac{\xi_2 q_2}{R_{HCV}} & 0 \\ 0 & \alpha & \lambda + (\psi + \mu + \delta) & 0 \\ 0 & 0 & \psi & \lambda + (\mu + \nu_1) \end{bmatrix}, \\
&= \lambda^4 + a_1\lambda^3 + a_2\lambda^2 + a_3\lambda + a_4,
\end{aligned}
$$

where I is a 4×4 identity matrix and

$$
\begin{aligned}
a_1 &= (\pi + \alpha + \mu) + (\psi + \mu + \delta) + (\mu + \nu_1) + f^* + \mu - \frac{\xi_2 q_2 \phi}{R_{HCV}}, \\
a_2 &= 3(\pi + \alpha + \mu)(\psi + \mu + \delta) + (\pi + \alpha + \mu)((\pi + \alpha + \mu) + f^* + \mu) \\
&\quad - \big(\pi f^* + \frac{\xi_2 q_2 \phi}{R_{HCV}}((\pi + \alpha + \mu) + 2(\psi + \mu + \delta) + \mu)\big), \\
a_3 &= (\psi + \mu + \delta)(\mu + \nu_1)((\pi + \alpha + \mu) + (f^* + \mu)) + (\pi + \alpha + \mu)(f^* + \mu) \\
&\quad - \big(\pi f^*((\psi + \mu + \delta) + (\mu + \nu_1)) + \frac{\xi_2 q_2}{R_{HCV}}(\phi(\psi + \mu + \delta)(\mu + \nu_1) \\
&\quad + \phi\mu((\psi + \mu + \delta) + (\mu + \nu_1)) + 2\alpha f^* + \alpha(\mu + (\mu + \nu_1))\big), \\
a_4 &= (\pi + \alpha + \mu)(\psi + \mu + \delta)(\mu + \nu_1)(f^* + \mu) - \big((\psi + \mu + \delta)(\mu + \nu_1)\pi f^* + \alpha\nu_1\psi f^* \\
&\quad + \frac{\xi_2 q_2(\mu + \nu_1)}{R_{HCV}}(\phi(\psi + \mu + \delta)\mu + 2\alpha f^* + \alpha\mu)\big).
\end{aligned}
$$

The local stability of the HCV endemic equilibrium is determined by the Routh-Hurwitz criterion which provides the necessary and sufficient conditions. The criterion requires that the Hurwitz determinants, H_i with $i = 1, 2, 3, 4$ are all non-negative. According to the Routh-Hurwitz, for a fourth-degree polynomial, these determinants are given by

$$
\begin{aligned}
H_1 &= a_1 > 1, \\
H_2 &= a_1 a_2 - a_3 > 0, \\
H_3 &= a_3(a_1 a_2 - a_3) - a_1^2 a_4 > 0, \\
H_4 &= a_4 > 0.
\end{aligned} \tag{4.100}
$$

When determinants in (4.100) are satisfied, thus a conclusion can be made that the endemic equilibrium

is locally asymptotically stable for $R_{HCV} > 1$. □

4.3.5.1 Global stability of HCV endemic equilibrium for HCV-only sub model with medication

Here, we investigate the global stability of HCV endemic equilibrium point E^*_{HCV}.

Lemma 4.9: The HCV infection endemic equilibrium point, E^*_{HCV} for HCV-only sub model is globally asymptotically stable if $R_{HCV} > 1$ and unstable otherwise.

Proof. To establish the global asymptotic stability of the HCV endemic equilibrium, we employ the Lyapunov function method.

Define a Lyapunov function, $L = L(S, I_A, I_C, R_H)$ as:

$$L = U_1\big(S - S^* - S^* In(\frac{S}{S^*})\big) + U_2\big(I_A - I^*_A - I^*_A In(\frac{I_A}{I^*_A})\big) + U_3\big(I_C - I^*_C - I^*_C In(\frac{I_C}{I^*_C})\big) + U_4\big(R_H - R^*_H - R^*_H In(\frac{R_H}{R^*_H})\big).$$

Evaluating the derivative of L with respect to time, t along with the equations of system (4.68), we have

$$\begin{aligned}\frac{dL}{dt} &= U_1\Big(1 - \frac{S^*}{S}\Big)\frac{dS}{dt} + U_2\Big(1 - \frac{I^*_A}{I_A}\Big)\frac{dI_A}{dt} + U_3\Big(1 - \frac{I^*_C}{I_C}\Big)\frac{dI_C}{dt} + U_4\Big(1 - \frac{R^*_H}{R_H}\Big)\frac{dR_H}{dt} \\ &= U_1\Big(1 - \frac{S^*}{S}\Big)(\Lambda + \pi I_A + \nu_1 R_H - \lambda_H S - \mu S) + U_2\Big(1 - \frac{I^*_A}{I_A}\Big)(\lambda_H S - (\pi + \alpha + \mu)I_A \\ &+ U_3\Big(1 - \frac{I^*_C}{I_C}\Big)(\alpha I_A - (\psi + \mu + \delta)I_C + U_4\Big(1 - \frac{R^*_H}{R_H}\Big)(\psi I_C - (\mu + \nu_1))R_H,\end{aligned} \tag{4.101}$$

where $U_1, U_2, ..., U_4$ are positive constants.

At the HCV infection endemic equilibrium point, we have:

$$\begin{aligned}\Lambda &= \xi_2 q_2\Big(\frac{\phi I^*_A + I^*_C}{N^*_{HCV}}\Big)S^* + \mu S^* - \pi I^*_A - \nu_1 R^*_H, \\ (\pi + \alpha + \mu) &= \xi_2 q_2\Big(\frac{\phi I^*_A + I^*_C}{N^*_{HCV}}\Big)S^*, \\ (\psi + \mu + \delta) &= \frac{\alpha I^*_A}{I^*_C}, \\ (\mu + \nu_1) &= \frac{\psi I^*_C}{R^*_H}.\end{aligned} \tag{4.102}$$

Substituting Equation (4.102) into (4.101), we have

$$\begin{aligned}\frac{dL}{dt} &= U_1\Big(1-\frac{S^*}{S}\Big)(\xi_2 q_2\Big(\frac{\phi I_A^* + I_C^*}{N_{HCV}^*}\Big)S^* + \mu S^* - \pi I_A^* - \nu_1 R_H^* + \pi I_A + \nu_1 R_H - \lambda_H S - \mu S)\\ &+ U_2\Big(1-\frac{I_A^*}{I_A}\Big)(\lambda_H S - \xi_2 q_2\Big(\frac{\phi I_A^* + I_C^*}{N_{HCV}^*}\Big)S^* I_A \\ &+ U_3\Big(1-\frac{I_C^*}{I_C}\Big)(\alpha I_A - \frac{\alpha I_A^*}{I_C^*} I_C + U_4\Big(1-\frac{R_H^*}{R_H}\Big)(\psi I_C - \frac{\psi I_C^*}{R_H^*} R_H).\end{aligned} \tag{4.103}$$

Now, expanding and collecting positive terms together and negative terms together, we have:

$$\frac{dL}{dt} = Q - R,$$

where

$$\begin{aligned}Q &= U_1\xi_2 q_2(\frac{\phi I_A^* + I_C^*}{N_{HCV}^*})S^* + U_1\mu S^* + U_1\pi I_A + U_1\nu_1 R_H + U_1\pi I_A^*\frac{S^*}{S} U_1\nu_1 R_H^*\frac{S^*}{S}\\ &+ U_1\xi_2 q_2(\frac{\phi I_A + I_C}{N_{HCV}})S + U_1\mu S^* + U_2\xi_2 q_2(\frac{\phi I_A + I_C}{N_{HCV}})S + U_2\xi_2 q_2(\frac{\phi I_A^* + I_C^*}{N_{HCV}^*})S^*\\ &+ U_3\alpha I_A + U_4\psi I_C + U_4\psi I_C^*,\end{aligned}$$

and

$$\begin{aligned}R &= U_1\pi I_A^* + U_1\nu_1 R_H^* + U_1\xi_2 q_2(\frac{\phi I_A + I_C}{N_{HCV}})S + U_1\mu S + U_1\xi_2 q_2(\frac{\phi I_A^* + I_C^*}{N_{HCV}^*})S^*\frac{S^*}{S} + U_1\mu S^*\frac{S^*}{S}\\ &+ U_1\pi I_A\frac{S^*}{S} + U_1\nu_1 R_H\frac{S^*}{S} + U_2\xi_2 q_2(\frac{\phi I_A^* + I_C^*}{N_{HCV}^*})S^*\frac{I_A}{I_A^*} + U_2\xi_2 q_2(\frac{\phi I_A + I_C}{N_{HCV}})S\frac{I_A^*}{I_A} + U_A\alpha_A^*\frac{I_C}{I_A^*}\\ &+ U_3\alpha I_A\frac{I_C^*}{I_C} + U_4\psi I_C\frac{R_H}{R_H^*} + U_4\psi I_C\frac{R_H^*}{R_H}.\end{aligned}$$

Thus, we can guarantee that $\frac{dL}{dt} \leq 0$ when $Q < R$ and $\frac{dL}{dt} = 0$ when $S = S^*, I_A = I_A^*, I_C = I_C^*$ and $R_H = R_H^*$. Therefore, the largest compact invariant set in $(S, I_A^*, I_C^*, R^*H) \in \Omega_{HCV}$ such that $\frac{dL}{dt} = 0$ is the singleton E_{HCV}^*, where E_{HCV}^* is the HCV endemic equilibrium for HCV-only sub model system. By LaSalle's invariant principle [71], it implies that E_{HCV}^* is globally asymptotically stable in Ω_H when $Q < R$.

□

4.3.6 Analysis of TB-HCV Co-infection Model with Medication

In this subsection, the TB-HCV disease-free equilibrium, E^0, and the effective reproduction number, R_{TH}, for the TB-HCV co-infection model (4.3) are established.

At the equilibrium point where both TB and HCV are absent, $S^0 = \frac{\Lambda}{\mu}$,
$I_L^0 = I_T^0, H^0 = R_T^0 = I_A^0 = I_C^0 = R_H^0 = I_{AL}^0 = I_{CL}^0 = I_{AT}^0 = I_{CT}^0 = R^0 = 0.$
Therefore, the disease-free equilibrium point is given by

$$E^0 = (\frac{\Lambda}{\mu}, 0, 0, 0, 0, 0, 0, 0, 0, 0, 0, 0, 0).$$

Lemma 4.10: The effective reproduction number for TB-HCV co-infection model,
$R_{TH} = \max\{R_{TB}, R_{HCV}\}$.

Proof: The next generation method is used to calculate R_{TH}. Now, using Driessche and Watmough [35] method on TB-HCV co-infection model system (4.3), the matrices for rate of appearance of new infections in compartment i, F_i, and for the rate of transfer into and out of compartment i by all other processes, V_i, are obtained as follows:

$$F_i = \begin{bmatrix} \lambda_T S \\ 0 \\ 0 \\ 0 \\ \lambda_H S \\ 0 \\ 0 \\ \lambda_T I_A + \lambda_H I_L \\ \lambda_T I_C \\ \lambda_H I_T \\ 0 \\ 0 \end{bmatrix},$$

and

$$V_i = \begin{bmatrix} (\theta+\eta+\mu+\lambda_H)I_L \\ -\theta I_L + (\omega_1+\rho+\mu+\sigma_1+\lambda_H)I_T \\ -\rho I_T + (\omega_2+\mu+\sigma_2)II \\ -\omega_2 H - \omega_1 I_T + (\nu_2+\mu)R_T \\ (\pi+\alpha+\mu+\lambda_T)I_A \\ -\alpha I_A + (\psi+\mu+\delta+\lambda_H)I_C \\ -\psi I_C + (\nu_1+\mu)R_H \\ (\tau_1+\mu+\beta_1)I_{AL} \\ -\beta_1 I_{AL} + (r_1+\tau_2+\mu+\delta)I_{CL} \\ -\tau_1 I_{AL} + (r_2+\beta_2+\mu+d_1)I_{AT} \\ -\tau_2 I_{CL} - \beta_2 I_{AT} + (r_3+\mu+d_2)I_{CT} \\ -r_1 I_{CL} - r_2 I_{AT} - r_3 I_{CT} + (\nu_3+\mu)R \end{bmatrix}.$$

The Jacobian matrix, F, of the new infections at disease-free equilibrium point, E^0, is given by

$$F = \begin{bmatrix} 0 & \xi_1 q_1 & \xi_1 q_1 \epsilon & 0 & 0 & 0 & 0 & 0 & 0 & \xi_1 q_1 & \xi_1 q_1 a_2 & 0 \\ 0 & 0 & 0 & 0 & 0 & 0 & 0 & 0 & 0 & 0 & 0 & 0 \\ 0 & 0 & 0 & 0 & 0 & 0 & 0 & 0 & 0 & 0 & 0 & 0 \\ 0 & 0 & 0 & 0 & 0 & 0 & 0 & 0 & 0 & 0 & 0 & 0 \\ 0 & 0 & 0 & 0 & \xi_2 q_2 \phi & \xi_2 q_2 & 0 & \xi_2 q_2 b_1 & \xi_2 q_2 b_2 & \xi_2 q_2 b_3 & \xi_2 q_2 b_4 & 0 \\ 0 & 0 & 0 & 0 & 0 & 0 & 0 & 0 & 0 & 0 & 0 & 0 \\ 0 & 0 & 0 & 0 & 0 & 0 & 0 & 0 & 0 & 0 & 0 & 0 \\ 0 & 0 & 0 & 0 & 0 & 0 & 0 & 0 & 0 & 0 & 0 & 0 \\ 0 & 0 & 0 & 0 & 0 & 0 & 0 & 0 & 0 & 0 & 0 & 0 \\ 0 & 0 & 0 & 0 & 0 & 0 & 0 & 0 & 0 & 0 & 0 & 0 \\ 0 & 0 & 0 & 0 & 0 & 0 & 0 & 0 & 0 & 0 & 0 & 0 \\ 0 & 0 & 0 & 0 & 0 & 0 & 0 & 0 & 0 & 0 & 0 & 0 \end{bmatrix}.$$

The rate of exchange between compartment i and other compartments through various processes at the disease-free equilibrium point E^0 are represented by the Jacobian matrix V, which is given by

$$V = \begin{bmatrix} h_1 & 0 & 0 & 0 & 0 & 0 & 0 & 0 & 0 & 0 & 0 & 0 \\ -\theta & h_2 & 0 & 0 & 0 & 0 & 0 & 0 & 0 & 0 & 0 & 0 \\ 0 & -\rho & h_3 & 0 & 0 & 0 & 0 & 0 & 0 & 0 & 0 & 0 \\ 0 & \omega_1 & -\omega_2 & h_4 & 0 & 0 & 0 & 0 & 0 & 0 & 0 & 0 \\ 0 & 0 & 0 & 0 & h_5 & 0 & 0 & 0 & 0 & 0 & 0 & 0 \\ 0 & 0 & 0 & 0 & -\alpha & h_6 & 0 & 0 & 0 & 0 & 0 & 0 \\ 0 & 0 & 0 & 0 & 0 & \psi & h_7 & 0 & 0 & 0 & 0 & 0 \\ 0 & 0 & 0 & 0 & 0 & 0 & 0 & h_8 & 0 & 0 & 0 & 0 \\ 0 & 0 & 0 & 0 & 0 & 0 & 0 & -\beta_1 & h_9 & 0 & 0 & 0 \\ 0 & 0 & 0 & 0 & 0 & 0 & 0 & -\tau_1 & 0 & h_{10} & 0 & 0 \\ 0 & 0 & 0 & 0 & 0 & 0 & 0 & 0 & -\tau_2 & -\beta & h_{11} & 0 \\ 0 & 0 & 0 & 0 & 0 & 0 & 0 & 0 & -r_1 & -r_2 & -r_3 & h_{12} \end{bmatrix},$$

where

$$h_1 = (\theta + \eta + \mu),\ h_2 = (\omega_1 + \rho + \mu + \sigma_1),\ h_3 = (\omega_2 + \mu + \sigma_2),\ h_4 = (\nu_2 + \mu),$$
$$h_5 = (\pi + \alpha + \mu),\ h_6 = (\psi + \mu + \delta),\ h_7 = (\nu_1 + \mu),\ h_8 = (\tau_1 + \mu + \beta_1),$$
$$h_9 = (r_1 + \tau_2 + \mu + \delta),\ h_{10} = (r_2 + \beta_2 + \mu + d_1),\ h_{11} = (r_3 + \mu + d_2),\ h_{12} = (\nu_3 + \mu).$$

However, the effective reproduction number, R_{TH}, for the TB-HCV co-infection model is the greatest of eigenvalues $\lambda_1, \lambda_2, \lambda_3, \lambda_4, \lambda_5, \lambda_6, \lambda_7, \lambda_8, \lambda_9, \lambda_{10}, \lambda_{11}$ and λ_{12} of the next generation matrix, FV^{-1}. That is,

$$R_{TH} = \max\Big\{\frac{\xi_1 q_1 \theta}{(\eta + \mu + \theta)(\omega_1 + \rho + \mu)}\Big(1 + \frac{\epsilon\rho}{(\omega_2 + \mu + \sigma_2)}\Big),$$
$$\frac{\xi_2 q_2\big(\phi(\psi + \mu + \delta) + \alpha\big)}{(\pi + \alpha + \mu)(\psi + \mu + \delta)}, 0,\ 0\ , 0\ , 0\ , 0\ , 0\ , 0\ , 0\ , 0\Big\}.$$

Therefore,

$$R_{TH} = \max\{R_{TB}, R_{HCV}\}, \tag{4.104}$$

where R_{TB} and R_{HCV} are the effective reproduction numbers of TB and HCV-only sub models respectively. This means that the spread of TB-HCV co-infection will be largely influenced by the disease with higher transmission potential.

The following Theorem (5) follows from Theorem (2) of Driessche and Watmough [35].

Theorem 9. *The disease-free equilibrium point, E^0, of the TB-HCV co-infection model (4.3) is locally asymptotically stable if $R_{TH} < 1$ and unstable otherwise.*

4.3.6.1 Global Stability of Disease-free Equilibrium Point for TB-HCV Co-infection Model with Medication

In order to investigate the global stability of the disease-free equilibrium point, E^0, for the TB-HCV co-infection model system (4.3), we apply the same approach as in subsection (4.3.4).
Re-writing the TB-HCV co-infection model (4.3) in the form:

$$\begin{aligned} \frac{dX}{dt} &= F(X,Z) \\ \frac{dZ}{dt} &= G(X,Z), \quad G(X,0) = 0, \end{aligned} \tag{4.105}$$

where $X = (S)$ and $Z = (I_L, I_T, H, R_T, I_A, I_C, R_H, I_{AL}, I_{CL}, I_{AT}, I_{CT}, R)$, with $X \in R_+$ denoting the number of uninfected humans and $Z \in R_+^{12}$ whose components denote the number of humans infected with TB, HCV or both TB and HCV including those under treatment of TB or HCV.
Let $E^0 = (X^0.0) = (\frac{\Lambda}{\mu}, 0)$ be the disease-free equilibrium of system (4.105). To ensure global asymptotic stability, we need to ascertain that conditions (S_1) and (S_2) are satisfied.

$$(S_1): \text{ For } \frac{dX}{dt} = F(X,0), X^0 \text{ is globally asymptotically stable,}$$
$$(S_2): G(X,Z) = NZ - \hat{G}(X,Z) \geq 0 \text{ for } (X,Z) \in \Omega,$$

where $N = D_Z G(X^0, 0)$ is an M-matrix and Ω is the region where the model makes biological meaning. Therefore, when system (4.105) satisfies conditions (S_1) and (S_2), we have the following Theorem 6 satisfied.

Theorem 10. *The fixed point $E^0 = (X, 0)$ is a globally asymptotic stable equilibrium of (4.105) provided $R_{TH} < 1$ and that the conditions (S1) and (S2) are satisfied.*

Proof. From Theorem 5, E^0 is locally asymptotically stable if $R_{TH} < 1$.

Considering the first condition $(S1)$, that is , the global asymptotic stability of X^0, we have

$$F(X,Z) = \begin{bmatrix} \Lambda + \nu_1 R_H + \nu_2 R_T + \nu_3 R + \pi I_A + \eta I_L - (\lambda_T + \lambda_H + \mu)S \\ 0 \end{bmatrix} \tag{4.106}$$

and

$$\frac{dX}{dt} = F(X,0) = \Lambda - \mu S, \tag{4.107}$$

which takes the form of a linear differential equation. Solving Equation (4.107), gives

$$S(t) = \frac{\Lambda}{\mu} - \frac{\Lambda}{\mu}e^{-\mu t} + S(0)e^{-\mu t}. \tag{4.108}$$

Now, as $t \to \infty$, $S(t) \to \frac{\Lambda}{\mu}$ regardless of the value of $S(0)$. Thus, there is convergence in Ω, implying that condition $(S1)$ holds.

For the second condition, $(S2)$, consider

$$G(X,Z) = \begin{bmatrix} \lambda_T S - (\theta + \eta + \mu + \lambda_H)I_L \\ \theta I_L - (\omega_1 + \rho + \mu + \sigma_1 + \lambda_H)I_T \\ \rho I_T - (\omega_2 + \mu + \sigma_2)H \\ \omega_2 H + \omega_1 I_T - (\nu_2 + \mu)R_T \\ \lambda_H S - (\pi + \alpha + \mu + \lambda_T)I_A \\ \alpha I_A - (\psi + \mu + \delta + \lambda_T)I_C \\ \psi I_C - (\nu_1 + \mu)R_H \\ \lambda_T I_A + \lambda_H I_L - (\tau_1 + \mu + \beta_1)I_{AL} \\ \beta_1 I_{AL} + \lambda_T I_C - (r_1 + \tau_2 + \mu + \delta)I_{CL} \\ \tau_1 I_{AL} + \lambda_H I_T - (r_2 + \beta_2 + \mu + d_1)I_{AT} \\ \tau_2 I_{CL} + \beta_2 I_{AT} - (r_3 + \mu + d_2)I_{CT} \\ r_1 I_{CL} + r_2 I_{AT} + r_3 I_{CT} - (\nu_3 + \mu)R \end{bmatrix},$$

and

$$N = \begin{bmatrix} -j_1 & \xi_1 q_1 & \xi_1 q_1 \epsilon & 0 & 0 & 0 & 0 & 0 & 0 & \xi_1 q_1 a_1 & \xi_1 q_1 a_2 & 0 \\ \theta & -j_2 & 0 & 0 & 0 & 0 & 0 & 0 & 0 & 0 & 0 & 0 \\ 0 & \rho & -j_3 & 0 & 0 & 0 & 0 & 0 & 0 & 0 & 0 & 0 \\ 0 & \omega_1 & \omega_2 & -j_4 & 0 & 0 & 0 & 0 & 0 & 0 & 0 & 0 \\ 0 & 0 & 0 & 0 & -j_5 & \xi_2 q_2 & 0 & \xi_2 q_2 b_1 & \xi_2 q_2 b_2 & \xi_2 q_2 b_3 & \xi_2 q_2 b_4 & 0 \\ 0 & 0 & 0 & 0 & \alpha & -j_6 & 0 & 0 & 0 & 0 & 0 & 0 \\ 0 & 0 & 0 & 0 & 0 & \psi & -j_7 & 0 & 0 & 0 & 0 & 0 \\ 0 & 0 & 0 & 0 & 0 & 0 & 0 & -j_8 & 0 & 0 & 0 & 0 \\ 0 & 0 & 0 & 0 & 0 & 0 & 0 & \beta_1 & -j_9 & 0 & 0 & 0 \\ 0 & 0 & 0 & 0 & 0 & 0 & 0 & \tau_1 & 0 & -j_{10} & 0 & 0 \\ 0 & 0 & 0 & 0 & 0 & 0 & 0 & 0 & \tau_2 & \beta_2 & -j_{11} & 0 \\ 0 & 0 & 0 & 0 & 0 & 0 & 0 & 0 & r_1 & r_2 & r_3 & -j_{12} \end{bmatrix},$$

where

$$j_1 = (\theta + \eta + \mu),\ j_2 = (\omega_1 + \rho + \mu + \sigma_1),\ j_3 = (\omega_2 + \mu + \sigma_2),\ j_4 = (\nu_2 + \mu),$$
$$j_5 = \xi_2 q_2 \phi - (\pi + \alpha + \mu),\ j_6 = (\psi + \mu + \delta),\ j_7 = (\nu_1 + \mu),\ j_8 = (\tau_1 + \mu + \beta_1),$$
$$j_9 = (r_1 + \tau_2 + \mu + \delta),\ j_{10} = (r_2 + \beta_2 + \mu + d_1),\ j_{11} = (r_3 + \mu + d_2),\ j_{12} = (\nu_3 + \mu).$$

Then

$$\hat{G}(X,Z) = \begin{bmatrix} \hat{G}_1(X,Z) \\ \hat{G}_2(X,Z) \\ \hat{G}_3(X,Z) \\ \hat{G}_4(X,Z) \\ \hat{G}_5(X,Z) \\ \hat{G}_6(X,Z) \\ \hat{G}_7(X,Z) \\ \hat{G}_8(X,Z) \\ \hat{G}_9(X,Z) \\ \hat{G}_{10}(X,Z) \\ \hat{G}_{11}(X,Z) \\ \hat{G}_{12}(X,Z) \end{bmatrix} = NZ - G(X,Z),$$

$$= \begin{bmatrix} \lambda_H I_L + \xi_1 q_1 \left(1 - \frac{S}{N}\right)(I_T + cII + a_1 I_{AT} + a_2 I_{CT}) \\ \theta I_L + \lambda_H I_T \\ 0 \\ 0 \\ \lambda_T I_A + \xi_2 q_2 (\phi I_A + I_C + b_1 I_A + b_2 I_C + b_3 I_{AT} + b_4 I_{CT})\left(1 - \frac{S}{N}\right) \\ \lambda_T I_C \\ 0 \\ -(\lambda_T I_A + \lambda_H I_L) \\ -\lambda_T I_C \\ -\lambda_H I_T \\ 0 \\ 0 \end{bmatrix}.$$

Since $\hat{G}_8(X,Z) < 0$ $\hat{G}_9(X,Z) < 0$ and $\hat{G}_{10}(X,Z) < 0$, which implies that condition (S_2) does not hold. Thus, $E_0 = (X^0, 0)$ may not be stable in the long run for $R_{TH} < 1$. □

4.3.6.2 Existence and Stability of the Endemic Equilibrium of the TB-HCV Co-infect Model with Medication

The analytical determination of the endemic equilibrium point for the TB-HCV co-infection mo is strenuous. Therefore, its existence and stability shall be numerically established as in Chapter The initial states of the variables, $S, I_L, I_T, H, R_T, I_A, I_C, R_H, I_{AL}, I_{CL}, I_{AT}, I_{CT}$ and R are adjus to determine if they converge to the same positive equilibrium values over time despite different ini variable values. The values of the parameters used in the numerical study are presented in Table -

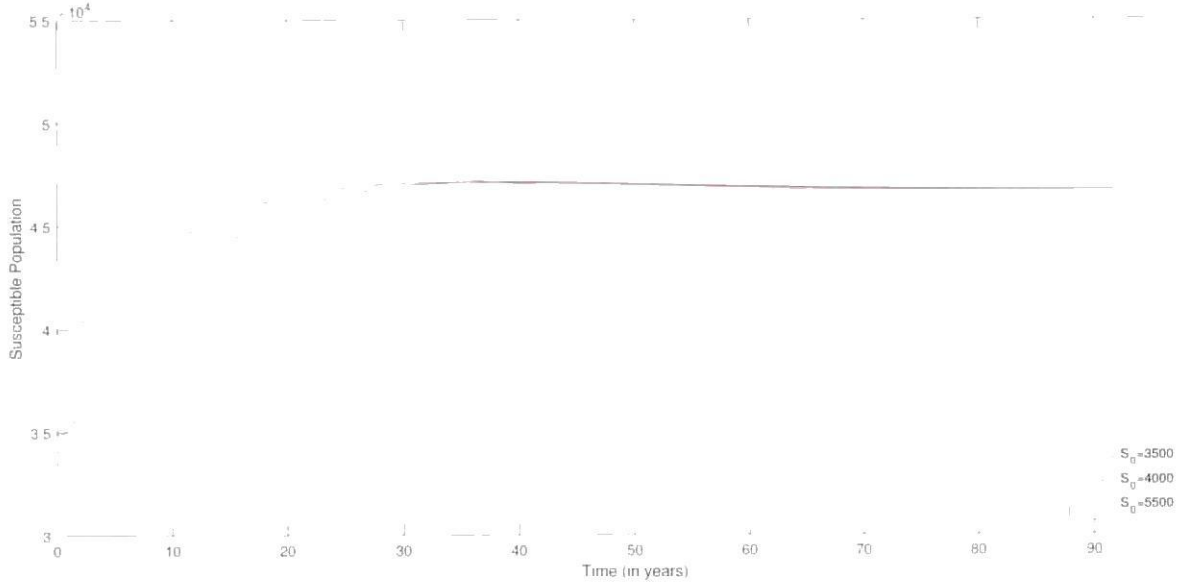

Figure 4.2: A graph of Susceptible humans against time with varied values of Susceptibles only.

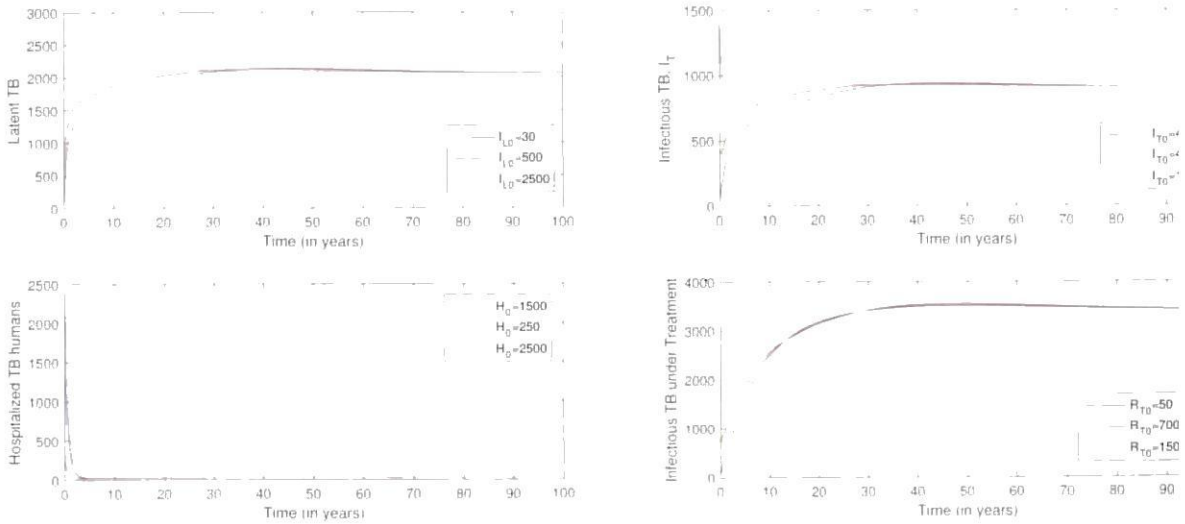

Figure 4.3: Graphs of TB infected humans against time.

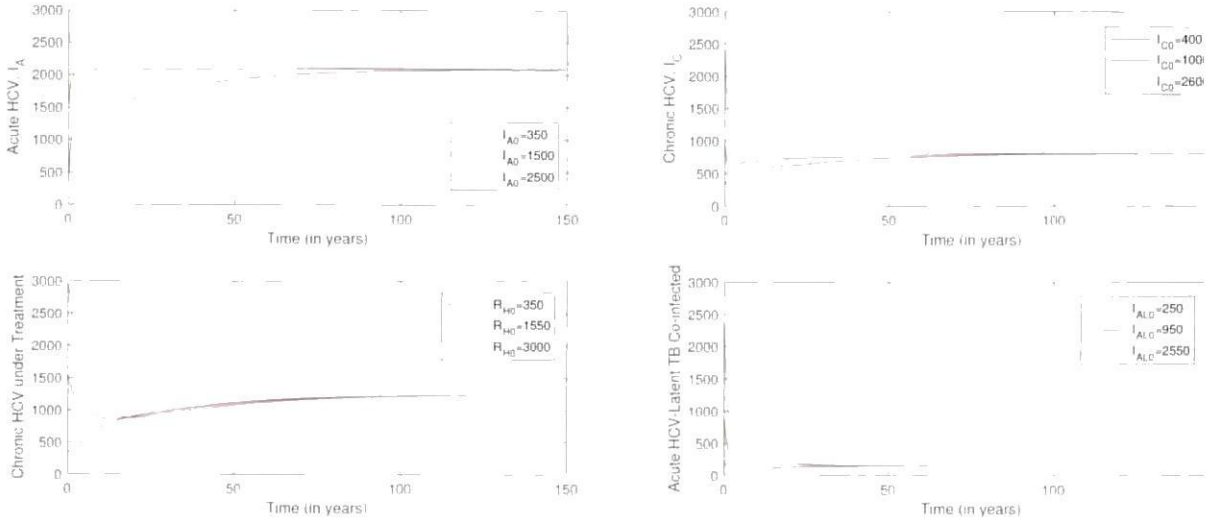

Figure 4.4: Graphs of HCV infected humans against time.

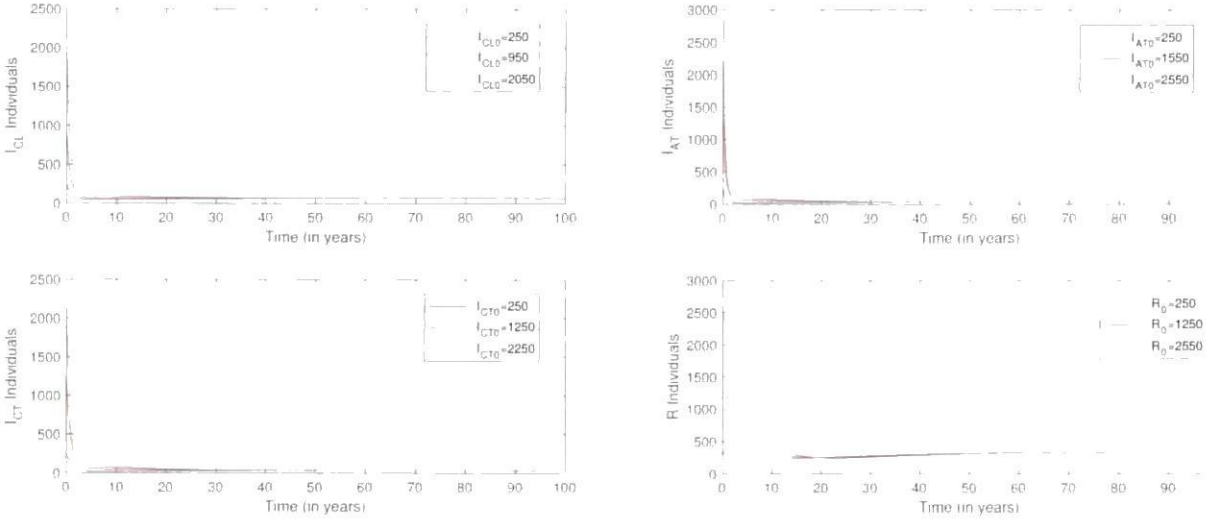

Figure 4.5: Graphs of co-infected humans against time.

Now, in Figures 4.2, 4.3, 4.4 and 4.5, the starting values of the specified variable are varied whi keeping the starting values of other variables of the TB-HCV co-infection model constant so as t ascertain whether the corresponding graphs would in the due course level off to the same non-zer values regardless of the different starting values of the variables. Curves in Figures 4.2, 4.3, 4.4 an 4.5 eventually level off to the same non-zero values regardless of the different starting values of th variables.

In Figure 4.6, we further demonstrate the existence and stability of the endemic state of the TB-HC

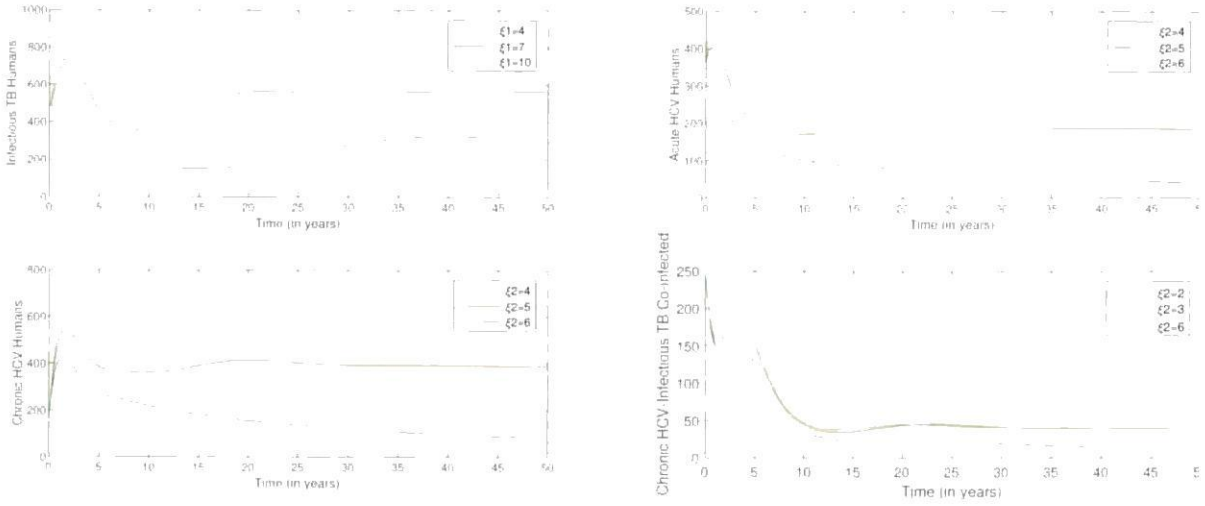

Figure 4.6: Figure displaying TB infectious humans, HCV acute humans, HCV chronic humans and chronic HCV-infectious TB co-infected humans against time with ξ_1 and ξ_2 respectively varied.

co-infection model. The values of some singled-out parameters say, the rate of human-to-human contact between the TB infected individuals and susceptible population, ξ_1 and the rate of human-to-human contact between the HCV infected individuals and susceptible population, ξ_2 are varied for some singled-out variables, say, TB infectious individuals assumed not on medication, I_T, acute HCV infected individuals, I_A, chronic HCV infected individuals, I_C and dually infected individuals with chronic HCV infections in the TB infectious stage, I_{CT}. This is done to ascertain whether these variables would in the due course level off to non-zero values regardless of the varying values of ξ_1 and ξ_2. Figure 4.6 reveals that despite the varying values of ξ_1 and ξ_2, in the long term, I_T, I_A, I_C and I_{CT} attain a non-zero steady- state, hence verifying the presence of a globally stable endemic equilibrium for the TB-HCV co-infection model.

4.3.7 Sensitivity Analysis

The sensitivity analysis is performed to assess the model's ability to withstand parameter fluctuations. This analysis can reveal which parameter has the greatest influence on R_{TH} [67]. Additionally, it facilitates the assessment of the relative impact of parameter changes on the state variable. The normalized forward sensitivity index shall be used to assess the sensitivity of each parameter of the model [67].

Definition: Let the variable W be a differentiable function of the parameter, p, then the normalized

forward sensitivity index of a variable W with respect to a parameter p is defined as

$$i_p^W = \frac{\partial W}{\partial p} \times \frac{p}{W}.$$

4.3.7.1 Computation of Sensitivity indices of the effective reproduction numbers with respect to the parameters of the Model

Now, proceeding like in subsection (3.3.3) of Chapter 3, the sensitivity analysis of the basic reproduction number of the TB-HCV co-infection model, R_{TH}, to each of the parameter is performed by computing the sensitivity indices of R_{TH} with respect to the parameters of the model using the normalized forward sensitivity index method [67]. Since $R_{TH} = \max\{R_{TB}, R_{HCV}\}$, sensitivity analysis of R_{TH} with respect to each of the parameters is carried out separately for R_{TB} and R_{HCV}. The sensitivity indices of R_{TB} and R_{HCV} have been calculated using formulas (4.109) and (4.110) respectively:

$$i_p^{R_{TB}} = \frac{\partial R_{TB}}{\partial p} \times \frac{p}{R_{TB}}, \tag{4.109}$$

and

$$i_p^{R_{HCV}} = \frac{\partial R_{HCV}}{\partial p} \times \frac{p}{R_{HCV}}. \tag{4.110}$$

The parameter values used with their respective sources and others assumed are presented in Table 4.3. The sensitivity indices of R_{TB} with respect to $\xi_1, q_1, \theta, \omega_1, \omega_2, \sigma_1, \sigma_2, \mu, \epsilon, \rho$ and η are respectively:

$$i_{\xi_1}^{R_{TB}} = \frac{\partial R_{TB}}{\partial \xi_1} \times \frac{\xi_1}{R_{TB}} = \frac{q_1\theta\big((\omega_2+\mu+\sigma_2)+\epsilon\rho\big)}{(\eta+\mu+\theta)(\omega_1+\rho+\mu+\sigma_1)(\omega_2+\mu+\sigma_2)} \times \frac{\xi_1}{R_{TB}} = 1.0000,$$

$$i_{q_1}^{R_{TB}} = \frac{\partial R_{TB}}{\partial q_1} \times \frac{q_1}{R_{TB}} = \frac{\xi_1\theta\big((\omega_2+\mu+\sigma_2)+\epsilon\rho\big)}{(\eta+\mu+\theta)(\omega_1+\rho+\mu+\sigma_1)(\omega_2+\mu+\sigma_2)} \times \frac{q_1}{R_{TB}} = 1.0000,$$

$$i_{\theta}^{R_{TB}} = \frac{\partial R_{TB}}{\partial \theta} \times \frac{\theta}{R_{TB}} = \frac{(\eta+\mu)}{(\eta+\mu+\theta)} = 0.6481,$$

$$i_{\omega_1}^{R_{TB}} = \frac{\partial R_{TB}}{\partial \omega_1} \times \frac{\omega_1}{R_{TB}} = \frac{-\omega_1}{(\omega_1+\rho+\mu+\sigma_1)} = -0.8600,$$

$$i_{\omega_2}^{R_{TB}} = \frac{\partial R_{TB}}{\partial \omega_2} \times \frac{\omega_2}{R_{TB}} = \frac{-\epsilon\rho\omega_2}{(\omega_2+\mu+\sigma_2)\big((\omega_2+\mu+\sigma_1)\big)} = -0.5610,$$

$$i_{\sigma_1}^{R_{TB}} = \frac{\partial R_{TB}}{\partial \sigma_1} \times \frac{\sigma_1}{R_{TB}} = \frac{-\sigma_1}{(\omega_1+\rho+\mu+\sigma_1)} = -0.0676,$$

$$i_{\sigma_2}^{R_{TB}} = \frac{\partial R_{TB}}{\partial \sigma_2} \times \frac{\sigma_2}{R_{TB}} = \frac{-\epsilon\rho\sigma_2}{(\omega_2+\mu+\sigma_2)\big((\omega_2+\mu+\sigma_1)\big)} = -0.0366,$$

$$i_{\epsilon}^{R_{TB}} = \frac{\partial R_{TB}}{\partial \epsilon} \times \frac{\epsilon}{R_{TB}} = \frac{\rho\epsilon}{(\omega_2+\mu+\sigma_2+\epsilon\rho)} = 0.0160,$$

$$i_{\eta}^{R_{TB}} = \frac{\partial R_{TB}}{\partial \eta} \times \frac{\eta}{R_{TB}} = \frac{-\eta}{(\eta+\mu+\theta)} = 0.6200,$$

$$i_{\rho}^{R_{TB}} = \frac{\partial R_{TB}}{\partial \rho} \times \frac{\rho}{R_{TB}} = \frac{\big(\epsilon(\omega_1+\rho+\mu+\sigma_1)-((\omega_2+\mu+\sigma_2)+\epsilon\rho)\big)}{((\omega_2+\mu+\sigma_2)+\epsilon\rho)(\omega_1+\rho+\mu+\sigma_1)} = -0.0312,$$

$$i_{\mu}^{R_{TB}} = \frac{\partial R_{TB}}{\partial \mu} \times \frac{\mu}{R_{TB}} = -0.0398.$$

The sensitivity indices of R_{HCV} with respect to $\xi_2, q_2, \phi, \psi, \delta, \alpha, \pi$and$\mu$ are respectively:

$$
\begin{aligned}
i_{\xi_2}^{R_{HCV}} &= \frac{\partial R_{HCV}}{\partial \xi_2} \times \frac{\xi_2}{R_{HCV}} = \frac{q_2(\phi(\psi+\mu+\delta)+\alpha)}{(\pi+\alpha+\mu)(\psi+\mu+\delta)} \times \frac{\xi_2}{R_{HCV}} = 1.0000,\\
i_{q_2}^{R_{HCV}} &= \frac{\partial R_{HCV}}{\partial q_2} \times \frac{q_2}{R_{HCV}} = \frac{\xi_2(\phi(\psi+\mu+\delta)+\alpha)}{(\pi+\alpha+\mu)(\psi+\mu+\delta)} \times \frac{q_2}{R_{HCV}} = 1.0000,\\
i_{\phi}^{R_{HCV}} &= \frac{\partial R_{HCV}}{\partial \phi} \times \frac{\phi}{R_{HCV}} = \frac{\phi(\psi+\mu+\delta)}{\phi(\psi+\mu+\delta)+\alpha} = 0.1023,\\
i_{\psi}^{R_{HCV}} &= \frac{\partial R_{HCV}}{\partial \psi} \times \frac{\psi}{R_{HCV}} = \frac{-\alpha\psi}{(\psi+\mu+\delta)(\phi(\psi+\mu+\delta)+\alpha)} = -0.2362,\\
i_{\delta}^{R_{HCV}} &= \frac{\partial R_{HCV}}{\partial \delta} \times \frac{\delta}{R_{HCV}} = \frac{-\alpha\delta}{(\psi+\mu+\delta)(\phi(\psi+\mu+\delta)+\alpha)} = -0.6457,\\
i_{\alpha}^{R_{HCV}} &= \frac{\partial R_{HCV}}{\partial \alpha} \times \frac{\alpha}{R_{HCV}} = \frac{\alpha\big((\pi+\alpha+\mu)-(\phi(\psi+\mu+\delta)+\alpha)\big)}{(\pi+\alpha+\mu)(\phi(\psi+\mu+\delta)+\alpha)} = 0.0243,\\
i_{\pi}^{R_{HCV}} &= \frac{\partial R_{HCV}}{\partial \pi} \times \frac{\pi}{R_{HCV}} = \frac{-\pi}{(\pi+\alpha+\mu)} = -0.1179,\\
i_{\mu}^{R_{HCV}} &= \frac{\partial R_{HCV}}{\partial \mu} \times \frac{\mu}{R_{HCV}} = -0.0168.
\end{aligned}
$$

Table 4.2: Sensitivity indices of R_{TB} and R_{HCV} with respect to parameters

Effective reproduction number	Parameter	Sensitivity index
R_{TB}	ξ_1	1.0000
	q_1	1.0000
	ω_1	-0.8600
	θ	0.6481
	η	0.6200
	ω_2	-0.5610
	σ_1	-0.0676
	μ	-0.0398
	σ_2	-0.0366
	ρ	-0.0312
	ϵ	0.0160
R_{HCV}	ξ_2	1.0000
	q_2	1.0000
	δ	-0.6457
	ψ	-0.2362
	π	-0.1179
	ϕ	0.1023
	α	0.0243
	μ	-0.0168

Table 4.2 presents sensitivity indices of both R_{TB} and R_{HCV} where the parameters are arranged from the most sensitive to the least ones.

4.3.7.2 Interpretation of the Sensitivity Indices

The sensitivity indices presented in Table 4.2 are explained in such a way that, when a parameter with a positive sensitivity index increases (or decreases) with the rest of other parameter values maintained constant, the related effective reproduction number increases (or decreases). On the other hand, when a parameter with a negative sensitivity index increases (or decreases) with other parameter values kept constant, the associated effective reproduction number decreases (or increases). For instance, raising (or lowering) the value of the rate of human-to-human contact between the TB infected individuals and susceptible population, ξ_1, by 100% while other parameters are kept constant, raises (lowers) the value of R_{TB} by 100%. Then, increasing (or decreasing) the value of the rate of natural recovery η, of TB latent individuals by 100% while keeping the values of other parameters constant, decreases (or increases) the value of R_{TB} by 62%. Comparably, the sensitivity indices of all other parameters can be explained. Therefore, we conclude that the prevalence of TB infection increases when the values of the rate of human-to-human contact between the TB infected individuals and

susceptible population ξ_1, the likelihood of a contact resulting in TB transmission q_1, and the rate of progression of individuals from latent to active stage θ are increased. However, the prevalence is observed to decrease when the values of the rate of treatment of TB infectious individuals ω_1, rate of natural recovery of TB latent individuals η, the rate of hospitalization of TB infectious individuals ρ, per capita natural mortality rate μ and the rate at which the hospitalized TB infectious individuals are put on treatment ω_2, are increased. The key factors of TB infection are ξ_1 and q_1 which are just as sensitive, followed by θ.

From Table 4.2, it is deduced that HCV infection becomes more prevalent when the values of rate of human-to-human contact between the HCV infected individuals and susceptible population ξ_2, the likelihood of a contact resulting in HCV transmission q_2, transmission coefficient for the acute HCV individuals ϕ and the rate of progression of individuals from acute to chronic HCV stage α, are increased while those of rate at which chronic HCV individuals are put on treatment ψ, rate at which the chronic HCV die δ, natural recovery rate for the acute HCV humans π and the per capita natural mortality rate μ are decreased. The key factors of HCV infection are ξ_2 and q_2 which have equal sensitivity, followed by ϕ and α. Therefore, efforts should focus on decreasing the values of ξ_2, q_2, ϕ and α. Hence, for reduced transmission of TB (or HCV) infection, interventions like health education campaigns involving screening and isolation of the infectious individuals, wearing masks by TB infectious individuals (or screening, sterilization of surgical instruments and condom use for HCV infectious individuals) should be implemented. Also seeking for early treatment of TB (or HCV) infectious individuals should be encouraged for those that test positive of TB (or HCV) infection.

Computation of R_{TH}: Inserting the parameter values from Table 4.3 into Equations (4.17) and (4.73), the values of $R_{TB} = 1.9407$ and $R_{HCV} = 1.1521$ are yielded.
From Equation (4.104), the effective reproduction number of the TB-HCV co-infection model is determined as follows:

$$R_{TH} = \max\{R_{TB}, R_{HCV}\} = \max\{1.9407, 1.1521\} = 1.9404.$$

Since $R_{TB} > R_{HCV}$, this implies that the interaction between TB and HCV infections in co-infected individuals is dominated by TB infection. This indicates that TB infection is more prevalent than HCV infection in a given community. This would mean more attention given to TB infection if the

co-infection burden is to be reduced.

4.4 Numerical Simulations

In the preceding subsections, we have examined the analytical dynamics and characteristics of TB-HCV co-infection model with treatment as well as the sub models. The numerical simulations were carried out to validate and support the analytical findings, providing a deeper understanding of the TB-HCV co-infection dynamics with treatment. Assuming the initial values of the state variables as $S(0) = 40,000, I_L(0) = 500, I_T(0) = 450, H(0) = 250, R_T(0) = 500, I_A(0) = 350, I_C(0) = 400, R_H(0) = 350, I_{AL}(0) = 250, I_{CL}(0) = 250, I_{AT}(0) = 250, I_{CT}(0) = 250$ and $R(0) = 250$. A number of parameters have been obtained from existing literature, that is, $\mu, \sigma_1, \sigma_2, \delta, \theta, \rho, \omega_1, \omega_2, \alpha, \psi, \iota$ as described in Table 4.3. Other parameters were carefully assumed depending on the dynamics of the co-infection, for example $\tau_2 > \tau_1$ implying that I_{CL} individuals are more likely to progress to I_{CT} than I_{AL} progressing to I_{AT}. Similarly, the progression rate, β_2 from I_{AT} to I_{CT} is greater than the progression rate, β_1 from I_{AL} to I_{CL} since I_{AT} are more infectious of TB than I_{AL}. MATLAB software was employed to simulate the model using the ODE 45 solver. Both cases for $R_{TH} < 1$ and $R_{TH} > 1$ are catered for with parameter modification.

Table 4.3: The TB-HCV Co-infection Model Parameter values

Parameter	Value/yr^{-1}	Source
μ	0.02	[49]
σ_1	0.0575	[49]
σ_2	0.00205	[59]
δ	0.82	[58]
d_1	0.6	Assumed
d_2	0.8	Assumed
θ	0.25	[57]
ρ	0.0415	[54]
ω_1	0.7311	[49]
ω_2	0.8733	[59]
α	2	[54]
ψ	0.30	[56]
ϵ	0.35	Assumed
τ_1	0.00013	Assumed
τ_2	0.00015	Assumed
β_1	0.00014	Assumed
β_2	0.00016	Assumed
r_1	0.5	Assumed
r_2	0.6	Assumed
r_3	0.4	Assumed
ν_1	0.025	[58]
ν_2	0.03	[59]
ν_3	0.05	Assumed
η	0.4405	[54]
π	0.27	[54]
ϕ	0.20	Assumed
ξ_1, ξ_2	4, 2 people respectively	[57, 58]
q_1, q_2	0.08, 0.07 respectively	[57, 58]
a	1.002	Assumed
b_1, b_2, b_3 and b_4	1.003, 1.002, 1.005, 1.001 respectively	Assumed

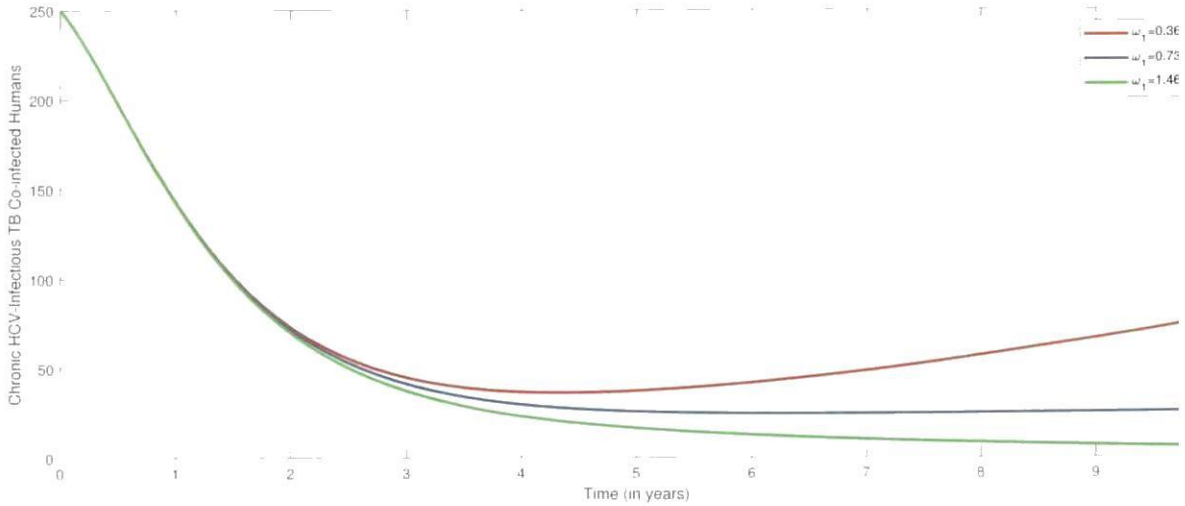

Figure 4.7: Figure displaying the number of chronic HCV-infectious TB co-infected humans against ti with TB treatment rate, ω_1 varied.

4.4.1 Effect of Treating TB on the Co-infection Dynamics of TB ai HCV

The results presented in Figure 4.7 indicate that enhancing the TB treatment rate by 100% le to a substantial decrease in the prevalence of chronic HCV-infectious TB co-infected humans fr about 12% to 8% in 5 years. Furthermore, in Figures 4.8a and 4.8b, a similar decreasing trenc observed in the populations of humans co-infected with chronic HCV-latent TB, as well as peo with acute HCV and infectious TB co-infection.

4.4.2 Effect of Hospitalization on the Co-infection Dynamics of TB ai HCV

Figure 4.9 illustrates that enhancing the TB hospitalization rate by 0.3735 yields a proportio and substantial reduction in the number of humans with chronic HCV-infectious TB co-infect from 12% to 10% in 5 years. Consistent with the observed trend in Figure 4.9, 4.10a and 4.1 demonstrate that the populations of chronic HCV-latent TB co-infected and acute HCV-infecti TB co-infected humans also exhibits a corresponding decline respectively.

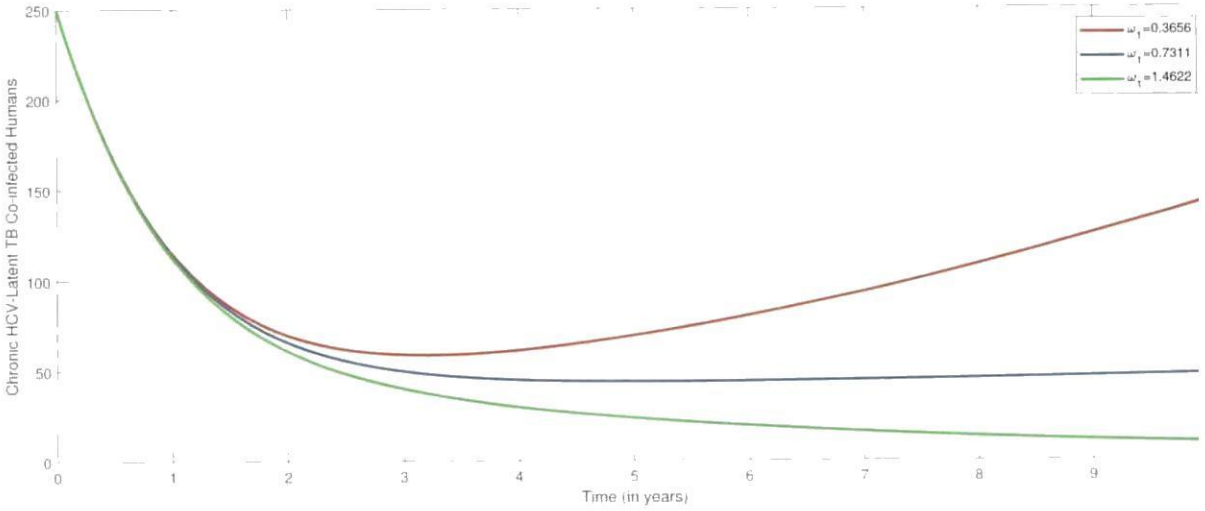

(a) Figure displaying the number of chronic HCV-latent TB co-infected humans against time with TB treatment ra ω_1 varied.

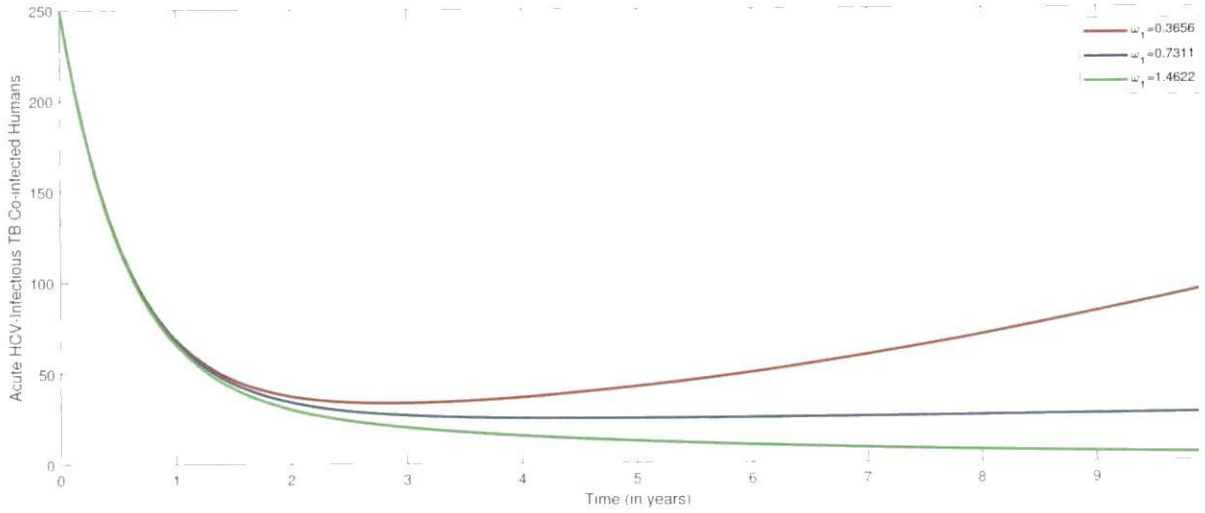

(b) Figure displaying the number of acute HCV-infectious TB co-infected humans against time with TB treatme rate ω_1 varied.

Figure 4.8: Figure displaying the number of chronic HCV-latent TB co-infected humans against time, a number of acute HCV-infectious TB co-infected humans against time with TB treatment rate ω_1 varied.

4.4.3 Role of Treatment rates, r_1, r_2 and r_3 on the Co-infection Dynamic of TB and HCV

Figures 4.11a, 4.11b and 4.12a, 4.12b indicate that when the rates r_1 and r_2 respectively at whic humans are put on HCV and TB medication rises, the number of people infected by chron HCV-infectious TB and chronic HCV-latent TB co-infection decreases. Similarly, Figures 4.1 4.14a and 4.14b reveal that increasing the rate r_3 at which humans are put on TB and HCV medic treatment by 1.2, decreases the number of chronic HCV-infectious TB from10% to 4%, chron

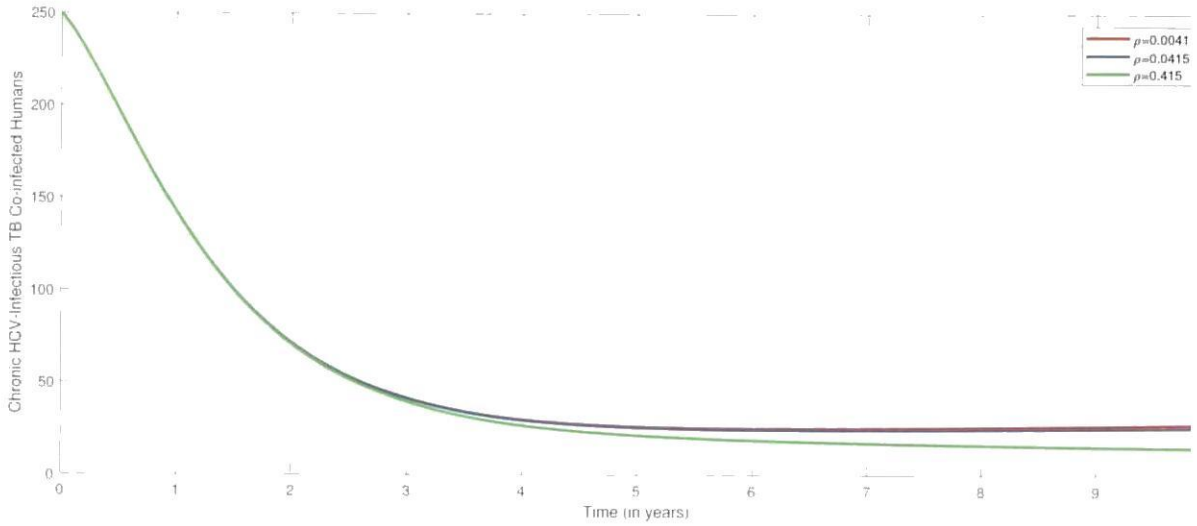

Figure 4.9: Figure displaying the number of chronic HCV-infectious TB co-infected humans against tir with hospitalization rate, ρ varied.

HCV-latent TB co-infected humans from 17.2% to 12% and acute HCV-infectious TB co-infecte humans from 10% to 8% in 5 years.

4.4.4 Effect of Treating HCV on the Co-infection Dynamics of TB an HCV

Figure 4.15 demonstrates that enhancing the HCV treatment rate by 1.5 yields a proportional ar substantial reduction in the number of humans with chronic HCV-infectious TB co-infection from 10 to 7.2% in 5 years. Consistent with the trend observed in Figure 4.15, 4.16a and 4.16b demonstra a concomitant decline in the population of chronic HCV-latent TB co-infected from 16% to 8% ar acute HCV-infectious TB co-infected individuals from 8% to 4.8% in a period of 5 years.

4.5 Discussion and Conclusion

In this Chapter, we developed and analysed a mathematical model to investigate the behaviour TB and HCV co-infection with medication, extending the previous work in Chapter 3. The mod was intended to assess the impact of the medication on the progression of TB and HCV co-infectio Under medication for both TB and HCV, the intricate dynamics of TB-HCV co-infection is dominate by TB. From sensitivity analysis, it is deduced that the rate of human-to-human contact betwee the TB (or HCV) infectious individuals and susceptible population and the likelihood of a conta resulting in TB (or HCV) transmission have an equal potential to lead to a surge in TB (or HCV

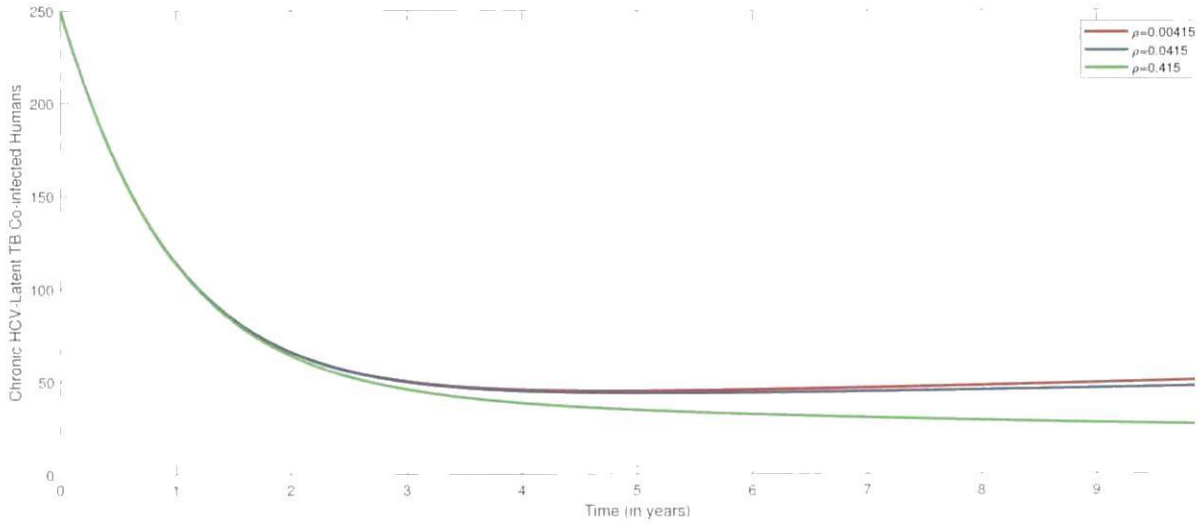

(a) Figure displaying the number of chronic HCV-latent TB co-infected humans against time with hospitalization ra ρ varied.

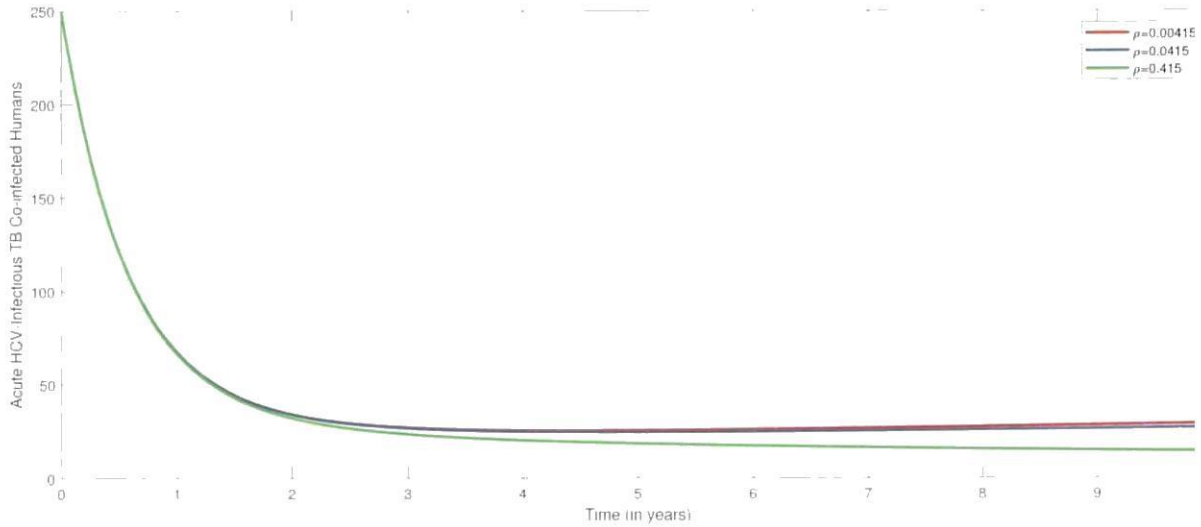

(b) Figure displaying the number of acute HCV-infectious TB co-infected humans against time with hospitalizati rate ρ varied.

Figure 4.10: Figure displaying the number of chronic HCV-latent TB co-infected humans against time, a number of acute HCV-infectious TB co-infected humans against time with hospitalization rate ρ varied.

cases. Furthermore, enhancing these parameters also boosts TB (or HCV) infection levels. Therefo for decreased TB (or HCV) infections, humans need to greatly reduce the rate of human-to-hum contact between the TB (or HCV) infectious individuals and susceptible population and the likelihoo of a contact resulting in TB (or HCV) transmission. Numerical simulation results unequivocal reveal that over time, increasing the TB treatment rate, HCV treatment rate, hospitalization rate a the rates at which individuals in co-infected classes are identified and put on TB and HCV treatme can significantly reduce the prevalence of TB-HCV co-infection. These findings are consistent wi

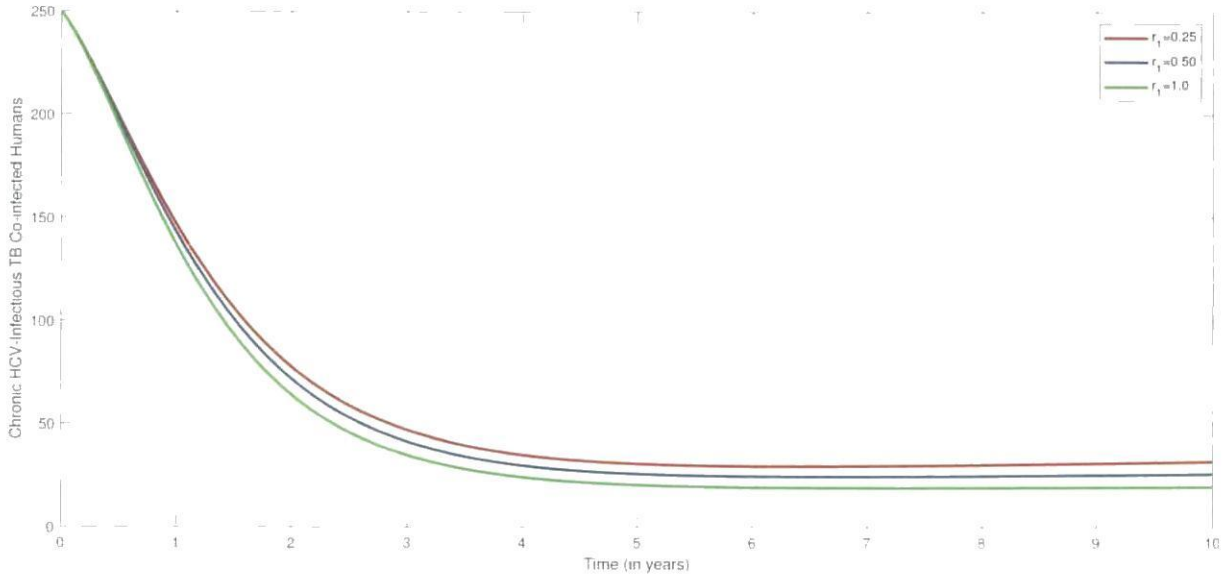

(a) Figure displaying the number of chronic HCV-infectious TB co-infected humans against time with HCV treatment rate, r_1 varied.

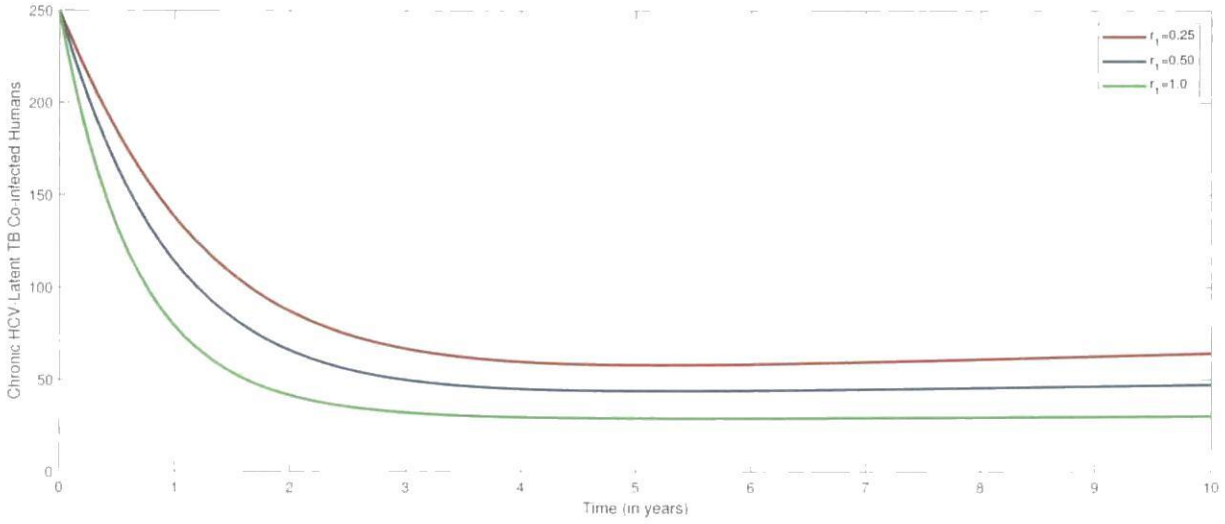

(b) Figure displaying the number of acute HCV-infectious TB co-infected humans against time with HCV treatment rate, r_1 varied.

Figure 4.11: Figure displaying the number of chronic HCV- latent TB co-infected humans against time, and number of acute HCV-infectious TB co-infected humans against time with HCV treatment rate, r_1 varied.

statistical evidence reported in earlier studies [20, 40, 65, 80]. Implementing the above interventions can have a profound impact on reducing the burden of TB-HCV co-infection and improving public health outcomes. We therefore, recommend that health facilities be stocked with antibiotics for TB and antiviral medications to facilitate access for those diagnosed with particular infections. It is realized that treatment intervention plays a big role in TB-HCV co-infection reduction as compared to the study in Chapter 3 where there was no intervention. This study can be further expanded to

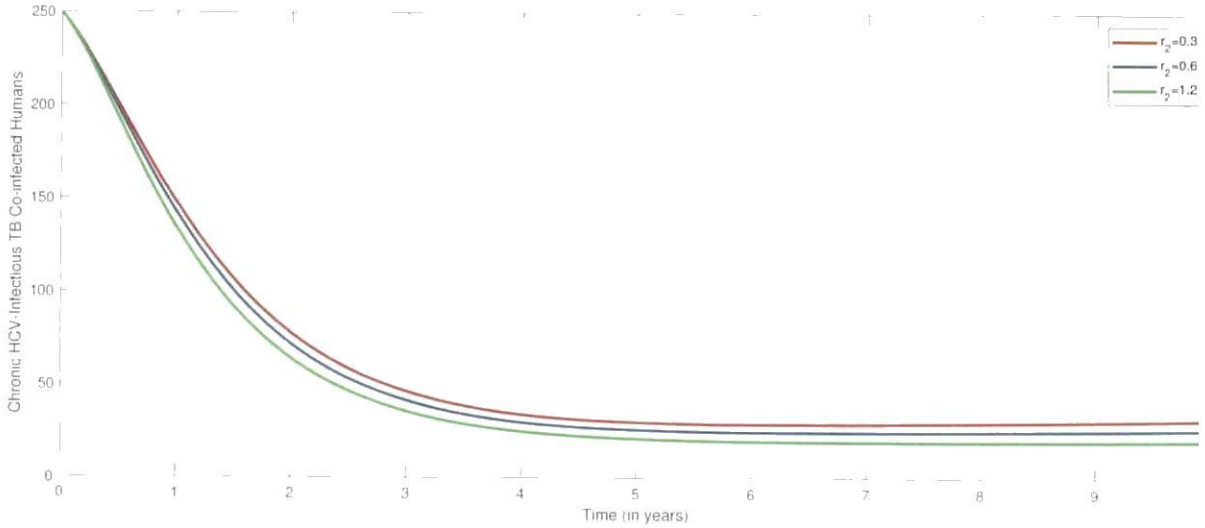

(a) Figure displaying the number of chronic HCV-infectious TB co-infected humans against time with TB treatmer rate, r_2 varied.

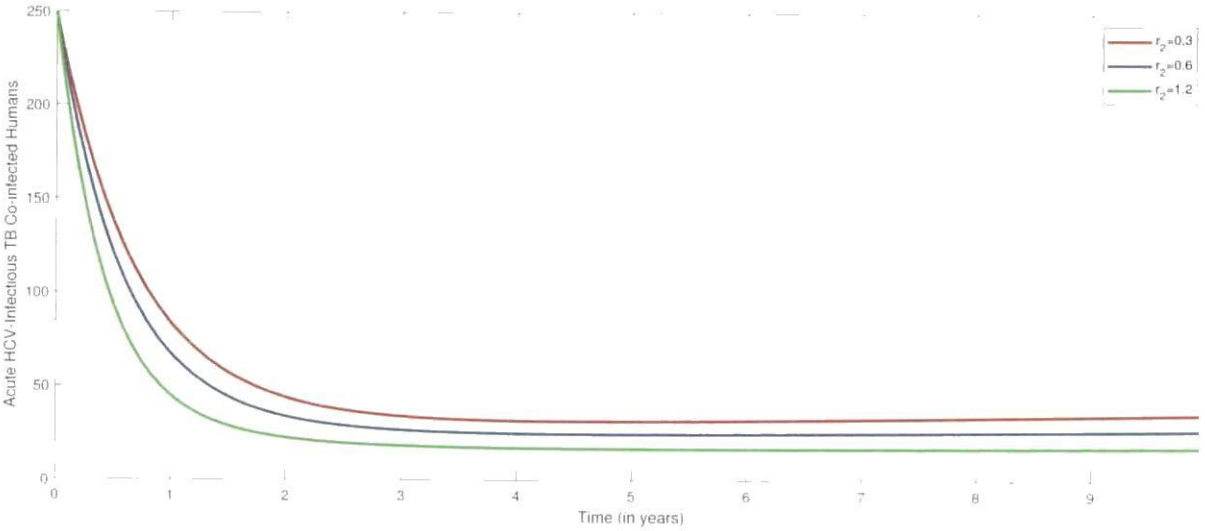

(b) Figure displaying the number of acute HCV-infectious TB co-infected humans against time with TB treatmer rate, r_2 varied.

Figure 4.12: Figure displaying the number of chronic HCV- latent TB co-infected humans against time. an number of acute HCV-infectious TB co-infected humans against time with TB treatment rate, r_2 varied.

include optimal control strategies in the model.

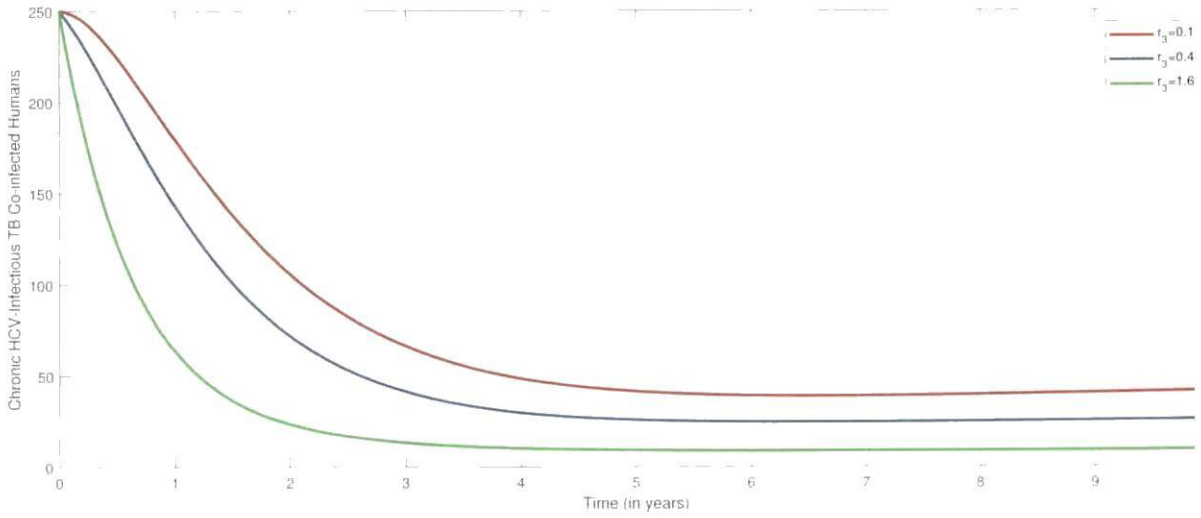

Figure 4.13: Figure displaying the number of chronic HCV-infectious TB co-infected humans against tin with treatment rate, r_3 varied.

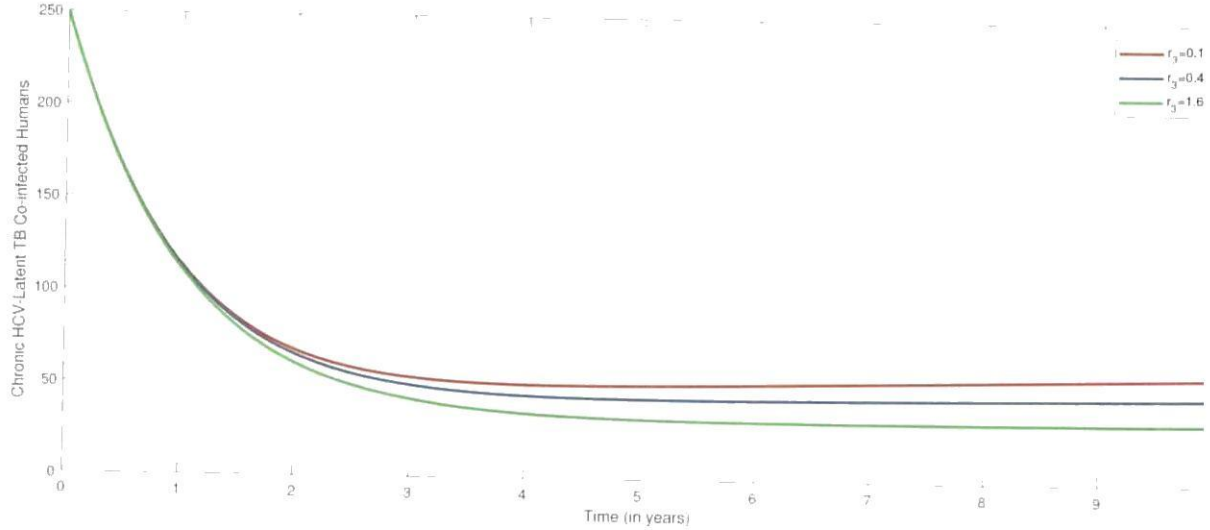

(a) Figure displaying the number of chronic HCV-latent TB co-infected humans against time with treatment rate r varied.

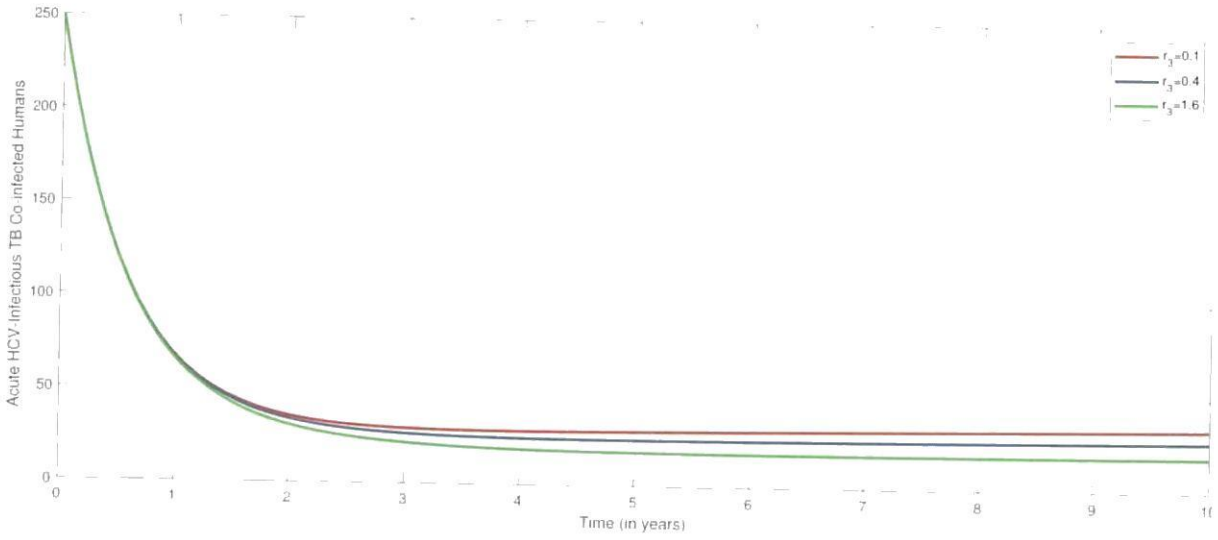

(b) Figure displaying the number of acute HCV-infectious TB co-infected humans against time with treatment rate r_3 varied.

Figure 4.14: Figure displaying the number of chronic HCV-latent TB co-infected humans against time, and number of acute HCV-infectious TB co-infected humans against time with treatment rate r_3 varied.

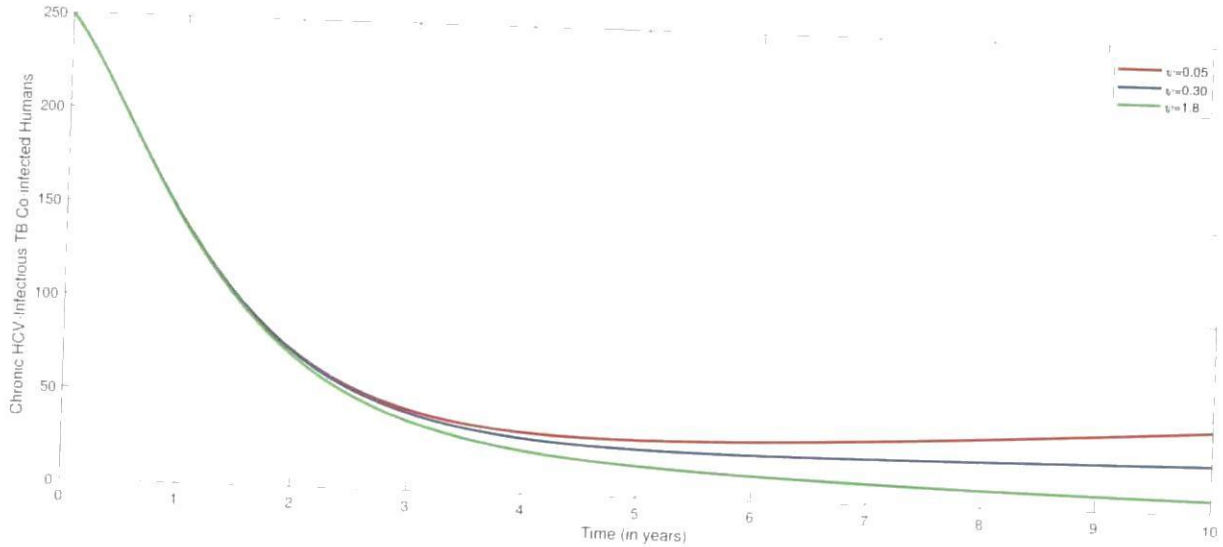

Figure 4.15: Figure displaying the number of chronic HCV-infectious TB co-infected humans against time with HCV treatment rate, ψ varied.

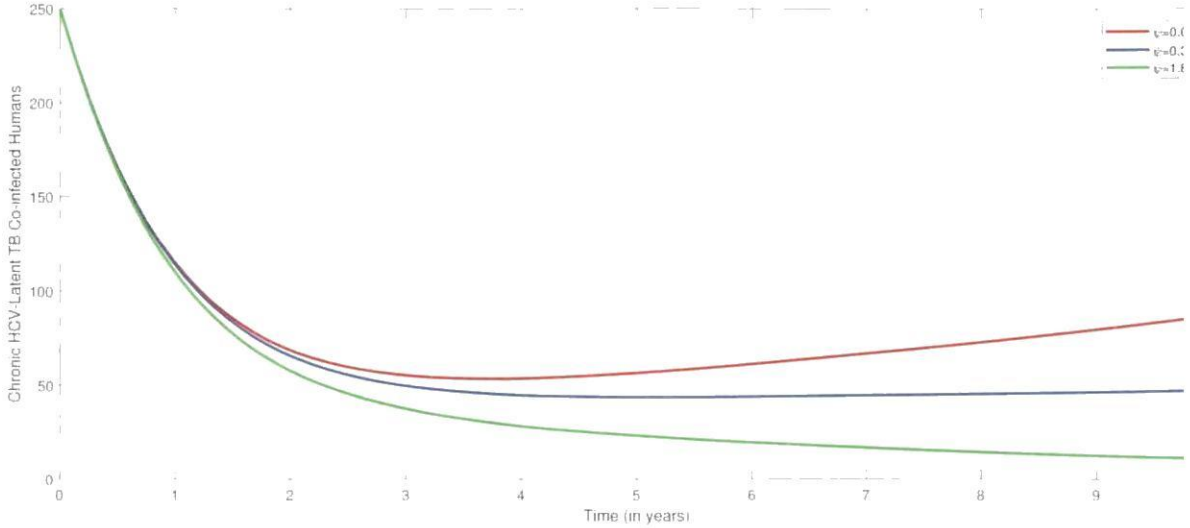

(a) Figure displaying the number of chronic HCV-latent TB co-infected humans against time with HCV treatm rate ψ varied.

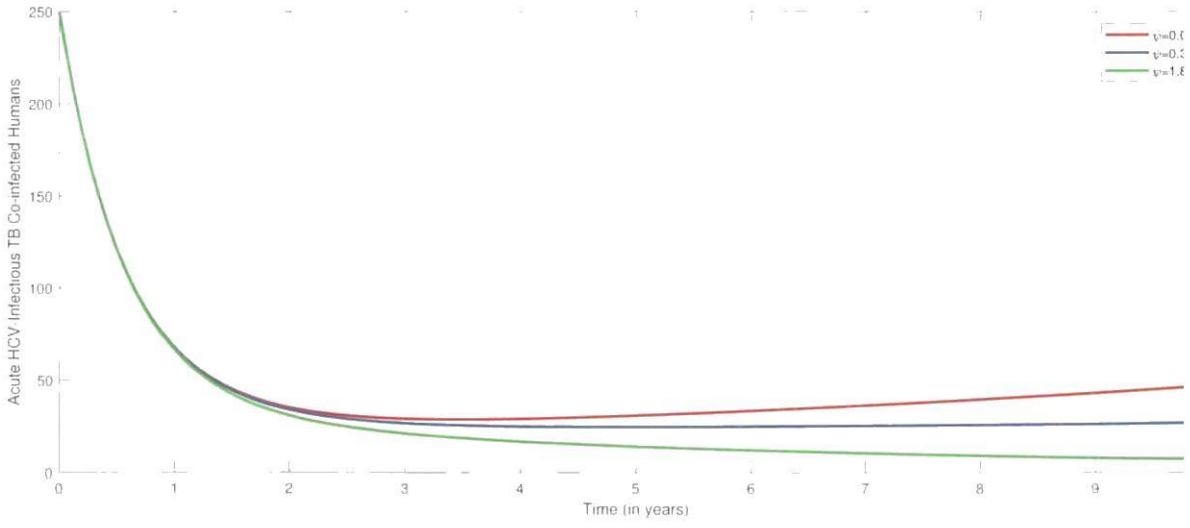

(b) Figure displaying the number of acute HCV-infectious TB co-infected humans against time with HCV treatm rate ψ varied.

Figure 4.16: Figure displaying the number of chronic HCV-latent TB co-infected humans against time, a number of acute HCV-infectious TB co-infected humans against time with HCV treatment rate ψ varied

Chapter 5

Analysis of Optimal Control on the Dynamics of TB-HCV Co-infection

5.1 Introduction

This Chapter investigates the optimal control strategies for managing the dynamics of TB-HCV co-infection. Despite the efforts to combat these diseases, co-infection remains a formidable challenge, necessitating innovative approaches.

Optimal control theory offers a powerful tool to identify effective interventions and resource allocation strategies. In this Chapter, we employ mathematical modelling and optimal control techniques to explore the dynamics of TB-HCV co-infection and determine the best control strategies to mitigate its impact. Our analysis aims to provide insights into the most effective interventions, such as treatment rates, screening efforts and resource allocation, to inform public health policy and decision-making.

To determine the optimal control strategies for managing TB-HCV co-infection, we employ Pontryagin's Maximum Principle [36], a powerful tool in optimal control theory. By applying Pontryagin's Maximum Principle to our model of TB-HCV co-infection, we can determine the optimal control strategies that minimise the spread of the diseases, while also considering the constraints and costs associated with the interventions. The Hamiltonian function and the adjoint equations provide valuable insights into the optimal control dynamics, allowing us to determine the most effective interventions and resource allocation strategies.

5.2 Optimal Control Problem

Optimal control has been applied in the study of infectious diseases such as those in [25, 43, 44, 45, 47, 107, 108, 109, 110]. For this model, to analyse the optimal level of effort needed to control the spread of tuberculosis and hepatitis C. Time-dependent controls $u_1(t)$, $u_2(t)$, $u_3(t)$ and $u_4(t)$ are introduced into the TB-HCV co-infection model (4.3).

The TB prevention control $u_1(t)$ is a strategy designed to reduce the risk of TB infection among susceptible population. The implementation of TB prevention strategy $u_1(t)$ can be facilitated through targeted health education campaigns, focusing on raising awareness about TB and its complex implications in the context of TB-HCV co-infection. The TB detecting and treatment control $u_2(t)$ strategy is aimed at identifying and managing humans exposed to or infected with TB. This is achieved through a combination of active case finding, rapid diagnostics, directly observed treatment, and healthcare system strengthening. The HCV prevention control $u_3(t)$ is strategy designed to reduce the risk of HCV infection among susceptible population. This strategy is achieved through education initiatives that inform individuals about HCV prevention measures and promote responsible behaviour among those already infected. The HCV detecting and treatment control $u_4(t)$ is a strategy aiming to identify and treat HCV-infected individuals through timely medication intervention. The strategy is accomplished by ensuring immediate initiation of antiviral therapy for all individuals testing positive for HCV. Ultimately, this will guide efforts to develop evidence-based interventions that can effectively curb the TB and HCV co-infection epidemic.

5.2.1 Formulation of the Model

Let

$$\big(S(t), I_L(t), I_T(t), H(t), R_T(t), I_A(t), I_C(t), R_H(t), I_{AL}(t), I_{CL}(t), I_{AT}(t), I_{CT}(t), R(t)\big)$$

be the state variables of the process at time t, and $\big(u_1(t), u_2(t), u_3(t), u_4(t)\big)$, with $0 \leq u_i \leq 1$, where $i = 1, 2, 3, 4$ be the control inputs to the model (4.3) at time t. Then the system is described by 13

first-order differential equations as shown below:

$$
\begin{aligned}
\frac{dS(t)}{dt} &= \Lambda + \nu_1 R_H(t) + \nu_2 R_T(t) + \nu_3 R(t) + \pi I_A(t) + \eta I_L(t) - \big((1-u_1(t))\lambda_T + (1-u_3(t))\lambda_H + \mu\big)S \\
\frac{dI_L(t)}{dt} &= (1-u_1(t))\lambda_T S(t) - (\theta + \eta + \mu + (1-u_3(t))\lambda_H) I_L(t), \\
\frac{dI_T(t)}{dt} &= \theta I_L(t) - ((\omega_1 + u_2(t)) + \rho + \mu + \sigma_1 + (1-u_3(t))\lambda_H) I_T(t), \\
\frac{dH(t)}{dt} &= \rho I_T(t) - (\omega_2 + \mu + \sigma_2) H(t), \\
\frac{dR_T(t)}{dt} &= \omega_2 H(t) + (\omega_1 + u_2(t)) I_T(t) - (\nu_2 + \mu) R_T(t), \\
\frac{dI_A(t)}{dt} &= (1-u_3(t))\lambda_H S(t) - (\pi + \alpha + \mu + u_4(t) + (1-u_1(t))\lambda_T) I_A(t), \\
\frac{dI_C(t)}{dt} &= \alpha I_A(t) - ((\psi + u_4(t)) + \mu + \delta + (1-u_1(t))\lambda_T) I_C(t), \qquad (5.1 \\
\frac{dR_H(t)}{dt} &= (\psi + u_4(t)) I_C(t) - (\nu_1 + \mu) R_H(t) + u_4(t) I_A, \\
\frac{dI_{AL}(t)}{dt} &= (1-u_1(t))\lambda_T I_A(t) + (1-u_3(t))\lambda_H I_L(t) - (\tau_1 + \mu + \beta_1 + u_4(t)) I_{AL}(t), \\
\frac{dI_{CL}(t)}{dt} &= \beta_1 I_{AL}(t) + (1-u_1(t))\lambda_T I_C(t) - ((r_1 + u_4(t)) + \tau_2 + \mu + \delta) I_{CL}(t), \\
\frac{dI_{AT}(t)}{dt} &= \tau_1 I_{AL}(t) + (1-u_3(t))\lambda_H I_T(t) - ((r_2 + u_2(t) + u_4(t)) + \beta_2 + \mu + d_1) I_{AT}(t), \\
\frac{dI_{CT}(t)}{dt} &= \tau_2 I_{CL}(t) + \beta_2 I_{AT}(t) - ((r_3 + u_2(t) + u_4(t)) + \mu + d_2) I_{CT}(t), \\
\frac{dR(t)}{dt} &= ((r_1 + u_4(t)) + u_2(t)) I_{CL}(t) + ((r_2 + u_2(t) + u_4(t)) I_{AT}(t) + (r_3 + u_2(t) + u_4(t)) I_{CT}(t) \\
&\quad - (\nu_3 + \mu) R(t) + u_4(t) I_{AL},
\end{aligned}
$$

with initial conditions $S(0) = S_0, I_L(0) = I_{L0}, I_T(0) = I_{T0}, II(0) = II_0, R_T(0) = R_{T0}$,
$I_A(0) = I_{A0}, I_C(0) = I_{C0}, R_H(0) = R_{H0}, I_{AL}(0) = I_{AL0}, I_{CL}(0) = I_{CL0}, I_{AT}(0) = I_{AT0}$,
$I_{CT}(0) = I_{CT0}, R(0) = R_0$.

The goal will be to minimize the number of infected humans in the community while keeping th cost associated with controls $u_1(t)$, $u_2(t)$, $u_3(t)$ and $u_4(t)$ as minimum as possible.

Thus, we design an objective functional by keeping the biomedical goal in our mind. Our goal is t minimize the number of infected individuals (including acute and infectious humans in the respectiv categories) with *Mycobacterium tuberculosis* bacteria, HCV virus or both, while at the same tim keeping the cost of implementing the four control strategies very low.

Therefore, we seek to minimise the objective functional J, defined over a feasible set of controls u_1

u_2, u_3 and u_4 applied over the pre-defined finite time interval $[0, t_f]$ given by

$$J(u_1, u_2, u_3, u_4) = \int_0^{t_f} [A_1 I_T + A_2 I_A + A_3 I_C + A_4 I_{AL} + A_5 I_{AT} + A_6 I_{CL} + A_7 I_{CT} + \frac{1}{2} B_1 u_1^2 + \frac{1}{2} B_2 u_2^2 + \frac{1}{2} B_3 u_3^2 + \frac{1}{2} B_4 u_4^2] dt,$$

where t_f is a fixed final time, whereas the coefficients $A_1, A_2, ..., A_7, B_1, ..., B_4$ are positive we constants, which balance the cost factors associated with variables and control measures I_T, I_A, $I_{AL}, I_{AT}, I_{CL}, I_{CT}, u_1, u_2, u_3$ and u_4 respectively.

In a finite time interval $[0, t_f]$, the total cost consists of the cost due to the disease and the due to the control efforts. The disease cost is proportional to the number of infected humans in respective compartments, whereas it is assumed that costs of the control strategies are non-li and take a quadratic nature, which is found to be consistent with previous works in the litera [47].

In the objective functional (5.2), we split the disease cost into $A_1 I_T$ as the cost associated TB infectious humans, $A_2 I_A$ as cost associated with HCV acutely infected humans, $A_3 I_C$ as associated with HCV chronically infected humans, $A_4 I_{AL}$ as cost associated with infected human I_{AL} class, $A_5 I_{AT}$ as cost associated with infected humans in I_{AT} class, $A_6 I_{CL}$ as cost associated infected humans in I_{CL} class and $A_7 I_{CT}$ as cost associated with infected humans in I_{CT} class.

B_1, B_2, B_3 and B_4 are relative or additional cost weights for each control measure u_1, u_2, u_3 an respectively. The control functions, $u_1(t)$, $u_2(t)$, $u_3(t)$ and $u_4(t)$ are bounded, *Lebesgue* measur functions. This implies that the control functions denoted by $u_i(t)$, $i = 1, 2, 3, 4$, have a fi magnitude, i.e., $|u_i(t)| \leq M, \forall t \in (0, t_f)$, where M is a constant. This means that the control in are restricted to a certain range, preventing excessively large or small values. Also, the cor functions are integrable in the sense of *Lebesgue*, meaning that the integral of $|u(t)|$ over a g interval $(0, t_f)$ exists and is finite, i.e., $\int_0^{t_f} |u(t)| dt < \infty$. This ensures that the control inputs ha finite energy or effort over the entire interval.

Thus, we seek to find optimal controls $u_1^*, u_2^*, u_3^*, u_4^*$ such that

$$J(u_1^*, u_2^*, u_3^*, u_4^*) = \min\{J(u_1, u_2, u_3, u_4) | u_1, u_2, u_3, u_4 \in \mathcal{U}\},$$

where the control set, $\mathcal{U} = \{(u_1, u_2, u_3, u_4)$ such that u_1, u_2, u_3, u_4 are measurable with $a_i \leq u$ $b_i, i = 1, 2, 3, 4$, for $t \in [0, t_f]$ and $a_i, b_i, i = 1, 2, 3, 4$ are fixed constants.$\}$

5.2.2 Existence and Characterization of Optimal Control Solution

In this subsection, the existence and characterization of an optimal control of system (5.1) are studied.

5.2.2.1 The Existence of an Optimal Control

Optimal control theory is concerned with finding the best control strategy to achieve a desired goal, subject to constraints and uncertainties. Here, the fundamental question is whether an optimal control exists, and under what conditions. In other words, can we guarantee the existence of a control strategy that minimizes a given performance criterion? The existence of an optimal control is a crucial issue, as it ensures that the optimization problem is well-posed and that the search for an optimal solution is meaningful.

The boundedness of solutions to system (5.1), previously established in Chapter (4), is essential for investigating the existence of optimal control. To ensure epidemiological significance, it is crucial to demonstrate that all state variables of system (5.1) remain non-negative for all time $t > 0$.

Consider a scenario where the variable S becomes zero at some time $t_1 > 0$, that is $S(t_1) = 0$, while the other variables remain non-negative. Then,

$$\begin{aligned}\frac{dS(t_1)}{dt} &= \Lambda + \nu_1 R_H(t_1) + \nu_2 R_T(t_1) + \nu_3 R(t_1) + \pi I_A(t_1) + \eta I_L(t_1) \\ &\quad - \big((1-u_1(t_1))\lambda_T + (1-u_3(t_1))\lambda_H + \mu\big)S(t_1), \\ &= \Lambda + \nu_1 R_H(t_1) + \nu_2 R_T(t_1) + \nu_3 R(t_1) + \pi I_A(t_1) + \eta I_L(t_1) > 0.\end{aligned}$$

This indicates $S(t)$ remains positive for all $t > 0$. By similar arguments, it follows that $I_L(t) \geq 0, I_T(t) \geq 0, H(t) \geq 0, R_T(t) \geq 0, I_A(t) \geq 0, I_C(t) \geq 0, R_H(t) \geq 0, I_{AL}(t) \geq 0, I_{CL}(t) \geq 0, I_{AT}(t) \geq 0, I_{CT}(t) \geq 0$ and $R(t) \geq 0$.

Consequently, model (5.1) demonstrates mathematical and epidemiological validity.

Theorem 11. *There exist optimal controls u_1^*, u_2^*, u_3^* and u_4^* with state variables in system (5.1) that minimize the objective functional (5.2).*

Proof. To prove this theorem, we intend to satisfy the conditions of Fleming and Rishel [123];

(i) The set of controls u_1, u_2, u_3, u_4 and the corresponding state variables $S, I_L, H, R_T, I_A, I_C, R_H, I_{AL}, I_{CL}, I_{AT}, I_{CT}, R$ is non empty.

(ii) The admissible control $\mathcal{U}$ is convex and closed.

(iii) The right hand side of the state system (5.1) is bounded by a linear function in the state an control variables.

(iv) The integrand of the objective functional (5.2) is concave on $\mathcal{U}$.

(v) There exists constants $p_1, p_2 > 0$ such that the integrand $J(u_1, u_2, u_3, u_4)$ is bounded above b $p_1|u_1, u_2, u_3, u_4|^{\iota} - p_2$.

If the state equations are continuous and its solutions are bounded and Lipschitz in the state variable then there is a unique solution corresponding to every admissible control $\mathcal{U}$. This implies that sta variables of system (5.1) with control set $\{(u_1, u_2, u_3, u_4) \in \mathcal{U}\}$ is non empty as is non negative shown in Chapter (4). This satisfies condition (i).

From objective functional (5.2), the control set is closed and convex, which satisfies condition (ii Now, condition (iii) is proven by re-writing the right hand side of system (5.1) as $g(t, X, u)$ whe $X = (S. I_L, I_T, H, R_T, I_A, I_C, R_H, I_{AL}, I_{CL}, I_{AT}.I_{CT}, R)$ and $u = (u_1, u_2, u_3, u_4)$.

Let

$$g(t, X, u) = g_1(t, X) + g_2(t, X)u, \tag{5.}$$

such that

$$g_1(t, X) = \begin{bmatrix} \Lambda + \nu_1 R_H + \nu_2 R_T + \nu_3 R + \pi I_A + \eta I_L - (\lambda_T + \lambda_H + \mu)S \\ \lambda_T S - (\theta + \eta + \mu + \lambda_H) I_L \\ \theta I_L - (\omega_1 + \rho + \mu + \sigma_1 + \lambda_H) I_T \\ \rho I_T - (\omega_2 + \mu + \sigma_2) H \\ \omega_2 H + \omega_1 I_T - (\nu_2 + \mu) R_T \\ \lambda_H S - (\pi + \alpha + \mu + \lambda_T) I_A \\ \alpha I_A - (\psi + \mu + \delta + \lambda_T) I_C \\ \psi I_C - (\nu_1 + \mu) R_H \\ \lambda_T I_A + \lambda_H I_L - (\tau_1 + \mu + \beta_1) I_{AL} \\ \beta_1 I_{AL} + \lambda_T I_C - (r_1 + \tau_2 + \mu + \delta) I_{CL} \\ \tau_1 I_{AL} + \lambda_H I_T - (r_2 + \beta_2 + \mu + d_1) I_{AT} \\ \tau_2 I_{CL} + \beta_2 I_{AT} - (r_3 + \mu + d_2) I_{CT} \\ r_1 I_{CL} + r_2 I_{AT} + r_3 I_{CT} - (\nu_3 + \mu) R \end{bmatrix}, \tag{5.}$$

and

$$g_2(t,X) = \begin{bmatrix} \lambda_T S & 0 & \lambda_H S & 0 \\ -\lambda_T S & 0 & -\lambda_H I_L & 0 \\ 0 & -I_T & \lambda_H I_T & 0 \\ 0 & 0 & 0 & 0 \\ 0 & I_T & 0 & 0 \\ \lambda_T I_C & 0 & -\lambda_H S & -I_A \\ \lambda_T I_C & 0 & 0 & -I_C \\ 0 & 0 & 0 & I_C + I_A \\ -\lambda_T I_A & 0 & -\lambda_T I_L & -I_{AL} \\ -\lambda_T I_C & 0 & 0 & -I_{CL} \\ 0 & -I_{AT} & -\lambda_H I_T & -I_{AT} \\ 0 & -I_{CT} & 0 & -I_{CT} \\ 0 & I_{CL} + I_{AT} + I_{CT} & 0 & I_{CL} + I_{AT} + I_{CT} + I_{AL} \end{bmatrix}. \tag{5.6}$$

Now, applying norm inequality on equation (5.4), we obtain

$$|g(t,X,u)| \leq |g_1(t,X)| + |g_2(t,X)||u|,$$

where g_1 and g_2 are continuous functions in state variables.

The boundedness of state variables has already been discussed in Chapter (4) and this implies that g_1 and g_2 are bounded. Suppose that, there are constants n_1 and n_2, such that $|g_1| \leq n_1$ and $|g_2| \leq n_2$, and for some $m = \max\{n_1, n_2\}$, then

$$\begin{aligned} |g(t,X,u)| &\leq |g_1(t,X)| + |g_2(t,X)||u|, \\ &\leq n_1 + n_2|u|, \\ &\leq m + m|u|, \\ &\leq m(1+|u|). \end{aligned}$$

Therefore, condition (iii) is satisfied. The objective functional (5.2) is concave, which fulfils condition (iv).

For the last condition, the integrand of the objective function (5.2), that is

$$A_1 I_T + A_2 I_A + A_3 I_C + A_4 I_{AL} + A_5 I_{AT} + A_6 I_{CL} + A_7 I_{CT} + \frac{1}{2}B_1 u_1^2 + \frac{1}{2}B_2 u_2^2 + \frac{1}{2}B_3 u_3^2 + \frac{1}{2}B_4 u_4^2$$

satisfied the condition

$$J(t, X, u) \geq p_1|(u_1, u_2, u_3, u_4)|^{\epsilon} - p_2,$$

where $p_1 = \min\left(\frac{B_1}{2}, \frac{B_2}{2}, \frac{B_3}{2}, \frac{B_4}{2}\right), p_2 = \frac{B_4}{2}$ and $\epsilon = 2$.

Therefore, the optimal control set exists. □

5.2.2.2 Characterisation of an Optimal Control

Here, we explore the fundamental concepts of optimal control theory, characterising the optimal control strategies that minimise the spread of TB-HCV co-infection. By applying Pontryagin's Maximum Principle, we derive the necessary conditions for optimality, which reveal the precise characteristics of the optimal control. We explore the properties of the optimal control, including its dynamics, constraints and cost considerations. The characterisation provides a comprehensive understanding of the optimal interventions and resource allocation strategies, enabling the development of effective public health policies and decision-making. Specifically, we investigate the following key aspects of the optimal control: the adjoint control dynamics, including the switching points and singular arcs; the adjoint equations and their role in determining the optimal control; the Hamiltonian function and its relationship to the performance index and the constraints and cost considerations that shape the optimal control.

By elucidating the characteristics of the optimal control, we lay the foundation for the numerical simulations and results presented in the subsequent sections.

Necessary conditions that optimal solutions need to satisfy are obtained from Pontryagin's maximum principle [36]. This principle converts Equations (5.1)-(5.3) into a problem of minimizing pointwise a Hamiltonian $\mathcal{H}$ with respect to u_1, u_2, u_3 and u_4 given by

$$\begin{aligned}\mathcal{H} = {} & A_1 I_T + A_2 I_A + A_3 I_C + A_4 I_{AL} + A_5 I_{AT} + A_6 T_{CL} + A_7 I_{CT} \\ & + \frac{1}{2}B_1 u_1^2 + \frac{1}{2}B_2 u_2^2 + \frac{1}{2}B_3 u_3^2 + \frac{1}{2}B_4 u_4^2 \\ & + P_1\frac{dS}{dt} + P_2\frac{dI_L}{dt} + P_3\frac{dI_T}{dt} + P_4\frac{dH}{dt} + P_5\frac{dR_T}{dt} + P_6\frac{dI_A}{dt} + P_7\frac{dI_C}{dt} \\ & + P_8\frac{dR_H}{dt} + P_9\frac{dI_{AL}}{dt} + P_{10}\frac{dI_{CL}}{dt} + P_{11}\frac{dIAT}{dt} + P_{12}\frac{dI_{CT}}{dt} + P_{13}\frac{dR}{dt},\end{aligned} \tag{5.7}$$

where $P_i, i = 1, 2, 3, ..., 13$ are adjoint variable functions.

Now, substituting for $\frac{dS}{dt}, \frac{dI_L}{dt}, \frac{dI_T}{dt}, ..., \frac{dR}{dt}$ in Equation (5.7) gives;

$$
\begin{aligned}
\mathcal{H} = {} & A_1 I_T + A_2 I_A + A_3 I_C + A_4 I_{AL} + A_5 I_{AT} + A_6 T_{CL} + A_7 I_{CT} \\
& + \frac{1}{2} B_1 u_1^2 + \frac{1}{2} B_2 u_2^2 + \frac{1}{2} B_3 u_3^2 + \frac{1}{2} B_4 u_4^2 \\
& + P_1\big(\Lambda + \nu_1 R_H(t) + \nu_2 R_T(t) + \nu_3 R(t) + \pi I_A(t) + \eta I_L(t) - \big((1-u_1)\lambda_T \\
& + (1-u_3)\lambda_H + \mu\big) S(t)\big) + P_2\big((1-u_1)\lambda_T S(t) - (\theta + \eta + \mu + (1-u_3)\lambda_H) I_L(t)\big) \\
& + P_3\big(\theta I_L(t) - ((\omega_1 + u_2) + \rho + \mu + \sigma_1 + (1-u_3)\lambda_H) I_T(t)\big) \\
& + P_4\big(\rho I_T(t) - (\omega_2 + \mu + \sigma_2) H(t)\big) \\
& + P_5\big(\omega_2 H(t) + (\omega_1 + u_2) I_T(t) - (\nu_2 + \mu) R_T(t)\big) \\
& + P_6\big((1-u_3)\lambda_H S(t) - (\pi + \alpha + \mu + u_4 + (1-u_1)\lambda_T) I_A(t)\big) \\
& + P_7\big(\alpha I_A(t) - ((\psi + u_4) + \mu + \delta + (1-u_1)\lambda_T) I_C(t)\big) \\
& + P_8\big((\psi + u_4) I_C(t) - (\nu_1 + \mu) R_H(t) + u_4 I_A\big) \\
& + P_9\big((1-u_1)\lambda_T I_A(t) + (1-u_3)\lambda_H I_L(t) - (\tau_1 + \mu + \beta_1 + u_4) I_{AL}(t)\big) \\
& + P_{10}\big(\beta_1 I_{AL}(t) + (1-u_1)\lambda_T I_C(t) - ((r_1 + u_4) + \tau_2 + \mu + \delta) I_{CL}(t)\big) \\
& + P_{11}\big(\tau_1 I_{AL}(t) + (1-u_3)\lambda_H I_T(t) - ((r_2 + u_2 + u_4) + \beta_2 + \mu + d_1) I_{AT}(t)\big) \\
& + P_{12}\big(\tau_2 I_{CL}(t) + \beta_2 I_{AT}(t) - ((r_3 + u_2 + u_4) + \mu + d_2) I_{CT}(t)\big) \\
& + P_{13}\big(((r_1 + u_4) + u_2) I_{CL}(t) + ((r_2 + u_2 + u_4) I_{AT}(t) + (r_3 + u_2 + u_4) I_{CT}(t) \\
& - (\nu_3 + \mu) R(t) + u_4 I_{AL}\big).
\end{aligned} \tag{5.8}
$$

Then, applying the Pontryagin's maximum principle, we obtain the following result.

Theorem 12. *There exist optimal controls u_1^*, u_2^*, u_3^* and u_4^* and the corresponding state solutions $S^*, I_L^*, I_T^*, H^*, R_T^*, I_A^*, I_C^*, R_H^*, I_{AL}^*, I_{AT}^*, I_{CL}^*, I_{CT}^*$ and R^* that minimize $J(u_1, u_2, u_3, u_4)$ over $\mathcal{U}$ and*

therefore, there exist adjoint variables $P_1, P_2, ..., P_{13}$ *such that*

$$
\begin{aligned}
\frac{dP_1}{dt} &= (P_1 - P_2)(1-u_1)\lambda_T + (P_1 - P_6)(1-u_3)\lambda_H + P_1\mu, \\
\frac{dP_2}{dt} &= (P_2 - P_3)\theta + (P_2 - P_1)\eta + (P_2 - P_9)(1-u_3)\lambda_H + \mu P_2, \\
\frac{dP_3}{dt} &= -A_1 + (P_1 - P_2)\xi_1 q_1 (1-u_1)\frac{S}{N} + (P_3 - P_4)\rho + (P_3 - P_5)(\omega_1 + u_2) \\
&\quad + (P_3 - P_{11})(1-u_3)\lambda_H + (P_6 - P_9)(1-u_1)\xi_1 q_1 \frac{I_A}{N} \\
&\quad + (P_7 - P_{10})(1-u_1)\xi_1 q_1 \frac{I_C}{N} + P_3(\sigma_1 + \mu), \\
\frac{dP_4}{dt} &= (P_1 - P_2)(1-u_1)\xi_1 q_1 \epsilon \frac{S}{N} + (P_4 - P_5)\omega_2 \\
&\quad + (P_7 - P_{10})(1-u_1)\xi_1 q_1 \epsilon \frac{I_C}{N} + (P_6 - P_9)(1-u_1)\xi_1 q_1 \epsilon \frac{I_A}{N} + P_4(\mu + \sigma_2), \\
\frac{dP_5}{dt} &= (P_5 - P_1)\nu_2 + \mu P_5, \\
\frac{dP_6}{dt} &= -A_2 + (P_6 - P_1)\pi + (P_1 - P_6)(1-u_3)\xi_2 q_2 \phi \frac{S}{N} + (P_3 - P_{11})(1-u_3)\xi_2 q_2 \phi \frac{I_T}{N} \\
&\quad + (P_4 - P_{11})(1-u_3)\xi_2 q_2 \phi \frac{H}{N} + (P_6 - P_7)\alpha + (P_6 - P_8)u_4 + P_6\mu \\
&\quad + (P_6 - P_9)(1-u_1)\lambda_T, \\
\frac{dP_7}{dt} &= -A_3 + (P_1 - P_6)(1-u_3)\xi_2 q_2 \frac{S}{N} + (P_3 - P_{11})(1-u_3)\xi_2 q_2 \frac{I_T}{N} \\
&\quad + (P_4 - P_{11})(1-u_3)\xi_2 q_2 \frac{H}{N} + (P_2 - P_9)(1-u_3)\xi_2 q_2 \frac{I_T}{N} + (P_7 - P_8)(\psi + u_4) \\
&\quad + (P_7 - P_9)(1-u_1)\lambda_T + P_7(\mu + \delta), \qquad (5.9) \\
\frac{dP_8}{dt} &= (P_8 - P_1)\nu_1 + \mu P_8, \\
\frac{dP_9}{dt} &= -A_4 + (P_1 - P_6)(1-u_3)\xi_2 q_2 b_1 \frac{S}{N} + (P_2 - P_9)(1-u_3)\xi_2 q_2 b_1 \frac{I_L}{N} \\
&\quad + (P_3 - P_{11})\xi_2 q_2 b_1 \frac{I_T}{N} + (P_4 - P_{11})\xi_2 q_2 b_1 \frac{H}{N} + (P_9 - P_{10})\beta_1 + (P_9 - P_{11})\tau_1 \\
&\quad + (P_9 - P_{13})u_4 + P_9\mu, \\
\frac{dP_{10}}{dt} &= -A_6 + (P_1 - P_6)(1-u_3)\xi_2 q_2 b_2 \frac{S}{N} + (P_2 - P_9)(1-u_3)\xi_2 q_2 b_2 \frac{I_L}{N} \\
&\quad + (P_4 - P_{11})(1-u_3)\xi_2 q_2 b_2 \frac{H}{N} + (P_3 - P_{11})(1-u_3)\xi_2 q_2 b_2 \frac{I_T}{N} + (P_{10} - P_{12})\tau_2 \\
&\quad + (P_{10} - P_{13})(r_1 + u_4) + P_{10}(\mu + \delta),
\end{aligned}
$$

$$
\begin{aligned}
\frac{dP_{11}}{dt} &= -A_5 + \Big((P_1 - P_2)\frac{S}{N} + (P_6 - P_9)\frac{I_A}{N} + (P_7 - P_{10})\frac{I_C}{N}\Big)(1-u_1)\xi_1 q_1 a_1 \\
&\quad + \Big((P_1 - P_6)\frac{S}{N} + (P_2 - P_9)\frac{I_L}{N} + (P_3 - P_{11})\frac{I_T}{N}\Big)(1-u_3)\xi_2 q_2 b_3, \\
&\quad + (P_{11} - P_{12})\beta_2 + (P_{11} - P_{13})(r_2 + u_2 + u_4) + P_{11}(\mu + d_1) \\
\frac{dP_{12}}{dt} &= -A_7 + \Big((P_1 - P_2)\frac{S}{N} + (P_6 - P_9)\frac{I_A}{N} + (P_7 - P_{10})\frac{I_C}{N}\Big)(1-u_1)\xi_1 q_1 a_2 \\
&\quad + \Big((P_1 - P_6)\frac{S}{N} + (P_2 - P_9)\frac{I_L}{N} + (P_3 - P_{11})\frac{H}{N}\Big)(1-u_3)\xi_2 q_2 b_4 \\
&\quad + (P_{12} - P_{13})(r_3 + u_2 + u_4) + P_{12}(\mu + d_2), \\
\frac{dP_{13}}{dt} &= (P_{13} - P_1)\nu_3 + P_{13}\mu.
\end{aligned}
$$

with transversality conditions

$$P_j(t_f) = 0 \text{ for } j = 1, 2, ..., 13. \tag{5.10}$$

Furthermore, the characterization of the optimal controls is given by

$$
\begin{aligned}
u_1^* &= \max\{0, \min\{1, \tau_1'\}\}, \\
u_2^* &= \max\{0, \min\{1, \tau_2'\}\}, \\
u_3^* &= \max\{0, \min\{1, \tau_3'\}\}, \\
u_4^* &= \max\{0, \min\{1, \tau_4'\}\},
\end{aligned} \tag{5.11}
$$

where

$$
\begin{aligned}
\tau_1' &= \frac{(P_2 - P_1)\lambda_T S + (P_9 - P_6)\lambda_T I_A + (P_{10} - P_7)\lambda_T I_C}{B_1}, \\
\tau_2' &= \frac{(P_3 - P_5)I_T + (P_{11} - P_{13})I_{AT} + (P_{12} - P_{13})I_{CT}}{B_2}, \\
\tau_3' &= \frac{(P_6 - P_1)\lambda_H S + (P_9 - P_2)\lambda_H I_L + (P_{11} - P_3)\lambda_H I_T}{B_3}, \\
\tau_4' &= \frac{(P_7 - P_8)I_C + (P_{10} - P_{13})I_{CL} + (P_{11} - P_{13})I_{AT} + (P_9 - P_{13})I_{AL}}{B_4}.
\end{aligned} \tag{5.12}
$$

Proof. The adjoint system is obtained by taking the negative partial derivatives of $\mathcal{H}$ with respect to

each state variable [122], evaluated at optimal controls and corresponding state variables as follow

$$\begin{aligned}
\frac{dP_1}{dt} &= -\frac{\partial \mathcal{H}}{\partial S} = (P_1 - P_2)(1-u_1)\lambda_T + (P_1 - P_6)(1-u_3)\lambda_H + P_1\mu, \quad P_1(t_f) = 0,\\
\frac{dP_2}{dt} &= -\frac{\partial \mathcal{H}}{\partial I_L} = (P_2 - P_3)\theta + (P_2 - P_1)\eta + (P_2 - P_9)(1-u_3)\lambda_H + \mu P_2, \quad P_2(t_f) = 0,\\
\frac{dP_3}{dt} &= -\frac{\partial \mathcal{H}}{\partial I_T} = -A_1 + (P_1 - P_2)\xi_1 q_1 (1-u_1)\frac{S}{N} + (P_3 - P_4)\rho + (P_3 - P_5)(\omega_1 + u_2)\\
&\quad + (P_3 - P_{11})(1-u_3)\lambda_H + (P_6 - P_9)(1-u_1)\xi_1 q_1 \frac{I_A}{N}\\
&\quad + (P_7 - P_{10})(1-u_1)\xi_1 q_1 \frac{I_C}{N} + P_3(\sigma_1 + \mu), \quad P_3(t_f) = 0,\\
\frac{dP_4}{dt} &= -\frac{\partial \mathcal{H}}{\partial H} = (P_1 - P_2)(1-u_1)\xi_1 q_1 \epsilon \frac{S}{N} + (P_4 - P_5)\omega_2\\
&\quad + (P_7 - P_{10})(1-u_1)\xi_1 q_1 \epsilon \frac{I_C}{N} + (P_6 - P_9)(1-u_1)\xi_1 q_1 \epsilon \frac{I_A}{N} + P_4(\mu + \sigma_2), \quad P_4(t_f) = 0,\\
\frac{dP_5}{dt} &= -\frac{\partial \mathcal{H}}{\partial R_T} = (P_5 - P_1)\nu_2 + \mu P_5, \quad P_5(t_f) = 0,\\
\frac{dP_6}{dt} &= -\frac{\partial \mathcal{H}}{\partial I_A} = -A_2 + (P_6 - P_1)\pi + (P_1 - P_6)(1-u_3)\xi_2 q_2 \phi \frac{S}{N} + (P_3 - P_{11})(1-u_3)\xi_2 q_2 \phi \frac{I_T}{N}\\
&\quad + (P_4 - P_{11})(1-u_3)\xi_2 q_2 \phi \frac{H}{N} + (P_6 - P_7)\alpha + (P_6 - P_8)u_4 + P_6\mu\\
&\quad + (P_6 - P_9)(1-u_1)\lambda_T, \quad P_6(t_f) = 0,\\
\frac{dP_7}{dt} &= -\frac{\partial \mathcal{H}}{\partial I_C} = -A_3 + (P_1 - P_6)(1-u_3)\xi_2 q_2 \frac{S}{N} + (P_3 - P_{11})(1-u_3)\xi_2 q_2 \frac{I_T}{N}\\
&\quad + (P_4 - P_{11})(1-u_3)\xi_2 q_2 \frac{H}{N} + (P_2 - P_9)(1-u_3)\xi_2 q_2 \frac{I_T}{N} + (P_7 - P_8)(\psi + u_4)\\
&\quad + (P_7 - P_9)(1-u_1)\lambda_T + P_7(\mu + \delta), \quad P_7(t_f) = 0, \qquad (5.1\\
\frac{dP_8}{dt} &= -\frac{\partial \mathcal{H}}{\partial R_H} = (P_8 - P_1)\nu_1 + \mu P_8, \quad P_8(t_f) = 0,\\
\frac{dP_9}{dt} &= -\frac{\partial \mathcal{H}}{\partial I_{AL}} = -A_4 + (P_1 - P_6)(1-u_3)\xi_2 q_2 b_1 \frac{S}{N} + (P_2 - P_9)(1-u_3)\xi_2 q_2 b_1 \frac{I_L}{N}\\
&\quad + (P_3 - P_{11})\xi_2 q_2 b_1 \frac{I_T}{N} + (P_4 - P_{11})\xi_2 q_2 b_1 \frac{H}{N} + (P_9 - P_{10})\beta_1 + (P_9 - P_{11})\tau_1\\
&\quad + (P_9 - P_{13})u_4 + P_9\mu, \quad P_9(t_f) = 0,\\
\frac{dP_{10}}{dt} &= -\frac{\partial \mathcal{H}}{\partial I_{AT}} = -A_6 + (P_1 - P_6)(1-u_3)\xi_2 q_2 b_2 \frac{S}{N} + (P_2 - P_9)(1-u_3)\xi_2 q_2 b_2 \frac{I_L}{N}\\
&\quad + (P_4 - P_{11})(1-u_3)\xi_2 q_2 b_2 \frac{H}{N} + (P_3 - P_{11})(1-u_3)\xi_2 q_2 b_2 \frac{I_T}{N} + (P_{10} - P_{12})\tau_2\\
&\quad + (P_{10} - P_{13})(r_1 + u_4) + P_{10}(\mu + \delta), \quad P_{10}(t_f) = 0,
\end{aligned}$$

$$\begin{aligned}
\frac{dP_{11}}{dt} &= -\frac{\partial \mathcal{H}}{\partial I_{CL}} = -A_5 + \Big((P_1 - P_2)\frac{S}{N} + (P_6 - P_9)\frac{I_A}{N} + (P_7 - P_{10})\frac{I_C}{N}\Big)(1-u_1)\xi_1 q_1 a_1 \\
&\quad + \Big((P_1 - P_6)\frac{S}{N} + (P_2 - P_9)\frac{I_L}{N} + (P_3 - P_{11})\frac{I_T}{N}\Big)(1-u_3)\xi_2 q_2 b_3 \\
&\quad + (P_{11} - P_{12})\beta_2 + (P_{11} - P_{13})(r_2 + u_2 + u_4) + P_{11}(\mu + d_1), \quad P_{11}(t_f) = 0, \\
\frac{dP_{12}}{dt} &= -\frac{\partial \mathcal{H}}{\partial I_{CT}} = -A_7 + \Big((P_1 - P_2)\frac{S}{N} + (P_6 - P_9)\frac{I_A}{N} + (P_7 - P_{10})\frac{I_C}{N}\Big)(1-u_1)\xi_1 q_1 a_2 \\
&\quad + \Big((P_1 - P_6)\frac{S}{N} + (P_2 - P_9)\frac{I_L}{N} + (P_3 - P_{11})\frac{H}{N}\Big)(1-u_3)\xi_2 q_2 b_4 \\
&\quad + (P_{12} - P_{13})(r_3 + u_2 + u_4) + P_{12}(\mu + d_2), \quad P_{12}(t_f) = 0, \\
\frac{dP_{13}}{dt} &= -\frac{\partial \mathcal{H}}{\partial R} = (P_{13} - P_1)\nu_3 + P_{13}\mu, \quad P_{13}(t_f) = 0.
\end{aligned}$$

Also, for characterization of the optimal controls, we first obtain the optimality conditions by applying Lagrangian maximum principle [111] as applied in [44, 124]. That is

$$\frac{\partial \mathcal{H}}{\partial u_1} = \frac{\partial \mathcal{H}}{\partial u_2} = \frac{\partial \mathcal{H}}{\partial u_3} = \frac{\partial \mathcal{H}}{\partial u_4} = 0.$$

Thus,

$$\begin{aligned}
\frac{\partial \mathcal{H}}{\partial u_1} &= B_1 u_1 + (P_1 - P_2)\lambda_T S + (P_6 - P_9)\lambda_T I_A + (P_7 - P_{10})\lambda_T I_C = 0, \\
\frac{\partial \mathcal{H}}{\partial u_2} &= B_2 u_2 + (P_5 - P_3) I_T + (P_{13} - P_{11}) I_{AT} + (P_{13} - P_{12}) I_{CT} = 0, \\
\frac{\partial \mathcal{H}}{\partial u_3} &= B_3 u_3 + (P_1 - P_6)\lambda_H S + (P_2 - P_9)\lambda_H I_L + (P_3 - P_{11})\lambda_H I_T = 0, \\
\frac{\partial \mathcal{H}}{\partial u_4} &= B_4 u_4 + (P_8 - P_7) I_C + (P_{13} - P_{10}) I_{CL} + (P_{13} - P_{11}) I_{AT} + (P_{13} - P_9) I_{AL} = 0.
\end{aligned} \tag{5.14}$$

From $\frac{\partial \mathcal{H}}{\partial u_1} = 0$, we have

$$B_1 u_1 + (P_1 - P_2)\lambda_T S + (P_6 - P_9)\lambda_T I_A + (P_7 - P_{10})\lambda_T I_C = 0. \tag{5.15}$$

Re-arranging (5.15), we have

$$u_1 = \frac{(P_2 - P_1)\lambda_T S + (P_9 - P_6)\lambda_T I_A + (P_{10} - P_7)\lambda_T I_C}{B_1}.$$

Using the same approach, it can be shown that

$$\begin{aligned} u_2 &= \frac{(P_3 - P_5)I_T + (P_{11} - P_{13})I_{AT} + (P_{12} - P_{13})I_{CT}}{B_2}, \\ u_3 &= \frac{(P_6 - P_1)\lambda_H S + (P_9 - P_2)\lambda_H I_L + (P_{11} - P_3)\lambda_H I_T}{B_3}, \\ u_4 &= \frac{(P_7 - P_8)I_C + (P_{10} - P_{13})I_{CL} + (P_{11} - P_{13})I_{AT} + (P_9 - P_{13})I_{AL}}{B_4}. \end{aligned} \tag{5.16}$$

Then, using the property of the control bounds $0 \leq u_i \leq 1, i = 1, 2, 3, 4$, the controls are given as

$$u_1^* = \begin{cases} 0 & \text{if } (P_2 - P_1)\lambda_T S + (P_9 - P_6)\lambda_T I_A + (P_{10} - P_7)\lambda_T I_C < 0, \\ u_1^* & \text{if } 0 \leq (P_2 - P_1)\lambda_T S + (P_9 - P_6)\lambda_T I_A + (P_{10} - P_7)\lambda_T I_C \leq 1, \\ 1 & \text{if } (P_2 - P_1)\lambda_T S + (P_9 - P_6)\lambda_T I_A + (P_{10} - P_7)\lambda_T I_C > 1, \end{cases}$$

$$u_2^* = \begin{cases} 0 & \text{if } (P_3 - P_5)I_T + (P_{11} - P_{13})I_{AT} + (P_{12} - P_{13})I_{CT} < 0, \\ u_2^* & \text{if } 0 \leq (P_3 - P_5)I_T + (P_{11} - P_{13})I_{AT} + (P_{12} - P_{13})I_{CT} \leq 1, \\ 1 & \text{if } (P_3 - P_5)I_T + (P_{11} - P_{13})I_{AT} + (P_{12} - P_{13})I_{CT} > 1, \end{cases}$$

$$u_3^* = \begin{cases} 0 & \text{if } (P_6 - P_1)\lambda_H S + (P_9 - P_2)\lambda_H I_L + (P_{11} - P_3)\lambda_H I_T < 0, \\ u_3^* & \text{if } 0 \leq (P_6 - P_1)\lambda_H S + (P_9 - P_2)\lambda_H I_L + (P_{11} - P_3)\lambda_H I_T \leq 1, \\ 1 & \text{if } (P_6 - P_1)\lambda_H S + (P_9 - P_2)\lambda_H I_L + (P_{11} - P_3)\lambda_H I_T > 1, \end{cases}$$

and

$$u_4^* = \begin{cases} 0 & \text{if } (P_7 - P_8)I_C + (P_{10} - P_{13})I_{CL} + (P_{11} - P_{13})I_{AT} + (P_9 - P_{13})I_{AL} < 0, \\ u_4^* & \text{if } 0 \leq (P_7 - P_8)I_C + (P_{10} - P_{13})I_{CL} + (P_{11} - P_{13})I_{AT} + (P_9 - P_{13})I_{AL} \leq 1, \\ 1 & \text{if } (P_7 - P_8)I_C + (P_{10} - P_{13})I_{CL} + (P_{11} - P_{13})I_{AT} + (P_9 - P_{13})I_{AL} > 1. \end{cases}$$

This can be written in a compact form as follows:

$$\begin{aligned} u_1^* &= \max\left\{0, \min\{1, \tau_1'\}\right\}, \\ u_2^* &= \max\left\{0, \min\{1, \tau_2'\}\right\}, \\ u_3^* &= \max\left\{0, \min\{1, \tau_3'\}\right\}, \\ u_4^* &= \max\left\{0, \min\{1, \tau_4'\}\right\}, \end{aligned} \tag{5.17}$$

where

$$\begin{aligned} \tau_1' &= \frac{(P_2 - P_1)\lambda_T S + (P_9 - P_6)\lambda_T I_A + (P_{10} - P_7)\lambda_T I_C}{B_1}, \\ \tau_2' &= \frac{(P_3 - P_5)I_T + (P_{11} - P_{13})I_{AT} + (P_{12} - P_{13})I_{CT}}{B_2}, \\ \tau_3' &= \frac{(P_6 - P_1)\lambda_H S + (P_9 - P_2)\lambda_H I_L + (P_{11} - P_3)\lambda_H I_T}{B_3}, \\ \tau_4' &= \frac{(P_7 - P_8)I_C + (P_{10} - P_{13})I_{CL} + (P_{11} - P_{13})I_{AT} + (P_9 - P_{13})I_{AL}}{B_4}. \end{aligned} \tag{5.18}$$

□

We point out that the optimal controls and the corresponding state solutions are found by solving the following optimality system, which consists of the state system (5.1) with its initial conditions coupled with the adjoint system (5.9) and its transversality conditions (5.10) together with the characterization of the optimal controls (5.11):

$$
\begin{aligned}
\frac{dS(t)}{dt} &= \Lambda + \nu_1 R_H(t) + \nu_2 R_T(t) + \nu_3 R(t) + \pi I_A(t) + \eta I_L(t) - \big((1-u_1^*)\lambda_T + (1-u_3^*)\lambda_H + \mu\big)S(t),\\
\frac{dI_L(t)}{dt} &= (1-u_1^*)\lambda_T S(t) - (\theta + \eta + \mu + (1-u_3^*)\lambda_H)I_L(t),\\
\frac{dI_T(t)}{dt} &= \theta I_L(t) - ((\omega_1 + u_2^*) + \rho + \mu + \sigma_1 + (1-u_3^*)\lambda_H)I_T(t),\\
\frac{dH(t)}{dt} &= \rho I_T(t) - (\omega_2 + \mu + \sigma_2)H(t),\\
\frac{dR_T(t)}{dt} &= \omega_2 H(t) + (\omega_1 + u_2^*)I_T(t) - (\nu_2 + \mu)R_T(t),\\
\frac{dI_A(t)}{dt} &= (1-u_3^*)\lambda_H S(t) - (\pi + \alpha + \mu + u_4^* + (1-u_1^*)\lambda_T)I_A(t),\\
\frac{dI_C(t)}{dt} &= \alpha I_A(t) - ((\psi + u_4^*) + \mu + \delta + (1-u_1^*)\lambda_T)I_C(t),\\
\frac{dR_H(t)}{dt} &= (\psi + u_4^*)I_C(t) - (\nu_1 + \mu)R_H(t) + u_4^* I_A(t),\\
\frac{dI_{AL}(t)}{dt} &= (1-u_1^*)\lambda_T I_A(t) + (1-u_3^*)\lambda_H I_L(t) - (\tau_1 + \mu + \beta_1 + u_4^*)I_{AL}(t),\\
\frac{dI_{CL}(t)}{dt} &= \beta_1 I_{AL}(t) + (1-u_1^*)\lambda_T I_C(t) - ((r_1 + u_4^*) + \tau_2 + \mu + \delta)I_{CL}(t),\\
\frac{dI_{AT}(t)}{dt} &= \tau_1 I_{AL}(t) + (1-u_3^*)\lambda_H I_T(t) - ((r_2 + u_2^* + u_4^*) + \beta_2 + \mu + d_1)I_{AT}(t),\\
\frac{dI_{CT}(t)}{dt} &= \tau_2 I_{CL}(t) + \beta_2 I_{AT}(t) - ((r_3 + u_2^* + u_4^*) + \mu + d_2)I_{CT}(t),\\
\frac{dR(t)}{dt} &= ((r_1 + u_4^*) + u_2^*)I_{CL}(t) + ((r_2 + u_2^* + u_4^*)I_{AT}(t) + (r_3 + u_2^* + u_4^*)I_{CT}(t) - (\nu_3 + \mu)R(t) + u_4^* I_{AL}\\
\frac{dP_1}{dt} &= (P_1 - P_2)(1-u_1^*)\lambda_T + (P_1 - P_6)(1-u_3^*)\lambda_H + P_1\mu,\\
\frac{dP_2}{dt} &= (P_2 - P_3)\theta + (P_2 - P_1)\eta + (P_2 - P_9)(1-u_3^*)\lambda_H + \mu P_2,\\
\frac{dP_3}{dt} &= -A_1 + (P_1 - P_2)\xi_1 q_1 (1-u_1^*)\frac{S}{N} + (P_3 - P_4)\rho + (P_3 - P_5)(\omega_1 + u_2^*)\\
&\quad + (P_3 - P_{11})(1-u_3^*)\lambda_H + (P_6 - P_9)(1-u_1^*)\xi_1 q_1 \frac{I_A}{N}\\
&\quad + (P_7 - P_{10})(1-u_1^*)\xi_1 q_1 \frac{I_C}{N} + P_3(\sigma_1 + \mu),\\
\frac{dP_4}{dt} &= (P_1 - P_2)(1-u_1^*)\xi_1 q_1 \epsilon \frac{S}{N} + (P_4 - P_5)\omega_2\\
&\quad + (P_7 - P_{10})(1-u_1^*)\xi_1 q_1 \epsilon \frac{I_C}{N} + (P_6 - P_9)(1-u_1^*)\xi_1 q_1 \epsilon \frac{I_A}{N} + P_4(\mu + \sigma_2),
\end{aligned}
\tag{5.19}
$$

$$
\begin{aligned}
\frac{dP_5}{dt} &= (P_5 - P_1)\nu_2 + \mu P_5,\\
\frac{dP_6}{dt} &= -A_2 + (P_6 - P_1)\pi + (P_1 - P_6)(1 - u_3^*)\xi_2 q_2 \phi \frac{S}{N} + (P_3 - P_{11})(1 - u_3^*)\xi_2 q_2 \phi \frac{I_T}{N}\\
&\quad + (P_4 - P_{11})(1 - u_3^*)\xi_2 q_2 \phi \frac{H}{N} + (P_6 - P_7)\alpha + (P_6 - P_8)u_4^* + P_6\mu\\
&\quad + (P_6 - P_9)(1 - u_1^*)\lambda_T,\\
\frac{dP_7}{dt} &= -A_3 + (P_1 - P_6)(1 - u_3^*)\xi_2 q_2 \frac{S}{N} + (P_3 - P_{11})(1 - u_3^*)\xi_2 q_2 \frac{I_T}{N}\\
&\quad + (P_4 - P_{11})(1 - u_3^*)\xi_2 q_2 \frac{H}{N} + (P_2 - P_9)(1 - u_3^*)\xi_2 q_2 \frac{I_T}{N} + (P_7 - P_8)(\psi + u_4^*)\\
&\quad + (P_7 - P_9)(1 - u_1^*)\lambda_T + P_7(\mu + \delta),\\
\frac{dP_8}{dt} &= (P_8 - P_1)\nu_1 + \mu P_8,\\
\frac{P_9}{dt} &= -A_4 + (P_1 - P_6)(1 - u_3^*)\xi_2 q_2 b_1 \frac{S}{N} + (P_2 - P_9)(1 - u_3^*)\xi_2 q_2 b_1 \frac{I_L}{N}\\
&\quad + (P_3 - P_{11})\xi_2 q_2 b_1 \frac{I_T}{N} + (P_4 - P_{11})\xi_2 q_2 b_1 \frac{H}{N} + (P_9 - P_{10})\beta_1 + (P_9 - P_{11})\tau_1\\
&\quad + (P_9 - P_{13})u_4^* + P_9\mu,\\
\frac{dP_{10}}{dt} &= -A_6 + (P_1 - P_6)(1 - u_3^*)\xi_2 q_2 b_2 \frac{S}{N} + (P_2 - P_9)(1 - u_3^*)\xi_2 q_2 b_2 \frac{I_L}{N}\\
&\quad + (P_4 - P_{11})(1 - u_3^*)\xi_2 q_2 b_2 \frac{H}{N} + (P_3 - P_{11})(1 - u_3^*)\xi_2 q_2 b_2 \frac{I_T}{N} + (P_{10} - P_{12})\tau_2\\
&\quad + (P_{10} - P_{13})(r_1 + u_4^*) + P_{10}(\mu + \delta),\\
\frac{dP_{11}}{dt} &= -A_5 + \Big((P_1 - P_2)\frac{S}{N} + (P_6 - P_9)\frac{I_A}{N} + (P_7 - P_{10})\frac{I_C}{N}\Big)(1 - u_1^*)\xi_1 q_1 a_1\\
&\quad + \Big((P_1 - P_6)\frac{S}{N} + (P_2 - P_9)\frac{I_L}{N} + (P_3 - P_{11})\frac{I_T}{N}\Big)(1 - u_3^*)\xi_2 q_2 b_3\\
&\quad + (P_{11} - P_{12})\beta_2 + (P_{11} - P_{13})(r_2 + u_2^* + u_4^*) + P_{11}(\mu + d_1),\\
\frac{dP_{12}}{dt} &= -A_7 + \Big((P_1 - P_2)\frac{S}{N} + (P_6 - P_9)\frac{I_A}{N} + (P_7 - P_{10})\frac{I_C}{N}\Big)(1 - u_1^*)\xi_1 q_1 a_2\\
&\quad + \Big((P_1 - P_6)\frac{S}{N} + (P_2 - P_9)\frac{I_L}{N} + (P_3 - P_{11})\frac{H}{N}\Big)(1 - u_3^*)\xi_2 q_2 b_4\\
&\quad + (P_{12} - P_{13})(r_3 + u_2^* + u_4^*) + P_{12}(\mu + d_2),\\
\frac{dP_{13}}{dt} &= (P_{13} - P_1)\nu_3 + P_{13}\mu,
\end{aligned}
$$

$$S(0) = S_0, I_L(0) = I_{L0}, I_T(0) = I_{T0}, H(0) = H_0, R_T(0) = R_{T0}, I_A(0) = I_{A0}, I_C(0) = I_{C0},$$

$$R_H(0) = R_{H0}, I_{AL}(0) = I_{AL0}, I_{AT}(0) = I_{AT0}, I_{CL}(0) = I_{CL0}, I_{CT}(0) = I_{CT0}, R(0) = R_0$$

$$P_j(t_f) = 0, \quad j = 1, 2, ..., 13.$$

Next, we discuss the numerical solutions and the corresponding control measures of the optimality

system.

5.3 Numerical Results and Discussions

With the optimal control characterized, we now turn to numerical simulations to explore the practical implications of our results. Numerical simulations offer a powerful tool for testing the efficacy of the optimal control strategies, allowing us to simulate various scenarios and evaluate the impact of different interventions.

The results of our simulations have an important implication for public health policy and decision-making offering insights into the most effective ways to mitigate the spread of TB-HCV co-infection.

The optimal control solution is obtained by solving the optimality system, which consists of the state system and the adjoint system. A fourth-order Runge-Kutta method is employed to obtain a numerical solution to the optimality system in this subsection. System (5.1) is numerically integrated forward in time using a fourth-order Runge-Kutta method, subject to the specified initial conditions for the state variables. The solution of the adjoint system (5.9) is computed backward in time, utilizing the current iteration results of system (5.1) and the transversality conditions (5.10), and applying the same numerical method. The state and adjoint values are utilized to update the control inputs based on the characterization provided in (5.11), after which the iterative process is repeated. The iterative process continues until the state, adjoint, and control values converge to a satisfactory level. In this subsection, we investigate numerically the effect of the following itemized optimal control strategies listed below on the spread of TB-HCV co-infection in a population.

(a) Strategy A: Using all intervention efforts ($u_1 \neq 0, u_2 \neq 0, u_3 \neq 0, u_4 \neq 0$).

(b) Strategy B: Prevention effort through health educational campaigns, and the detect and treat effort for TB ($u_1 \neq 0, u_2 \neq 0, u_3 = 0, u_4 = 0$).

(c) Strategy C: Prevention effort through health educational campaigns, and the detect and treat effort for HCV ($u_1 = 0, u_2 = 0, u_3 \neq 0, u_4 \neq 0$).

(d) Strategy D: Detecting and treatment effort for both TB and HCV ($u_1 = 0, u_2 \neq 0, u_3 = 0, u_4 \neq 0$).

(e) Strategy E: Prevention effort through health educational campaigns for both TB and HCV ($u_1 \neq 0, u_2 = 0, u_3 \neq 0, u_4 = 0$).

We employed parameter values similar to those reported in previous studies whenever possible. Table 4.3 provides a summary of the parameter values used in numerical simulation of model (5.1). Due to lack of data, we make hypothesis on some parameter values within realistic ranges. The initial values for the states are given by $S(0) = 40000, I_L(0) = 500, I_T(0) = 450, H(0) = 350, R_T(0) = 500, I_A(0) = 350, I_C(0) = 400, R_H(0) = 350, I_{AL}(0) = 250, I_{CL}(0) = 250, I_{AT}(0) = 250, I_{CT}(0) = 250, R(0) = 250$. The weights in the objective functional are $A_1 = 20, A_2 = 25, A_3 = 50, A_4 = 40, A_5 = 60, A_6 = 30, A_7 = 30, B_1 = 20, B_2 = 30, B_3 = 25$ and $B_4 = 40$, which means that minimization of the number of latent, infectious, co-infections and treated has different importance. The bounds on the control are based on the effectiveness of the intervention strategy. It is reasonable to assume that the upper bound for $u_1(t), u_2(t), u_3(t). u_4(t)$ is 1 and lower bound is 0. We choose optimal control for a period of 5 years in keeping with what is in other literature on treatment of tuberculosis and hepatitis C such as [25, 96, 112].

5.3.1 Control with a Combination of all Intervention Strategies

The controls u_1, u_2, u_3 and u_4 are used to evaluate their effect on the control of TB, HCV and their co-infection. The results in Figures 5.1, 5.2 and 5.3 demonstrate increase in the number of susceptible individuals by 25% in 5 years and a sharp drop in the number of TB and HCV infected individuals to 10% in 5 and 3.5 years respectively. Results show that the co-infection burden would be wiped out in a period of about three years. Further, it would take about 5 years to considerably reduce the TB infected individuals and about 4.5 years to wipe out HCV only infected individuals.

5.3.2 Controls Fixed on TB only

The controls u_1 and u_2 are used to check how protecting against TB, testing and timely treatment against TB affects the co-dynamics of TB and HCV. The results in Figures 5.4 and 5.6 show a gradual increase in the number of susceptible individuals and a decrease in the number of TB infected and co-infected individuals. Figure 5.5 shows a slight reduction in HCV infected individuals when controls u_1 and u_2 for TB are applied. This indirect reduction in the number of HCV only cases is due to reduction in the number of co-infected individuals. Furthermore, controlling TB increases the number of healthy individuals, thus lower risk or reduced exposure to HCV. There is however a possibility of significantly reducing acute HCV-infectious TB and chronic HCV-infectious TB co-infection in

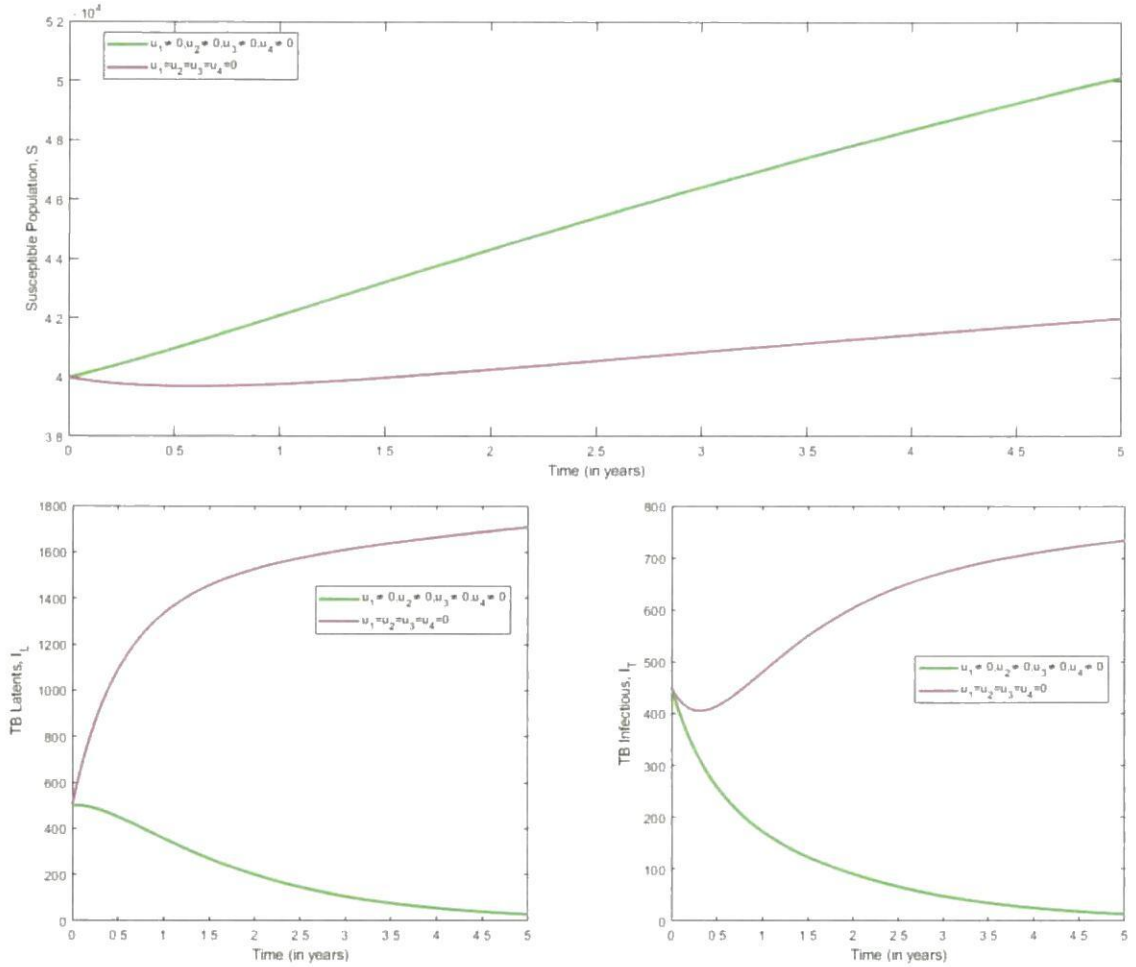

Figure 5.1: Effect of all intervention strategies on susceptible and TB infected populations.

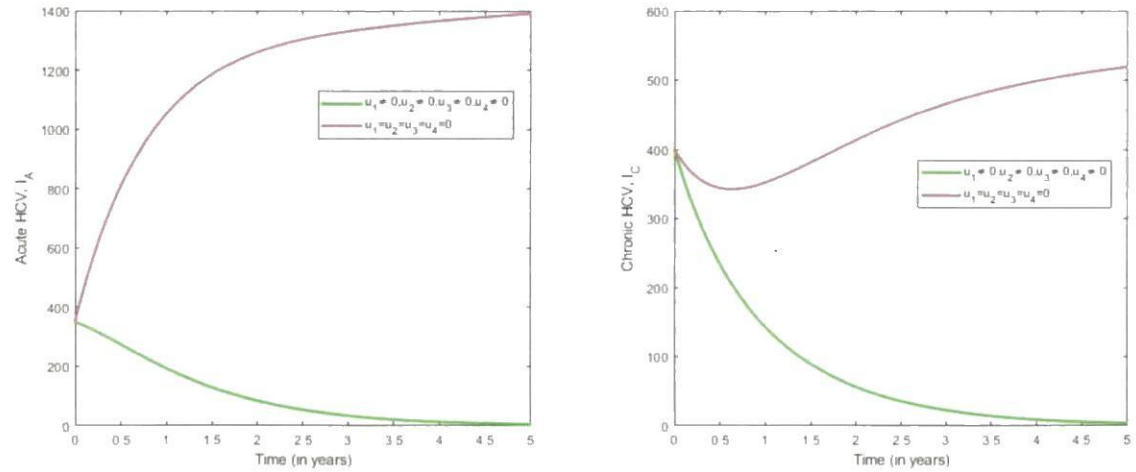

Figure 5.2: Effect of all intervention strategies on HCV infectious populations.

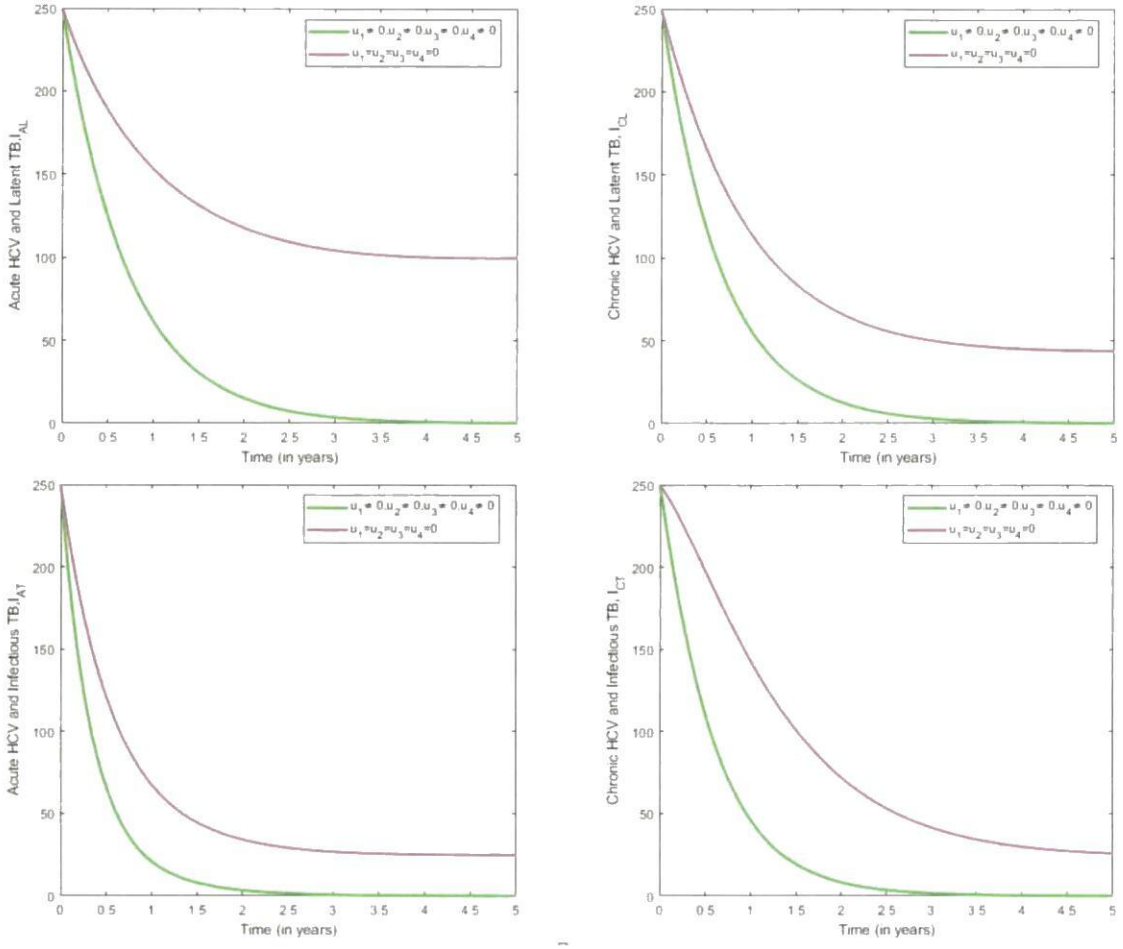

Figure 5.3: Effect of all intervention strategies on co-infected populations.

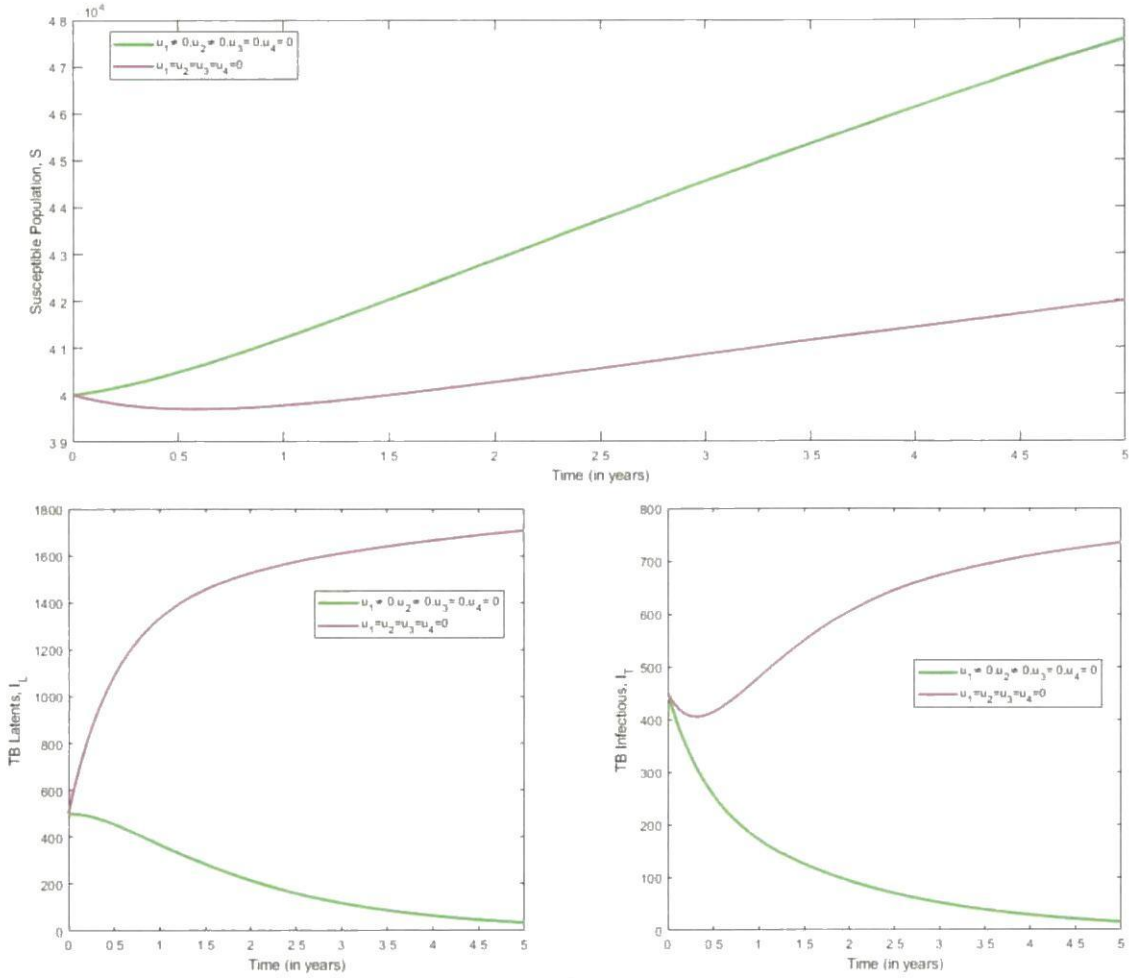

Figure 5.4: Effect of controls u_1 and u_2 on susceptible and TB infected populations.

about five years of implementing these controls.

5.3.3 Controls Fixed on HCV only

The controls u_3 and u_4 are used to check how protecting against HCV, testing and timely treatme against HCV affects the co-dynamics of TB and HCV. The results in Figures 5.7 show a gradu increase in the number of susceptible individuals and a slight decrease in the number of TB infect individuals. Figures 5.8 and 5.9 indicate a significant decrease in the number of HCV infect and co-infected individuals. The indirect slight reduction in the number of TB only cases is d to reduction in the number of co-infected individuals. Furthermore, controlling HCV increases t number of healthy individuals, thus lower risk or reduced exposure to TB. The plan shows a char of co-infection elimination in about 3.5 years of enforcement.

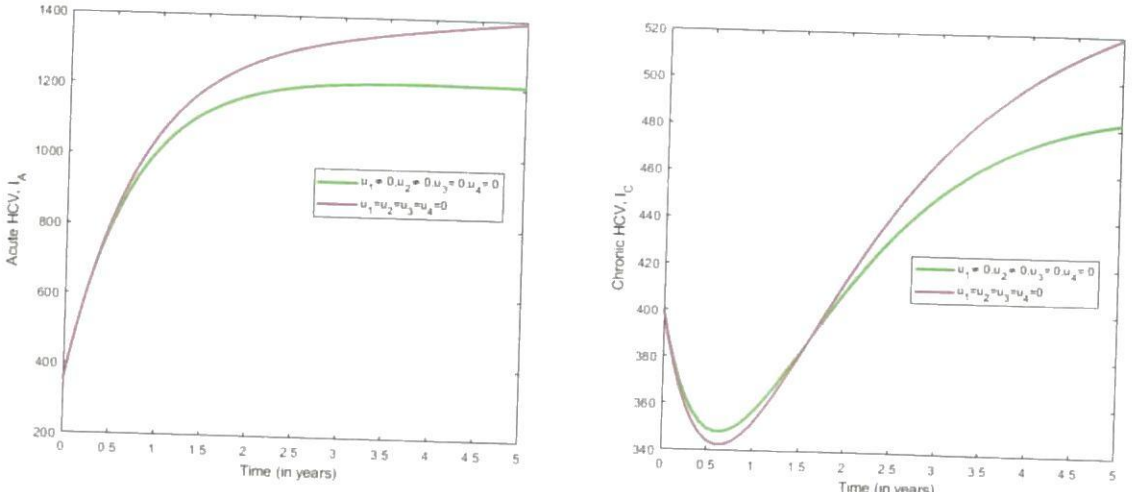

Figure 5.5: Effect of controls u_1 and u_2 on HCV infected populations.

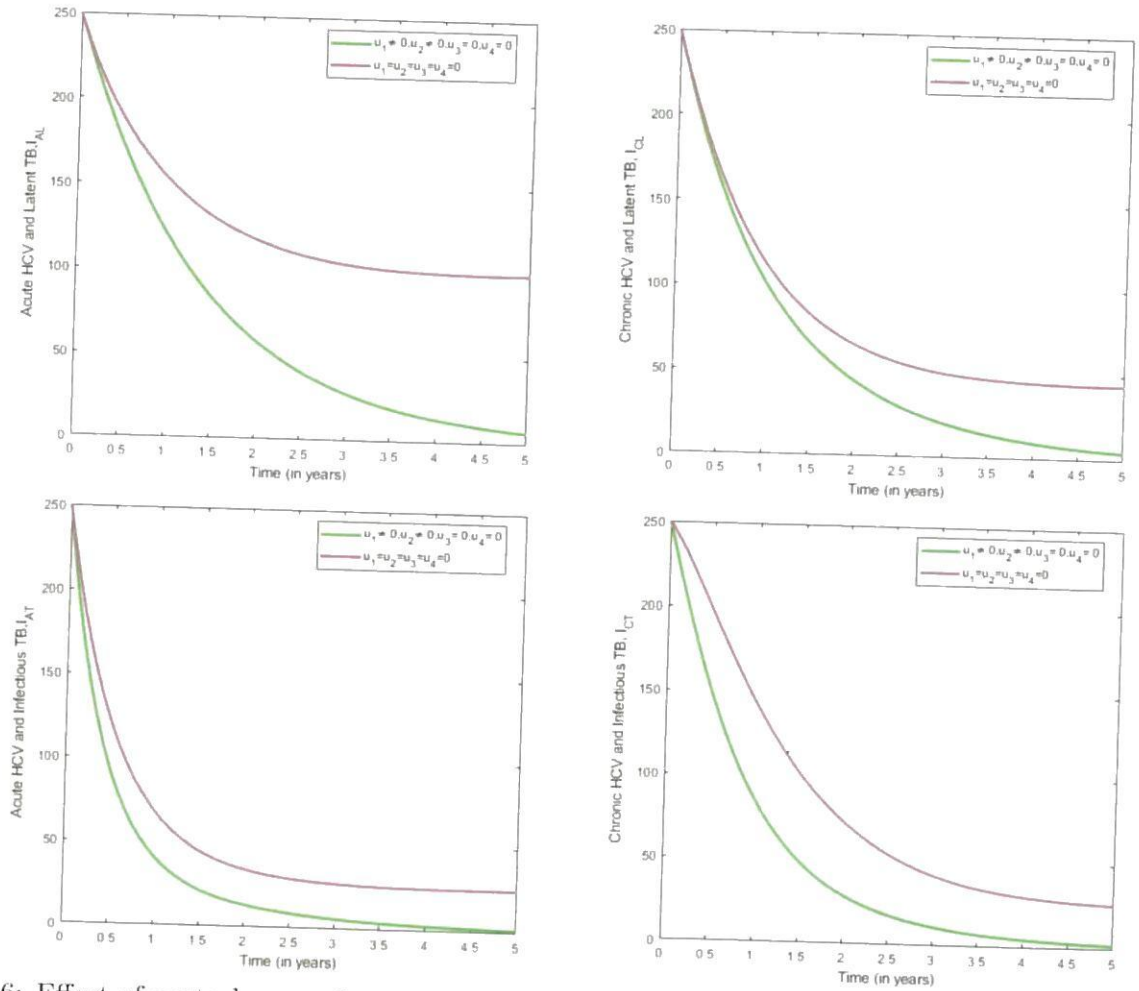

igure 5.6: Effect of controls u_1 and u_2 on co-infected populations.

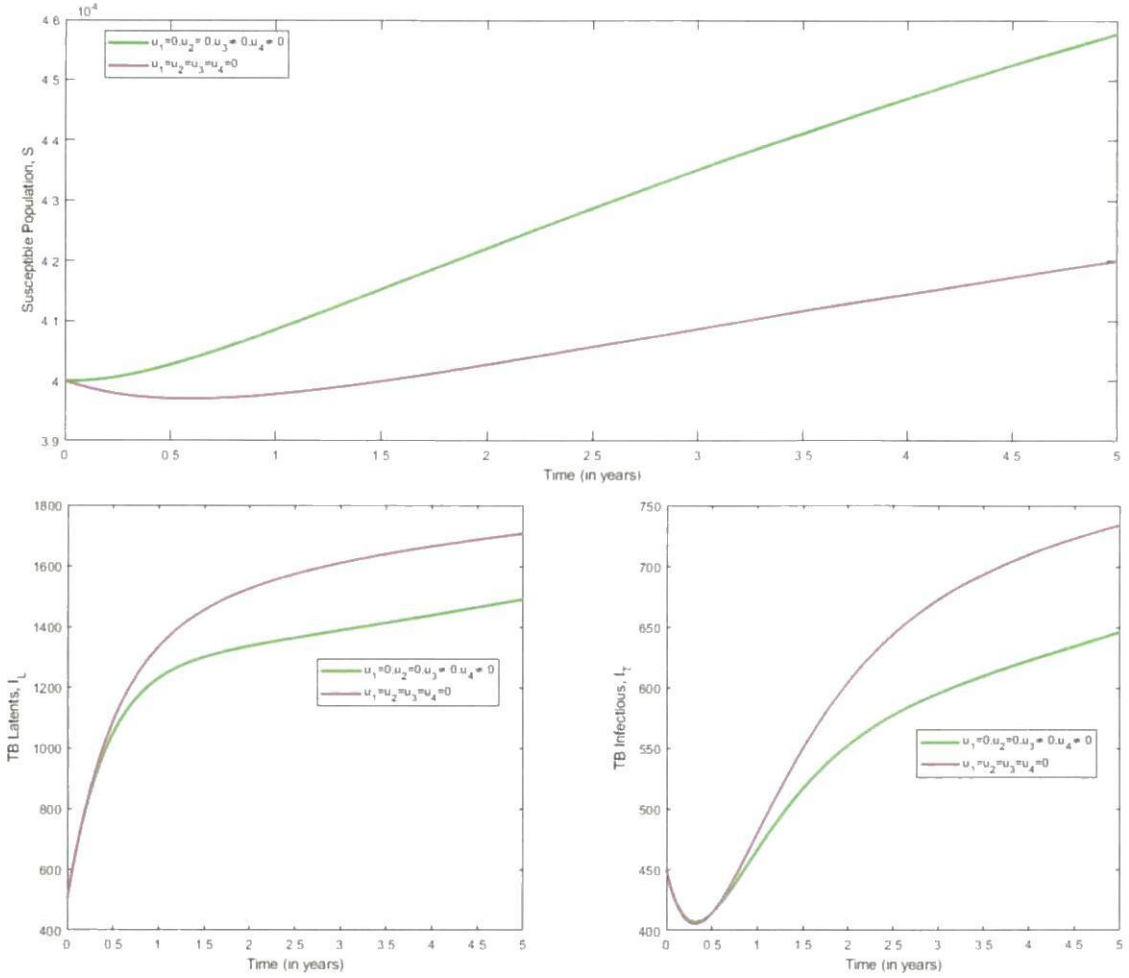

Figure 5.7: Effect of controls u_3 and u_4 on susceptible and TB infected populations.

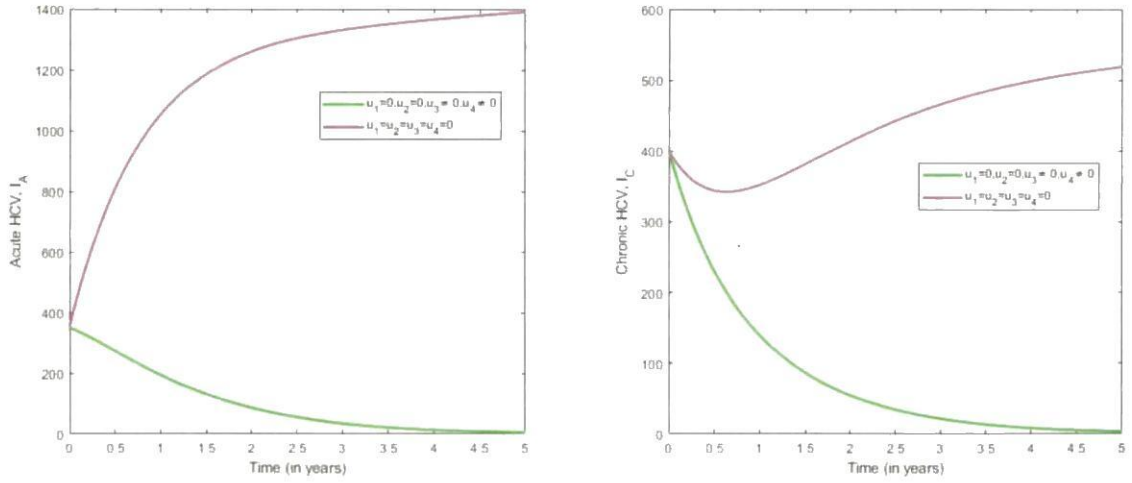

Figure 5.8: Effect of controls u_3 and u_4 on HCV infected populations.

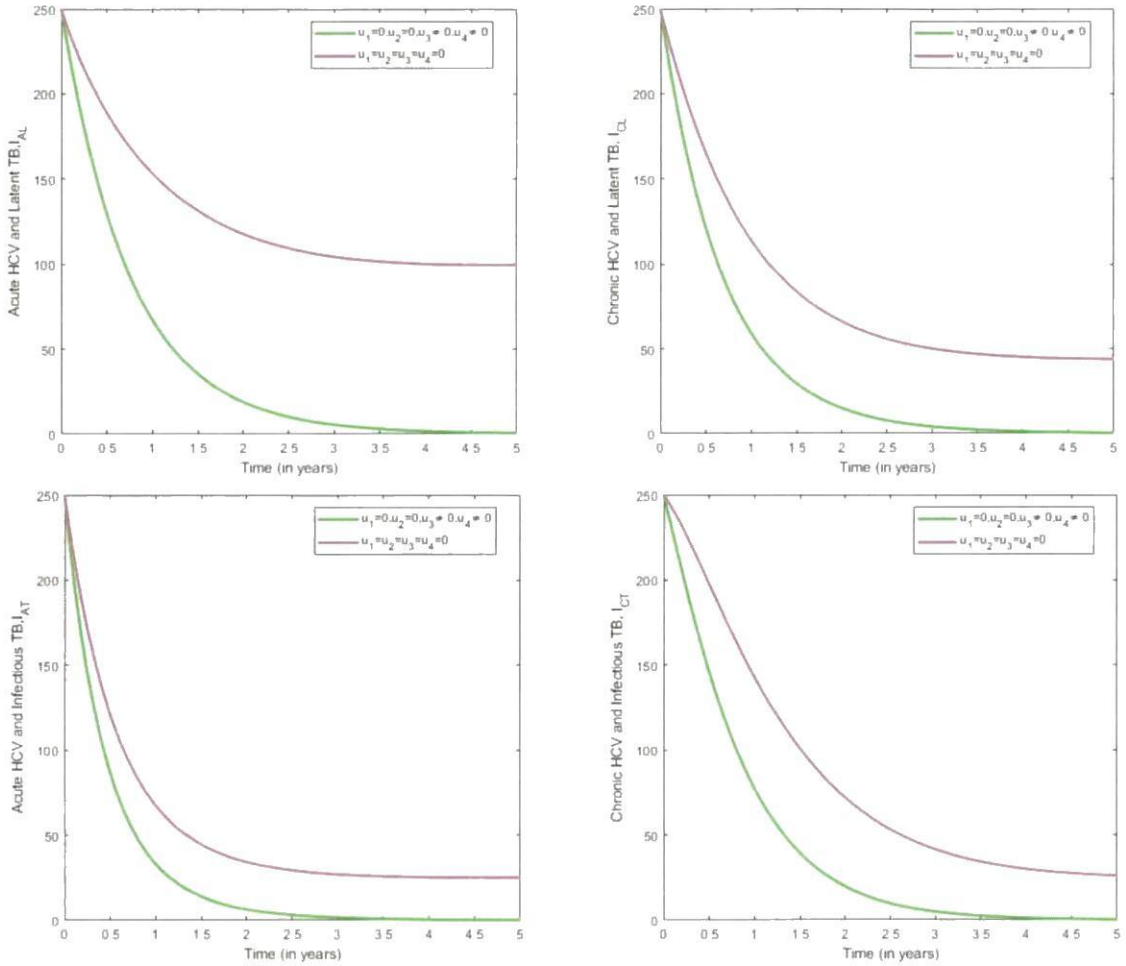

Figure 5.9: Effect of controls u_3 and u_4 on co-infected populations.

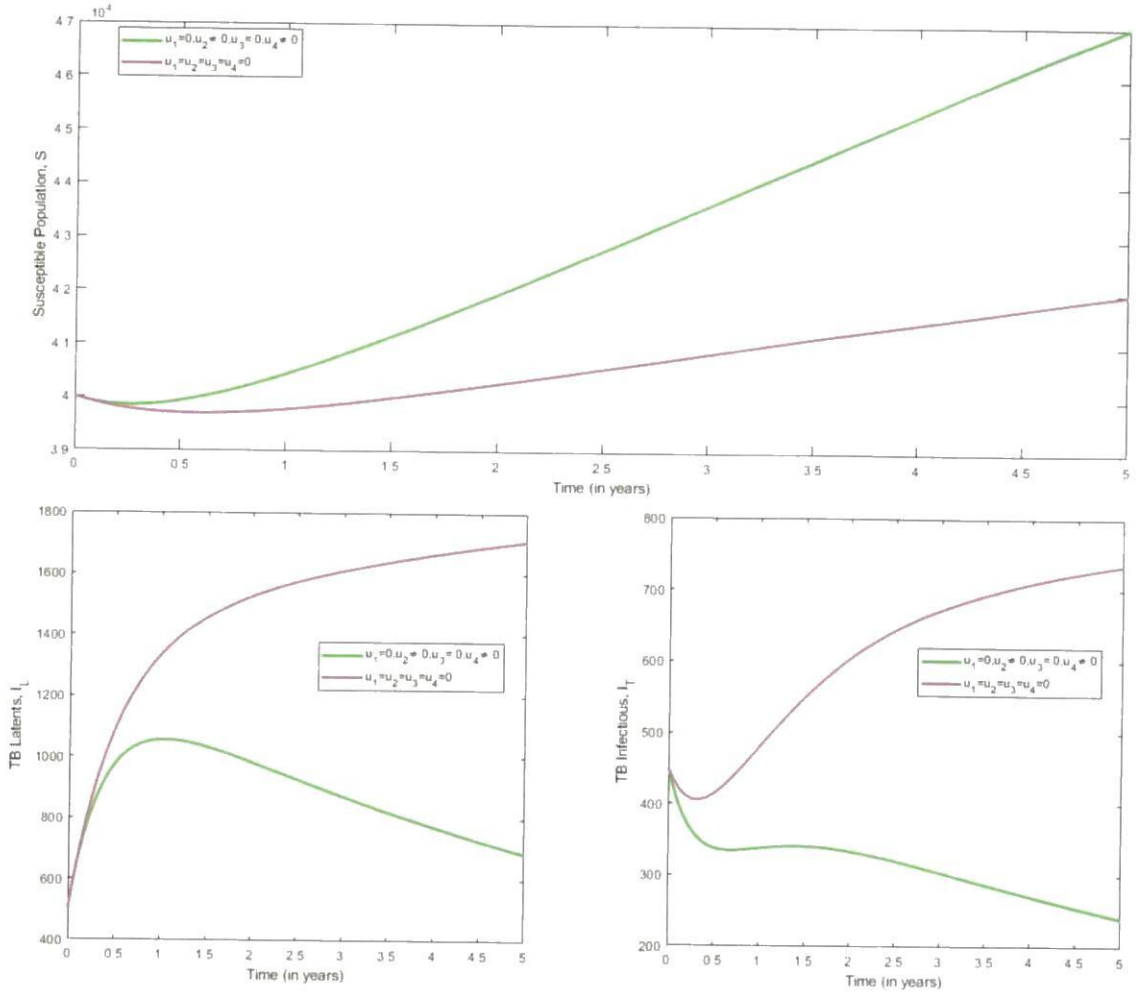

Figure 5.10: Effect of controls u_2 and u_4 on susceptible and TB infected populations.

5.3.4 Controls with Screen and Treat against TB and HCV

Figures 5.10, 5.11 and 5.12 show the impact of utilizing controls u_2 and u_4 in the control of TB-HC co-infection. Figure 5.10 shows an increase in the number of susceptible individuals and a gradu reduction of TB latent and infectious populations. Figure 5.11 portrays a gradual decrease in HC acute and chronic infected populations. There is a chance of drastically reducing the co-infectic burden if screening and early treatment of TB and HCV are implemented as seen in Figure 5.9.

5.3.5 Controls with Prevention against TB and HCV

Controls u_1 and u_3 are used in the dynamics of TB and HCV co-infection. Figure 5.13 show a increase in the number of susceptible individuals and a minimal decrease in the number of TB later and TB infectious individuals. There is also a minimal reduction in the number of HCV acute an chronically infected individuals as seen in Figure 5.14. Figure 5.15 also shows that the co-infecte individuals are always reducing. The minimal reduction in the number of infected and co-infecte

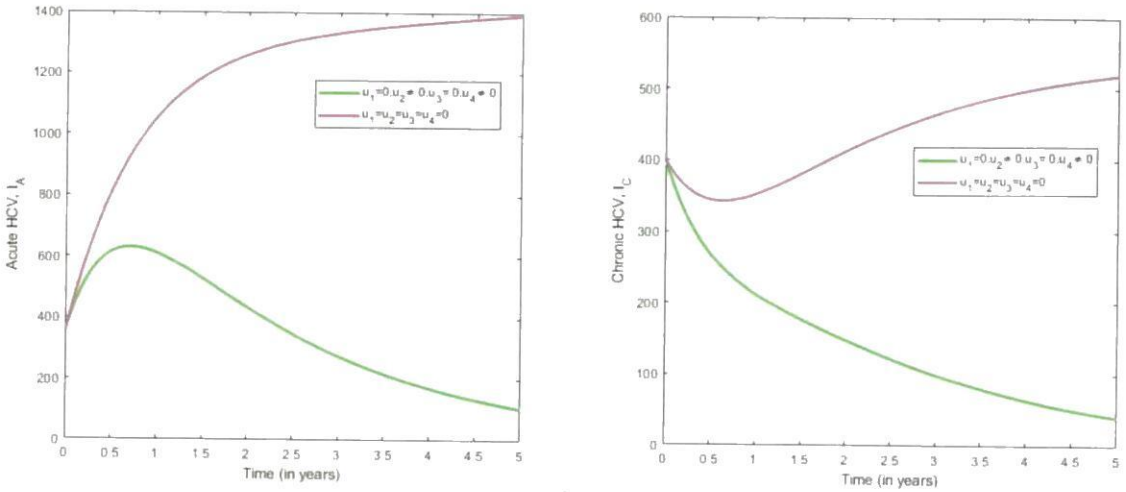

Figure 5.11: Effect of controls u_2 and u_4 on HCV infected populations.

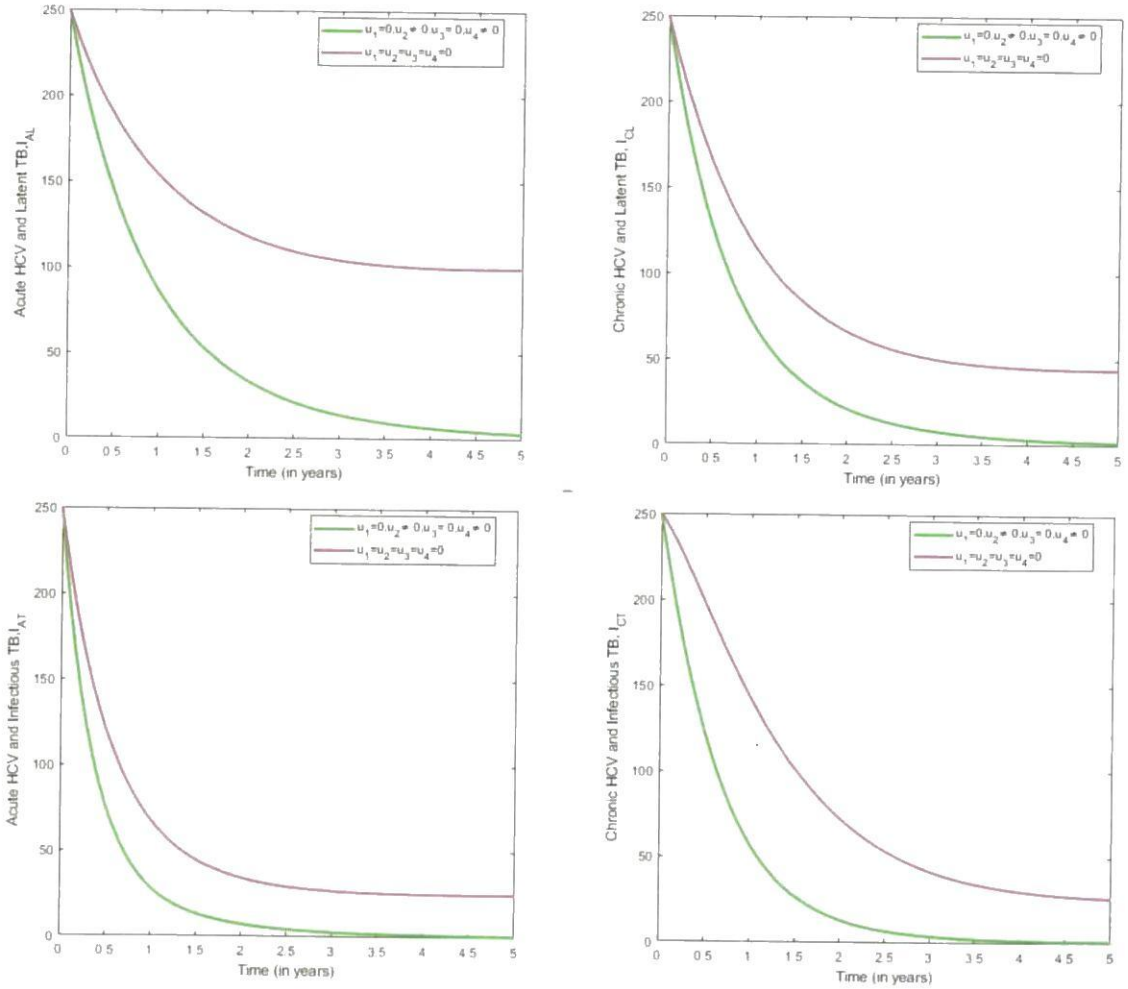

Figure 5.12: Effect of controls u_2 and u_4 on co-infected populations.

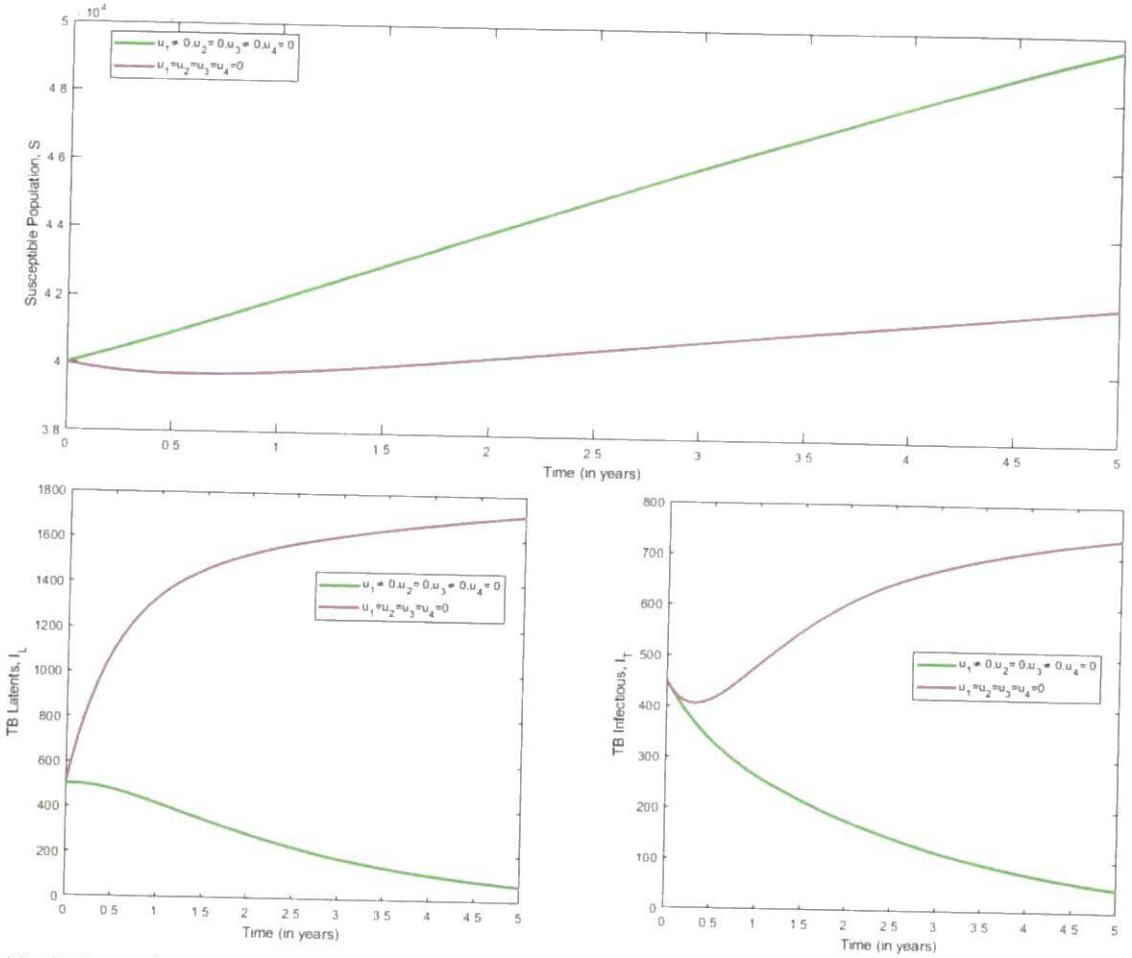

Figure 5.13: Effect of controls u_1 and u_3 on susceptible and TB infected populations.

individuals is because when u_1 and u_3 are applied, the strategy targets only the susceptible individua but not the existing infections. Diseases like TB remain latent for long time and thus prevention partially effective.

5.4 Discussion and Conclusion

The model system presented in Equation (4.3) of Chapter 4 was extended to incorporate time-depend control variables u_1, u_2, u_3 and u_4 as detailed in Section 5.2. The extended model was analyzed usin Pontryagin's Maximum Principle, leading to the derivation of the associated optimality system.

Simulation results based on the optimality system demonstrated the effectiveness of each propose control strategy in reducing the incidence of TB, HCV, and TB-HCV co-infection. Notably, th implementation of all the four control strategies concurrently yielded the most significant impact, witl potential to eliminate co-infection within approximately three years. This outcome underscore

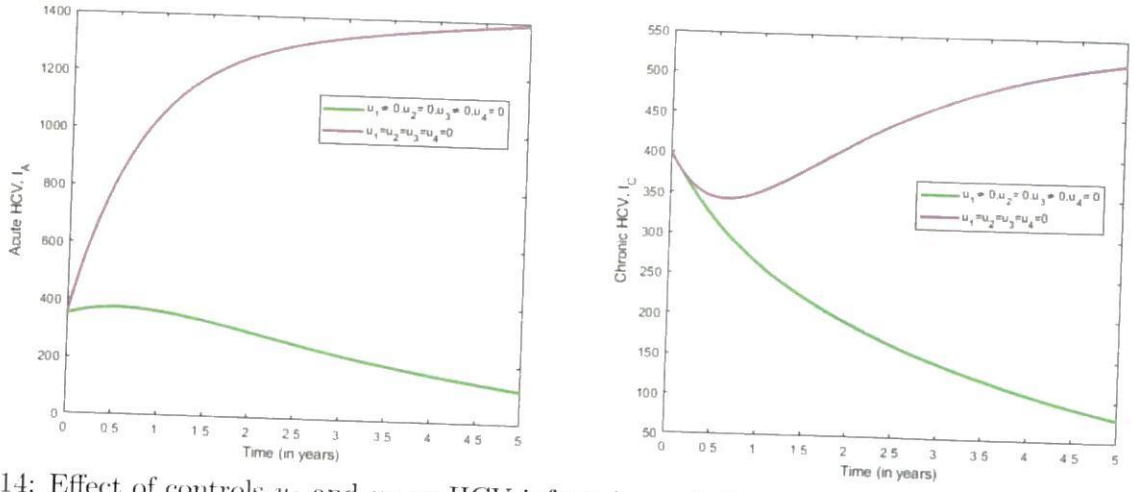

Figure 5.14: Effect of controls u_1 and u_3 on HCV infected populations.

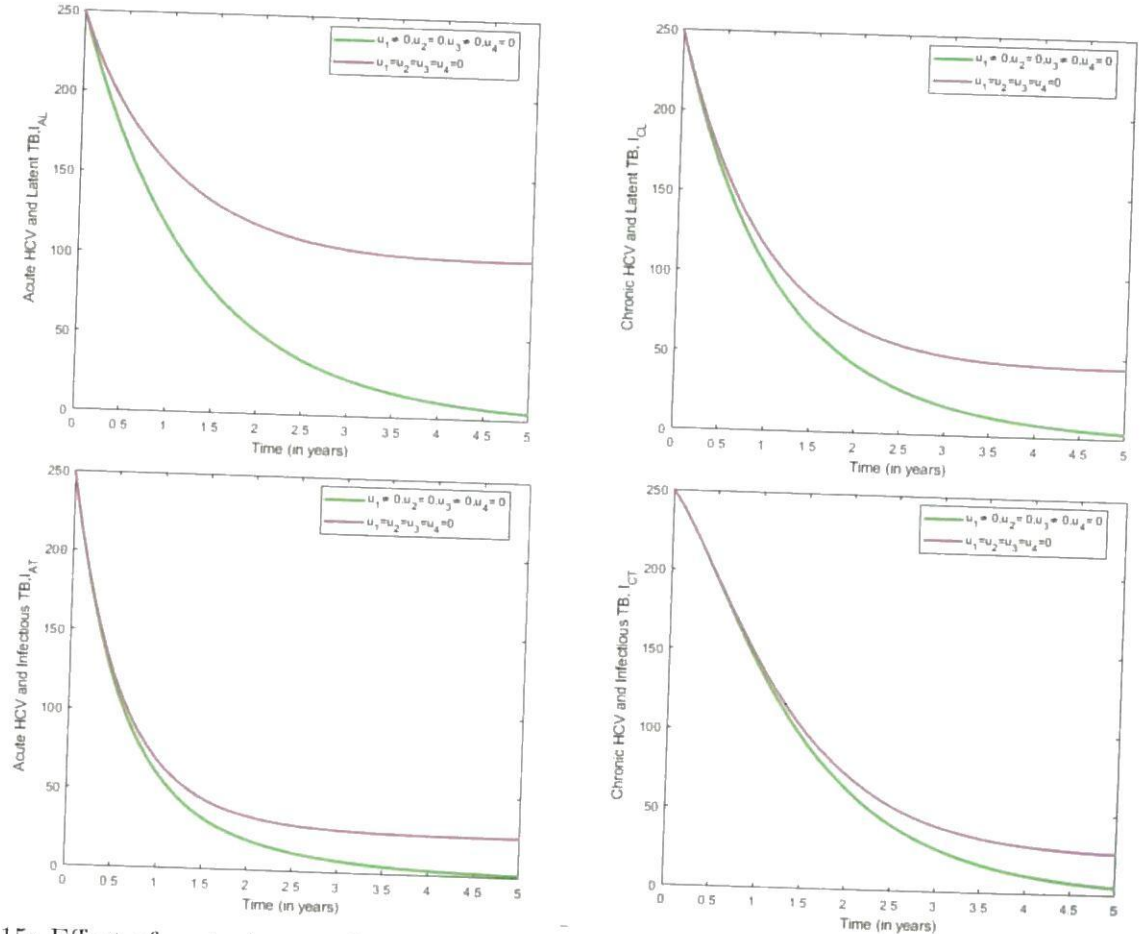

igure 5.15: Effect of controls u_1 and u_3 on co-infected populations.

the synergistic benefit of a comprehensive intervention approach.

Further, comparative analysis indicated that strategy C outperformed B and D because reducing HCV incidence and rapidly treating existing chronic cases substantially shrinks the pool of HCV-infecte individuals who can become coinfected with TB with projected co-infection elimination within 3.5 years. In the model, this dual approach lowers both new HCV infections and the chronic reservoir, producing a larger indirect reduction in TB–HCV coinfection than TB-focused strategies, which are limited by the persistence of latent TB and slower treatment impact. Additionally, if HCV infection accelerates progression to active TB in the model, then HCV control indirectly curtails TB transmission, further amplifying the benefit of Strategy C. Control strategies focused exclusively on TB and HCV prevention alone, though beneficial, were found to be less effective when applied in isolation, achieving slower reductions in infection prevalence.

These findings suggest that for a significant and sustained reduction of both mono-infections and co-infections, a multifaceted control strategy is essential. In light of this, it is recommended that public health systems prioritize integrated health education campaigns, promote widespread screening, and ensure timely treatment for both TB and HCV. Such coordinated efforts are crucial for moving toward the elimination of TB-HCV co-infection and improving overall population health outcomes.

Chapter 6

Discussion, Conclusion, Recommendations and Future Work

6.1 Discussion

Globally, TB and HCV pose a significant burden on health, accounting for considerable morbidity and mortality rates. TB primarily affects the respiratory system, causing lung damage, inflammation and scarring, but can also impact other body systems. If left untreated, TB can result in severe outcomes such as respiratory failure, heart failure, haemoptysis and pneumothorax. Untreated HCV can have dire consequences, including liver damage, cirrhosis, liver cancer and fatal outcomes. The lack of a vaccine underscores the importance of early detection and intervention. Although TB-HCV co-infection is a pressing global issue, it has not received adequate focus in resource-scarce countries like Uganda. TB-HCV co-infection severely impacts multiple body system, causing respiratory damage, liver cirrhosis, immunity suppression, gastrointestinal issues, cardiovascular disease and neurological problems [20, 21]. If left untreated, co-infection can lead to life-threatening complications, including liver cancer, respiratory failure, cardiac arrest, sepsis and multi-organ failure, thus, the need for early diagnosis and integrated care. In this study, we formulated and analysed mathematical models for the TB-HCV co-infection so as to find the conditions for the disease control; determine the synergistic effects of dual therapy on TB-HCV co-infection progression; and investigate the optimal strategy in management of TB-HCV co-infection.

6.1.1 TB-HCV Co-infection Dynamics with no Intervention

The study presented in Chapter 3 focused on modelling the progression of TB-HCV co-infection in the absence of intervention strategies. A compartmental model was developed, and preliminary analysis confirmed that the model was biologically meaningful and mathematically well-posed. To facilitate analysis, the overall model was decomposed into two sub models: the TB-only sub model and the HCV-only sub model.

For the TB-only sub model, equilibrium points were derived, and the basic reproduction number, R_T, was computed. It was established that the TB-free equilibrium is both locally and globally asymptotically stable when $R_T < 1$, indicating the eventual elimination of the disease in such scenarios. Conversely, the TB-endemic equilibrium was found to be both locally and globally stable when $R_T > 1$, signifying persistent transmission within the population under those conditions.

Similarly, analysis of the HCV-only sub model yielded the equilibrium points and its basic reproduction number R_H. The stability of the disease-free and endemic equilibria for HCV was determined based on the value of R_H. These findings collectively highlighted that the co-infection dynamics are inherently dependent on the behavior of the individual sub models.

A key outcome of the study was the derivation of the basic reproduction number for the full TB-HCV co-infection model, R_0. It was shown that $R_0 = \max\{R_T, R_H\}$, reflecting the dominance of the more transmissible infection in driving the co-infection dynamics. As demonstrated in Subsection 3.3.3, TB was found to play a dominant role in the absence of intervention, primarily due to its higher basic reproduction number. The analysis further suggested that, in a fully susceptible population, a TB-HCV co-infected individual generates the same number of secondary TB cases as an individual infected with TB alone, underscoring the independence of TB transmission from HCV co-infection.

Moreover, the local and global stability of the co-infection-free equilibrium were analytically established under the condition $R_0 < 1$, which implies that both $R_T < 1$ and $R_H < 1$. Numerical simulations were employed to examine the behavior of the endemic equilibrium, revealing that, regardless of initial population distributions, the system's trajectories converged to a unique endemic state, indicating its global stability.

Sensitivity analysis was conducted to identify parameters that significantly influence R_0. The results indicated that R_0 is most sensitive to the rate of human-to-human contact involving TB-infected individuals and the susceptible population, the probability of transmission upon contact, and the rate at which individuals progress from latent TB to active TB. These findings mirror the sensitivity structure observed in the TB-only sub-model. Additionally, it was found that the rate of contact and transmission probability between infected and susceptible individuals were equally influential in both TB and HCV transmission dynamics. As detailed in Subsection 3.3.3, variations in these parameters had the most substantial effect on the amplification of TB and HCV infections, reinforcing their critical role in disease spread.

6.1.2 TB-HCV Co-infection Dynamics with Medication

The primary objective of Chapter 4 was to investigate the synergistic effects of dual therapy on the progression of TB-HCV co-infection through a mathematical modelling framework. A compartmental model was developed and its basic properties analyzed, confirming that the model is biologically well-posed and mathematically meaningful. To facilitate analytical tractability, the full model was decomposed into two sub models: a TB-only sub model and an HCV-only sub model.

For the TB-only sub model, the disease-free and endemic equilibria were derived, and the corresponding effective reproduction number, R_{TB}, was obtained. Stability analysis revealed that the TB-free equilibrium is both locally and globally asymptotically stable when $R_{TB} < 1$, while the endemic equilibrium is locally and globally stable for $R_{TB} > 1$. A similar analysis was carried out for the HCV-only sub model, where the equilibrium points and the associated effective reproduction number, R_{HCV}, were determined. The stability of the HCV equilibria was likewise governed by the threshold condition $R_{HCV} < 1$ and $R_{HCV} > 1$.

The analysis of the individual sub models demonstrated that the overall dynamics of the co-infection model are intrinsically linked to the dynamics of the constituent sub models. In particular, it was shown that the effective reproduction number for the full TB-HCV co-infection model, R_{TH}, is given by $R_{TH} = \max\{R_{TB}, R_{HCV}\}$. This result implies that for the co-infection-free equilibrium to be locally and globally stable, both R_{TB} and R_{HCV} must be less than one.

Furthermore, the global stability of the co-infection-free equilibrium was established under the

condition $R_{TH} < 1$, confirming the eradication of both infections in this regime. The stability of the endemic equilibrium was investigated numerically, and simulations indicated that regardless of initial population conditions, all solution trajectories converge to the same endemic equilibrium point. This suggests a globally attracting endemic state when $R_{TH} > 1$, thereby underscoring the importance of reducing both reproduction numbers below unity to control the co-infection dynamics effectively. The results in subsection 3.3.3 indicate that, despite treatment for both diseases, TB remains the dominant factor in the dynamics of TB-HCV co-infection as observed in Chapter 3.

From sensitivity analysis, it was deduced that TB (or HCV) rate of human-to-human contact between the infected individuals and susceptible population and the likelihood of a contact resulting in TB (or HCV) transmission are equally likely to result into increased TB (or HCV) infections. An increase in the values of these parameters contributes to a rise in TB (or HCV) infections through a corresponding increase in other related parameters, just like in Chapter 3 when there was no intervention.

Numerical simulation results unequivocally reveal that over time, increasing the TB treatment rate, HCV treatment rate, hospitalization rate and the rates at which individuals in co-infected classes are identified and put on TB and HCV treatment, can reduce the prevalence of TB-HCV co-infection. These findings are consistent with statistical evidence reported in earlier studies [20, 40, 65, 80]. However, treatment alone without behavioural changes and public health interventions may not lead to optimal outcomes in controlling TB-HCV co-infection.

6.1.3 Optimal Control Management Strategy for TB-HCV Co-infection

The mathematical model in Chapter 4 was extended to incorporate time-dependent control functions: u_1 representing TB prevention measures, u_2 targeting the identification and management of individuals exposed to or infected with TB, u_3 for reducing the risk of HCV transmission, and u_4 for the identification and treatment of HCV-infected individuals. The resulting optimal control model was analyzed to establish the existence of optimal control solutions. This was achieved by verifying the standard conditions required for existence, including the boundedness and measurability of the control set, the Lipschitz continuity of the state system, and the convexity of the integrand in the objective functional with respect to control variables. Furthermore, the characterization of the optimal controls was derived using Pontryagin's Maximum Principle, which provided necessary conditions for optimality in the form of adjoint equations and associated transversality conditions.

Simulation results presented in Section 5.3 demonstrated that the implementation of each individual control strategy significantly contributed to reducing the burden of TB-HCV co-infection. However, the combined implementation of all the four strategies produced the most pronounced impact on controlling the dual epidemic. Notably, the simulations suggested the potential for achieving a co-infection-free population under the full implementation of all control measures, as depicted in Figure 5.3 of Section 5.3. These findings underscore the importance of an integrated public health response, including interventions such as comprehensive health education campaigns, routine screening and isolation of infectious TB cases, the use of masks by TB-infectious individuals, and preventive measures for HCV transmission such as sterilization of surgical equipment, consistent condom use, and prompt treatment of HCV-infected persons.

6.2 Conclusion

In Chapter 3, the study developed a compartmental model to examine the progression of TB-HCV co-infection without interventions. The model, shown to be mathematically sound, was decomposed into TB-only and HCV-only sub-models to facilitate analysis. For each sub-model, equilibrium points and basic reproduction numbers (R_T and R_H) were derived, with stability analyses confirming disease elimination when reproduction numbers are below one, and persistence when they exceed one.

The co-infection model's basic reproduction number was determined as $R_0 = \max\{R_T, R_H\}$, indicating that the more transmissible infection drives the overall dynamics. TB emerged as the dominant force due to its higher R_T, and its transmission was shown to be independent of HCV co-infection. The co-infection-free equilibrium was proven to be globally stable when both $R_T < 1$ and $R_H < 1$, while simulations confirmed the unique global stability of the endemic equilibrium when $R_0 > 1$.

Sensitivity analysis revealed that R_0 is most influenced by TB-related transmission and progression parameters, aligning with the findings of the TB-only model. These results underscore the critical role of TB in co-infection dynamics and highlight key parameters for targeted disease control.

Chapter 4 investigated the synergistic dynamics of TB-HCV co-infection using a compartmental mathematical model. By decomposing the full model into TB-only and HCV-only sub-models, the

analysis confirmed that the overall dynamics are governed by the effective reproduction numbers of the individual infections, with the threshold condition for disease eradication given by $R_{TH} = \max\{R_{TB}, R_{HCV}\} < 1$. Stability analyses demonstrated that the co-infection-free equilibrium is globally stable when both R_{TB} and R_{HCV} are below unity, while the system converges to a unique endemic state when $R_{TH} > 1$.

Sensitivity analysis identified key parameters driving the transmission of both infections, particularly contact rates and transmission probabilities. Numerical simulations revealed that increasing treatment and intervention rates can significantly reduce co-infection prevalence. However, treatment alone is insufficient, behavioral and public health strategies are essential for optimal control.

Chapter 5 analyzed an optimal control model addressing the co-dynamics of TB and HCV, incorporating four time-dependent intervention strategies. The existence of optimal solutions was established using standard mathematical criteria, and optimal controls were characterized via Pontryagin's Maximum Principle.

Simulation results demonstrated that while each control measure individually reduces the burden of TB-HCV co-infection, their combined implementation yields the most significant impact, with the potential to eliminate co-infection entirely. These findings emphasize the necessity of integrated public health strategies combining prevention, early detection, and treatment to effectively control and potentially eradicate TB-HCV co-infection.

This study presents a comprehensive mathematical investigation into the dynamics of tuberculosis (TB) and hepatitis C virus (HCV) co-infection, a growing public health concern in many parts of the world. By formulating and analyzing a deterministic compartmental model, the research captures the transmission mechanisms, progression, and interaction between the two infections within a population. The study examines the model's theoretical properties, including positivity, boundedness, and stability of equilibria, and explores the impact of key epidemiological parameters through numerical simulations. The findings reveal that co-infection significantly increases the disease burden and that isolated control measures are insufficient for effective management. As such, the research emphasizes the need for integrated intervention strategies, early detection, and combined treatment approaches. This work not only advances the mathematical understanding of

TB-HCV co-infection but also provides valuable guidance for public health policy and future research in infectious disease modelling.

6.3 Recommendations

The results of this research inform the following suggested strategies:
A comprehensive approach to raise public awareness about TB and HCV is necessary, incorporating information campaigns, educational seminars, and mass media engagement. Regular community sensitization programmes should be implemented to educate individuals on the transmission modes of TB and HCV, and provide guidance on prevention strategies and behavioural changes to reduce the disease transmission and promote overall well-being.

For instance, people can be educated on TB prevention strategies by promoting good hygiene practices, such as covering the mouth when coughing, wearing of a face mask when infected with TB, avoiding close contact with infected individuals and ensuring good ventilation. Additionally, encouraging people to get tested for TB, especially if they have symptoms or have been exposed to someone with TB, can help them prevent transmission. Healthcare providers should also be trained to provide accurate information and testing services.

To prevent HCV transmission, people should be educated on the risks associated with sharing needles, syringes, and other equipment. Promoting safe injection practices, providing access to clean needles and syringes, and encouraging testing for HCV can help reduce transmission. Furthermore, raising awareness about the importance of proper infection control practices in healthcare settings can also help prevent HCV transmission.

It is crucial to encourage individuals infected with TB and HCV to seek medical attention early and comply with treatment guidelines to ensure effective management of the diseases. As a result, the progression of latent TB to infectious TB and acute HCV to chronic HCV will be slowed, and the individuals' ability to spread the diseases will be diminished.

To address the significant global morbidity and mortality associated with HCV, resource-constrained countries like Uganda must allocate equitable priority to HCV, comparable to that given to TB.

ICV testing and treatment should be made a regular practice, mirroring the standard procedures or TB. Dedicating resources and programmes specifically to HCV will allow tackling the disease ıore effectively. To make HCV screening and treatment more accessible, these countries should seek ut affordable options and consider seeking assistance from the international community, including eveloped countries and global health organisation.

'ountries should also strengthen their healthcare systems to effectively manage TB and HCV. This an be achieved by training healthcare workers, improving diagnostic facilities, and ensuring a steady ıpply of medications.

'urthermore, governments and international organizations should support research and development f new diagnostic tools, treatments, and vaccines for HCV and TB. This can help improve treatment utcomes, reduce costs, and increase access to care. Collaboration between governments, civil society, nd private sector is crucial to achieving these goals and ultimately controlling the spread of TB and ICV.

5.4 Future Work

ı this research, significant progress has been made in understanding the dynamics of TB-HCV o-infection. However, several research gaps remain. Therefore, future studies should focus on ddressing these gaps to inform the development of effective and sustainable control strategies.

'eveloping a model that evaluates the cost-effectiveness of different treatment strategies for TB-HCV o-infection. This model could incorporate parameters such as treatment costs, healthcare system osts, patient outcomes, and quality of life. The model could help policymakers and healthcare ecision-makers determine the most cost-effective treatment strategies for TB-HCV co-infection.

nalysing a model that incorporates time delays in the treatment process, such as delays in diagnosis, 'eatment initiation, and treatment completion. This model could help researchers understand how me delays affect treatment outcomes and how to optimize treatment strategies to minimize the npact of time delays.

Formulating a model that simulates the impact of liver disease on TB-HCV co-infection treatment outcomes. This model could help researchers understand how liver disease affects the treatment outcomes of TB-HCV co-infection and how to optimize treatment strategies for individuals with liver disease.

The parameter values utilized in simulating the models developed in this study are grounded in existing literature. A potential direction for future research is to validate these models by fitting their simulations to empirical data. This would enable a comparative analysis between the deterministic model results and real-world data, providing a more comprehensive understanding of TB-HCV dynamics.

Bibliography

[1] He, S., Lin, B., Chu, V., Hu, Z., Hu, X., Xiao, J., ... & Liang, T. J. (2015). Repurposing of the antihistamine chlorcyclizine and related compounds for treatment of hepatitis C virus infection. *Science translational medicine*, 7(282), 282ra49-282ra49.

[2] Dhiman, R. K. (2014). Future of therapy for Hepatitis C in India: A Matter of Accessibility and Affordability. *Journal of clinical and experimental hepatology*, 4(2), 85-86.

[3] Ekstedt, M., Franzén, L. E., Mathiesen, U. L., Thorelius, L., Holmqvist, M., Bodemar, G., & Kechagias, S. (2006). Long-term follow-up of patients with NAFLD and elevated liver enzymes. *Hepatology*, 44(4), 865-873.

[4] Choo, Q. L., Kuo, G., Weiner, A. J., Overby, L. R., Bradley, D. W., & Houghton, M. (1989). Isolation of a cDNA clone derived from a blood-borne non-A, non-B viral hepatitis genome. *Science*, 244(4902), 359-362.

[5] World Health Organisation. (2013). Global policy report on the prevention and control of viral hepatitis in WHO Member States.

[6] Onyekwere, C. A., & Hameed, L. (2015). Hepatitis B and C virus prevalence and association with demographics: report of population screening in Nigeria. *Tropical doctor*, 45(4), 231-235.

[7] Negro, F., & Alberti, A. (2011). The global health burden of hepatitis C virus infection. *Liver International*, 31, 1-3.

[8] Munir, S., Saleem, S., Idrees, M., Tariq, A., Butt, S., Rauff, B., ... & Awan, Z. (2010). Hepatitis C treatment: current and future perspectives. *Virology journal*, 7(1), 1-6.

[9] Gretch, D. R. (1997). Diagnostic tests for hepatitis C. *Hepatology*, 26(S3), 43S-47S.

[10] Castillo, I., Bartolomé, J., Quiroga, J. A., Barril, G., & Carreño, V. (2010). Diagnosis of occult hepatitis C without the need for a liver biopsy. *Journal of medical virology*, 82(9), 1554-1559.

[11] Raja, N. S., & Janjua, K. A. (2008). Epidemiology of hepatitis C virus infection in Pakistan. *Journal of microbiology, immunology, and infection= Wei mian yu gan ran za zhi*, 41(1), 4-8.

[12] Khokhar, N., Gill, M. L., & Malik, G. J. (2004). General seroprevalence of hepatitis C and hepatitis B virus infections in population. *Journal of the College of Physicians and Surgeons–pakistan*: JCPSP, 14(9), 534-536.

[13] Kiyosawa, K., Sodeyama, T., Tanaka, E., Nakano, Y., Furuta, S., Nishioka, K., ... & Alter, H. J. (1991). Hepatitis C in hospital employees with needlestick injuries. *Annals of internal medicine*, 115(5), 367-369.

[14] Jumbo, J., Obaseki, D. O., & Ikuabe, P. O. (2013). Tuberculosis and gender parity in a TB Referral Centre, South–South Nigeria. *Greener Journal of Medical Sciences*, 3(7), 270-275.

[15] Pan, R., Silva, M. T. R., Fidelis, T. L. N., Vilela, L. S., Silveira-Monteiro, C. A., & Nascimento, L. C. (2018). Knowledge of health professionals concerning initial in-hospital care for burn victims. *Revista Gaúcha de Enfermagem*, 39.

[16] Tchuenche, J. M., Dube, N., Bhunu, C. P., Smith, R. J., & Bauch, C. T. (2011). The impact of media coverage on the transmission dynamics of human influenza. *BMC public health*, 11(1), 1-14.

[17] World Health Organization. (2015). Tuberculosis Fact sheet N 104. 2015. *Avaialble at http://www. who. int/mediacentre/factsheets/fs104/en.*

[18] World Health Organization. (2005). Addressing poverty in TB control: options for national TB control programmes. World Health Organization.

[19] Bhatt, C. P., Bhatt, A. B., & Shrestha, B. (2009). Nepalese People's knowledge about Tuberculosis. *SAARC Journal of Tuberculosis, Lung Diseases and HIV/AIDS*, 6(2), 31-37.

[20] Lomtadze, N., Kupreishvili, L., Salakaia, A., Vashakidze, S., Sharvadze, L., Kempker, R. R., ... & Blumberg, H. M. (2013). Hepatitis C virus co-infection increases the risk of anti-tuberculosis drug-induced hepatotoxicity among patients with pulmonary tuberculosis. *PLoS One*, 8(12), e83892.

[21] Yee, D., Valiquette, C., Pelletier, M., Parisien, I., Rocher, I., & Menzies, D. (2003). Incidence of serious side effects from first-line antituberculosis drugs among patients treated for active tuberculosis. *American journal of respiratory and critical care medicine*, 167(11), 1472-1477.

[22] Neumann, A. U., Lam, N. P., Dahari, H., Gretch, D. R., Wiley, T. E., Layden, T. J., & Perelson, A. S. (1998). Hepatitis C viral dynamics in vivo and the antiviral efficacy of interferon -α therapy. *Science*, 282(5386), 103-107.

[23] Dahari, H., Lo, A., Ribeiro, R. M., & Perelson, A. S. (2007). Modeling hepatitis C virus dynamics: Liver regeneration and critical drug efficacy. *Journal of theoretical biology*, 247(2), 371-381.

[24] Khan, A., Sial, S., & Imran, M. (2014). Transmission dynamics of hepatitis C with control strategies. *Journal of Computational Medicine*, 2014.

[25] Okosun, K. O., & Makinde, O. D. (2014). Optimal control analysis of hepatitis C virus with acute and chronic stages in the presence of treatment and infected immigrants. *International journal of Biomathematics*, 7(02), 1450019.

[26] Waaler, H., Geser, A., & Andersen, S. (1962). The use of mathematical models in the study of the epidemiology of tuberculosis. *American Journal of Public Health and the Nations Health*, 52(6), 1002-1013.

[27] Trauer, J. M., Denholm, J. T., & McBryde, E. S. (2014). Construction of a mathematical model for tuberculosis transmission in highly endemic regions of the Asia-Pacific. *Journal of theoretical biology*, 358, 74-84.

[28] Castillo-Chavez, C., & Feng, Z. (1998). Global stability of an age-structure model for TB and its applications to optimal vaccination strategies. *Mathematical biosciences*, 151(2), 135-154.

[29] Kasereka Kabunga, S., Doungmo Goufo, E. F., & Ho Tuong, V. (2020). Analysis and simulation of a mathematical model of tuberculosis transmission in Democratic Republic of the Congo. *Advances in Difference Equations*, 2020(1), 1-19.

[30] Ayobami, S. L. (2020). Mathematical Modelling of Spread and Control of the Hepatitis C Virus. *International Journal of Science and Research (IJSR)* ISSN: 2319-7064 SJIF (2022): 7.942

[31] Behzadifar, M., Behzadifar, M., & Bragazzi, N. L. (2020). A systematic review and meta-analysis of the prevalence of hepatitis C virus infection in people who inject drugs in Iran. *BMC Public Health*, 20, 1-12.

[32] El-Mokhtar, M. A., Elgendy, S. G., Eldin, A. S., Hassan, E. A., Hasan, A. A. A., Abdel Hameed M. R., ... & Salama, E. H. (2020). Hepatitis C virus affects tuberculosis-specific T cells i HIV-negative patients. *Viruses*, 12(1), 101.

[33] Mengistu, A. K., & Witbooi, P. J. (2020, December). Mathematical analysis of TB model wit vaccination and saturated incidence rate. *In Abstract and Applied Analysis* (Vol. 2020). Hindaw

[34] Witbooi, P. J., & Mengistu, A. K. (2020). Mathematical analysis of TB model with vaccinatio and saturated incidence rate.

[35] Van den Driessche, P., & Watmough, J. (2002). Reproduction numbers and sub-threshol endemic equilibria for compartmental models of disease transmission. *Mathematical Bioscience.* 180(1), 29-48.

[36] Pontryagin, L. S. (1987). Mathematical theory of optimal processes. CRC press.

[37] da Costa, A. L. P., Neto, O. A. R., & Silva-Júnior, A. C. S. (2019). Conditioners of the infectiou diseases dynamics. *Estação Científica (UNIFAP)*, 8(3), 09-23.

[38] Wang, Z., Andrews, M. A., Wu, Z. X., Wang, L., & Bauch, C. T. (2015). Couple disease–behavior dynamics on complex networks: A review. *Physics of life reviews*, 15, 1-29.

[39] Fauci, A. S. (2001). Infectious diseases: considerations for the 21st century. *Clinical Infectiou Diseases*, 32(5), 675-685.

[40] Wu, T., Perrings, C., Kinzig, A., Collins, J. P., Minteer, B. A., & Daszak, P. (2017). Economi growth, urbanization, globalization, and the risks of emerging infectious diseases in China: A review. *Ambio*, 46(1), 18-29.

[41] Wu, P. H., Lin, Y. T., Hsieh, K. P., Chuang, H. Y., & Sheu, C. C. (2015). Hepatitis C virus infection is associated with an increased risk of active tuberculosis disease: a nationwid population-based study. *Medicine*, 94(33).

[42] Ungo, J. R., Jones, D., Ashkin, D., Hollender, E. S., Bernstein, D., Albanese, A. P., & Pitchenik A. E. (1998). Antituberculosis drug–induced hepatotoxicity: the role of hepatitis C virus anc the human immunodeficiency virus. *American journal of respiratory and critical care medicine* 157(6), 1871-1876.

[43] Gao, D. P., & Huang, N. J. (2018). Optimal control analysis of a tuberculosis model. *Applied Mathematical Modelling*, 58, 47-64.

[44] Kereyu, D., & Demie, S. (2021). Transmission dynamics model of Tuberculosis with optimal control strategies in Haramaya district, Ethiopia. *Advances in Difference Equations*, 2021(1), 1-22.

[45] Zhang, S., & Xu, X. (2017). Dynamic analysis and optimal control for a model of hepatitis C with treatment. *Communications in Nonlinear Science and Numerical Simulation*, 46, 14-25.

[46] Lienhardt, C. (2001). From exposure to disease: the role of environmental factors in susceptibility to and development of tuberculosis. *Epidemiologic reviews*, 23(2), 288-301.

[47] Jung, E., Lenhart, S., & Feng, Z. (2002). Optimal control of treatments in a two-strain tuberculosis model. *Discrete and Continuous Dynamical Systems Series B*, 2(4), 473-482.

[48] Nampala, H., Luboobi, L. S., Mugisha, J. Y., Obua, C., & Jablonska-Sabuka, M. (2018). Modelling hepatotoxicity and antiretroviral therapeutic effect in HIV/HBV coinfection. *Mathematical biosciences*, 302, 67-79.

[49] Bowong, S., & Kurths, J. (2010). Modelling tuberculosis and hepatitis b co-infections. *Mathematical Modelling of Natural Phenomena*, 5(6), 196-242.

[50] Gurmu, E. D., Bole, B. K., & Koya, P. R. (2020). Mathematical model for co-infection of HPV with cervical cancer and HIV with AIDS diseases. *International journal of scientific research in mathematical and statistical sciences*, 7(2).

[51] Bhunu, C. P., Garira, W., & Mukandavire, Z. (2009). Modeling HIV/AIDS and tuberculosis coinfection. *Bulletin of mathematical biology*, 71(7), 1745.

[52] Sanga, G. G., Makinde, O. D., Massawe, E. S., & Namkinga, L. (2017). Modeling co-dynamics of cervical cancer and HIV diseases. *Global journal of pure and applied mathematics*, 13(6), 2057-2078.

[53] Carvalho, A. R., & Pinto, C. M. (2014). A coinfection model for HIV and HCV. Biosystems, 124, 46-60.

[54] Mayanja, E., Luboobi, L. S., Kasozi, J., & Nsubuga, R. N. (2020). Mathematical modelling HIV-HCV coinfection dynamics in absence of therapy. *Computational and Mathematical metho in Medicine*, 2020.

[55] Nannyonga, B., Mugisha, J. Y. T., & Luboobi, L. S. (2011). The role of HIV positive immigran and dual protection in a co-infection of malaria and HIV/AIDS. *Applied Mathematical Science* 5(59), 2919-2942.

[56] Bhunu, C. P., & Mushayabasa, S. (2013). Modelling the transmission dynamics of HIV/AID and hepatitis C virus co-infection. *HIV & AIDS Review*, 12(2), 37-42.

[57] Ronoh, M., Jaroudi, R., Fotso, P., Kamdoum, V., Matendechere, N., Wairimu, J., ... & Lugoye, J (2016). A mathematical model of tuberculosis with drug resistance effects. *Applied Mathematics* 7(12), 1303-1316.

[58] Shi, R., & Cui, Y. (2016). Global analysis of a mathematical model for Hepatitis C virus transmissions. *Virus Research*, 217, 8-17.

[59] Zhang, J., Li, Y., & Zhang, X. (2015). Mathematical modeling of tuberculosis data of China. *Journal of theoretical biology*, 365, 159-163.

[60] Chen, S. L., & Morgan, T. R. (2006). The natural history of hepatitis C virus (HCV) infection. *International journal of medical sciences*, 3(2), 47.

[61] Zumla, A., George, A., Sharma, V., Herbert, R. H. N., Oxley, A., & Oliver, M. (2015). The WHO 2014 global tuberculosis report—further to go. *The Lancet Global Health*, 3(1), e10-e12.

[62] Karimi, S. E., Bayani, A., Higgs, P., Bayat, A. H., Hemmat, M., Ahounbar, E., ... & Fakhri, Y. (2020). Prevalence and high-risk behaviours associated with HCV testing among people who inject drugs: a systematic review and Meta-analysis. *Substance Abuse Treatment, Prevention, and Policy*, 15(1), 1-16.

[63] Diekmann, O., Heesterbeek. J. A. P., & Metz. J. A. (1990). On the definition and the computation of the basic reproduction ratio R_0 in models for infectious diseases in heterogeneous populations. *Journal of Mathematical Biology*, 28(4), 365-382.

[64] Elbasha, Elamin H., and Abba B. Gumel. "Theoretical assessment of public health impact of imperfect prophylactic HIV-1 vaccines with therapeutic benefits." *Bulletin of mathematical biology* 68.3 (2006): 577.

[65] Olaru, I. D., Meier, M. B., Mirzayev, F., Prodanovic, N., Kitchen, P. J., Schumacher, S. G., & Denkinger, C. M. (2023). Global prevalence of hepatitis B or hepatitis C infection among patients with tuberculosis disease: systematic review and meta-analysis. *Eclinicalmedicine*, 58.

[66] World Health Organization. (2022). Global tuberculosis report 2022. In *Global tuberculosis report 2022*.

[67] Chitnis, N., Hyman, J. M., & Cushing, J. M. (2008). Determining important parameters in the spread of malaria through the sensitivity analysis of a mathematical model. *Bulletin of Mathematical Biology*, 70(5), 1272-1296.

[68] World Health Organization. (2016). *Guidelines for the screening care and treatment of persons with chronic hepatitis C infection updated version April 2016: guidelines*. World Health Organization.

[69] Feng, Z., Castillo-Chavez, C., & Capurro, A. F. (2000). A model for tuberculosis with exogenous reinfection. *Theoretical population biology*, 57(3), 235-247.

[70] Cai, Z., Fan, J., & Li, R. (2000). Efficient estimation and inferences for varying-coefficient models. *Journal of the American Statistical Association*, 95(451), 888-902.

[71] LaSalle, J. P. (1976). The stability of dynamical systems, Regional Conference Series in Applied Mathematics, Society for Industrial and Applied Mathematics. *American Naturalist*, 110, 79-99.

[72] F. R. Gantmacher, "The theory of matrices," Chelsea Publishing Company, New York,1959

[73] Gao, D. P., & Huang, N. J. (2018). Optimal control analysis of a tuberculosis model. *Applied Mathematical Modelling*, 58, 47-64.

[74] Okosun, K. O., & Makinde, O. D. (2014). Optimal control analysis of hepatitis C virus with acute and chronic stages in the presence of treatment and infected immigrants. *International journal of Biomathematics*, 7(02), 1450019.

[75] Jung, E., Lenhart, S., & Feng, Z. (2002). Optimal control of treatments in a two-strain tuberculosis model. *Discrete and Continuous Dynamical Systems Series B*, 2(4), 473-482.

[76] Castillo-Chavez, C. (2002). ON THE COMPUTATION OF R. AND ITS ROLE ON GLOBAL STABILITY CARLOS CASTILLO-CHAVEZ*, ZHILAN FENG, AND WENZHANG HUANG.

Mathematical approaches for emerging and reemerging infectious diseases: an introduction, 1, 229.

[77] Kizito, M., & Tumwiine, J. (2018). A mathematical model of treatment and vaccination interventions of pneumococcal pneumonia infection dynamics. *Journal of Applied Mathematics*, 2018.

[78] Liu, J., & Zhang, T. (2011). Global stability for a tuberculosis model. *Mathematical and Computer Modelling*, 54(1-2), 836-845.

[79] Nino, C., Rukhadze, N., Svanidze, M., Sharvadze, L., Dehovitz, J. A., Tsertsvadze, T., ... & Del Rio, C. (2014). Evaluation of multiple measures of antiretroviral adherence in the Eastern European country of Georgia. *African Journal of Reproduction and Gynaecological Endoscopy*, 17(1).

[80] Meysam, B., Heydarvand, S., Behzadifar, M., & Bragazzi, N. L. (2019). Prevalence of hepatitis C virus in tuberculosis patients: a systematic review and meta-analysis. *Ethiopian journal of health sciences*, 29(1).

[81] Liao, C. M., Lin, Y. J., & Cheng, Y. H. (2013). Modeling the impact of control measures on tuberculosis infection in senior care facilities. *Building and environment*, 59, 66-75.

[82] Ai, J. W., Ruan, Q. L., Liu, Q. H., & Zhang, W. H. (2016). Updates on the risk factors for latent tuberculosis reactivation and their managements. *Emerging microbes & infections*, 5(1), 1-8.

[83] Zhang, S., & Xu, X. (2017). Dynamic analysis and optimal control for a model of hepatitis C with treatment. *Communications in Nonlinear Science and Numerical Simulation*, 46, 14-25.

[84] Zhang, S., & Zhou, Y. (2012). Dynamics and application of an epidemiological model for hepatitis C. *Mathematical and Computer Modelling*, 56(1-2), 36-42.

[85] Ozcaglar, C., Shabbeer, A., Vandenberg, S. L., Yener, B., & Bennett, K. P. (2012). Epidemiological models of Mycobacterium tuberculosis complex infections. *Mathematical biosciences*, 236(2), 77-96.

[86] Lönnroth, K., Migliori, G. B., Abubakar, I., D'Ambrosio, L., De Vries, G., Diel, R., ... & Raviglione, M. C. (2015). Towards tuberculosis elimination: an action framework for low-incidence countries. *European Respiratory Journal*, 45(4), 928-952.

7] Carvalho, A. R., & Pinto, C. M. (2018). Non-integer order analysis of the impact of diabetes and resistant strains in a model for TB infection. *Communications in Nonlinear Science and Numerical Simulation*, 61, 104-126.

8] Mandal, S., & Arinaminpathy, N. (2015). Transmission modeling and health systems: the case of TB in India. *International Health*, 7(2), 114-120.

9] Khan, M. A., Bonyah, E., Hammouch, Z., & Shaiful, E. M. (2020). A mathematical model of tuberculosis (TB) transmission with children and adults groups: Afractional model. *AIMS Mathematics*, 5(4), 2813-2842.

0] Porco, T. C., & Blower, S. M. (1998). Quantifying the intrinsic transmission dynamics of tuberculosis. *Theoretical Population Biology*, 54(2), 117-132.

1] Zhao, Y., Li, M., & Yuan, S. (2017). Analysis of transmission and control of tuberculosis in Mainland China, 2005–2016, based on the age-structure mathematical model. *International journal of environmental research and public health*, 14(10), 1192.

2] Dodd, P. J., Yuen, C. M., Sismanidis, C., Seddon, J. A., & Jenkins, H. E. (2017). The global burden of tuberculosis mortality in children: a mathematical modelling study. *The Lancet Global Health*, 5(9), e898-e906.

3] Kim, S., & Jung, E. (2018). Mathematical model and intervention strategies for mitigating tuberculosis in the Philippines. *Journal of theoretical biology*, 443, 100-112.

4] Ullah, S., Ullah, O., Khan, M. A., & Gul, T. (2020). Optimal control analysis of tuberculosis (TB) with vaccination and treatment. *The European Physical Journal Plus*, 135(7), 602.

5] Choi, S., & Jung, E. (2014). Optimal tuberculosis prevention and control strategy from a mathematical model based on real data. *Bulletin of mathematical biology*, 76, 1566-1589.

6] Bi, Y., Liu, S., & Liu, Y. (2020). Modeling and dynamic analysis of tuberculosis in mainland China from 1998 to 2017: the effect of DOTS strategy and further control. *Theoretical Biology and Medical Modelling*, 17(1), 6.

] Fang, K., Wang, H. L., Lin, Y., Li, S., & Wu, J. (2023). Modeling the impacts of prevention and treatment interventions on hepatitis C among people who inject drugs in China. *Infectious Diseases and Therapy*, 12(4), 1043-1055.

[98] Conway, J. M., & Perelson, A. S. (2014). A hepatitis C virus infection model with time-varyin drug effectiveness: solution and analysis. *PLoS computational biology*, 10(8), e1003769.

[99] Kwon, J. A., Chambers, G. M., Luciani, F., Zhang, L., Kinathil, S., Kim, D., ... & Butler T. (2021). Hepatitis C treatment strategies in prisons: A cost-effectiveness analysis. *Plos one* 16(2), e0245896.

[100] Butler, T., Boonwaat, L., Hailstone, S., Falconer, T., Lems, P., Ginley, T., ... & Kaldor J. (2007). The 2004 Australian prison entrants' blood-borne virus and risk behaviour survey *Australian and New Zealand journal of public health*, 31(1), 44-50.

[101] Elbasha, E. H. (2013). Model for hepatitis C virus transmissions. *Mathematical Biosciences & Engineering*, 10(4), 1045-1065.

[102] Heffernan, A., Cooke, G. S., Nayagam, S., Thursz, M., & Hallett, T. B. (2019). Scaling up prevention and treatment towards the elimination of hepatitis C: a global mathematical model. *The Lancet*, 393(10178), 1319-1329.

[103] Feleke, B. E., Feleke, T. E., Adane, W. G., & Girma, A. (2020). Impacts of hepatitis B and hepatitis C co-infection with tuberculosis, a prospective cohort study. *Virology Journal*, 17, 1-8.

[104] Musso, M., Mosti, S., Gualano, G., Mencarini, P., Urso, R., Ghirga, P., ... & Palmieri, F. (2019). Hepatitis C virus infection: a challenge in the complex management of two cases of multidrug-resistant tuberculosis. *BMC Infectious Diseases*, 19, 1-4.

[105] Nageeb, E. S., Abu-Bakr, S. M., Eid, H. A., & Abou Elhassan, H. A. (2021). Impact of Hepatitis C Virus Co-Infection on Tuberculous Patients. *International Journal of Medical Arts*, 3(4), 1884-1890.

[106] Wahid, B., Saleem, K., Waqar, M., Wasim, M., Sajjad, & Idrees, M. (2018). Successful treatment of HCV/TB co-infected patient with sofosbuvir and daclatasvir: a case report. *Future Virology*, 13(5), 317-321.

[107] Singh, M., & Goyal, S. (2023). Newer Advances in the Management of Hepatitis C. *GMC Patiala Journal of Research and Medical Education*, 6(02), 73-79.

[108] Agusto, F. B. (2009). Optimal chemoprophylaxis and treatment control strategies of a tuberculosis transmission model. *World J Model Simul*, 5(3), 163-173.

[109] Agusto, F. B., & Okosun, K. O. (2010). Optimal seasonal biocontrol for Eichhornia crassipes emphInternational Journal of Biomathematics, 3(03), 383-397.

[110] Kirschner, D., Lenhart, S., & Serbin, S. (1997). Optimal control of the chemotherapy of HIV *Journal of mathematical biology*, 35, 775-792.

[111] Lenhart, S., & Workman, J. T. (2007). Optimal control applied to biological models. *Chapman and Hall/CRC.*

[112] Yang, Y., Tang, S., Xlaohong, R. E. N., Zhao, H., & Guo, C. (2016). GLOBAL STABILITY AND OPTIMAL CONTROL FOR A TUBERCULOSIS MODEL WITH VACCINATION AND TREATMENT. *Discrete & Continuous Dynamical Systems-Series B*, 21(3).

[113] Cui, J. A., Zhao, S., Guo, S., Bai, Y., Wang, X., & Chen, T. (2020). Global dynamics of an epidemiological model with acute and chronic HCV infections. *Applied Mathematics Letters*, 103, 106203.

[114] Byamukama, M., Kajunguri, D., & Karuhanga, M. (2023). A Mathematical Model for Co-infection Dynamics of Pneumocystis Pneumonia and HIV/AIDS with Treatment. *arXiv preprint arXiv:2306.04407.*

[115] Convery, O., Gargan, S., Kickham, M., Schröder, M., O'Farrelly, C., & Stevenson, N. J. (2019). The hepatitis C virus (HCV) protein, p7, suppresses inflammatory responses to tumor necrosis factor (TNF)-alpha via signal transducer and activator of transcription (STAT) 3 and extracellular signal-regulated kinase (ERK)-mediated induction of suppressor of cytokine signaling (SOCS) 3. *FASEB Journal*, 33(8), 8732-8744.

[116] World Health Organization. (2024). Global tuberculosis report 2024. In *Global tuberculosis report 2022.*

[117] World Health Organization. (2023). Global hepatitis report 2023. In *Global hepatitis report 2022.*

[118] Namasopo, S. O. M., Ndugwa, C., & Tumwine, J. K. (2013). Hepatitis C and blood transfusion among children attending the Sickle Cell Clinic at Mulago Hospital, Uganda. *African health sciences*, 13(2), 255-260.

[119] Seremba, E., Ocama, P., Opio, C. K., Kagimu, M., Thomas, D. L., Yuan, H. J., ... & Lee, W. M. (2010). Poor performance of hepatitis C antibody tests in hospital patients in Uganda. *Journal of medical virology*, 82(8), 1371-1378.

[120] Hladik, W., Kataaha, P., Mermin, J., Purdy, M., Otekat, G., Lackritz, E., ... & Downing, R. (2006). Prevalence and screening costs of hepatitis C virus among Ugandan blood donors. *Tropical medicine & international Health*, 11(6), 951-954.

[121] Nankya-Mutyoba, J., Apica, B. S., Otekat, G., Kyeyune, D. B., Nakyagaba, L., Nabunje, J., ... & Ocama, P. (2021). Hepatitis C in Uganda: identification of infected blood donors for micro-elimination. *Journal of Virus Eradication*, 7(2), 100041.

[122] Lenhart, S., & Workman, J. T. (2007). Optimal control applied to biological models. *Chapman and Hall/CRC.*

[123] Fleming, W. H., & Rishel, R. W. (2012). Deterministic and stochastic optimal control (Vol. 1). *Springer Science & Business Media.*

[124] Coddington, E. A., Levinson, N., & Teichmann, T. (1956). Theory of ordinary differential equations.

[125] World Health Organization. (2024). *Global hepatitis report 2024: action for access in low-and middle-income countries.* World Health Organization.

[126] Anbesu, E. W., Aychiluhm, S. B., Alemayehu, M., Asgedom, D. K., & Kifle, M. E. (2023). A systematic review and meta-analysis of sexually transmitted infection prevention practices among Ethiopian young people. *SAGE Open Medicine*, 11, 20503121221145640.

[127] Hiebert-Suwondo, L., Manning, J., Tohme, R. A., Buti, M., Kondili, L. A., Spearman, C. W., ... & Nartey, Y. (2025). A 2024 global report on national policies, programmes, and progress towards hepatitis C elimination: findings from 33 hepatitis elimination profiles. *The Lancet Gastroenterology & Hepatology.*

[128] Ocama, P., Ssekitoleko, R., Nankya-Mutyoba, J., Apica, B., Otekat, G., & Seremba, E. (2024). High false hepatitis C antibody positivity rate in a regionally-inclusive population of non-renumerated blood donors in Uganda. *African Health Sciences*, 24(3), 41-46.

[129] Kempker, R. R., Alghamdi, W. A., Al-Shaer, M. H., Burch, G., & Peloquin, C. A. (2019). A pharmacology perspective on simultaneous tuberculosis and hepatitis C treatment. *Antimicrobia agents and chemotherapy*, 63(12), 10-1128.

[130] Tanvi, & Aggarwal, R. (2021). Estimating the impact of antiretroviral therapy on HIV-TB co-infection: optimal strategy prediction. *International Journal of Biomathematics*, 14(01), 2150004.

[131] Aggarwal, R. (2020). Stability analysis of a delayed HIV-TB co-infection model in resource limitation settings. *Chaos, Solitons & Fractals*, 140, 110138.

[132] Cintrón-Arias, A., Castillo-Chávez, C., Bettencourt, L. M., Lloyd, A. L., & Banks, H. T. (2009). The estimation of the effective reproductive number from disease outbreak data. *Mathematical Biosciences & Engineering*, 6(2), 261-282.

Appendices

Appendix I: MATLAB Code for Chapter 3 Simulations

Model without any interventions

```
function dy = nointerventionmmdf(t,y)
dy = zeros(5,1);S=y(1);IL=y(2);IT=y(3);IA=y(4);IC=y(5);IAL=y(6);ICL=y(7);IAT=y(8);
ICT=y(9);
N=S+IL+IT+IA+IC+IAL+ICL+IAT+ICT;
Lambda= 2000; mu = 0.07; sigma1=0.757; delta1=0.35; delta2=0.42;d1=0.7; d2=0.78;
theta=0.25; alpha=2;tau1=0.35;tau2=0.35;beta1=0.4;beta2=0.6; eta=0.4405;pi=0.3;
phi=0.1;xi1=7;q1=0.3;a1=1.3;a2=1.3;xi2=3;q2=0.2;b1=1.1;b2=1.4;b3=1.2;b4=1.5;
dy(1)=Lambda+pi*y(4)+eta*y(2)-((xi1*q1*(y(3)+a1*y(8)+a2*y(9)))/N
+(xi2*q2*(phi*y(4)+y(5)+b1*y(6)+b2*y(7)+b3*y(8)+b4*y(9)))/N).*y(1)-mu*y(1);
dy(2)=y(1).*(xi1*q1*(y(3)+a1*y(8)+a2*y(9)))/N-(theta+eta+mu)*y(2)
-((xi2*q2*(phi*y(4)+y(5)+b1*y(6)+b2*y(7)+b3*y(8)+b4*y(9)))/N).*y(2);
dy(3)=theta*y(2)-(mu+sigma1)*y(3)-((xi2*q2*(phi*y(4)+y(5)+b1*y(6)+b2*y(7)+b3*y(8)
+b4*y(9)))/N).*y(3);
dy(4)=y(1).*(xi2*q2*(phi*y(4)+y(5)+b1*y(6)+b2*y(7)+b3*y(8)+b4*y(9)))/N
-(pi+alpha+mu+delta1)*y(4)-((xi1*q1*(y(3)+a1*y(8)+a2*y(9)))/N).*y(4);
dy(5)=alpha*y(4)-(mu+delta2)*y(5)-((xi1*q1*(y(3)+a1*y(8)+a2*y(9)))/N).*y(5);
dy(6)=y(4)*(xi1*q1*(y(3)+a1*y(8)+a2*y(9))/N)+y(2)*(xi2*q2*(phi*y(4)+y(5)
+b1*y(6)+b2*y(7)+b3*y(8)+b4*y(9))/N)-(tau1+mu+delta1+beta1)*y(6);
dy(7)=beta1*y(6)+y(5).*(xi1*q1*(y(3)+a1*y(8)+a2*y(9))/N)-(tau2+mu+delta2)*y(7);
dy(8)=tau1*y(6)+(xi2*q2*(phi*y(4)+y(5)+b1*y(6)+b2*y(7)+b3*y(8)+b4*y(9))/N).*(y(3))
-(beta2+mu+d1)*y(8);
```

```
dy(9)=tau2*y(7)+beta2*y(8)-(mu+d2)*y(9);
end
```

Appendix II: MATLAB Code for Chapter 4 Simulations

Model with medication

```
function dy = treatmentmother2(t,y)
dy = zeros(5,1);
S=y(1);IL=y(2);IT=y(3);H=y(4);RT=y(5);IA=y(6);IC=y(7);RH=y(8);IAL=y(9);ICL=y(10);
IAT=y(11);ICT=y(12);R=y(13);
N=S+IL+IT+H+RT+IA+IC+RH+IAL+ICL+IAT+ICT+R;
%constant parameters
Lambda=5000; mu = 0.07; sigma1=0.575; sigma2=0.5; delta=0.42;d1=0.7; d2=0.78; theta
rho=0.0415; omega1=0.7311; omega2=0.8733; alpha=0.32;tau1=0.35;tau2=0.35;
beta1=0.4;beta2=0.6;psi=0.3;r1=0.5;r2=0.6;r3=0.4;nu1=0.125;nu2=0.13;nu3=0.15;eta=0.
pi=0.13;episilon=0.35;phi=0.2;xi1=4;q1=0.55;a1=1.3;a2=1.3;xi2=3;q2=0.3;b1=1.1;b2=1
b3=1.2;b4=1.5;
dy(1)=Lambda+nu1*y(8)+nu2*y(5)+nu3*y(13)+pi*y(6)+eta*y(2)-((xi1*q1*(y(3)+episilon*
+a1*y(11)+a2*y(12)))/N+(xi2*q2*(phi*y(6)+y(7)+b1*y(9)+b2*y(10)+b3*y(11)+b4*y(12)))
*y(1)-mu*y(1);
dy(2)=y(1)*(xi1*q1*(y(3)+episilon*y(4)+a1*y(11)+a2*y(12)))/N-(theta+eta+mu)*y(2)
-((xi2*q2*(phi*y(6)+y(7)+b1*y(9)+b2*y(10)+b3*y(11)+b4*y(12)))/N)*y(2);
dy(3)=theta*y(2)-(omega1+rho+mu+sigma1)*y(3)-((xi2*q2*(phi*y(6)+y(7)+b1*y(9)+b2*y(
+b3*y(11)+b4*y(12)))/N)*y(3);
dy(4)=rho*y(3)-(omega2+mu+sigma2)*y(4);
dy(5)=omega2*y(4)+omega1*y(3)-(nu2+mu)*y(5);
dy(6)=y(1)*(xi2*q2*(phi*y(6)+y(7)+b1*y(9)+b2*y(10)+b3*y(11)+b4*y(12)))/N-(pi+alpha
*y(6)-((xi1*q1*(y(3)+episilon*y(4)+a1*y(11)+a2*y(12)))/N)*y(6);
dy(7)=alpha*y(6)-(psi+mu+delta)*y(7)-((xi1*q1*(y(3)+episilon*y(4)+a1*y(11)
+a2*y(12)))/N)*y(7);
dy(8)=psi*y(7)-(nu1+mu)*y(8);
dy(9)=y(6)*(xi1*q1*(y(3)+episilon*y(4)+a1*y(11)+a2*y(12))/N)+y(2)*(xi2*q2*(phi*y(
```

```
+b1*y(9)+b2*y(10)+b3*y(11)+b4*y(12))/N)-(tau1+mu+beta1)*y(9);
dy(10)=beta1*y(9)+y(7)*(xi1*q1*(y(3)+episilon*y(4)+a1*y(11)+a2*y(12))/N)
-(r1+tau2+mu+delta)*y(10);
dy(11)=tau1*y(9)+(xi2*q2*(phi*y(6)+y(7)+b1*y(9)+b2*y(10)+b3*y(11)+b4*y(12))/N)*y
(r2+beta2+mu+d1)*y(11);
dy(12)=tau2*y(10)+beta2*y(11)-(r3+mu+d2)*y(12);
dy(13)=r1*y(10)+r2*y(11)+r3*y(12)-(nu3+mu)*y(13);
```

Appendix IV: Publications and Manuscripts

Publications

As a result of this study, we contributed to the scientific literature through publication of the followi scholarly articles:

1. Kizito, M., Nampala, H., & Ariho, P. (2024). Mathematical Modelling of Tuberculosis a Hepatitis C Coinfection Dynamics with No Intervention. Journal of Mathematics, 2024(1 5521979. doi.org/10.1155/2024/5521979

2. Kizito, M., Nampala, H., & Ariho, P. (2024). Analysis of a Mathematical Model on t Dynamics of TB-HCV Co-infection with Medication. (Accepted in the Journal of Applie Mathematics, ID 8033235)

Manuscript

During the course of this research, we successfully submitted the following manuscript for peer revie and publication consideration:

1. Kizito, M., Nampala, H., & Ariho, P. (2025). Analysis of Optimal Control on the Dynamics o TB-HCV Co-infection in presence of Treatment (Manuscript submitted)